

Geological Survey of Finland, Special Paper 19

Geochemistry of Proterozoic supracrustal rocks in Finland

IGCP Project 179 Stratigraphic Methods as Applied to the Proterozoic Record
and
IGCP Project 217 Proterozoic Geochemistry

Edited by Mikko Nironen and Yrjö Kähkönen



Geologian tutkimuskeskus
Espoo 1994

Geological Survey of Finland, Special Paper 19

**Geochemistry of Proterozoic supracrustal rocks
in Finland**

**IGCP Project 179 Stratigraphic Methods as Applied to the Proterozoic Record
and
IGCP Project 217 Proterozoic Geochemistry**

Edited by Mikko Nironen and Yrjö Kähkönen

Geologian tutkimuskeskus
Espoo 1994

Nironen, Mikko & Kähkönen, Yrjö (editors) 1994. Geochemistry of Proterozoic supracrustal rocks in Finland. *Geological Survey of Finland, Special Paper* 19, 184 pages, 114 figures, 18 tables, 7 appendices.

The publication results from the activities of the Finnish National Working Groups of IGCP Projects 179 "Stratigraphic Methods as Applied to the Proterozoic Record" and 217 "Proterozoic Geochemistry". The majority of the 11 articles deal with the ca. 1.9 Ga Paleoproterozoic metavolcanic rocks in the Svecofennian Domain of southern and central Finland. Most of the metavolcanic successions studied have arc affinities but a few show features indicative of extensional setting. The topics of the three articles on metasedimentary rocks range from geochemistry and petrography of metaturbidites to rare earth elements in iron-formations.

Key words (GeoRef Thesaurus, AGI): supracrustals, metavolcanic rocks, metasedimentary rocks, geochemistry, Proterozoic, Paleoproterozoic, Finland

Mikko Nironen, Geological Survey of Finland, FIN-02150 Espoo, Finland
Yrjö Kähkönen, Department of Geology, P.O. Box 11 (Snellmaninkatu 3),
FIN-00014 University of Helsinki, Finland

ISBN 951-690-563-3
ISSN 0782-8535

Vammala Vammalan Kirjapaino Oy

CONTENTS

Introduction	5
IGCP Project 179 Stratigraphic Methods as Applied to the Proterozoic Record	
Petrology, geochemistry and dating of Paleoproterozoic metavolcanic rocks in the Pyhäjärvi area, central Finland, <i>Jukka Kousa, Erkki Marttila and Matti Vaasjoki</i>	7
Geochemistry of the Paleoproterozoic andesitic to rhyolitic arc-type metavolcanic rocks of Haukkamaa, Kuru, central Finland, <i>Markku Tiainen and Yrjö Kähkönen</i>	29
Geochemistry of the Paleoproterozoic metavolcanic rocks at Evijärvi, western Finland, <i>Markus Vaarma and Yrjö Kähkönen</i>	47
Geochemistry of calc-alkaline metavolcanic rocks in the Parikkala-Punkaharju area, southeastern Finland, <i>Ahti Viluksela</i>	61
IGCP Project 217 Proterozoic Geochemistry	
REE distribution in the phosphorite bands within the Paleoproterozoic Tuomivaara and Pahtavaara iron-formations, central and northern Finland, <i>Seppo Gehör</i>	71
Geology and geochemistry of the Hämeenlinna-Somero Volcanic Belt, southwestern Finland: a Paleoproterozoic island arc, <i>Gerhard Hakkarainen</i>	85
Shoshonitic and high-K metavolcanic rocks in the southern parts of the Paleoproterozoic Tampere Schist Belt, southern Finland: evidence for an evolved arc-type setting, <i>Yrjö Kähkönen</i>	101
Geochemistry of metasedimentary rocks of the Paleoproterozoic Tampere Schist Belt, southern Finland, <i>Yrjö Kähkönen and Jussi Leveinen</i>	117
Supracrustal rocks around the Paleoproterozoic Haveri Au-Cu deposit, southern Finland: evolution from a spreading center to a volcanic arc environment, <i>Yrjö Kähkönen and Mikko Nironen</i>	141
Post-depositional K-feldspar breakdown and its implications for metagraywacke provenance studies - an example from north Karelia, eastern Finland, <i>Jarmo Kohonen</i>	161
Emplacement, deformation and geochemistry of bimodal volcanics in Vestlax, SW Finland, <i>Alf Lindroos and Carl Ehlers</i>	173

INTRODUCTION

This Special Paper Volume is the final report of two IGCP (International Geological Correlation Programme) Projects in Finland. Project 179 **Stratigraphic Methods as Applied to the Proterozoic Record** was initiated 1981 by J. Sarfati (Montpellier, France), N. Clauer (Strasbourg, France), M. Semikhatov (Moscow, USSR) and G.M. Young (Ontario, Canada). The aim of the Project was intrabasinal and interregional correlations of Proterozoic supracrustal rocks by a combined use of all available methods. An attempt was made to work towards a more precise correlation of reference sections of the Proterozoic from different countries. The Finnish National Working Group, led by Dr. Kauko Meriläinen of the Geological Survey of Finland, was active during 1983-1987. The members of the Working Group were from the Geological Survey of Finland, from the Geology Departments of the Universities of Helsinki and Turku and from Rautaruukki Oy. The topic of the Project was the typology, evolution and stratigraphic setting of Svecokarelian volcanic and plutonic rocks, with the emphasis on geochemical methods. In addition to the ones presented in this Special Paper Volume, the studies by e.g. A. Kontinen on the Jormua Ophiolite Complex (Kontinen 1987), and J. Kousa, L. Pekkarinen and H. Lukkarinen on metavolcanics in eastern Finland (Kousa 1985, Pekkarinen & Lukkarinen 1991) were supported by the Project.

IGCP Project 217 **Proterozoic Geochemistry** was launched in 1984 by Kent C. Condie (Socorro, USA) and Randy Van Schmus (Lawrence, USA). The themes of the Project were: 1) a comparison of Archean and Proterozoic supracrustal associations; 2) crustal evolution as recorded by Proterozoic detrital sediments; 3) the apparent 2.4 to 2.0 Ga crustal generation gap; 4) precise geochronology of Proterozoic lithologic suites; 5) mantle evolution during the Proterozoic; 6) origin and evolution of rapakivi granite-anorthosite association; 7) reworking versus juvenile addition to the continents; 8) high-grade metamorphic terranes; and 9) evolution of metallogenic mineral deposits.

The Finnish National Working Group was established on February 14th, 1985, and it was led by Dr. Yrjö Kähkönen of the Department of Geology, University of Helsinki. The members of the Working Group were from the Geological Survey of Finland, from the Geology Departments of the Universities of Helsinki, Oulu, Turku and Åbo Akademi, from Outokumpu Oy and from the Technical Research Centre of Finland. As the closing event, the Working Group arranged the national symposium "Proterozoic Geochemistry, Helsinki '90", held at the University of Helsinki on December 13 and 14, 1990. Of the 23 papers given at the symposium seven are published here.

The Finnish Working Group, together with the Finnish and Swedish Working Groups of IGCP project 247 (Precambrian Ore Deposits and Tectonic Setting), arranged the international field conference "Tectonic Setting of Proterozoic Volcanism and Associated Ore Deposits" in central Sweden and southern Finland from August 15-21, 1988. Jointly with the Department of Geology, University of Helsinki and IGCP project 247, the Working Group arranged the international symposium "Precambrian Granitoids - Petrogenesis, Geochemistry and Metallogeny" at the University of Helsinki August 14-17, 1989. The proceedings of the symposium were published as volume 51 of Precambrian Research, edited by Ilmari Haapala and Kent C. Condie.

We would like to thank the authors and the referees for their kind cooperation in producing this Volume as well as the members of the National Working Groups for their activity. The financial support allocated by the Academy of Finland and the National IGCP Committee of Finland to the Projects is gratefully acknowledged.

REFERENCES

- Kontinen, A. 1987.** An early Proterozoic ophiolite - the Jormua mafic-ultramafic complex, northeastern Finland. *Precambrian Res.* 35, 313-341.
- Kousa, J. 1985.** Rantasalmen tholeiittisista ja komatiittisista vulkaniiteista. *Geologi* 2, 17-22. (in Finnish)
- Pekkarinen, L. J. & Lukkarinen, H. 1991.** Paleoproterozoic volcanism in the Kiihtelysvaara - Tohmajärvi district, eastern Finland. *Geol. Surv. Finland, Bull.* 357, 30 p.

PETROLOGY, GEOCHEMISTRY AND DATING OF PALEOPROTEROZOIC METAVOLCANIC ROCKS IN THE PYHÄJÄRVI AREA, CENTRAL FINLAND

by

Jukka Kousa, Erkki Marttila and Matti Vaasjoki

Kousa Jukka, Marttila Erkki & Vaasjoki Matti 1994. Petrology, geochemistry and dating of Paleoproterozoic metavolcanic rocks in the Pyhäjärvi area, central Finland. *Geological Survey of Finland, Special Paper 19*, 7–27, 12 figures and two tables.

The Pyhäjärvi area lies within the highly deformed NW-SE trending Ladoga - Bothnian Bay zone, between the Archean craton (east) and the Paleoproterozoic Central Finland Granitoid Complex (west). During the Svecokarelian orogeny the supracrustal rocks of Pyhäjärvi were metamorphosed to amphibolite facies grade.

The metavolcanic rocks of Pyhäjärvi have been divided into two groups on the basis of field observations and compositional differences. The metavolcanics in the eastern part of the study area have a distinctly bimodal nature and include low-K tholeiitic metabasalts, basaltic andesites and metarhyolites. Primary pyroclastic and pillow structures have been preserved locally, indicating at least partially subaqueous eruptions. This bimodal association is here termed as the Eastern Volcanic Sequence (EVS); a quartz porphyry within this unit gives a U-Pb zircon age of 1.92 Ga. The metavolcanic rocks west and southwest of Lake Pyhäjärvi (Western Volcanic Sequence, WVS) form a more evolved, probably calc-alkaline series of basaltic to dacitic rocks. Unfortunately, no reliable age determinations were obtained from these rocks, but evidence from adjacent plutonic and hypabyssal rocks (1.89-1.87 Ga) as well as many similarities with the nearby Pihlajavesi and Kuusaanjärvi metavolcanics strongly suggest that the rocks of the WVS are younger than rocks of the EVS.

Geochemically all of the metavolcanic rocks in the Pyhäjärvi area show arc affinities. The mafic metavolcanics of the EVS resemble primitive island arc tholeiites. On the other hand, the bimodal nature suggests a rifting episode, perhaps of an older Paleoproterozoic active continental margin crust. The younger, calc-alkaline WVS rocks resemble the volcanics of a more mature compressional stage arc system.

Key words (GeoRef Thesaurus, AGI): metavolcanic rocks, pillow lava, schist belts, stratigraphy, geochemistry, absolute age, U/Pb, Proterozoic, Paleoproterozoic, Pyhäjärvi, Finland

*Jukka Kousa, Geological Survey of Finland, P. O. Box 1237
FIN-70211 Kuopio, Finland*

Erkki Marttila, Samoiliijantie 3, FIN-70200 Kuopio, Finland,

*Matti Vaasjoki, Geological Survey of Finland, Betonimiehenkuja 4,
FIN-02150 Espoo, Finland*

INTRODUCTION

The Pyhäjärvi area lies within the Svecofennian Domain close to the western margin of the Archean craton (Fig. 1). The Svecofennian Domain formed in Paleoproterozoic times, predominantly from newly mantle-derived material (Huhma 1986). The study area is part of the Pyhäsalmi - Pielavesi district, well known for its sulfide ore deposits (e.g. Huhtala 1979, Ekdahl 1993). The Svecofennian supracrustal rocks underwent intense deformation and metamorphism during the Svecokarelian orogeny, which culminated 1900-1850 Ma ago (Korsman et al. 1984, Vaasjoki & Sakko 1988).

Huhtala et al. (1978) and Huhtala (1979) studied the volcanic rocks of the Vihanti-Pyhäsalmi-Pielavesi zone from an ore geologic point of view and noted that the Pyhäsalmi Zn-Pb-Cu sulfide deposit is surrounded by altered rocks in a volcanic environment. Helovuori (1979) studied the geology of the Pyhäsalmi mine and concluded that the ore is of volcanic-exhalative origin. Mäki (1986) and Mäkelä et al. (1987) carried out exploration-related geochemical studies in the volcanic rocks surround-

ing the Pyhäsalmi mine. These volcanics belong to the Ruotanen Schist Zone (p. 14) of this study.

Collaboration between geologists from Outokumpu Company and Geological Survey of Finland has led to the recognition of new aspects of the geology of the Pyhäjärvi area. This study is based on sample material collected during petrological mapping with emphasis on volcanic rocks (Table 1). Bulk chemical analyses (XRF) of the samples were carried out at the Research Centre of Rautaruukki Company at Raahe, the REE analyses (INAA) were performed at the Reactor Laboratory of the Technical Research Centre at Espoo, and the isotopic studies were done at the Geological Survey of Finland. The purpose of the study is to discuss the geochemical nature of the volcanic rocks, their geotectonic environment, and their temporal development.

The geological description in this text was made by E. Marttila and J. Kousa, the isotope geological work by M. Vaasjoki and the geochemical study by J. Kousa.

GENERAL CHARACTERISTICS OF THE METAVOLCANIC ROCKS IN THE PYHÄJÄRVI AREA

The metavolcanic rocks of the Pyhäjärvi area occur partly as long, narrow zones between updoming granitoid batholiths and partly as larger units containing a variety of rock types (Fig. 1; see also Marttila 1993). Due to polyphase deformation, intense foliation with widely varying dip angles characterizes the structure of the area. The metavolcanic

rocks were divided into two major units on the basis of their areal occurrence: 1) Eastern Volcanic Sequence and 2) Western Volcanic Sequence. Both units are composed of several types of volcanogenic rocks which are described below. The sites of the rocks analyzed are shown in Fig. 1.

EASTERN VOLCANIC SEQUENCE

Tetrimmäki Schist Zone

The Tetrimmäki Schist Zone (TSZ), 4 km in length, is located about 10-20 km NE of Lake Pyhäjärvi, in the NE part of the map area (Fig. 1). The metavolcanic rocks of this zone consist of both mafic lavas and pyroclastic rocks as well as felsic tuffaceous pyroclastic schists.

Lavas with well-preserved pillow structures occur in the TSZ, the largest being up to 1 m in diameter. They are either uralite porphyries or even-grained

amphibolites, and they commonly contain amygdules filled with epidote and/or albite. In the northern part of the zone the pillows are large and well-developed. Their size decreases eastwards and pillow breccias (Fig. 2) become more common. The breccias contain abundant yellowish-green fragments rich in epidote, and the interstices are filled with hyaloclastic material. In the southern part of the zone the lavas are dark green and massive, occasionally containing yellow-

ish-green epidote segregations and amygdules. The main minerals are hornblende, epidote and plagioclase; the last being clearly less abundant than the other two. Titanite and locally sulfides are common accessory minerals. In composition the pillow lavas are basalts and basaltic andesites (Table 1, analyses 8, 12, 14, 17 and 23).

Both the pillow lavas and the breccias are cut by a dense swarm of mafic and intermediate dykes (Koivula 1987). The dykes are usually 10-30 cm wide, although in exceptional cases they have widths of 70 cm, and their contacts with the metalavas are sharp. The trend of the dykes varies from N-S to NNW-SSE. North of the TSZ (sites 7 and 11 in Fig. 1) there are several outcrops of basaltic lavas with both massive and pillow lava beds. As in the TSZ, the lavas are crosscut by mafic dykes.

Felsic volcanoclastic rocks occur west of the lavas,

and the zone terminates against a fine- to medium-grained reddish granite which further away from the contact grades into a medium-grained gray variety. The contact is covered by till, and hence the age relationship between the granite and the Tetrinmäki pillow lavas is unknown.

An area of mafic metavolcanic rocks, as well as altered rock types such as sericite and chlorite schists and cordierite-bearing rocks, occurs to the east of the TSZ proper, separated from it by plutonic rocks. These rocks include mafic pillow lavas, fragmentary metalavas and pyroclastic breccias (sites 13, 19, 22 and 32). The pillows are slightly elongated, 20-50 cm in length, and are generally surrounded by a 1-2 cm thick epidote-quartz rim containing Fe-sulfides. The main minerals are hornblende, plagioclase (An₃₀) and diopside. The fragmented variety contains pale green pillow-like shards (5-50

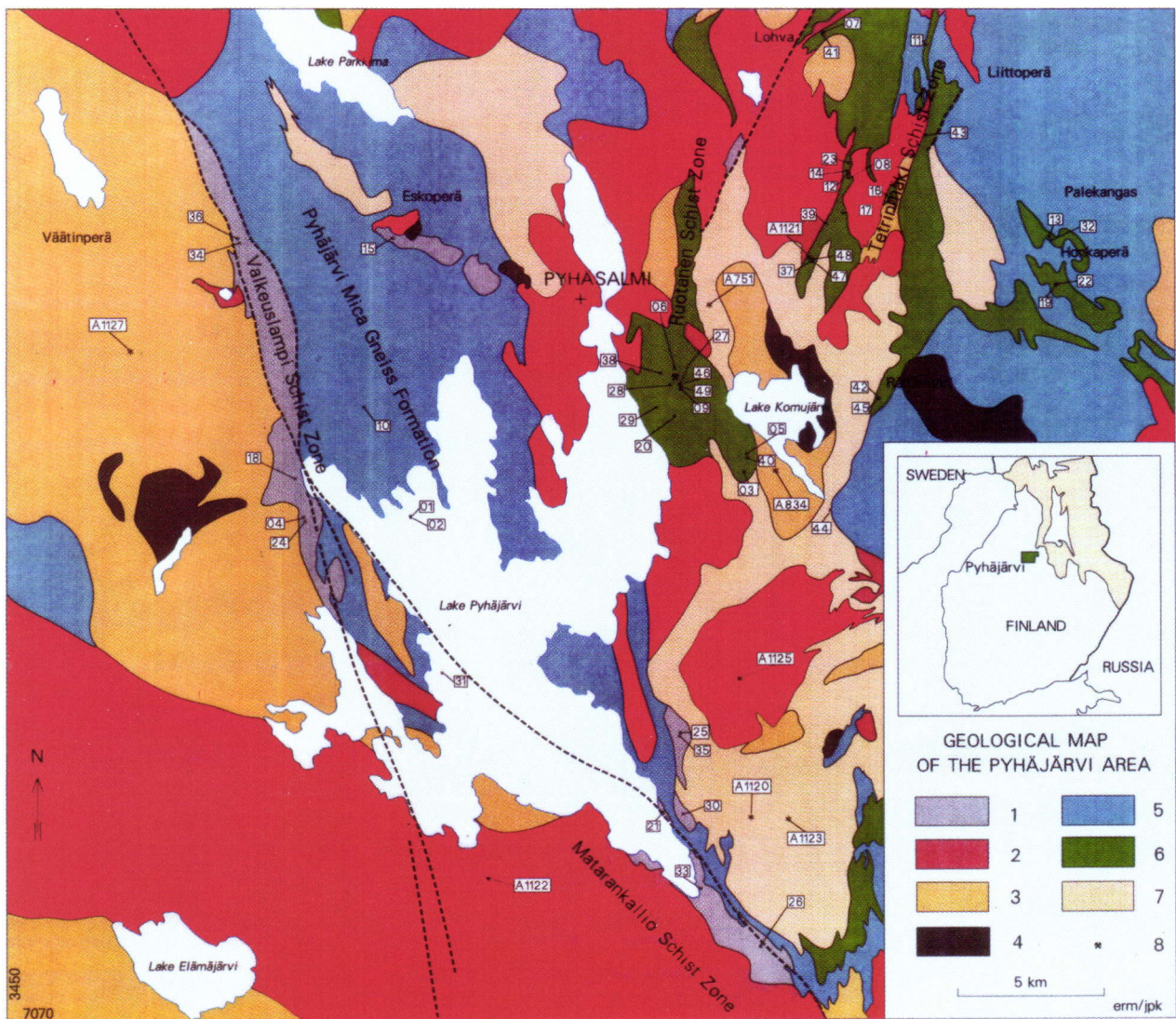


Fig. 1. Geological map of the Pyhäjärvi area (modified from Marttila 1977, 1992a, 1992b). Sample localities have been marked in the map with the same numbers as the analyses and samples in Tables 1 and 2. Lithologies in the legend: 1=Western Volcanic Sequence; 2=granite; 3=granodiorite and quartz diorite; 4=diorite and gabbro; 5=mica gneiss; 6=Eastern Volcanic Sequence; 7=ortho- and paragneiss complex; 8=Pyhäsalmi sulfide mine. Inset: locality of the study area in green, Archean basement in beige.

TABLE 1. Major and trace element analyses and sample locations of the metavolcanic rocks at the Pyhäjärvi area, Central Finland. Major elements and V, Cu, Zn, Ni, S, Ba, Sr and Zr by XRF. REE by INAA. Oxides in weight-% and trace elements in ppm.

	1	2	3	4	5	6	7	8	9	10	11	12	13
SiO ₂	44.01	45.54	46.97	47.48	48.26	48.75	49.50	49.66	49.70	50.11	50.29	50.31	50.32
TiO ₂	0.41	0.50	0.42	0.55	0.46	0.59	0.58	0.51	0.49	0.54	0.48	0.51	0.58
Al ₂ O ₃	15.39	16.07	15.99	17.96	15.95	17.76	17.07	13.92	16.21	11.17	15.32	14.04	14.43
Fe ₂ O _{3t}	10.49	11.42	11.53	12.42	11.85	12.63	10.29	12.27	11.59	12.22	9.99	10.64	12.02
MnO	0.17	0.20	0.23	0.21	0.24	0.19	0.17	0.41	0.18	0.21	0.20	0.40	0.18
MgO	11.69	9.59	9.26	6.78	8.11	5.47	6.14	7.73	7.67	12.65	7.30	8.40	8.30
CaO	14.19	12.04	11.52	11.54	12.00	9.52	9.95	12.25	11.08	10.02	12.77	12.70	11.18
Na ₂ O	1.11	0.98	2.83	1.95	1.08	4.22	3.25	2.40	2.56	0.71	1.05	2.05	1.73
K ₂ O	0.45	0.86	0.74	0.61	1.73	0.34	0.29	0.30	0.25	1.61	0.17	0.38	0.38
P ₂ O ₅	0.02	0.09	0.12	0.19	0.07	0.06	0.08	0.11	0.06	0.28	0.06	0.10	0.09
Total	97.92	97.27	99.60	99.69	99.74	99.53	97.31	99.57	99.78	99.51	97.62	99.54	99.21
V	250	200	270	260	280	330	300	280	270	260	250	270	270
Cu	50	60	30	100	160	350	10	20	20	60	90	10	50
Zn	50	70	140	90	80	100	130	100	80	110	120	90	80
Ni	150	130	130	50	80	30	50	160	70	290	2450	180	80
S	720	360	310	190	240	3250	460	30	30	1830	4070	10	270
Ba	100	270	150	200	240	110	130	90	110	460	150	200	140
Sr	270	290	100	460	150	40	230	160	170	280	80	180	150
Zr	20	30	30	50	30	40	40	40	30	70	40	40	30
La	1.1	-	-	6.8	-	3.0	-	-	-	11.2	3.0	5.3	4.6
Ce	2.0	-	-	13.1	-	9.1	-	-	-	21	7.1	10	9.9
Nd	-	-	-	9.8	-	3.1	-	-	-	16	-	-	6.1
Sm	1.2	-	-	2.6	-	1.5	-	-	-	3.7	1.3	1.8	1.9
Eu	0.46	-	-	0.76	-	0.54	-	-	-	0.91	0.5	0.61	0.66
Tb	0.26	-	-	0.34	-	0.36	-	-	-	0.46	0.37	0.37	0.34
Yb	0.83	-	-	1.3	-	1.5	-	-	-	1.4	1.4	1.3	1.6
Lu	0.11	-	-	0.16	-	0.19	-	-	-	0.2	0.14	0.16	0.18
	14	15	16	17	18	19	20	21	22	23	24	25	26
SiO ₂	50.37	51.06	51.11	51.43	51.65	51.72	51.95	52.00	52.16	52.57	53.08	53.81	54.06
TiO ₂	0.54	1.52	1.14	0.58	0.65	0.44	0.63	0.74	0.45	0.51	0.43	0.28	0.82
Al ₂ O ₃	14.42	17.14	17.23	17.72	17.53	14.66	15.68	16.20	14.89	13.61	17.42	12.20	18.15
Fe ₂ O _{3t}	10.16	11.20	13.29	10.01	11.98	9.93	10.66	9.06	10.53	11.85	10.74	5.41	10.47
MnO	0.35	0.16	0.20	0.22	0.18	0.18	0.19	0.20	0.18	0.34	0.19	0.18	0.18
MgO	8.05	5.63	4.53	5.45	3.71	6.61	6.38	8.21	7.54	6.77	5.30	11.98	3.38
CaO	12.39	7.34	8.21	10.26	9.92	12.03	10.78	10.39	9.53	10.79	9.07	13.82	7.62
Na ₂ O	2.34	3.45	2.72	3.40	2.49	3.85	2.67	2.49	4.09	2.65	2.55	1.85	2.76
K ₂ O	0.27	1.83	0.99	0.18	1.12	0.18	0.54	0.35	0.18	0.32	0.80	0.26	2.05
P ₂ O ₅	0.09	0.35	0.15	0.14	0.25	0.08	0.16	0.12	0.08	0.10	0.15	0.09	0.19
Total	98.98	99.69	99.57	99.40	99.48	99.67	99.63	99.76	99.64	99.50	99.74	99.88	99.68
V	270	200	390	320	280	240	250	200	230	220	210	40	220
Cu	10	20	40	320	90	50	60	-	140	10	210	-	20
Zn	80	100	120	250	110	60	120	140	80	300	80	90	130
Ni	290	60	30	210	30	60	60	150	60	170	40	10	20
S	410	850	770	610	230	610	720	20	570	120	60	30	90
Ba	130	490	360	100	360	70	100	100	50	140	170	100	750
Sr	160	470	180	220	580	70	250	250	110	150	340	270	210
Zr	50	180	60	40	50	20	60	80	30	40	40	160	80
La	5.2	-	-	-	-	-	-	8.4	3.3	-	-	18	-
Ce	9.6	-	-	-	-	-	-	16	7.2	-	-	37	-
Nd	7.2	-	-	-	-	-	-	12.1	4.9	-	-	22	-
Sm	1.8	-	-	-	-	-	-	3.0	1.5	-	-	5.1	-
Eu	0.61	-	-	-	-	-	-	0.89	0.48	-	-	1.0	-
Tb	0.29	-	-	-	-	-	-	1.1	0.30	-	-	0.66	-
Yb	1.2	-	-	-	-	-	-	1.8	0.95	-	-	3.1	-
Lu	0.18	-	-	-	-	-	-	0.25	0.14	-	-	0.40	-

TABLE 1. (continued)

	27	28	29	30	31	32	33	34	35	36	37	38	39
SiO ₂	54.10	54.26	54.27	54.37	55.08	55.25	57.07	61.49	61.66	63.53	67.70	72.26	73.35
TiO ₂	0.53	0.50	0.38	1.19	0.41	0.68	0.73	0.63	0.61	0.58	0.54	0.18	0.32
Al ₂ O ₃	16.32	17.52	14.53	16.00	19.43	16.74	18.84	16.50	16.96	16.58	15.30	13.85	13.51
Fe ₂ O _{3t}	11.20	9.54	9.00	10.54	7.83	7.65	9.51	6.81	7.24	6.51	3.08	3.98	3.52
MnO	0.17	0.18	0.11	0.12	0.15	0.09	0.21	0.10	0.10	0.12	0.06	0.11	0.06
MgO	5.26	4.51	8.14	5.01	3.05	5.44	2.47	2.66	2.61	1.70	1.31	0.88	0.25
CaO	5.91	7.76	9.93	8.47	8.88	8.48	7.69	5.13	4.65	5.31	4.04	1.71	1.84
Na ₂ O	3.88	5.05	2.80	2.40	2.91	4.80	0.85	3.61	3.04	2.47	6.25	2.50	4.59
K ₂ O	2.05	0.24	0.28	1.31	0.83	0.38	2.09	2.39	2.71	2.48	1.04	3.66	2.20
P ₂ O ₅	0.09	0.13	0.07	0.17	0.11	0.11	0.21	0.16	0.17	0.18	0.18	0.02	0.07
Total	99.51	99.68	99.51	99.58	98.68	99.63	99.67	99.49	99.75	99.46	99.50	99.15	99.70
V	270	290	250	220	130	280	190	150	120	110	80	-	20
Cu	70	10	70	70	-	30	70	20	20	-	-	-	0
Zn	110	90	80	90	80	80	200	90	90	90	30	150	50
Ni	30	50	60	60	30	120	20	20	30	10	20	10	10
S	2990	180	2070	2890	50	1750	1350	80	310	50	10	40	50
Ba	290	130	230	290	420	160	750	700	590	620	230	770	560
Sr	160	70	190	350	470	150	180	370	290	320	120	80	90
Zr	50	20	20	100	50	40	110	140	160	130	220	150	310
La	-	-	3.7	-	-	3.6	-	-	28	27	44	15	-
Ce	-	-	9.2	-	-	7.2	-	-	46	50	82	31	-
Nd	-	-	4.7	-	-	5.2	-	-	23	22	35	19	-
Sm	-	-	1.6	-	-	1.8	-	-	4.8	4.9	6.9	5.3	-
Eu	-	-	0.61	-	-	0.62	-	-	1.0	1.1	1.3	1.6	-
Tb	-	-	0.32	-	-	0.41	-	-	0.48	0.57	0.91	1.2	-
Yb	-	-	0.77	-	-	1.7	-	-	1.7	2.2	3.8	5.6	-
Lu	-	-	0.11	-	-	0.2	-	-	0.19	0.29	0.40	0.78	-
	40	41	42	43	44	45	46	47	48	49			
SiO ₂	76.04	76.13	76.71	76.78	76.88	78.10	78.37	78.96	79.71	79.99			
TiO ₂	0.18	0.17	0.20	0.17	0.16	0.15	0.12	0.12	0.11	0.11			
Al ₂ O ₃	11.43	12.99	12.32	12.37	11.75	11.82	11.95	12.53	12.50	11.64			
Fe ₂ O _{3t}	3.53	2.49	3.08	1.97	2.69	2.17	1.63	0.30	0.32	1.21			
MnO	0.05	0.03	0.03	0.03	0.09	0.04	0.02	0.02	0.01	0.02			
MgO	0.80	0.26	0.36	0.48	1.76	0.27	0.22	0.05	0.07	0.23			
CaO	1.59	1.95	1.97	0.97	0.85	2.35	1.31	0.37	0.44	0.70			
Na ₂ O	1.39	4.82	4.94	4.00	3.76	4.08	4.88	6.43	6.35	5.39			
K ₂ O	4.46	0.80	0.09	2.69	1.02	0.15	0.43	0.18	0.16	0.44			
P ₂ O ₅	0.03	0.03	0.04	0.03	0.01	0.03	0.01	0.01	0.01	0.01			
Total	99.51	99.67	99.73	99.49	98.97	99.16	98.95	98.97	99.68	99.75			
V	10	20	10	20	10	10	-	-	-	10			
Cu	20	10	-	10	-	-	40	-	-	-			
Zn	60	30	20	20	130	10	20	-	10	20			
Ni	10	20	10	20	20	10	10	10	10	10			
S	3910	290	160	200	1720	60	960	10	-	180			
Ba	520	410	60	1020	340	150	390	70	80	380			
Sr	30	110	80	70	60	120	120	30	30	50			
Zr	130	230	170	260	240	180	180	210	220	190			
La	13.6	-	19	22	-	-	29	79	-	-			
Ce	26	-	38	40	-	-	51	145	-	-			
Nd	13.5	-	21	23	-	-	26	57	-	-			
Sm	2.9	-	4.6	5.1	-	-	6.2	12	-	-			
Eu	0.69	-	1.1	1.4	-	-	1.1	0.71	-	-			
Tb	0.48	-	0.77	0.57	-	-	0.99	1.1	-	-			
Yb	3.2	-	3.4	1.6	-	-	4.7	4.3	-	-			
Lu	0.40	-	0.44	0.22	-	-	0.61	0.46	-	-			

TABLE 1. (continued)

1. Mafic metalava; Pyhäsalmi, Lokinkivi; 3321 08B, x=7057.550, y=3443.820
2. Mafic metalava; Pyhäsalmi, Lokinkivi; 3321 08B, x=7057.550, y=3443.820
3. Mafic metalava; Pyhäsalmi, Soidinmäki; 3321 11B, x=7059.000, y=3455.000
4. Uraliteporphyry metatuff; Pyhäsalmi, Olkkosenmäki; 3321 08B, x=7056.940, y=3440.220
5. Mafic metavolcanic rock; Pyhäsalmi, Topiskonräme; 3321 11D, x=7059.620, y=3455.440
6. Mafic metalava; Pyhäsalmi, mine area; 3321 12A, x=7062.650, y=3452.770
7. Mafic metalava; Pyhäsalmi, Lauttasaari; 3322 10C, x=7074.030, y=3457.860
8. Mafic pillow lava; Pyhäsalmi, Tetrinmäki; 3321 12D, x=7069.140, y=3458.940
9. Mafic metalava; Pyhäsalmi, mine area; 3321 12A, x=7061.810, y=3453.180
10. Mafic metavolcanic rock; Pyhäsalmi, Lamminaho; 3321 09A, x=7060.800, y=3441.880
11. Mafic pillow lava; Pyhäsalmi, Murtoerä; 3324 01A, x=7073.580, y=3461.430
12. Mafic pillow lava; Pyhäsalmi, Tetrinmäki; 3321 12D, x=7069.180, y=3458.920
13. Mafic pillow lava; Kiuruvesi, Palekangas; 3323 03D, x=7066.700, y=3465.730
14. Mafic pillow lava; Pyhäsalmi, Tetrinmäki; 3321 12D, x=7069.240, y=3458.920
15. Mafic metavolcanic rock; Pyhäsalmi, Eskoperä; 3321 09B, x=7067.290, y=3443.140
16. Mafic metavolcanic rock; Pyhäsalmi, Äyhynkorpi; 3323 03B, x=7068.590, y=3460.320
17. Mafic pillow lava; Pyhäsalmi, Jylkynkangas; 3321 12D, x=7067.830, y=3458.640
18. Mafic metatuff; Pyhäsalmi, Kärkelä; 3321 05D, x=7058.700, y=3439.940
19. Mafic pillow lava; Kiuruvesi, Kyntölänkangas; 3323 03D, x=7065.230, y=3466.130
20. Mafic metavolcanic rock; Pyhäsalmi, Lippikylä; 3321 12A, x=7060.860, y=3452.960
21. Uraliteporphyry metatuff; Pyhäsalmi, Olinniemi; 3321 10B, x=7047.160, y=3452.300
22. Mafic pillow lava; Kiuruvesi, Kyntölänkangas; 3323 03D, x=7065.180, y=3466.000
23. Mafic pillow lava; Pyhäsalmi, Tetrinmäki; 3321 12D, x=7069.670, y=3458.880
24. Mafic metatuff; Pyhäsalmi, Olkkosemäki; 3321 08B, x=7056.880, y=3440.240
25. Mafic metatuff; Pyhäsalmi, Jokelaisneva; 3321 10B, x=7049.800, y=3453.150
26. Mafic metatuff; Pyhäsalmi, Matarankallio; 3321 10C, x=7042.440, y=3455.960
27. Mafic metatuff; Pyhäsalmi, mine area; 3321 12A, x=7062.100, y=3453.000
28. Mafic metalava; Pyhäsalmi, mine area; 3321 12A, x=7062.070, y=3452.600
29. Mafic pillow lava; Pyhäsalmi, Mukurinperä; 3321 12A, x=7061.340, y=3452.060
30. Uraliteporphyry metatuff; Pyhäsalmi, Pullosuo; 3321 10B, x=7046.900, y=3453.180
31. Mafic metatuff; Pyhäsalmi, Kirjavatsaari; 3321 08A, x=7052.000, y=3444.770
32. Mafic pillow lava; Kiuruvesi, Palekangas; 3323 03D, x=7066.700, y=3465.730
33. Intermediate metavolcanic rock; Pyhäsalmi, Maaselänlahti; 3321 10A, x=7044.600, y=3453.550
34. Intermediate metatuff; Pyhäsalmi, Valkeuslampi; 3321 06D, x=7066.960, y=3437.900
35. Intermediate metatuff; Pyhäsalmi, Jokelaisneva; 3321 10B, x=7049.830, y=3453.300
36. Intermediate metatuff; Pyhäsalmi, Valkeuslampi; 3321 06D, x=7067.030, y=3437.880
37. Intermediate metatuff; Pyhäsalmi, Riitavuori; 3321 12D, x=7066.220, y=3457.530
38. Quartzporphyry; Pyhäsalmi, mine area; 3321 12A, x=7062.460, y=3452.500
39. Felsic metavolcanic rock; Pyhäsalmi, Heikinaho; 3321 12D, x=7067.640, y=3458.080
40. Felsic metavolcanic rock; Pyhäsalmi, Topiskonräme; 3321 11D, x=7059.620, y=3455.440
41. Felsic metatuff; Pyhäsalmi, Lauttasaari; 3321 10C, x=7074.030, y=3457.860
42. Felsic metatuff; Pyhäsalmi, Rättävuori; 3321 12C, x=7061.520, y=3459.900
43. Felsic tuffaceous metasediment; Pyhäsalmi, Liitoperä; 3324 01A, x=7070.400, y=3461.320
44. Felsic metatuff; Pyhäsalmi, Salmelanperä; 3321 11D, x=7057.620, y=3458.250
45. Felsic metavolcanic rock; Pyhäsalmi, Rättävuori; 3321 12C, x=7061.500, y=3459.880
46. Quartzporphyry; Pyhäsalmi, mine area; 3321 12A, x=7061.930, y=3453.120
47. Quartzporphyry; Pyhäsalmi, Riitavuori; 3321 12D, x=7066.190, y=3457.490
48. Quartzporphyry; Pyhäsalmi, Riitavuori; 3321 12D, x=7066.260, y=3457.440
49. Quartzporphyry; Pyhäsalmi, mine area; 3321 12A, x=7061.920, y=3453.160

cm in diameter) with diopside, hornblende, epidote and minor amounts of plagioclase. The metalavas comprise basalts, basaltic andesites and basaltic trachyandesites and they locally contain abundant epidote-rich fragments which are either broken pillows or pyroclasts. Some agglomerates stratigraphically overlie the pillow lavas (Marttila 1976, 1981; Karvinen 1978). The size and composition of the pyroclasts varies, with sizes up to 15 cm. The rims of the fragments contain a large amount of diopside and epidote. Pale fragments have a greenish outer rim, and the anorthite content of plagioclase increases from the center of the fragment (An_{36}) towards the rim (An_{43}). In the mafic interstitial matrix between clasts, the An content of plagioclase is about 50%. The mafic "bombs" consist of plagioclase (An_{69}) and diopside with accessory twinned titanite, carbonate and tremolite.

The rhyolitic (analyses 47 and 48) and rhyodacitic (analysis 37) metavolcanics from Riitavuori are separated by a breccia from the eastern pillow lava of the TSZ. The pyroclastic material contains intercalations of quartz porphyry, volcanic breccia and arkosic sediments. The phenocrysts in the quartz porphyry are 1-2 mm in size. The tuffaceous arkosite in this area is a fine-grained, strongly recrystallized reddish rock. Beside quartz, the other main mineral is oligoclase. Minor minerals are hornblende and

biotite, and accessory constituents are epidote, titanite, muscovite and carbonate. Numerous N-S trending uralite and plagioclase porphyry veins and amphibolitic dykes crosscut the rock. Similar recrystallized tuffaceous rhyolite occurs N of Riitavuori (site 39).

In the northern part of the TSZ, skarn material, sulfide disseminations, cordierite-anthophyllite gneiss and sericite quartzite occur among the rhyolites. The metavolcanics at Lohvanperä (site 41) resemble the felsic volcanic rocks of the Ruotanen Schist Zone (see page 14).

A N-S striking zone at site 43 contains mafic and felsic volcanics. The basaltic metavolcanics contain skarns consisting of abundant diopside with plagioclase (An_{50}), hornblende and epidote. Accessory minerals are titanite, sulfides and carbonate.

At the southern end of the TSZ a distinctly layered rhyolitic pyroclastic schist is encountered at Rättävuori (site 42). Thin (cm scale) layers of fine-grained anthophyllite-cordierite rock occur in the SW part of the outcrop (site 45). The sequence is crosscut by mafic dykes and a pegmatite.

A rhyolitic metatuffite (site 44), southeast of Lake Komujärvi probably belongs to the zone of schists extending from Ruotanen to Rättävuori. This zone is penetrated and brecciated by quartz diorites and granodiorites.

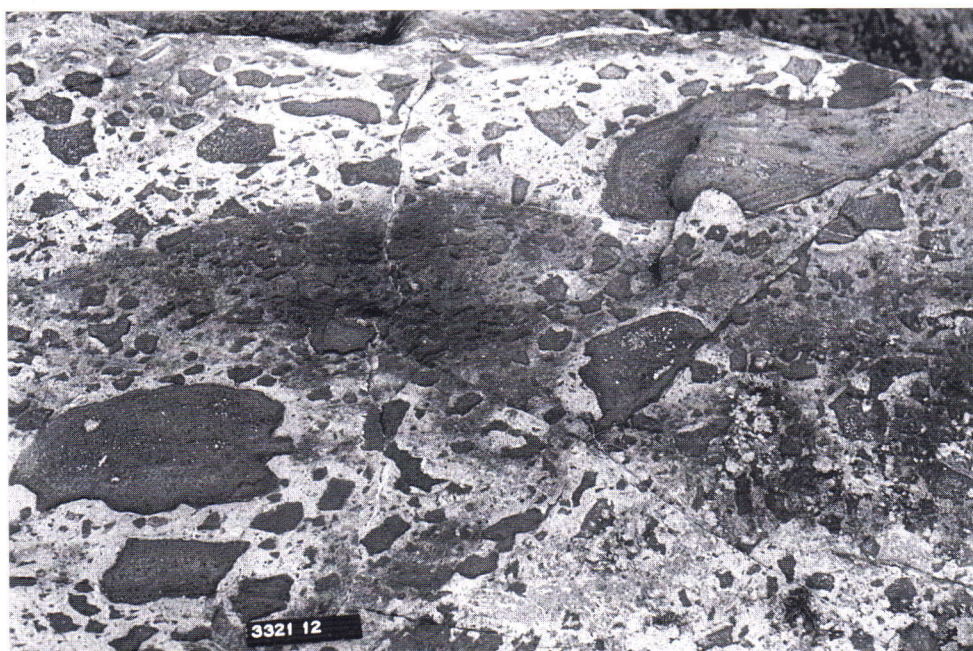


Fig. 2. Basaltic pillow breccia at Tetrinmäki, Pyhäjärvi. Length of code bar 15 cm. x=7069.17, y=3458.96.

Ruotanen Schist Zone

The heterogeneous Ruotanen Schist Zone (RSZ), immediately east of Lake Pyhäjärvi, can be correlated lithologically with the metavolcanic rocks of the TSZ. A high degree of hydrothermal alteration is typical of the RSZ. Large and small-scale tectonic features in the RSZ indicate isoclinal folding, with axial planes trending N-S, which causes repetition of lithologic units from west to east.

Weakly deformed pillow lavas of basaltic andesite composition occur about 1 km SW of the Pyhäsalmi



Fig. 3. Schistose felsic pyroclastic rock 4 km S-SE from the Pyhäsalmi mine, Topiskonrämpe, Pyhäjärvi. Length of paper 15 cm. $x=7059.95$, $y=3454.70$.

mine (analysis 29). The pillows are 10-50 cm in diameter and the interstitial material between the pillows contains some disseminated pyrite. A basaltic pillow lava also occurs at a railroad cut in the Pyhäsalmi mine area (site 6). The pillows are deformed into long ribbons or lenses, and the lava - together with the other pillow lava in the RSZ - is thought to be part of the older (bimodal) volcanic sequence. The deformed basaltic-andesitic lavas of the mine area are represented by analysis 28. Other basaltic and basaltic-andesitic rocks of the mine area, both lavas and pyroclastic rocks, are documented by analyses 9, 20 and 27.

Basalts similar to those of the RSZ and rhyolitic metavolcanic rocks occur SE of the Pyhäsalmi mine (sites 3 and 5). In spite of complex deformation, their original lava and pyroclastic structures are easily recognized.

The volcanic rocks of the RSZ are intensely altered around the Pyhäsalmi ore deposit (Helovuori 1979, Mäki 1986). Within the hydrothermal alteration zone there are sericite schists, sericite quartzites, garnet-cordierite-biotite gneisses, cordierite-anthophyllite rocks and talc-chlorite schists. The felsic volcanic rocks contain thin tremolitic layers. The original rock type was mainly pyroclastic rhyolite; however, some quartz porphyries may have been lavas. Layering, accentuated by amphibolitic bands, is visible on weathered surfaces. In places the rock contains lapilli. The main minerals in the rhyolitic rocks are quartz and oligoclase, which occur occasionally as phenocrysts a few millimeters in diameter (analyses 38, 46 and 49).

The amphibolites consist of cummingtonite- and hornblende-bearing layers, but intermediate volcanics are absent. The felsic metavolcanics in the mine area are associated with sericite schists and sericite quartzites, which also are present in the RSZ south of the ore deposit. The felsic rocks SE of the mine are predominantly pyroclastic, but massive quartz porphyries (Fig. 3, site 40) occur as well. Mafic dykes intrude all these rock types.

WESTERN VOLCANIC SEQUENCE

Pyhäjärvi mica gneiss formation

The mica gneiss formation W and NW of Lake Pyhäjärvi consists of metagraywacke which is partly migmatitic and contains abundant garnet and sillimanite. Rare mafic metavolcanic intercalations occur within the metagraywacke (see Marttila 1993).

On an island in Lake Pyhäjärvi (sites 1 and 2) uralite porphyry rocks occur that are proposed here to be of volcanic origin. The diffuse contact zone between a pyroclastic and lava-like layer can be seen at this outcrop. The pyroxene pseudomorphs (in places partly preserved) are 5-7 mm in size. The groundmass consists of pale green hornblende and

labradorite (An_{60}). Plagioclase is partly scapolitized, and calcite occurs as a secondary accessory mineral. The chemical composition of the rock is suggestive of picritic basalt (analyses 1 and 2, Table 1).

A strongly deformed basaltic lava occurs in a road cut which is intercalated with a mica gneiss (site 10). It deviates from the other volcanics in the area due to its high MgO content (12.65%) and K_2O/Na_2O ratio (2.27). Main minerals are tremolite-actinolite and biotite. Plagioclase occurs as a secondary accessory mineral.

Valkeuslampi Schist Zone

The N-S trending Valkeuslampi Schist Zone (VSZ) can be traced some 10-15 km between the Väätinperä granodiorite (west) and Pyhäjärvi mica gneiss (east; see Fig. 1). The contact between the Väätinperä granodiorite and the VSZ volcanic rocks is highly tectonized. The VSZ consists of reddish, strongly tectonized pyroclastic schists which are andesitic-dacitic in composition (analyses 34 and 36). In places amphibolitic interlayers occur. The rock is porphyritic, with abundant plagioclase phenocrysts ca. 5 mm in diameter. To the south more mafic varieties, such as uralite porphyrite of pyroclastic origin (sites 4 and 18) and basaltic-andesitic metatuff (site 24) are present. A similar metatuff also occurs

on an island in Lake Pyhäjärvi (site 31).

Volcanic conglomerate and pyroclastic breccia occur at Eskoperä, about 10 km NW of the Pyhäsalmi sulfide mine. The heterogeneous fragments, comprising mafic, intermediate and felsic metavolcanic rocks and a variety of gneisses, are 10-15 cm in size. Some of the fragments are angular, while others are more rounded or oval. The clasts are densely packed (clast-supported), fine pyroclastic material filling the interstices. The volcanic rock is intruded by a reddish porphyritic syenite. Fine-grained, banded hornblende-labradorite tuff schists (site 15) in the southern part of the deposit also contain lapilli tuff layers.

Matarankallio Schist Zone

The Matarankallio Schist Zone is a volcanic unit SE of Lake Pyhäjärvi (sites 25, 35, 21, and 30) containing mainly mafic and intermediate tuffaceous schists with rare primary pyroclastic breccia structures. The metavolcanics are folded isoclinally with fold axes plunging gently S. West of this zone, a sillimanite gneiss has been intersected in drill holes, and graphitic gneisses occur between these two rock

units.

Diopside-tremolite skarns, garnet-bearing mica gneisses, and cordierite-biotite rocks as well as cordierite-anthophyllite rocks occur at Matarankallio. Intermediate and mafic metatuffs (site 26) are accompanied by minor felsic metatuffites. The zone curves eastwards and also contains occasional volcanic rocks (amphibolites and hornblende gneisses).

STRATIGRAPHY AND AGE OF THE VOLCANIC ROCKS

Figure 4 depicts the stratigraphic positions of the metavolcanic rocks in the Pyhäjärvi area. The oldest volcanic rocks, belonging to the Eastern Volcanic Sequence (EVS), lie upon a complex called the Kettuperä granodioritic gneiss, which consists of both para- and orthogneisses. Some age data for the Pyhäjärvi area were published by Helovuori (1979), with the Kettuperä gneiss registering the oldest U-Pb zircon age (1930 ± 15 Ma) in the area. Metavolcanic rocks at the Pyhäsalmi mine, belonging to the Ruotanen Schist Zone, have a whole rock Pb-Pb age of 1909 ± 27 Ma. The whole rock trend passes within experimental error through the Pb isotopic composition of the ore, thus supporting a common origin for the ore and its country rocks.

The EVS is overlain by gneissic metasediments which locally contain appreciable amounts of graphite. However, black schists proper are not encountered in these metasediments.

The EVS and the gneissic metasediments are overlain by rhyodacitic-dacitic and commonly porphyritic volcanics, the Western Volcanic Sequence (WVS), which have been documented from the Valkeuslampi and Matarankallio areas and northern part of Jokelaisneva. The stratigraphic scheme in Fig. 4 is interpretative because the contacts between the above mentioned lithological sequences, ob-

served in the field and/or in airborne magnetic graytone maps, are highly tectonized by shearing or thrusting.

Field observations suggest that the basement complex, the EVS and the sedimentogenic gneisses are crosscut and brecciated by a granodiorite - diorite suite. The Jusko granodiorite, representing these rocks, had previously yielded a U-Pb age of 1894 ± 2 Ma (Helovuori 1979). Clasts of similar quartz dioritic rocks have been encountered in a polymictic conglomerate at Settijärvi, 30 km NW from Pyhäsalmi, underlying or intercalated with the WVS (Marttila 1987). These upper metasediments and metavolcanics are crosscut by diabase and felsic porphyry dykes, and they are also intruded by a porphyritic granite suite.

The youngest magmatic rock found by Helovuori (1979) was an almost undeformed plagioclase-phyric rock, with a zircon Pb-Pb age of 1876 Ma. This age was regarded as the minimum age of the emplacement of the rock.

The present study aimed at placing further temporal constraints on the tectonic evolution and volcanism in the Pyhäjärvi area. Thus both the EVS (A1121 - Riitavuori) and the WVS (A1126 - Vasikkakallio) were sampled. The analysis of the Jusko granodiorite (A834) was enhanced by one abraded fraction, and four other granitoids were analyzed from the area (A1120 - Jänismäki, A1122 - Pieni Asikkamäki, A1123 - Hoikanlampi and A1125 - Vuohomäki). An attempt to determine the time of sedimentation was made from a mafic portion (dyke?) in the paleosome of a migmatitic rock at Hoikanlampi (A1124). The quartz-feldspar porphyries intersecting the WVS and the Väätinperä granodiorite were sampled at Jauhokangas (A1127). Unfortunately neither the suspected dyke at Hoikanlampi (A1124) nor the felsic volcanic rock from Vasikkakallio (A1126) yielded sufficient amounts of zircon for a reliable U-Pb age determination.

The results of the U-Pb analyses are presented in Table 2. The results are graphically presented in Fig. 5. A detailed consideration of the results suggests that:

1) The Riitavuori quartz porphyry (A1121), with an age of 1921 ± 2 Ma, is the oldest rock in the present sample material and the three fractions behave "normally", i.e. the abraded fraction is the most concordant one while the lightest fraction is the most discordant. The uranium contents increase as discordancy increases. An interesting feature is the relatively high content of ^{208}Pb , which suggests a high Th/U ratio in the source of this rock.

2) The revised age of the Jusko granodiorite (A834) is 1886 ± 9 Ma, which is consistent with other

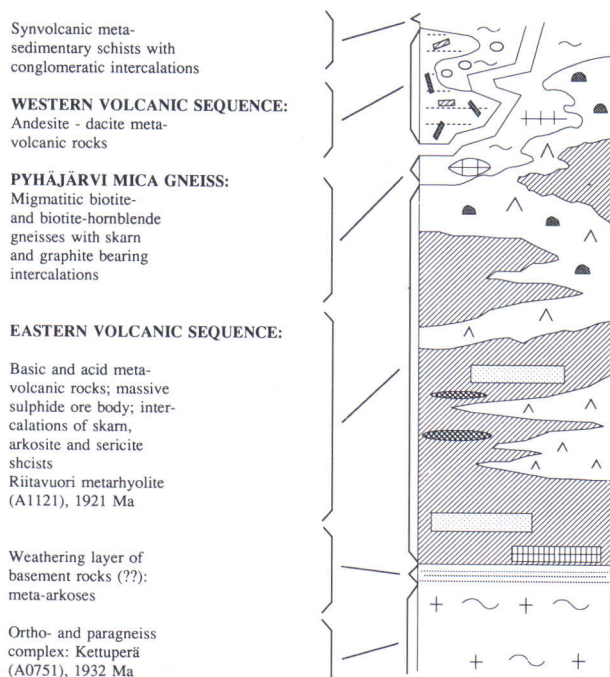


Fig. 4. Schematic stratigraphic column (not to scale) of the rocks in the Pyhäjärvi area.

Table 2. U-Pb mineral data from igneous rocks in the Pyhäjärvi area.

Sample	Fraction	Uconc ppm	Pbconc ppm	206/204 meas.	206/238 Corrected	207/235 for blank	206/207	Apparent age in Ma 6/8	7/5	7/6
A486-Pyhäsalmi amphibolite										
A	Titanite	44.6	15.39	1196	.3209	4.945	.1118	1793	1809	1828
A500-Pyhäsalmi quartz porphyry										
A	Total	277.7	88.17	1073	.2943	4.635	.1142	1663	1755	1867
A620-Pyhäsalmi plagioclase porphyrite										
A	Titanite	65.2	21.88	1564	.2948	4.601	.1132	1665	1749	1851
A536-Kettukallio porphyritic granite										
A	4.3-4.6, >150 μm	527.0	183.80	332	.2904	4.497	.1123	1643	1730	1837
B	4.3-4.6, 70-150 μm	443.6	139.80	4208	.3056	4.775	.1133	1718	1780	1853
C	4.2-4.3, HF	654.8	195.97	4810	.2951	4.628	.1137	1667	1754	1859
D	4.2-4.3, 70-150 μm	720.2	219.80	1212	.2900	4.511	.1129	1641	1733	1845
E	4.2-4.3, HF	669.8	204.72	5485	.3012	4.719	.1136	1697	17701	1858
F	4.0-4.2	942.1	275.26	2001	.2852	4.416	.1123	1617	1715	1837
G	4.0-4.2, HF	814.9	253.19	4831	.3067	4.804	.1136	1724	1785	1857
A751-Kettuperä granitic gneiss										
A	+4.2, >150 μm	355.5	99.95	6624	.2631	4.202	.1159	1505	1674	1893
B	+4.2	495.7	126.63	7381	.2422	3.839	.1150	1398	1600	1879
C	4.0-4.2	830.2	171.80	5520	.1976	3.061	.1124	1162	1423	1838
A834-Jusko quartz diorite										
A	+4.2, >150 μm	210.6	73.13	4784	.3204	5.087	.1152	1791	1834	1882
B	+4.2, 70-150 μm	361.7	118.65	3551	.3053	4.825	.1146	1717	1789	1873
C	4.0-4.2, >70 μm	805.7	253.91	1615	.2920	4.589	.1140	1651	1747	1864
D	Titanite	95.9	38.53	383	.3157	4.961	.1140	1768	1812	1863
E	+4.2, abraded	166.2	61.02	5566	.3363	5.338	.1151	1868	1874	1882
A1120-Jänismäki granodioritic gneiss										
A	+4.5, abraded	135.9	48.85	19058	.3364	5.326	.1149	1869	1873	1878
B	+4.5, >150 μm	200.4	63.19	5935	.2972	4.638	.1132	1677	1756	1851
C	4.3-4.5, >150 μm	338.8	90.73	4270	.2535	3.930	.1125	1456	1619	1839
D	4.2-4.3, >70 μm	695.3	182.05	1769	.2433	3.730	.1112	1403	1577	1818
E	Titanite	227.7	116.52	331	.3160	4.886	.1122	1769	1799	1834
A1121-Riitavuori felsic volcanic rock										
A	4.3-4.5, abraded	383.8	141.59	23981	.3381	5.480	.1175	1877	1897	1919
B	4.3-4.5	422.9	147.58	12911	.3209	5.185	.1172	1794	1850	1913
C	4.2-4.3	571.6	186.82	11900	.2998	4.831	.1169	1690	1790	1909
A1122-Pieni Asikkämäki porphyritic granite										
A	4.0-4.2, >150 μm	1388	424.38	8306	.2964	4.599	.1126	1673	1749	1841
B	4.0-4.2, 70-150 μm	594.1	193.42	4962	.3112	4.813	.1122	1746	1749	1841
C	+4.5, abraded	218.5	73.47	8087	.3218	5.064	.1141	1798	1830	1866
D	+4.5	265.4	81.17	6145	.2936	4.581	.1132	1659	1745	1850
E	4.3-4.5, clear	407.2	115.16	5524	.2699	4.185	.1125	1540	1671	1839
F	4.3-4.5, dark	615.7	193.35	10164	.3063	4.786	.1133	1722	1782	1853
A1123-Hoikanlampi granitic gneiss										
A	+4.5	181.2	63.24	5739	.3315	5.226	.1144	1845	1856	1869
B	4.3-4.5, needles	481.4	158.41	2400	.3121	4.915	.1142	1751	1804	1867
C	4.3-4.5, rounded	476.9	152.54	7594	.3111	4.870	.1135	1746	1796	1856
A1124-Hoikanlampi amphibolite										
A	Titanite	183.8	61.36	1530	.3225	4.905	.1103	1802	1803	1804
A1125-Vuotomäki porphyritic granite										
A	4.0-4.2, <150 μm	1136	333.44	2685	.2814	4.390	.1131	1598	1710	1850
B	3.8-4.0, >150 μm	1713	425.86	1777	.2357	3.613	.1112	1364	1552	1818
C	4.2-4.3, abraded	770.5	253.40	4008	.3147	4.952	.1141	1763	1811	1866
D	4.2-4.3, >70 μm	787.7	246.55	3162	.2979	4.664	.1136	1680	1760	1857
E	4.2-4.3, >150 μm	696.9	214.98	4040	.2969	4.650	.1136	1675	1758	1857
A1127-Jauhokangas quartz-feldspar porphyry										
A	4.3-4.5, abraded	409.3	139.83	3056	.3176	4.991	.1140	1777	1817	1863
B	4.3-4.5	469.6	145.93	2409	.2878	4.495	.1133	1630	1730	1863
C	4.2-4.3	679.4	195.93	2217	.2681	4.156	.1125	1530	1665	1839
D	4.0-4.2, 70-150 μm	1036	274.48	2052	.2474	3.801	.1114	1424	1592	1823

Concentrations in μg/g. Common lead correction: ²⁰⁶Pb/²⁰⁴Pb 15.15; ²⁰⁷Pb/²⁰⁴Pb 15.15; ²⁰⁸Pb/²⁰⁴Pb 34.9.

data from syntectonic granitoid intrusions of the Svecokarelian orogeny.

3) The Jänismäki granodioritic gneiss (A1120), in contrast, is younger with an age of 1876 ± 15 Ma. The four analyzed fractions yielded a normal pattern of U content with respect to discordancy, and as the zircons exhibit a simple tetragonal prism-pyramid morphology, there is little doubt that the measured age represents the primary formation of this mineral. Moreover, because the abraded fraction (A) is nearly concordant, it is unlikely that the age of this rock exceeds 1885 Ma. A similar result was obtained from the granodioritic gneiss at Hoikanlampi (A1123).

4) The porphyritic granites at Pieni Asikkamäki (A1122) and at Vuohomäki (A1125) record zircon U-Pb ages of 1867 ± 12 Ma and 1875 ± 2 Ma, respectively. Thus they date the late tectonic phase at

approximately 1875 Ma in the Pyhäjärvi area.

5) The quartz-feldspar porphyry dyke at Jauhokangas (A1127), intersecting the granodioritic rock of Väätinperä (correlative with the Jusko granodiorite), registers an age 1874 ± 5 Ma which, in view of the normal discordancy pattern of the zircons as well as their simple morphology, must be regarded as a true crystallization age of the rock.

6) Titanite from A834 - Jusko granodiorite - has a $^{207}\text{Pb}/^{206}\text{Pb}$ age of 1867 Ma, which sets a minimum for either the formation or the closure of this mineral, and probably marks the regional cooling through the 500°C isotherm. A similar result was also obtained for titanite from the granodioritic gneiss at Jänismäki (A1120) while titanite from the amphibolite at Hoikanlampi (A1124) is much younger, with an age of 1803 Ma.

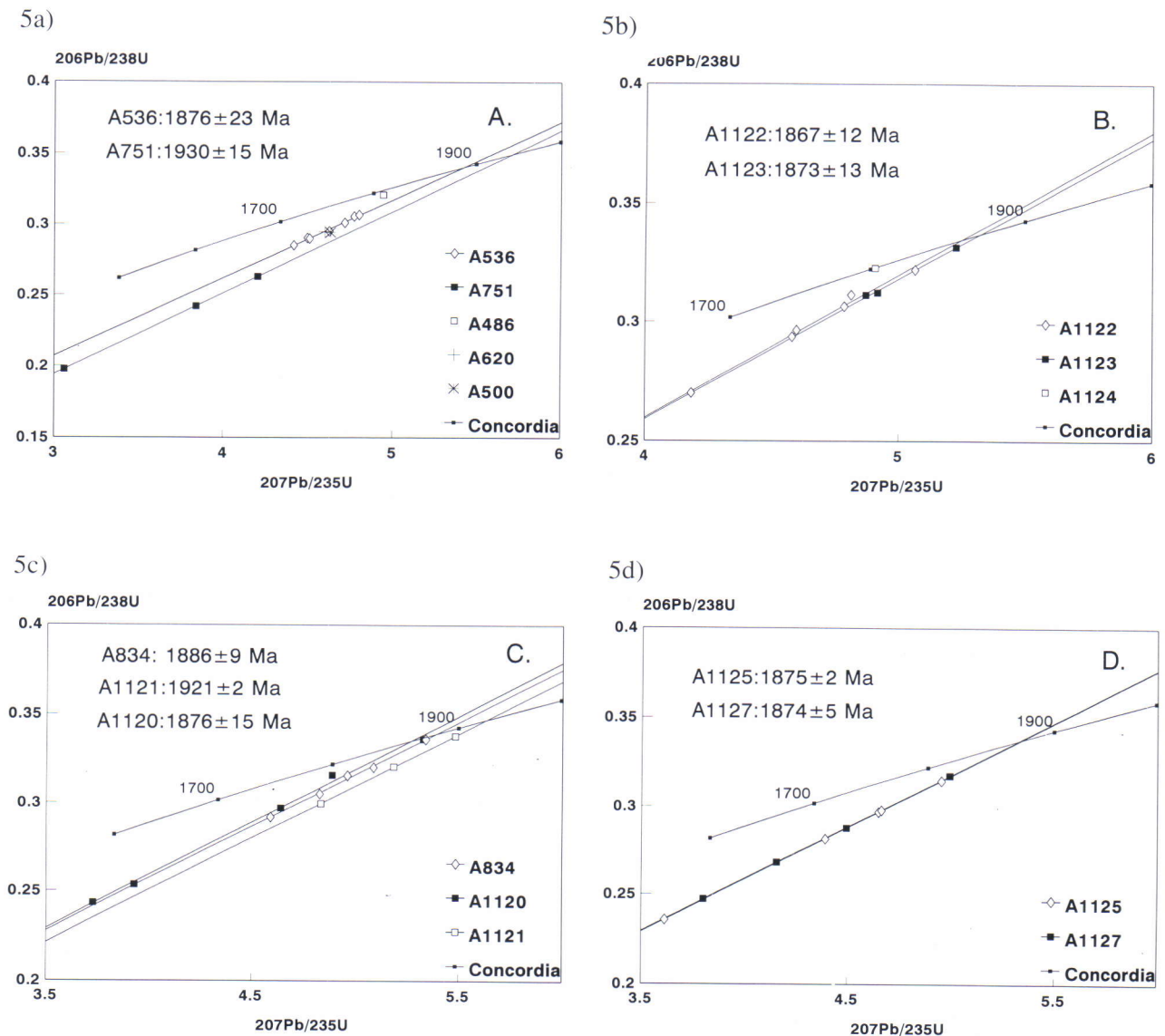


Fig. 5. U-Pb results of zircons and titanites from the Pyhäjärvi area. A. A536 - Kettukallio porphyritic granite, A751 - Kettuperä granitic gneiss, A486 - Pyhäsalmi amphibolite, A620 - Pyhäsalmi plagioclase porphyrite. B. A1122 - Pieni Asikkamäki porphyritic granite, A1123 - Hoikanlampi granitic gneiss, A1124 - Hoikanlampi amphibolite. C. A834 - Jusko quartz diorite, A1120 - Jänismäki granodioritic gneiss, A1121 - Riitavuori felsic volcanic rock. D. A1125 - Vuohomäki porphyritic granite, A1127 - Jauhokangas quartz-feldspar porphyry.

GEOCHEMISTRY

Alteration, postmagmatic hydrothermal activity, polyphase deformation, metamorphism up to medium-grade amphibolite facies conditions and related retrograde processes hamper the interpretation of geochemical results in the Pyhäjärvi area. For example the alteration zone around the Pyhäsalmi sulfide ore can be recognized from changes in certain elemental concentrations up to several hundred meters away from the contact of the ore (Mäki 1986, Mäkelä et al. 1987). Because of postmagmatic events, the samples of this study were chosen to represent the least altered compositions as possible.

Special attention was paid to the geochemistry of the less mobile elements (e.g. Pearce & Cann 1973). Davies et al. (1978) used the ternary $\text{MgO}/10\text{-CaO}/\text{Al}_2\text{O}_3\text{-SiO}_2/100$ diagram to evaluate alteration in

magmatic rocks. On this diagram, the samples studied are within the field of unaltered magmatic rocks (Fig. 6 a and b), suggesting that pronounced alteration has not occurred. However, Figs. 6 c and d show that the dispersion of the present data is considerable and spreads beyond the range of the igneous spectrum defined by Hughes (1973). Moreover, these diagrams show the compositional diversity of the EVS and the WVS, revealing in particular the bimodal nature and "spilitization" of the WVS (Fig. 6 b and d). In general, the Na content of the felsic metavolcanics in the WVS is relatively high compared to K content (Table 1). This keratophyric property may be attributed to hydrothermal activity during ore formation. The elevated K content in some samples could arise from regional alteration

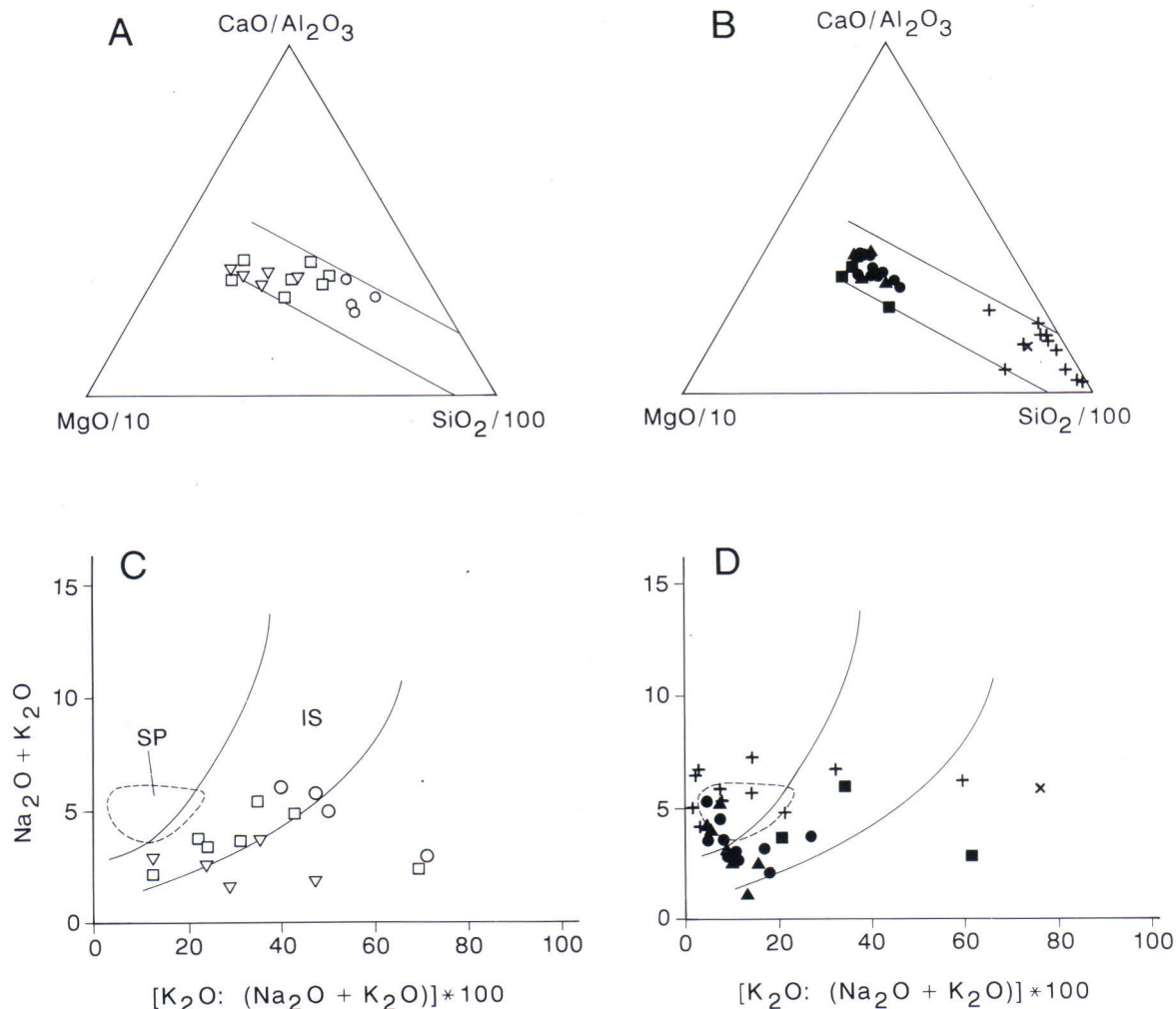


Fig. 6. Geochemical discrimination diagrams for the Pyhäjärvi metavolcanic rocks. A and B after Davis et al. (1978; the field between the solid lines in the diagram represents unaltered rocks), C and D after Hughes (1973; IS = igneous spectrum, SP = spilites). Figs. A and C represent the Western Volcanic Sequence (symbols: open square = mafic volcanic rock; open triangle = uraltite porphyrite; open circle = intermediate volcanic rock). Figs. B and D represent the Eastern Volcanic Sequence (symbols: black dot = mafic volcanic rock; black square = mafic high-K volcanic rock; black triangle = pillow lava; cross = felsic volcanic rock).

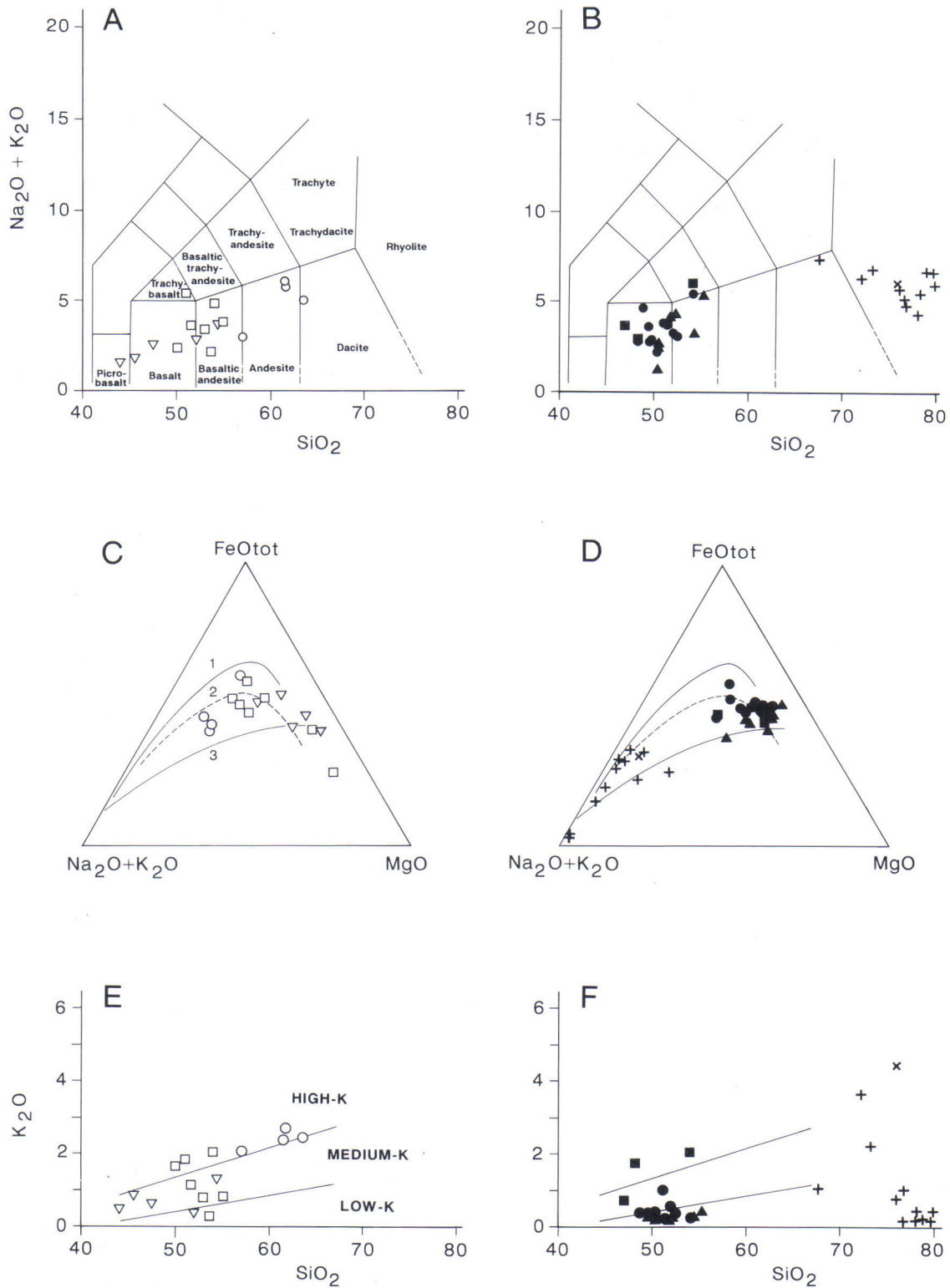


Fig. 7. Geochemical discrimination diagrams for the Pyhäjärvi metavolcanic rocks. The classification scheme of the total alkali vs. silica diagram (Figs. A and B) is after LeBas et al. (1986). The numbered trends in the AFM diagrams (Figs. C and D) also give a crude definition of the maturity of island arcs: 1) immature island arcs (Brown 1982); 2) discrimination line between tholeiitic (upper field) and calc-alkaline (lower field) volcanics (Irvine & Baragar 1971); 3) mature island arcs (Brown op cit.). The fields in the K_2O/SiO_2 diagram (Figs. E and F) are based on Ewart (1982) and Kähkönen (1989). Figs. A, C and E represent the Western Volcanic Sequence and Figs. B, D and F the Eastern Volcanic Sequence. Symbols as in Fig. 6.

during the intrusion of younger granitoids, although samples of this kind were avoided.

In the total alkali vs. silica diagram, the majority of the metavolcanic rocks of the WVS (Fig. 7a) form a continuous series from basalts to andesites, without a major compositional gap, while the EVS metavolcanics (Fig. 10b) comprise a bimodal association of basalts, basaltic andesites and rhyolites (see also Mäki 1986). Both the WVS and EVS metavolcanics represent subalkalic magmas.

On the AFM diagram the WVS rocks (Fig. 10c) display a calc-alkaline trend, but also show Fe enrichment typical of a tholeiitic trend. The dispersion is probably in part due to the cumulate nature of the uraltite and/or plagioclase -phyric lava varieties. If cumulates of thick lava flows are considered to be the reason for Fe-Mg variation, the WVS as a whole could represent a calc-alkaline magma series. The petrographic data available for the samples analyzed from the WVS is, however, too limited to solve this problem.

Mafic members of the EVS also have a tholeiitic affinity, although the most altered varieties among the pillow lavas resemble calc-alkaline rocks on the AFM diagram (Fig. 7d). On the other hand, the felsic metavolcanic rocks of the EVS have a distinct calc-alkaline affinity.

The WVS and EVS clearly form separate trends on the K_2O vs. SiO_2 diagram despite of a certain amount of dispersion in both sequences. Most of the WVS rocks show an increase in K_2O with increasing SiO_2 content, and they can be considered to belong to medium- to high-K varieties of calc-alkaline magma

series (Fig. 10e). The EVS metavolcanics have low K contents compared to the WVS rocks (Fig. 7f). A few EVS samples (marked as filled square and cross symbols in Fig. 7f) nevertheless resemble the WVS sequence rocks and might thus be correlated to them. Two of the EVS felsic samples showing medium- to high-K nature probably record secondary potassium increase due to hydrothermal alteration.

The chondrite-normalized REE distributions (Fig. 8) clearly discriminate between the WVS and EVS metavolcanic rocks. The total REE content of the mafic rocks is approximately twice as high in the WVS as in the EVS, although in both cases the pattern has the same slightly enriched LREE shape, with the $(La/Yb)_N$ ratio varying between 2 and 3. The intermediate WVS rocks show a marked LREE enrichment and have HREE patterns identical with those of the mafic members, indicating that they may be comagmatic. Notable exceptions to this general WVS chemistry include the rocks at Lokinkivi (analyses 1 and 2 in Table 1 and solid line in Fig. 8a) which are considered to represent a discrete magmatic event.

The bimodal nature of the EVS metavolcanics can also be seen in the REE patterns (Fig. 8b). Felsic members display marked LREE enrichment and flat HREE with a negative Eu anomaly while mafic rocks show a gently sloping trend. The two exceptions in Fig. 8b are samples of felsic tuffaceous metavolcanics at Topiskonrämpe and Liittoperä whose stratigraphic position is ambiguous (analyses 40 and 43 in Table 1; solid and dashed lines respectively in Fig. 8b). It is even possible that these samples belong to the WVS.

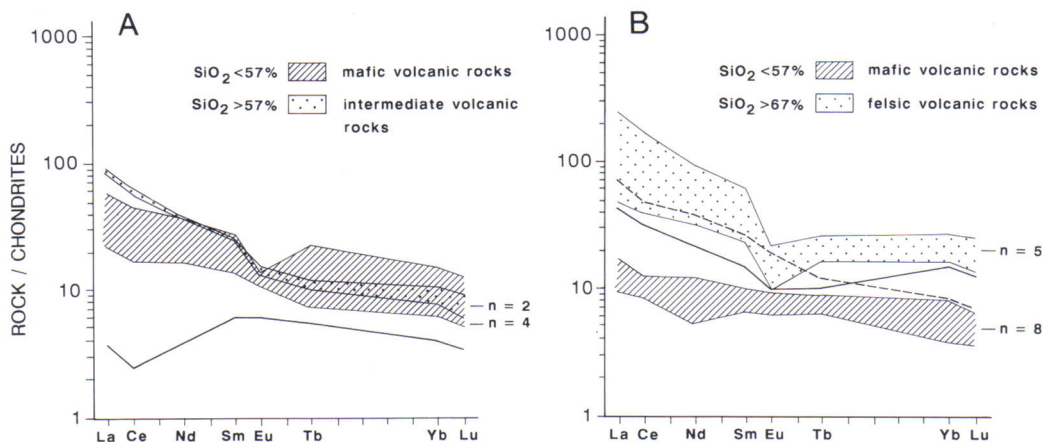


Fig. 8. REE patterns for Pyhäjärvi metavolcanic rocks. A: Western Volcanic Sequence. The solid line corresponds to sample 1 in Table 1. B: Eastern Volcanic Sequence. The solid line and dotted lines represent samples 40 and 43 in Table 1, respectively. n = number of analyzed samples. Normalization values after Hickey & Frey (1982).

TECTONOMAGMATIC AFFINITIES

With the help of selected major and trace elements an attempt has been made to relate the metavolcanic rocks in the Pyhäjärvi area to tectonomagmatic settings. The results for various diagrams are conflicting, but they do allow the inference of paleoenvironments to some extent. We emphasize that as the diagrams have been generated using data for modern volcanics, their tectonomagmatic significance for Precambrian rocks is not fully understood, and the fields depicting different tectonic regimes are used here mainly for reference.

The WVS and EVS cannot easily be separated from each other on major component diagrams. The AFM diagrams (Fig. 7 c and d) show a transitional affinity between immature and mature volcanic arc systems. Both sequences have $\text{Fe}_2\text{O}_3^{\text{tot}}/\text{MgO}$ ratios close to those of the arc tholeiite trend (Fig. 9 a and

b). On the $\text{MgO}/\text{FeO}^{\text{tot}}/\text{Al}_2\text{O}_3$ plot (Fig. 9 c and d) the basaltic andesite rocks of both WVS and EVS have characteristics of orogenic environments. EVS analyses disperse also in the field of OFB and MORB which in this case might simply indicate their more primitive nature compared to the WVS rocks. Trace element relations for selected immobile components confirm the results of major element discrimination diagrams. The samples of WVS and EVS rocks closely resemble recent arc volcanics when examined on the Ti/Zr plot (Fig. 10). Furthermore, the $\text{Zr}/\text{Ti}:100/\text{Sr}:2$ diagram (Fig. 11) more clearly discriminates between the WVS and EVS mafic metavolcanic rocks, so that the former can be classified mainly as calc-alkaline basalts while the latter resemble low-K tholeiites. Felsic members among both sequences have the La/Yb distribution close to the arc field (Fig. 12).

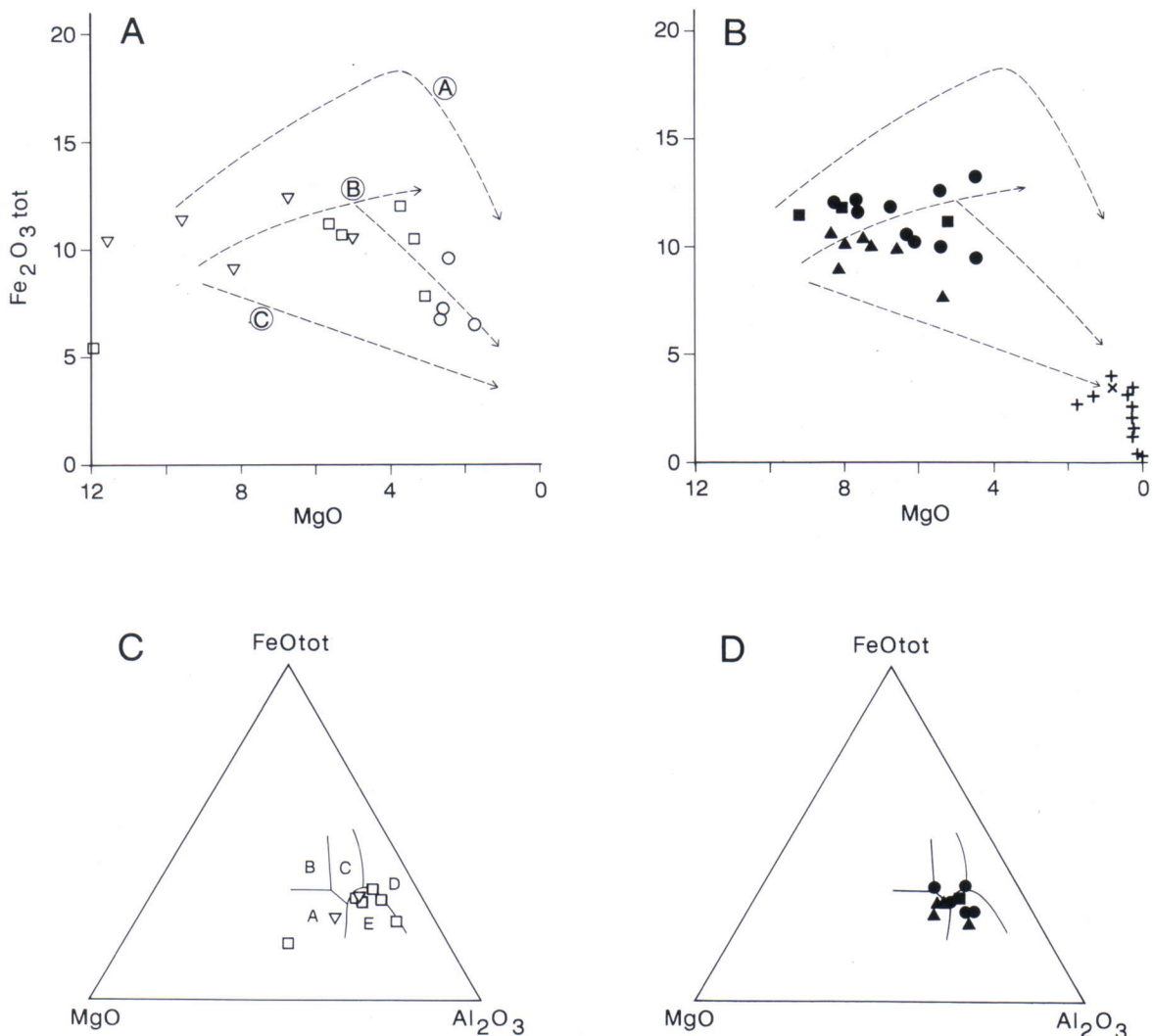


Fig. 9. Tectonomagmatic discrimination diagrams for the Pyhäjärvi metavolcanic rocks. Trend lines in Figs A and B after Pharaoh & Pearce (1984): A = ocean and continental tholeiites; B = island arc tholeiites; C = island arc calc-alkaline rocks. Figs. C and D: $\text{MgO}/\text{FeO}^{\text{tot}}/\text{Al}_2\text{O}_3$ diagram for basaltic andesites ($\text{SiO}_2 = 51\text{-}56$ wt %); fields after Pearce et al. (1977): A = ocean ridge and floor; B = ocean island (intra-plate); C = continental; D = spreading centre island (inter-plate); E = orogenic (island arcs and active continental margins). Figs. A and C represent the Western Volcanic Sequence and Figs. B and D the Eastern Volcanic Sequence. Symbols as in Fig. 6.

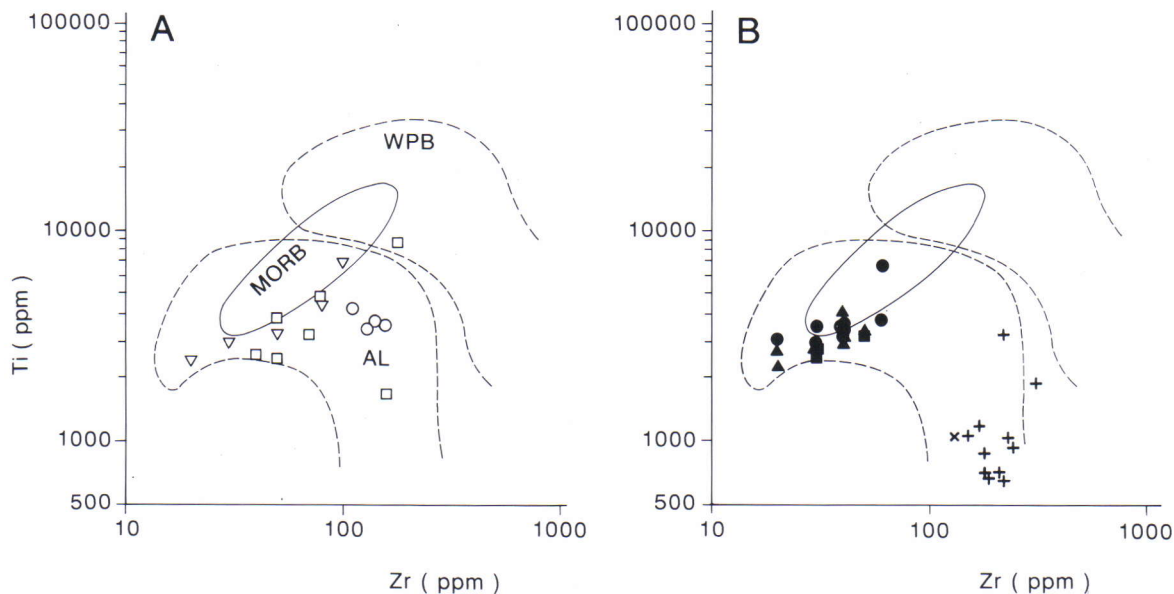


Fig. 10. Ti/Zr diagram for the Pyhäjärvi metavolcanic rocks. Fields after Pearce (1982): MORB = mid ocean ridge basalts; WPB = within plate basalts; AL = arc lavas. Fig. A represents the Western Volcanic Sequence and Fig. B the Eastern Volcanic Sequence. Symbols as in Fig. 6.

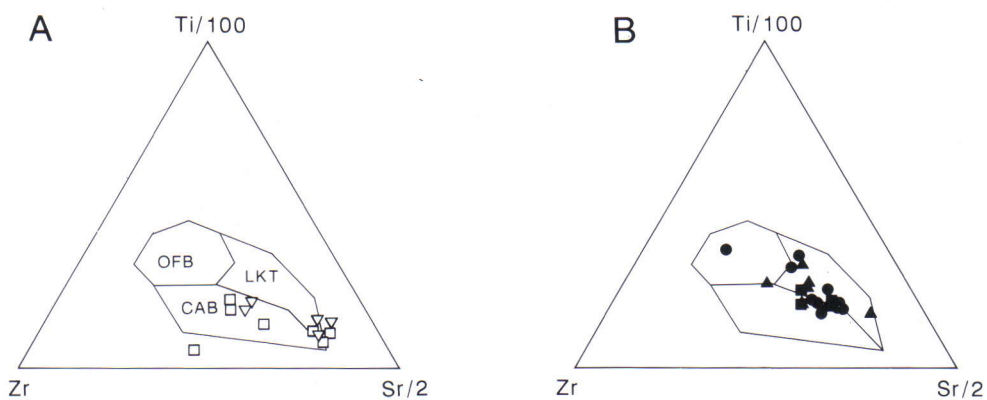


Fig. 11. Zr/(Ti:100)/(Sr:2) diagram for the Pyhäjärvi metavolcanic rocks. Fields after Pearce and Cann (1973): OFB = ocean floor basalts; LKT = low-K tholeiites (island arc tholeiites); CAB = calc-alkaline basalts (island arc basalts). Fig. A represents the Western Volcanic Sequence and Fig. B the Eastern Volcanic Sequence. Symbols as in Fig. 6.

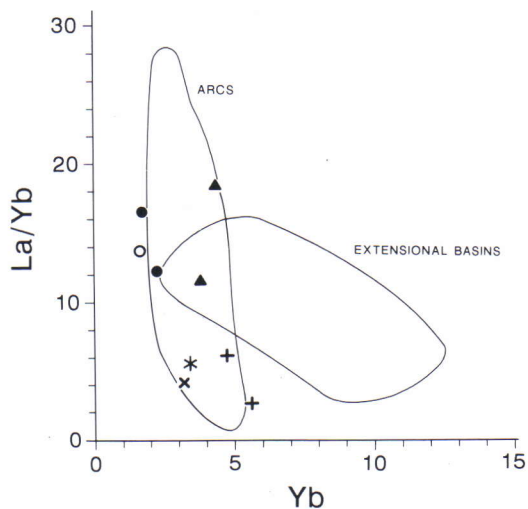


Fig. 12. La:Yb/Yb diagram of felsic metavolcanic rocks from Pyhäjärvi (after Condie 1986). Symbols: black circle = analyses 35 and 36 (Western Volcanic Sequence); black triangle = analyses 37 and 47 (Eastern Volcanic Sequence); open circle = analysis 43; * = analysis 42 (Eastern Volcanic Sequence); x = analysis 40; + = analyses 38 and 46 (Eastern Volcanic Sequence).

DISCUSSION

The volcanic activity of the EVS is only slightly younger than the 1930 Ma age, registered by the granodioritic gneiss at Kettuperä. The quartz porphyry at Riitavuori (A1121) yielded a zircon age of 1921 ± 2 Ma which is consistent with the Pb-Pb whole rock age of 1909 ± 27 Ma for the volcanic rocks in the Pyhäsalmi mine area (Helovuori 1979). In view of the fact that the 1930-1915 Ma granitoid intrusion event is fairly widespread in the Ladoga - Bothnian Bay zone (Vaasjoki & Sakko 1988) and that preliminary Sm-Nd data indicate these rocks to be primarily mantle-derived material (Huhma & Lahtinen 1993), the Kettuperä gneiss should be considered the basement of the EVS. Consequently, and bearing in mind the normal discordancy pattern of the zircon from the Riitavuori porphyry, the age obtained should be considered the age of the volcanic activity.

Within the Finnish part of the Fennoscandian shield geological observations suggest that rocks of the EVS are analogous to the nearby Kiuruvesi area in their stratigraphy (Marttila 1976, 1981). Within the Ladoga - Bothnian Bay zone, both granitoid and volcanic rocks of similar age have also been encountered elsewhere (Korsman et al. 1984, Vaasjoki & Sakko 1988, Nironen & Front 1992). The WVS, on the other hand, resembles the supracrustal rocks at Pihtipudas (Aho 1979), about 40 km SW of Pyhäjärvi, and the Kuusaanjärvi formation (Kousa 1990), 40 km NW of Pyhäjärvi. The volcanic rocks at Pihtipudas (Aho 1979), W and SW of Pyhäjärvi, can be timed close to the syntectonic intrusive phase of 1890-1875 Ma (Vaasjoki & Sakko 1988).

A probable hypabyssal counterpart for the WVS is the plagioclase porphyry in the Pyhäsalmi mine area, with a total zircon fraction $^{207}\text{Pb}/^{206}\text{Pb}$ age of 1875 Ma, representing a minimum emplacement age (Helovuori 1979). Hence, the WVS may be considerably younger than the EVS. Titanite ages mostly at 1870-1860 Ma from the plutonic rocks probably indicate the cooling of the terrain to temperatures below 500°C . However, some titanites both at Pyhäjärvi and at Pihtipudas register ages around 1800 Ma, which could be related to block uplift phenomena. Haudenschield (1988, 1990) interpreted block uplift to have reset mica K-Ar and whole rock Rb-Sr ages along the Ladoga - Bothnian Bay zone.

Within the bimodal EVS there are two small areas (Topiskonrämpe and Tetrinmäki) whose mafic components deviate slightly from the basalts of the "ordinary" bimodal sequence. At Topiskonrämpe the metabasalts (analyses 3, 5, and 9 in Table 1) are massive and in places amygdaloidal. They differ in composition from other EVS samples, especially in their higher potassium content and thus resemble

rocks of the WVS.

The other problem concerns the Tetrinmäki pillow lavas. According to the schematic stratigraphic column (Fig. 4), these metabasalts represent the uppermost supracrustal unit of the whole study area. This conclusion is based only on the observation (Marttila 1993) that the pillow structures are well-preserved in the Tetrinmäki basalts unlike the other mafic lavas of the bimodal system. On the other hand, the contacts of the Tetrinmäki lavas are covered by soil and thus the stratigraphic position of these lavas remains questionable. The chemical compositions of the Tetrinmäki pillow basalts do not differ from other mafic metavolcanic rocks of the EVS which probably therefore favor a genetic relationship between these rocks.

Exhalative-hydrothermal volcanism with concomitant sulfide ore formation and related tectono-metamorphic processes have caused alteration of the local rock types. Thus tuffaceous felsic volcanics underwent potassic and sericite alteration and in subsequent metamorphism became sericite quartzites or sericite schists and, similarly, mafic volcanics were altered into cordierite, garnet and anthophyllite rocks and talc-cordierite schists. These are encountered in the vicinity of the Pyhäsalmi mine and around minor sulfide occurrences at Tetrinmäki, Lohvanperä, Maaselänlahti and Hulanperä.

Lithologically the rocks in the Pyhäjärvi area bear some resemblance to the well-known Skellefte area in northern Sweden (Lundberg 1980, Claesson 1985, Vivallo 1987, Vivallo & Claesson 1987, Vivallo & Wildén 1988). The Skellefte volcanics are situated within the boundary zone between the Paleoproterozoic Bothnian basin and the Archean craton (interpreted to be covered by Proterozoic rocks). According to Lundberg (1980) the Skellefte group proper consists of basal rhyolitic-andesitic volcanic rocks and minor basaltic lavas. These are overlain by a turbiditic graywacke-pelite unit of the Bothnian basin with minor intercalated ultramafic volcanics (Nilsson 1986). The upper part of the Skellefte group consists mainly of basaltic rocks with minor sedimentary interlayers and an uppermost felsic volcanic unit. The older, bimodal volcanic sequence (EVS) at Pyhäjärvi resembles the volcanic rocks of the Skellefte group because the lower units in both areas are mainly felsic and the upper units basaltic in composition. The metaturbidites and associated ultramafic metavolcanic rocks of the Skellefte district could also be correlative with some remnants of mica schist with high magnesium basaltic rock intercalations in the Lamminaho area, which are termed here as the Pyhäjärvi mica gneiss formation.

Vivallo and Wildén (1988) concluded that the volcanic rocks in the Skellefte area represent an arc system related to subduction, associated with collision of an oceanic and a continental plate. Sporadic tensional processes led to rifting of the arc and the development of a sedimentary basin containing mafic volcanic rocks. On the basis of their chemical composition, it seems that the older volcanic rocks at Pyhäjärvi are more primitive than those of the Skellefte group, and thus represent volcanism at the early stages of arc formation. This is in conflict with the conclusion of Gaál (1990) that volcanism at the Vihanti - Pyhäsalmi district represent a mature island arc developed on Paleoproterozoic oceanic island arc. It is instead considered more likely that the EVS mafic volcanics are an early, mantle-derived part of the proposed oceanic island arc system. The felsic volcanics represent partly remobilized Paleoproterozoic crust having the same source as some 1930 Ma old tonalitic to granodioritic gneissose rocks of the Ladoga - Bothnian Bay zone. Solving the problem of the origin and nature of the basement to the supracrustals of the EVS needs much more detailed work than was possible during the course of this study.

The metavolcanic rocks of the Skellefte group belong compositionally to a calc-alkaline magma

series (Claesson 1985) or have slightly tholeiitic to calc-alkaline differentiation trends (Vivallo & Claesson 1987). At Pyhäjärvi, the volcanic rocks of the EVS can be divided into two different groups in which the mafic volcanics exhibit a distinct tholeiitic signature while the felsic members are calc-alkaline. The WVS is a scattered zone of metavolcanic rocks which probably has a calc-alkaline differentiation affinity. However, whereas the tectonic activity in the Pyhäjärvi area terminated soon after the syntectonic phase (most titanite ages at ca. 1860 Ma), the Skellefte area was intruded and the supracrustal rocks deformed by the Revsund granites about 1790 Ma ago (Skiöld 1988). Moreover, despite many similarities in lithology in the Pyhäjärvi and Skellefte areas there is a distinct difference in the age of volcanism. In the Skellefte area the age group 1930-1920 Ma is unknown. Also, there is a difference in the ore lead isotopic composition between the Ladoga - Bothnian Bay zone in Finland and the Skellefte area in Sweden (Vaasjoki & Vivallo 1990). Further, the seismic refraction data suggest that the observed depression of the Moho boundary in the Ladoga - Bothnian Bay zone has no continuation below the Skellefte area (Luosto 1991). Thus, in spite of many similarities, the Pyhäjärvi and Skellefte areas cannot be considered to be identical.

CONCLUSIONS

The main results for the metavolcanic rocks studied from the Pyhäjärvi area are:

1. According to field observations the metavolcanic rocks represent two sequences which differ from each other lithologically and stratigraphically. The older Eastern Volcanic Sequence (EVS) is bimodal consisting of mafic and felsic members, while the younger Western Volcanic Sequence (WVS) is a compositionally variable series of mafic to intermediate metavolcanics.

2. The age of the EVS is proposed here to be only slightly younger than the oldest rock yet dated in the area (1930 Ma). The U-Pb dating of zircon from a quartz porphyritic rhyolite at Riitavuori gives the age of 1921 ± 2 Ma.

3. The age group 1890-1865 Ma consists mainly of

granitoids and diorites, but gneissose granodiorites and felsic porphyry dykes exist in this group as well. The WVS may be the volcanic equivalent of these rocks.

4. In their chemical composition the mafic metavolcanics of the EVS are low-K tholeiitic basalts and basaltic andesites while the felsic intercalations have a calc-alkaline nature, suggesting a different petrogenesis for the mafic and felsic members of the bimodal EVS. In contrast, the metavolcanic rocks of the WVS resemble modern calc-alkaline magma series.

5. The mafic metavolcanics of the EVS resemble recent primitive island arc tholeiites in their chemical composition while the metavolcanic rocks of the WVS have a more mature arc affinity.

ACKNOWLEDGEMENTS

Dr. Kauko Meriläinen was the primus motor for this study. The study was financed by the Academy of Finland via IGCP Project 179 and the Geological Survey of Finland. Prof. Heikki Papunen, Dr. Yrjö Kähkönen and Dr. Mikko Nironen made critical and

fruitful comments that improved the manuscript. Ms. Anni Vuori made the drawings. Dr. Peter Sorjonen-Ward checked the English. Our warm thanks to all these persons.

REFERENCES

- Aho, L. 1979.** Petrogenetic and geochronological studies of metavolcanic rocks and associated granitoids in the Pihtipudas area, central Finland. *Geol. Surv. Finland, Bull.* 300, 22 p.
- Brown, G.C. 1982.** Calc-alkaline intrusive rocks: their diversity, evolution, and relation to volcanic arcs. In: Thorpe, R.S. (ed.) *Andesites, Orogenic Andesites and Related Rocks*. Chichester: John Wiley & Sons, 437-461.
- Claesson, L.-Å. 1985.** The geochemistry of early Proterozoic metavolcanic rocks hosting massive deposits in the Skellefte district, northern Sweden. *J. Geol. Soc. Lond.* 142, 899-909.
- Condie, K.C. 1986.** Geochemistry and tectonic setting of Early Proterozoic supracrustal rocks in the southwestern United States. *J. Geol.* 94, 845-864.
- Davis, A., Blackburn, W.H., Brown, W.R. & Ehmann, W.D. 1978.** Trace element geochemistry and origin of late Precambrian - early Cambrian Catoclin greenstones of the Appalachian Mountains. Univ. Calif., Davies, Calif. (unpubl. report)
- Ekdahl, E. 1993.** Early Proterozoic Karelian and Svecofennian formations and the evolution of the Raahe-Ladoga Ore Zone, based on the Pielavesi area, central Finland. *Geol. Surv. Finland, Bull.* 373, 137 p.
- Ewart, A. 1979.** A review of the mineralogy and chemistry of Tertiary-Recent dacitic, latitic, rhyolitic and related salic volcanic rocks. In: Barker, F. (ed.) *Trondhjemites, Dacites and Related Rocks*. Amsterdam: Elsevier, 13-121.
- Gaál, G. 1990.** Tectonic styles of Early Proterozoic ore deposition in the Fennoscandian Shield. *Precambrian Res.* 46, 83-114.
- Haudenschild, U. 1988.** K-Ar age determination on biotite and muscovite in the Pihtipudas-Iisalmi and Joroinen areas, eastern Finland. *Geol. Surv. Finland, Bull.* 343, 33-50.
- Haudenschild, U. 1990.** Cooling history of the eastern Svecofennian: whole-rock and mica Rb-Sr and hornblende K-Ar ages in the areas of Pihtipudas-Iisalmi and Joroinen-Sulkava, Finland. *Bull. Geol. Soc. Finland* 62, 39-59.
- Helovuori, O. 1979.** Geology of the Pyhäsalmi ore deposit, Finland. *Econ. Geol.* 74, 1084-1101.
- Hickey, R.L. & Frey, F.A. 1982.** Geochemical characteristics of boninite series volcanics: implications of their source. *Geochim. Cosmochim. Acta* 46, 2099-2115.
- Hughes, C.J. 1973.** Spilites, keratophyres and the igneous spectrum. *Geol. Mag.* 109, 513-527.
- Huhma, H. 1986.** Sm-Nd, U-Pb and Pb-Pb isotopic evidence for the origin of the early Proterozoic Svecofennian crust in Finland. *Geol. Surv. Finland Bull.* 337, 52 p.
- Huhma, H. & Lahtinen, R. 1993.** Isotopic studies on early Svecofennian crust. In: IGCP-275, Symposium on The Svecofennian Domain, Abstracts, Turku 23.-25.8.1993, 28.
- Huhtala, T. 1979.** The geology and zinc-copper deposits of the Pyhäsalmi-Pielavesi district, Finland. *Econ. Geol.* 74, 1069-1083.
- Huhtala, T., Mäkelä, T. & Rauhamäki, E. 1978.** Vihannin-Pyhäsalmien alueen sinkkimalmien vulkaanis-stratigrafinen asema. In: Laatokan-Perämeren malmivyöhyke symposio 16.2.1978, Vuorimiesyhdistys-Bergmannaföreningen, 111-120. (in Finnish)
- Irvine, T.N. & Baragar, W.R.A. 1971.** A guide to the classification of the common volcanic rocks. *Can. J. Earth Sci.* 8, 523-548.
- Kähkönen, Y. 1989.** Geochemistry and petrology of the metavolcanic rocks of the early Proterozoic Tampere schist belt, southern Finland. *Geol. Surv. Finland, Bull.* 345, 107 p.
- Karvinen, A. 1978.** Kiuruveden Niemisjärvi-Honkaperävyöhykkeen geologiasta ja kiisuesiintymistä. M.Sc. thesis, Univ. Turku, 111 p. (unpublished, in Finnish)
- Koivula, S. 1987.** Pyhäjärven (Ol.) alueen mafiset, intermediaariset ja felsiset juonikivet. M.Sc. thesis, Univ. Turku, 105 p. (unpublished, in Finnish)
- Korsman, K., Hölttä, P., Hautala, T. & Wasenius, P. 1984.** Metamorphism as an indicator of evolution and structure of the crust in eastern Finland. *Geol. Surv. Finland, Bull.* 328, 40 p.
- Kousa, J. 1990.** Paleoproterozoic metavolcanic rocks in the border zone of Savo and Pohjanmaa, Central Finland. In: Kähkönen, Y. (ed.) *Symposium Proterozoic Geochemistry, Helsinki '90: December 13-14, 1990 Helsinki, Finland: abstracts*. IGCP Project 217 Proterozoic Geochemistry. Univ. Helsinki, 29-30.
- Le Bas, M.J., Le Maitre, R.W., Streckeisen, A. & Zanettin, B. 1986.** A chemical classification of volcanic rocks based on the total alkali-silica diagram. *J. Petrol.* 27, 745-750.
- Lundberg, B. 1980.** Aspects of the geology of the Skellefte field, northern Sweden. *Geol. Fören. Stockholm Förh.* 102, 156-166.
- Luosto, U. 1991.** Moho depth map of the Fennoscandian shield based on seismic refraction data. In: *Proceedings of the 2nd Workshop on Investigation of the Lithosphere in Fennoscandian Shield by Seismological Methods*. Institute of Seismology, Univ. Helsinki, Report S-25.
- Mäkelä, M., Kuronen, U. & Mäki, T. 1987.** Syvämalminetsintä ja geokemia. *Geologi* 39, 180-184. (in Finnish)
- Mäki, T. 1986.** Litho-geochemistry of the Pyhäsalmi zinc-copper-pyrite deposit, Finland. In: *Prospecting in Areas of Glaciated Terrain*. 7th Int. Prospecting in areas of glaciated terrain symposium, Sept. 1-2, 1986 Kuopio, Finland. IMM, London. 69-82
- Marttila, E. 1976.** Evolution of the Precambrian volcanic complex in the Kiuruvesi area, Finland. *Geol. Surv. Finland, Bull.* 283, 109 p.
- Marttila, E. 1977.** Pre-Quaternary rocks, sheet 3323 Kiuruvesi.

- Geological map of Finland 1 : 100 000.
- Marttila, E. 1981.** Kiuruveden kartta-alueen kallioperä. Summary: Pre-Quaternary rocks of the Kiuruvesi map-sheet area. Explanation to the maps of Pre-Quaternary rocks, sheet 3323. Geological map of Finland 1 : 100 000, 48p.
- Marttila, E. 1987.** Haapajärven Settijärven konglomeraattikerrostuma - prekambriinen kivikkosorakerrostuma. Maa-selkä 24, 8. (in Finnish)
- Marttila, E. 1992a.** Pre-Quaternary rocks, sheet 3321 Pyhäjärvi. Geological map of Finland 1 : 100 000.
- Marttila, E. 1992b.** Pre-Quaternary rocks, sheet 3322 Kärsämäki. Geological map of Finland 1 : 100 000.
- Marttila, E. 1993.** Pyhäjärven kartta-alueen kallioperä. Summary: Pre-Quaternary rocks of the Pyhäjärvi map-sheet area. Explanation to the maps of Pre-Quaternary rocks, sheet 3321. Geological map of Finland 1 : 100 000, 64 p.
- Neuvonen, K.J., Korsman, K., Kouvo, O. & Paavola, J. 1981.** Paleomagnetism and age relations of the rocks in the Main Sulfide Ore Belt in central Finland. Bull. Geol. Soc. Finland 53, 109-133.
- Nironen, M. & Front, K. 1992.** The 1.88 Ga old Mäntylä complex, central Finland: emplacement and deformation of mafic to felsic plutonic rocks and associated Mo mineralization. Bull. Geol. Soc. Finland, 64, 75-90.
- Pearce, J.A. 1982.** Trace element characteristics of lavas from destructive plate margins. In: Thorpe, R.S. (ed.) Andesites, Orogenic Andesites and Related Rocks. Chichester: John Wiley & Sons, 525-548.
- Pearce, J.A. & Cann, J.R. 1973.** Tectonic setting of basic volcanic rocks using trace element analyses. Earth Planet. Sci. Lett. 19, 290-300.
- Pearce, T.H., Gorman, B.E. & Birkett, T.C. 1975.** The TiO_2 - K_2O - P_2O_5 diagram: a method of discriminating between oceanic and non-oceanic basalts. Earth Planet. Sci. Lett. 24, 419-426.
- Pearce, T.H., Gorman, B.E. & Birkett, T.C. 1977.** The relationship between major element chemistry and tectonic environment of basic and intermediate volcanic rocks. Earth Planet. Sci. Lett. 36, 121-132.
- Pharoah, T. & Pearce, J.A. 1984.** Geochemical evidence for the tectonic setting of early Proterozoic metavolcanic sequences in Lapland. Precambrian Res. 25, 283-308.
- Skiöld, T. 1988.** Implications of new U-Pb zircon chronology to early Proterozoic crustal accretion in northern Sweden. Precambrian Res. 38, 147-164.
- Vaasjoki, M. & Sakko, M. 1988.** The evolution of the Raahe-Ladoga zone in Finland: isotopic constraints. Geol. Surv. Finland, Bull. 343, 7-32.
- Vivallo, W. & Claesson, L.-Å. 1987.** Intra-arc rifting and massive sulphide mineralization in an early Proterozoic volcanic arc, Skellefte district, northern Sweden. In: Pharoah, T.C., Beckinsale, R.D. & Rickard, D. (eds.) Geochemistry and Mineralisation of Proterozoic Volcanic Suites. Oxford: Blackwell. Geol. Soc. Spec. Publ. 33, 69-79.
- Vivallo, W. & Willdén, M. 1988.** Geology and geochemistry of an early Proterozoic volcanic arc sequence at Kristineberg, Skellefte district, Sweden. Geol. Fören. Stockholm Förh. 110, 1-12.
- Wilkman, W.W. 1931.** Kivilajikartan selitys, lehti C4 Kajaani. The General Geological Map of Finland. Explanation to the maps of Pre-Quaternary rocks, sheet C4. Geological map of Finland, 1 : 400 000, 247 p. (in Finnish)

GEOCHEMISTRY OF THE PALEOPROTEROZOIC ANDESITIC TO RHYOLITIC ARC-TYPE METAVOLCANIC ROCKS OF HAUKKAMAA, KURU, CENTRAL FINLAND

by
Markku Tiainen and Yrjö Kähkönen

Tiainen, Markku & Kähkönen, Yrjö 1994. Geochemistry of the Paleoproterozoic andesitic to rhyolitic arc-type metavolcanic rocks at Haukkamaa, Kuru, central Finland. *Geological Survey of Finland, Special Paper 19*, 29–44, 14 figures, two tables and one appendix.

The Haukkamaa volcanogenic belt is situated within the 1.89–1.87 Ga old Central Finland Granitoid Complex. The belt is composed of intermediate and felsic rocks. The intermediate rocks are predominantly homogeneous and they may be of subvolcanic, lava or pyroclastic origin. There are also stratified and fragmental pyroclastic rocks showing structures of fallout and pyroclastic flow deposits. The felsic rocks are characterized by massive porphyritic types but they also include fine-grained stratified tuffs. Six zircon fractions from a stratified felsic tuff at Haukkamaa yield a U–Pb age of 1897 ± 2 Ma.

According to the major elements, most of the Haukkamaa volcanics are high-K andesites-rhyolites with calc-alkaline affinities, but some trace elements show characteristics of both high-K and medium-K rocks. LREE show an enrichment over HREE in chondrite-normalized diagrams ($La_N:Yb_N$ ranges from 5 to 11). Pronounced Eu minima are common in felsic rocks. Although a few of the rocks display signs of severe alteration, some conclusions about petrogenesis can be drawn. Fractionation of plagioclase played a major role in the genesis of the rhyolites and the solid assemblage also contained mafic silicates, magnetite, biotite and apatite.

Based on the Ti vs. Zr diagram and the absence of a bimodal frequency distribution of Si, the Haukkamaa volcanics have arc affinities. According to the La/Yb vs. Th diagram, the Haukkamaa andesites resemble andesites of evolved arcs.

Key words (GeoRef Thesaurus, AGI): metavolcanic rocks, andesites, rhyolites, geochemistry, genesis, island arcs, absolute age, U/Pb, Proterozoic, Paleoproterozoic, Haukkamaa, Ruovesi, Kuru, Finland

*Markku Tiainen, Geological Survey of Finland, Betonimiehenkuja 4,
FIN-02150 Espoo, Finland
Yrjö Kähkönen, Department of Geology, P.O. Box 11 (Snellmaninkatu 3),
FIN-00014 University of Helsinki, Finland*

INTRODUCTION

The Paleoproterozoic Svecofennian Domain was formed by mantle-derived crustal growth ca. 1.9 Ga ago and it bears many resemblances to young convergent plate margins (e.g. Hietanen 1975, Huhma 1986, Gaál & Gorbatshev 1987). The supracrustal rocks of the Svecofennian Domain are characterized by turbiditic metasedimentary rocks and basaltic to rhyolitic metavolcanic rocks (written from here on without the prefix meta-). The latter in many instances resemble volcanics of young volcanic arcs in chemical composition, but in places arc affinities are not evident (Latvalahti 1979, Mäkelä 1980, Ehlers et al. 1986, Kähkönen 1987, Vaarma & Kähkönen, this volume).

With regard to supracrustal lithologies, the Svecofennian Domain was divided into three parts by Gaál and Gorbatshev (1987). The Northern and Southern Svecofennian Subprovinces are characterized by volcanic rocks. Instead, the Central Svecofennian Subprovince (CSS) largely comprises graywackes and pelites deposited in a basin which Hietanen (1975) called the Bothnian Basin. The bedrock in the eastern part of the CSS is dominated by the 1.89-1.87 Ga Central Finland Granitoid Complex (CFGC) rich in I-type granitoids (Huhma 1986, Front & Nurmi 1987).

The volcanogenic belt of Haukkamaa is situated in the southern part of the CFGC (Fig. 1). In this paper,

we will discuss depositional types, age, geochemical features, alteration, petrogenesis and tectonomagmatic affinities of the Haukkamaa volcanics.

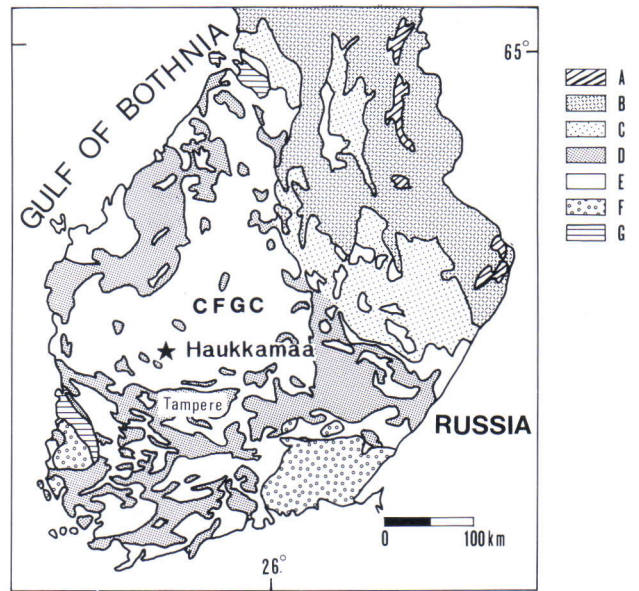


Fig. 1. Geological map of southern and central Finland. Modified from Simonen (1980). A = Archean greenstone belts, B = Archean granitoids, C = Karelian schists, D = Svecofennian schists, gneisses and migmatites, E = Svecofennian plutonic rocks, F = rapakivi granites, G = Jotnian sedimentary rocks. CFGC = Central Finland Granitoid Complex.

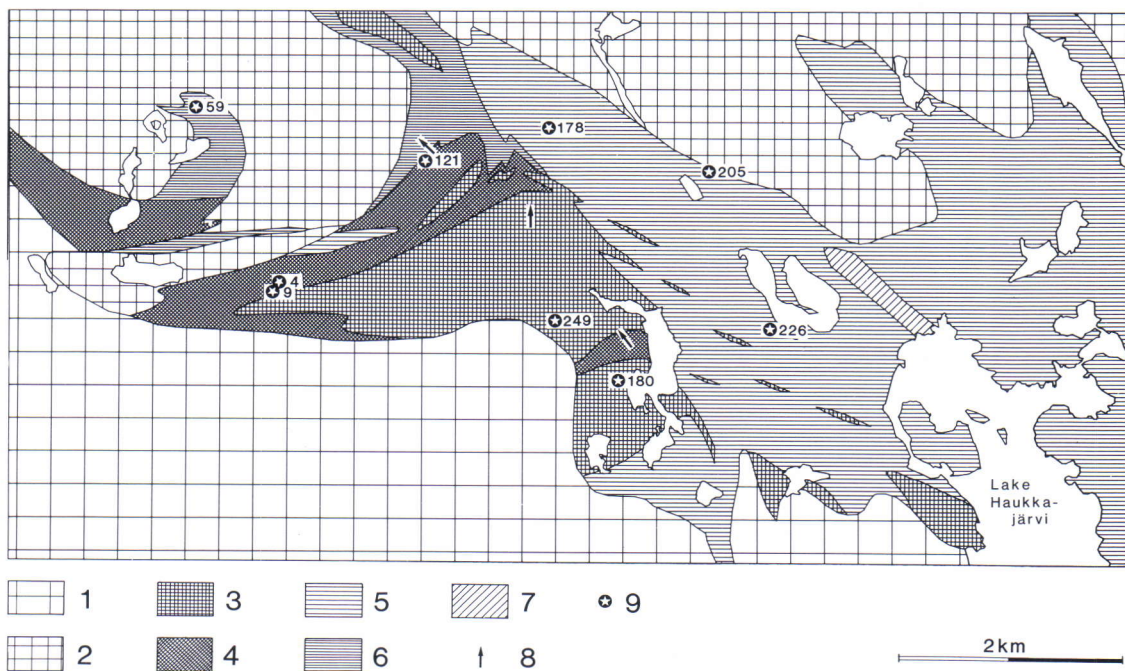


Fig. 2. A simplified lithological map of the Haukkamaa volcanogenic belt, after Matisto (1960) and Tiainen (1983). 1 = granites and granodiorites, 2 = quartz diorites and gabbros, 3 = massive intermediate volcanics, 4 = pyroclastic intermediate volcanics, 5 = fine- to coarse-grained felsic volcanics, 6 = fine-grained stratified felsic volcanics, 7 = conglomerate, 8 = top of strata, 9 = sample location.

PREVIOUS STUDIES AND GEOLOGICAL SETTING

The Haukkamaa belt, which is about 15 km long and 3 km wide, is composed of intermediate to felsic rocks (Fig. 2). The intermediate rocks consist mostly of amphibolites and uralite- and plagioclase-porphyrries which Matisto (1960, 1961) interpreted as pyroclastic and lava rocks. The rocks in the area dominated by felsic rocks were mapped by Sederholm (1903) as felsite schists, while Matisto (1960, 1961) regarded these rocks dyke-like granite porphyries. Bedrock mapping (Tiainen 1983) showed that the intermediate rocks consist of massive porphyritic rocks and of fragmental and stratified pyroclastic rocks. The felsic rocks comprise mainly

massive porphyritic volcanic or subvolcanic rocks but there are also fine-grained, in places stratified tuffs.

The intermediate rocks probably underlie the fine-grained felsic volcanics to the north (Fig. 2). The NE part of the belt, dominated by felsic rocks, may be separated by a NW-SE striking fault from the part rich in intermediate rocks. Notwithstanding that, it is probable that the felsic rocks also in the NE part are younger than the intermediate rocks. The polymictic conglomerate (Fig. 2) contains both intermediate and felsic volcanics as clasts, and it is regarded as the uppermost horizon of the belt.

PRIMARY STRUCTURES AND PETROGRAPHY

The intermediate rocks are dominated by massive or vaguely layered porphyritic rocks, but there are also indisputable pyroclastic rocks with stratified and fragmental structures. It is often difficult to decide whether the massive rocks are lavas, sills or tuffs. Faint layering in some lithologies suggests that some intermediate rocks are pyroclastic.

Indisputable pyroclastic rocks abound in the uppermost part of the succession dominated by intermediate rocks (Fig. 2). They vary in grain size from agglomerates and volcanic breccias to tuffs (Fig. 3). Some strata are evidently fallout deposits but there are also features indicating pyroclastic flows (Figs. 3c-d). Fragments rich in epidote are in places abundant. Because they originally may have been pumice later filled with carbonate (Laitakari 1980), the environments of eruption were possibly in part subaerial. The pyroclastic horizon also contains a unit, about 5 m thick, made up of graded graywackes-siltstones and matrix-supported breccias (Fig. 4). Redeposition is indicated by the breccias containing stratified fragments. The breccia was probably deposited from a debris flow and the graywackes-siltstones from related turbidity currents.

Plagioclase and clinopyroxene (now hornblende) are the most common phenocryst phases in the massive intermediate rocks. Some aggregates comprising mainly biotite exhibit crystal shapes of hornblende and biotite (Fig. 5; Appendix). Thus the phenocrystic assemblage also contained hornblende and biotite. Plagioclase phenocrysts are in part well-preserved andesine grains, but they have been altered

to epidote and sericite to some extent. The granoblastic matrix of the massive rocks consists mostly of quartz, plagioclase, biotite, epidote, and hornblende.

The intermediate rocks of indisputably pyroclastic origin often contain more epidote than the massive rocks. The coarse-grained pyroclastic rocks comprise both crystals (mostly plagioclase) and lithic fragments. Intermediate volcanics and clasts rich in epidote dominate among the lithic fragments but there are also clasts of felsic volcanics.

The felsic rocks are dominated by porphyritic massive types. Phenocrysts of quartz, plagioclase and K-feldspar are fairly abundant. Some biotite aggregates are evidently pseudomorphs of mafic phenocrysts. There are also a few rock fragments. Phenocrysts of quartz and K-feldspar are in part embayed and granulated (Fig. 6). The phenocrysts of plagioclase are commonly fragmental and in part they have been altered to epidote and sericite. The fine-grained granoblastic matrix consists of quartz, plagioclase, K-feldspar and, to a lesser amount, biotite. It is often difficult to decide conclusively whether the massive porphyritic felsic rocks are of volcanic or subvolcanic origin.

The fine-grained felsic rocks are in places stratified and show graded bedding, and a supracrustal origin is evident. They consist mainly of quartz, plagioclase, K-feldspar and biotite. In some samples, there are small phenocrysts of quartz and plagioclase as well as rock fragments. The fine-grained felsic rocks are tuffs, but they may have been redeposited to some extent.

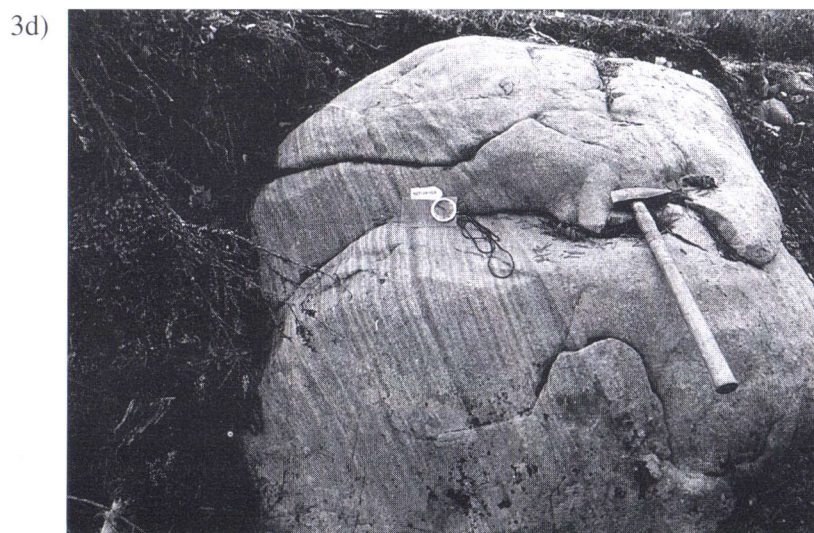
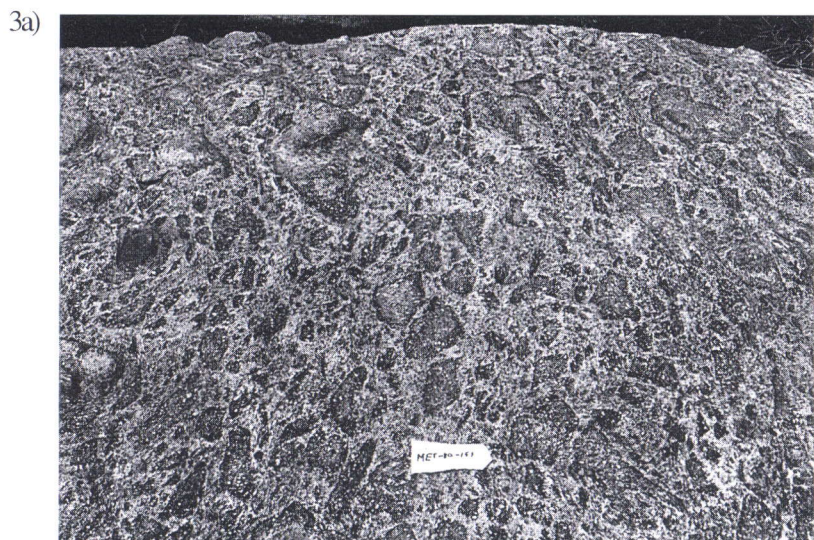


Fig. 3. Pyroclastic structures in the intermediate volcanic rocks at Haukkamaa. **a.** Pyroclastic breccia with intermediate volcanic blocks and some epidote-rich fragments in a matrix of crystal tuff. Length of code paper 10 cm. **b.** Coarse pyroclastics (to the left) grade to laminated strata (to the right). **c.** Strata interpreted to show features similar to those in idealized pyroclastic flow deposits (Sparks et al. 1973, Fisher 1979). Top of strata to the left. The fine-grained basal layer (b1) overlies the stratified precursor fall deposits, no cross bedded ground surge is visible. The pyroclastic flow unit (b2) shows reverse size grading with a horizon (b3) of pumice fragments, presently rich in epidote, at the top. The ash cloud deposit (c) is overlain by fallout tephra (d). **d.** Erosional base of a pyroclastic flow. Length of compass 12 cm.

4a)

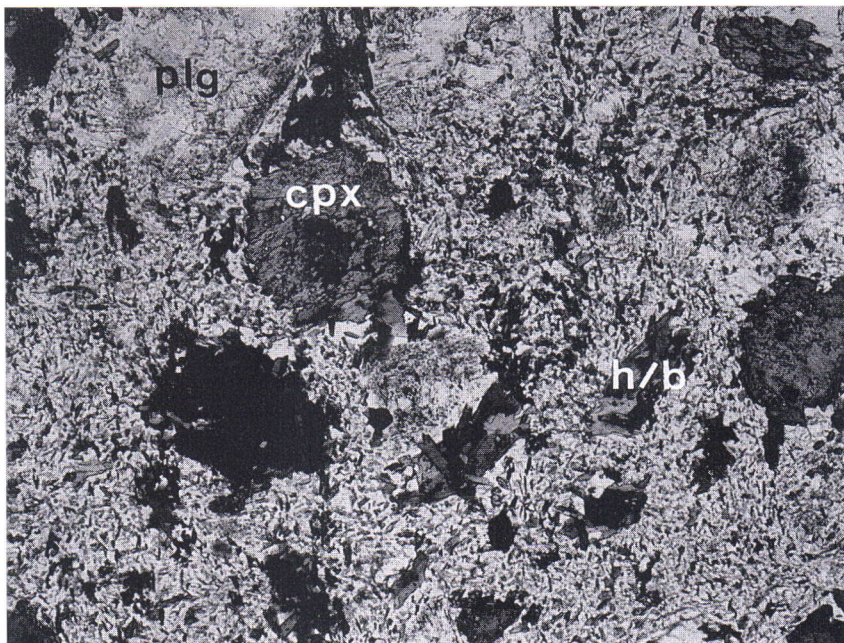


4b)

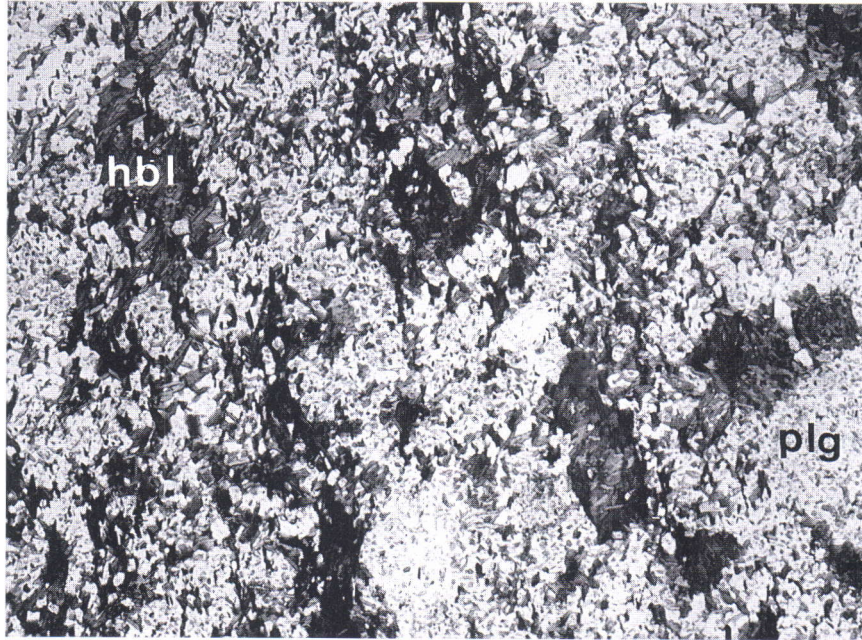


Fig. 4. a) Graded graywacke and siltstone at Haukkamaa. b) Breccia overlying the graywackes of Fig. 4a. Length of code paper 9 cm.

5a)



5b)



5c)

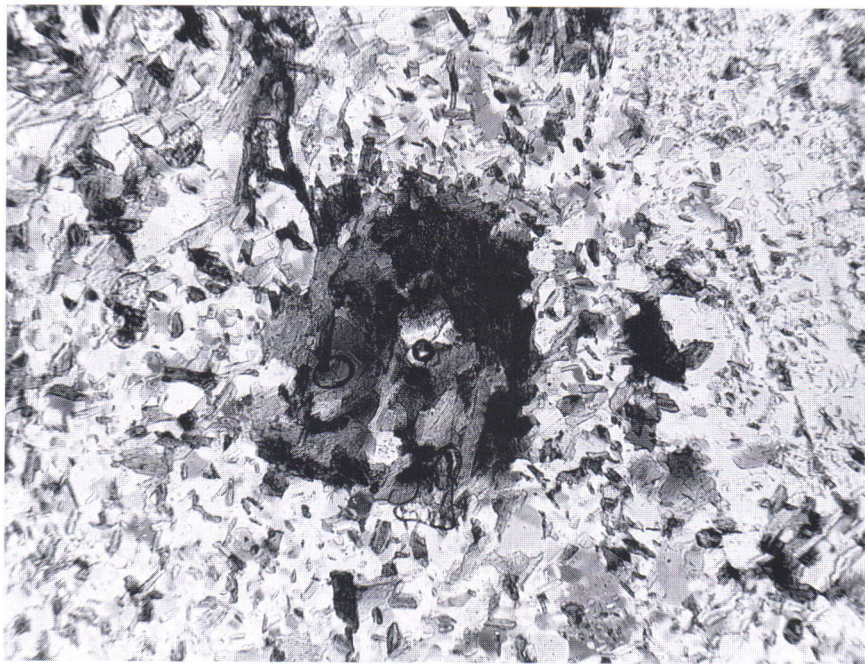
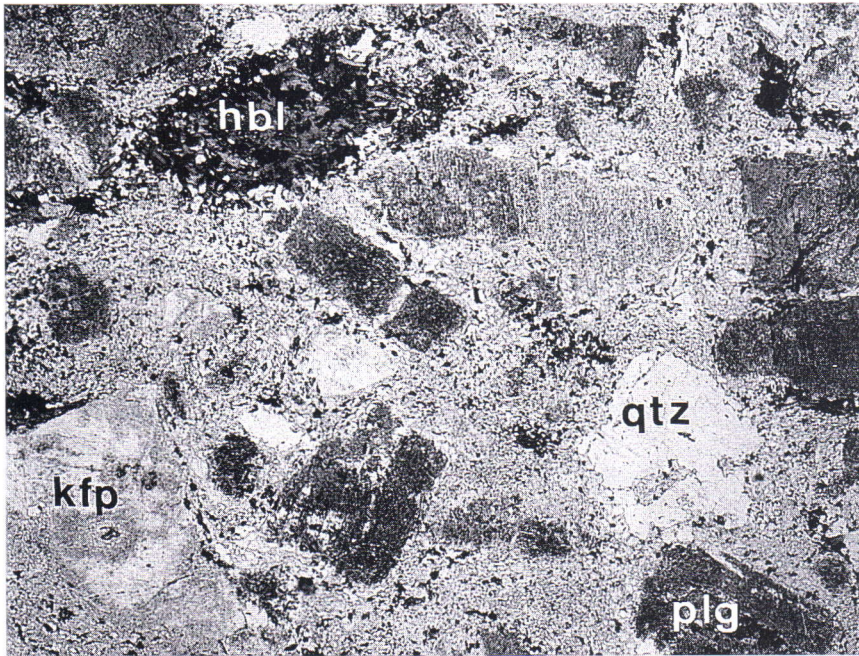


Fig. 5. Photomicrographs of the intermediate rocks at Haukkamaa. Nicols // . **a.** Relics of plagioclase (plg) and pseudomorphs of clinopyroxene (cpx, now hornblende). The aggregates of biotite to the right down (h/b) are pseudomorphs after hornblende or biotite. Sample 249. Field of view 3.7 mm wide. **b.** Biotite aggregates (hbl) with crystal shapes of phenocrystic amphibole. Relics of plagioclase phenocrysts (plg) are visible as pale areas. Sample 180. Field of view 4.7 mm wide. **c.** Biotite aggregate, probably a pseudomorph after phenocrystic mica. Sample 180. Field of view 1.3 mm wide.

6a)



6b)

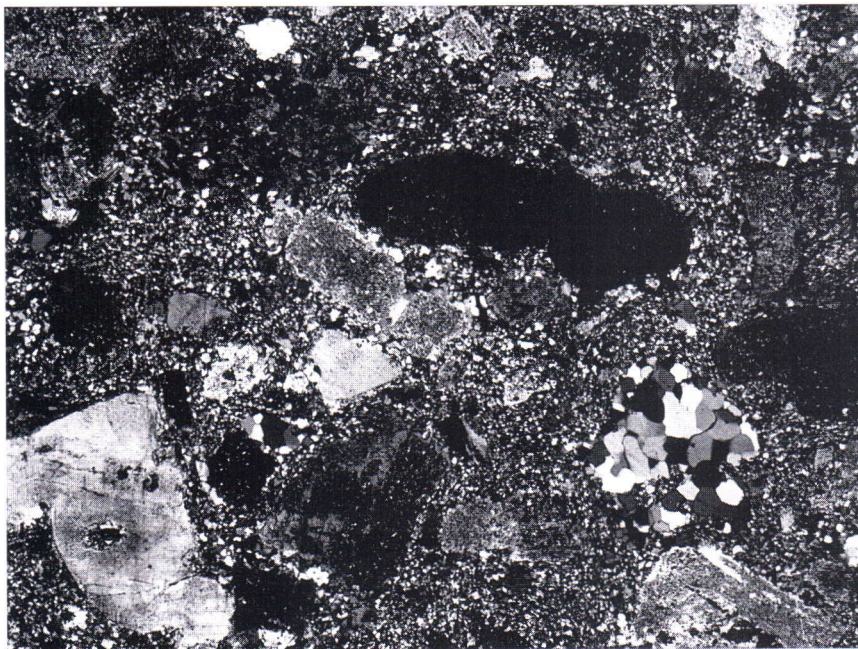


Fig. 6. Photomicrographs of sample 226. Pseudomorphs and relics after phenocrysts of plagioclase (plg), quartz (qtz), potassium feldspar (kfp) and hornblende (hbl, now aggregate of biotite). Quartz and potassium feldspar show embayments. Field of view 4.7 mm wide. **a.** nicols //, **b.** nixols x.

U-Pb ZIRCON AND SPHENE AGES OF THE HAUKKAMAA VOLCANICS

A sample from the outcrop of sample 121 (a crystal tuff) was taken for U-Pb age determinations on zircon and sphene. The zircon grains are mostly translucent but some are brown. Grains with easily visible crystal surfaces and rounded edges dominate. A part of the grains are long, poor in surfaces, and have sharp edges. Well-rounded grains are scarce. A characteristic feature of zircon is the abundance of grains coated with biotite. These features, and the abundance of zircon and sphene suggest that secondary enrichment of the grains is possible (O. Kouvo, pers. comm.). Sphene occurs as two types: as a translucent and euhedral type and as one coated with biotite and plagioclase.

The zircon fractions give an age of 1897 ± 2 Ma (Fig. 7). The very exact regression line indicates that, although secondary enrichment of zircon and sphene is possible, the zircon grains are derived from same sources or from coeval sources. The age is within the 1904-1889 Ma age range of the volcanics of the Tampere Schist Belt (Kähkönen et al. 1989) but is somewhat higher than the 1.89-1.87 Ga zircon ages of the CFGC (Huhma 1986). We interpret the age of 1897 ± 2 Ma to represent the age of volcanism at Haukkamaa.

The translucent sphene fraction B (Table 1) is, with the calculated error limits, concordant with an

age of 1869 ± 11 Ma (the age uncertainty is based on age calculated according to the $^{207}\text{Pb}/^{206}\text{Pb}$ ratio). This age probably reflects recrystallization during regional metamorphism.

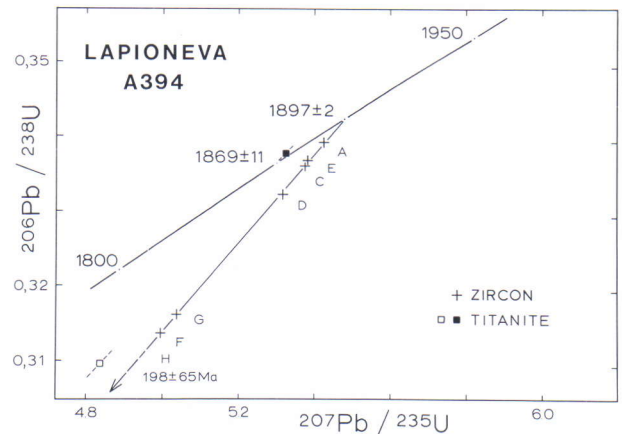


Fig. 7. Concordia plot for zircon and titanite from a tuff near Lapioneva, Haukkamaa. The outcrop of sample 121. The data are from Table 1. The zircon fractions in Table 1 are indicated with A, C, D, E, G and H. Filled square indicates translucent sphene; open square indicates coated sphene. The York (1969) method was used to regress the U-Pb data, and the age uncertainties of the concordia intersections are given at the 2 sigma level.

Table 1. U-Pb isotopic data of sample A394 (the outcrop of sample 121). The determinations were made by Dr. Olavi Kouvo at the Isotope Laboratory of the Geological Survey of Finland. The abrasion of the grains and isotopic measurements were performed following the methods of Krogh (1973). Further details, see Vaasjoki (1977) and Huhma (1986).

Fraction (g/cm ³)	Concentrations (ppm)			206Pb/ 204Pb measured	Isotopic composition of lead 206Pb = 100			Atom ratios and radiometric ages, Ma		
	238U	206Pb	208Pb		204Pb	207Pb	208Pb	206Pb/ 238U	207Pb/ 235U	207Pb/ 206Pb
A $d > 4.5$ abr 6 h	204.1	59.89	25887	.002031	11.625	11.786	.3392 ± 27 1882	5.424 ± 44 1888	.11598 ± 11 1895	
B titanite 3.4 < d < 3.5 translucent	24.5	7.16	314.2	.30946	15.621	24.185	.3377 ± 26 1875	5.324 ± 53 1872	.11435 ± 63 1869	
C 4.3 < d < 4.5 abr 9 h	291.2	84.63	20880	.003256	11.649	12.394	.3360 ± 18 1867	5.375 ± 30 1880	.11605 ± 8 1896	
D 4.2 < d < 4.3 $\phi > 70$ after abr	425.1	122.19	7181	.01278	11.774	13.820	.3322 ± 19 1849	5.314 ± 32 1871	.11601 ± 16 1895	
E 4.2 < d < 4.3 $\phi < 70$ after abr	426.5	124.30	2930	.03290	12.034	15.104	.3368 ± 19 1871	5.383 ± 39 1882	.11590 ± 51 1894	
F 4.0 < d < 4.2 $\phi > 70$ after abr	469.2	127.30	4723	.01977	11.818	13.700	.3136 ± 19 1758	4.994 ± 34 1818	.11551 ± 30 1888	
G 4.0 < d < 4.2 $\phi < 70$ after abr	599.0	163.84	5802	.01604	11.770	15.190	.3161 ± 21 1770	5.036 ± 34 1825	.11554 ± 13 1888	
H titanite abr, anhedral coated with biotite	98.5	26.39	905	.10777	12.788	21.787	.3096 ± 22 1738	4.835 ± 54 1791	.11328 ± 86 1852	

GEOCHEMISTRY

Most of the samples analyzed are subalkaline high-K andesites, dacites and rhyolites with calc-alkaline affinities (Fig. 8). The rocks plot mostly within the igneous spectrum (Fig. 9). Sample 9, an altered host rock of a sulfide mineralization, is a striking exception owing to its low K and Na content.

Although in part dispersed, the increase in K content with increasing Si content as well as the decreases in Al, Ca, Fe, Ti, Mg, Sr, Cr and V with increasing Si are quite coherent. The P contents are higher in the intermediate rocks than in the rhyolitic rocks. In general, the Zr, Th, La, U and Ba contents increase with the increasing Si content, but in the rhyolitic rocks the dispersions are large. The increases in Ba and Zr are less pronounced than those in Th and U. Sample 59, the one highest in Si and Th, is low in Zr and U.

The Haukkamaa samples show LREE-enriched patterns in the chondrite-normalized diagrams such that the chondrite-normalized La (La_N) values are 50-120, Yb_N values 7-17, and $La_N:Yb_N$ ratios 5-11 (Fig. 10; Table 2). Excluding samples 4 and 9, the dacitic and rhyolitic rocks tend to have higher contents of REE than the andesites but the Yb content of sample 59 is relatively low. The dacitic and rhyolitic rocks show Eu minima and sample 59 has the most pronounced Eu minimum. The two samples lowest in

silica, 121 and 180, do not show negative Eu anomalies and the former exhibits a slight Eu maximum. The REE patterns of samples 4 and 9 resemble those of the other Haukkamaa volcanics but sample 9 has the lowest contents for most REE.

A comparison with young andesites-dacites (Ewart 1979, 1982) suggests that the high-K character of the Haukkamaa andesites and dacites is not wholly unequivocal. The Haukkamaa andesites tend to be lower in P than young high-K andesites, and they are more like medium-K andesites in this respect. On the other hand, although young high-K andesites are mostly higher in La (30-90 ppm, Ewart 1982) than the Haukkamaa andesites (17-21 ppm) they also contain rocks relatively low in La (15-20 ppm). A comparison with high-K dacites is problematic since the averages of this group in Ewart (1979) contain shoshonitic rocks rich in P and La. However, the Haukkamaa dacites are similar to certain young high-K dacites in P contents, and they are distinctly higher in La than young medium-K dacites. The Ba contents in the Haukkamaa andesites and dacites are like those in young high-K andesites-dacites. In conclusion, the Haukkamaa andesites and dacites have characteristics of both high-K and medium-K andesites-dacites.

Alteration

Some of the dispersion in Fig. 8 may be attributed to alteration. Sample 9 (a silicified sulfide-bearing tuff; see Appendix) deviates from the other samples in many respects. Its high contents of Si, Ca and Sr, and the low contents of REE are petrographically attributed to the bytownitic plagioclase and the network of quartz veins (Appendix). Besides, the K, Na and Ba contents are so low that leaching of these elements is evident.

Also sample 4 contains felsic veinlets (Appendix). The veinlets are not as abundant as those in sample 9, but they are still so frequent that secondary increase of Si is evident. Therefore, sample 4 was dacite rather than rhyolite in original composition. This could explain its plotting outside the typical fields in the Th vs. SiO_2 and U vs. SiO_2 diagrams.

Sample 178 plots off the general trend in the K_2O vs. SiO_2 diagram and well outside the igneous spectrum. It contains phenocrysts of potassium feldspar (Appendix) which, in showing embayments, have primary rather than secondary forms. However, some of the phenocrysts contain inclusions of altered plagioclase. This may indicate that the phenocrysts were originally plagioclase. Metasomatism near a shear zone is possibly the reason for the deviating composition of sample 178.

Sample 121 is rich in plagioclase phenocrysts and epidote (Appendix). Accumulation of plagioclase and epidotization (Condie et al. 1977, Hellman et al. 1979) may account for the slight Eu maximum in this sample.

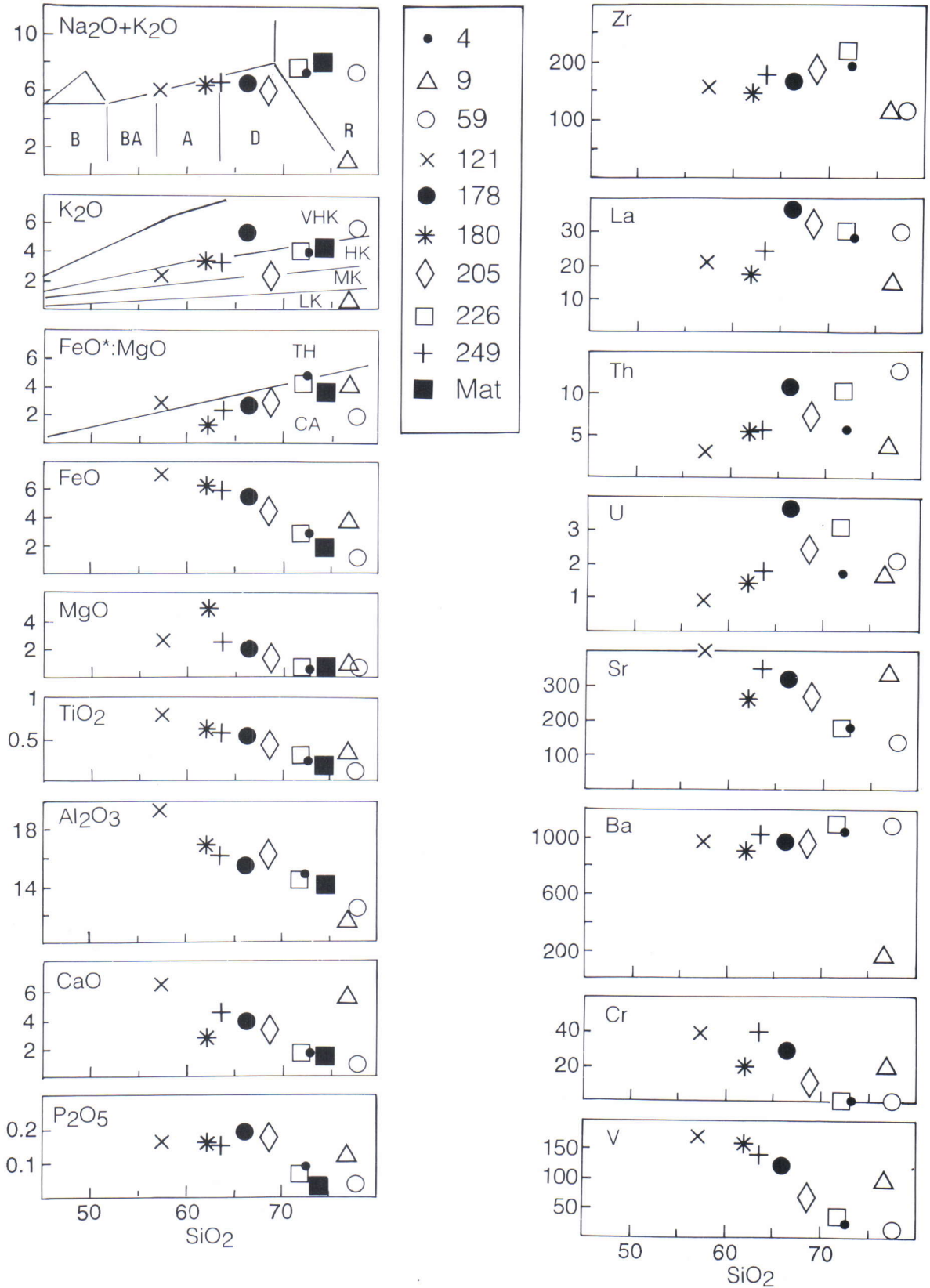


Fig. 8. Selected Harker diagrams of the Haukkamaa volcanics. Data from Table 2, "Mat" is a sample from Matisto (1961). The major element analyses were recalculated to 100%. The boundary lines in the (Na₂O + K₂O) vs. SiO₂ diagram are from Le Bas et al. (1986). BA = basaltic andesite, A = andesite, D = dacite, R = rhyolite. In the K₂O vs. SiO₂ diagram, the LK (low K), MK (medium K), HK (high K) and VHK (very high K) fields are from Kähkönen (1989). In the FeO*:MgO vs. SiO₂ diagram, the boundary line separating the tholeiitic (TH) and calc-alkaline (CA) fields is from Miyashiro (1974).

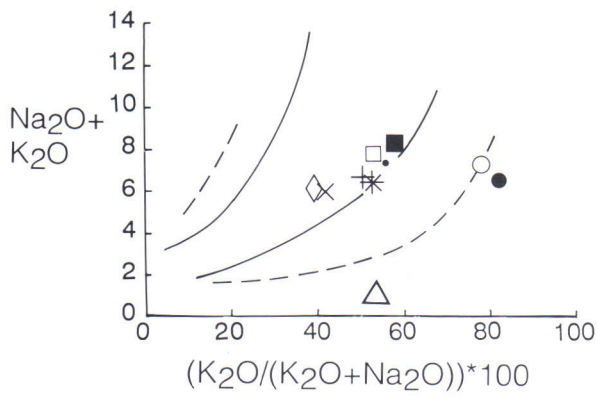


Fig. 9. Igneous spectrum of the Haukkamaa volcanics. Data, data processing and symbols as in Fig. 8. The solid lines give the boundaries of the original igneous spectrum (Hughes 1973) and the dashed lines those of the modified igneous spectrum (Kähkönen 1989).

Table 2. XRF and INAA analyses of the metavolcanic rocks at Haukkamaa, Kuru. Major elements in weight%, trace elements in ppm. Total Fe as FeO*. Major elements were analysed at the Geological Survey of Finland from fused discs using a Philips PW 1410/AHP XRF instrument, Zr, Cr, Ni, Sr, Ba, V, Zn and Cu by the XRF method from pressed rock powder briquettes at the Raahe Laboratory of Rautaruukki Oy, and rare earth elements, Th and U by instrumental neutron activation analysis at the Reactor Laboratory of the Technical Research Centre of Finland (Rosenberg 1977).

Sample	4	9	59	121	178	180	205	226	249
SiO ₂	69.53	72.10	75.44	55.53	65.00	59.91	65.97	69.81	62.28
TiO ₂	0.27	0.33	0.09	0.80	0.53	0.61	0.41	0.30	0.57
Al ₂ O ₃	14.32	10.88	12.02	19.01	15.16	16.35	15.71	14.20	15.93
FeO*	2.71	3.52	1.13	6.90	5.20	6.06	4.25	2.85	5.73
MnO	0.07	0.18	0.00	0.13	0.21	0.07	0.10	0.07	0.10
MgO	0.59	0.87	0.59	2.59	2.04	4.74	1.32	0.68	2.53
CaO	1.71	5.24	0.89	6.28	3.82	2.66	3.10	1.70	4.41
Na ₂ O	3.15	0.41	1.59	3.37	1.19	2.94	3.59	3.52	3.23
K ₂ O	3.98	0.47	5.49	2.41	5.26	3.27	2.26	4.02	3.28
P ₂ O ₅	0.08	0.12	0.04	0.16	0.19	0.16	0.17	0.07	0.15
sum	96.33	94.00	97.24	97.02	98.41	96.61	96.71	97.15	98.06
Zr	200	120	120	160	170	150	190	220	180
Cr	0	20	0	40	30	20	10	0	40
Ni	10	10	10	20	10	20	10	10	20
Sr	180	340	140	400	320	260	270	180	350
Ba	1060	160	1110	980	980	910	960	1120	1020
V	30	100	10	170	120	160	70	40	140
Zn	70	3580	30	90	490	60	100	60	70
Cu	10	4910	10	20	200	0	0	0	30
La	29	15	30	21	37	17	32	30	24
Ce	58	32	61	45	73	35	61	64	53
Nd	32	19	25	25	34	18	33	30	27
Sm	5.4	3.2	3.7	5.1	6.1	3.8	5.4	5.2	5.1
Eu	1.23	0.84	0.46	1.85	1.16	1.05	1.29	1.02	1.15
Tb	0.69	0.46	0.78	0.64	0.97	0.55	0.79	0.97	0.71
Yb	1.8	1.5	1.9	1.94	3.2	2.0	2.5	3.4	2.2
Th	5.9	3.7	13.1	3.0	11.0	5.5	7.4	10.7	5.7
U	1.7	1.7	2.1	0.9	3.7	1.4	2.4	3.1	1.8
FeO*/MgO	4.59	4.04	1.92	2.67	2.55	1.28	3.22	4.20	2.27
Na ₂ O+K ₂ O	7.13	0.88	7.08	5.78	6.45	6.21	5.85	7.54	6.51
La _N :Yb _N	10.64	6.60	10.43	7.15	7.63	5.61	8.45	5.83	7.20
Ti/V	54.00	19.80	54.00	28.24	26.50	22.88	35.14	45.00	24.43
Ti/Zr	8.10	16.50	4.50	30.00	18.71	24.40	12.95	8.18	19.00

Tectonomagmatic affinities

According to the Ti vs. Zr diagram (Fig. 11), the Haukkamaa volcanics have arc affinities. Also, since subduction-related plate margins are the happy home of calc-alkaline andesites and dacites, the Haukkamaa volcanics, which are rich in calc-alkaline andesites

and dacites, resemble the volcanic rocks of convergent plate margins.

The frequency distribution of silica of volcanic associations also reflects the tectonic setting. A bimodal frequency distribution of silica is character-

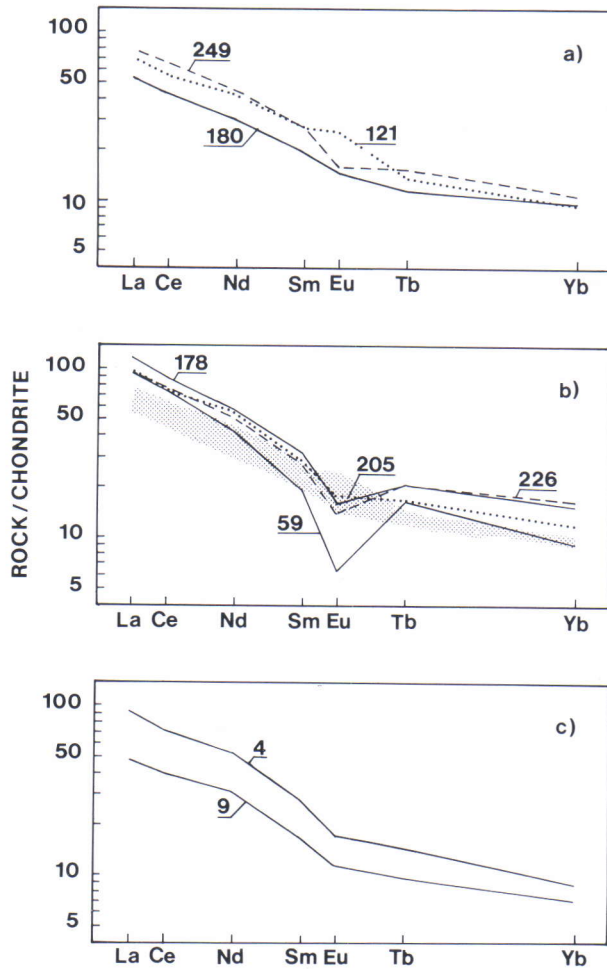


Fig. 10. Chondrite-normalized REE diagrams of the Haukkamaa volcanics. Data from Table 2. Chondrite values used for normalization: Leedeey-6 divided by factor 1.2 (Jahn et al. 1980, Tb from Koljonen & Rosenberg 1975). a. andesite samples 121, 180, 249; b. dacite and rhyolite samples 59, 178, 205, 226, the shaded area shows the field of the above andesites; c. samples 4 and 9.

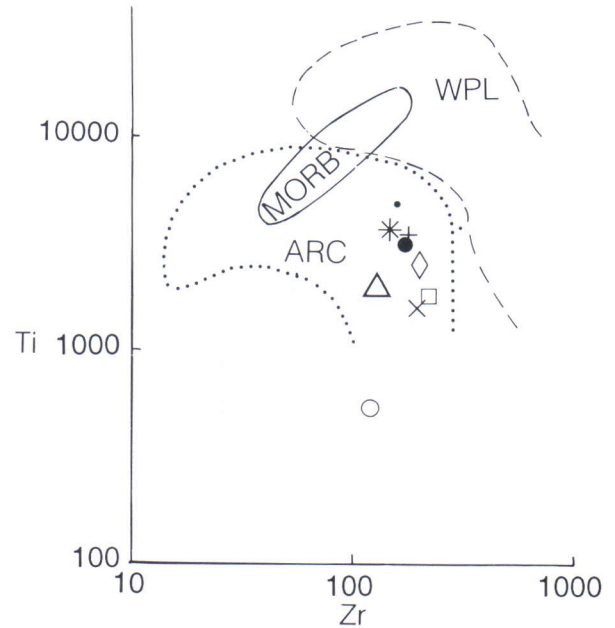


Fig. 11. Ti vs. Zr diagram of the Haukkamaa volcanics. Data and symbols as in Fig. 8. MORB = mid-ocean ridge basalts, ARC = arc lavas, WPL = within plate lavas (Pearce 1982).

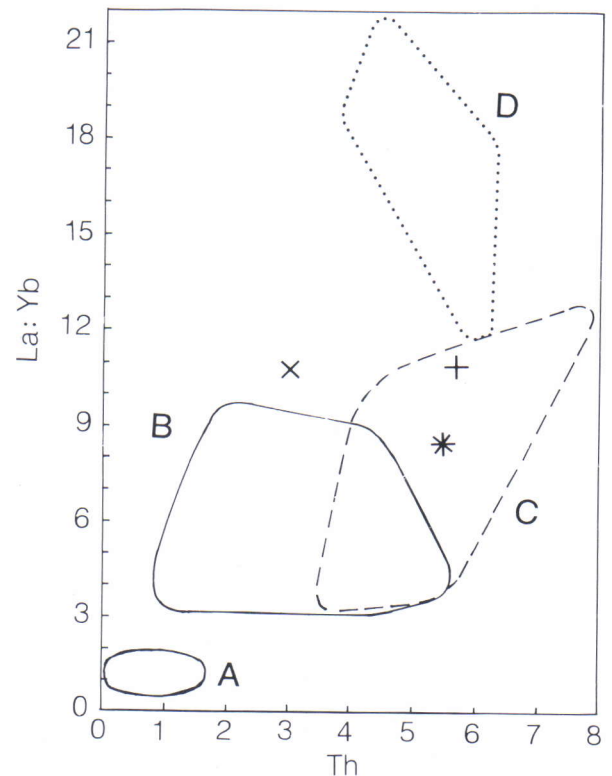


Fig. 12. La/Yb vs. Th diagram of the Haukkamaa andesites. Data and symbols as in Fig. 8. A = field of low-K oceanic island arc andesites, B = field of oceanic island arc andesites not low in K, C = field of continental island arc and thin continental margin andesites, D = field of Andean andesites of N Chile and Peru (Bailey 1981).

istic of volcanic rocks of extensional environments. For instance, certain Paleoproterozoic volcanogenic belts, which have similarities with convergent plate margins have been interpreted to represent extensional settings since they show bimodal frequency distribution of silica (Vivallo & Rickard 1984, Lagerblad & Gorbatshev 1985, Condie 1986). The relatively high proportion of felsic volcanics at Haukkamaa might be considered to indicate an extensional setting. However, although the chemical data from Haukkamaa are scarce, field observations indicate that andesites and dacites are common (Fig. 2). Also, the Haukkamaa rocks show mostly coherent trends in the Harker diagrams and, in particular, the content of Zr, an immobile and incompatible element, largely increases with increasing Si. Therefore, thorough

changes in the overall Si content are not probable and a bimodal frequency distribution of silica is not evident at Haukkamaa.

When compared with young arc andesites, the Haukkamaa andesites differ from both low-K oceanic andesites and Andean andesites (Fig. 12). Andesites with similar La/Yb vs. Th characteristics are common in continental margin island arcs, in arcs with thin continental crust and in certain oceanic island arcs containing volcanics not low in K. The abundance of andesites, dacites and rhyolites at Haukkamaa also indicates that these rocks deviate from the intra-oceanic island arc volcanics which are dominated by basalts and basaltic andesites (Leeman 1983).

PETROGENESIS

The Haukkamaa data are scarce and the samples are from widely dispersed localities. The effects of alteration are evident in some samples. For these reasons, we do not regard a quantitative petrogenetic discussion with detailed model calculations justified. Certain conclusions are, however, warranted.

The Haukkamaa andesites have rather low contents of Cr and Ni. Thus, if they are derived from mafic melts of the mantle, marked fractionation of mafic phases is implied. The relatively low La:Yb ratios suggest that the solid residue of melting did not contain significant amounts of garnet (e.g. Gill 1981).

The general decrease in Sr with increasing Si, and the frequent Eu anomalies in the rhyolitic rocks indicate that fractionation of plagioclase played a major role in the genesis of the felsic rocks. The general decreases in Cr, V and Ti suggest fractionation of mafic silicates and magnetite, and the low P content in the rhyolites is an indication of fractionation of apatite. As discussed below, the behavior of Zr and Ba suggest that the assemblage also contained hornblende and biotite. These features agree with the relics and pseudomorphs of phenocrysts of plagioclase, pyroxene, hornblende and biotite ob-

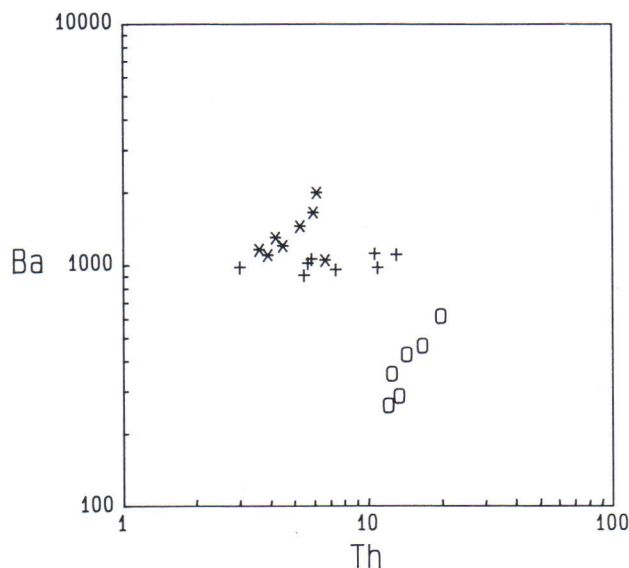


Fig. 13. Ba vs. Th diagram of the Haukkamaa volcanics (+) compared with those of the andesites - rhyodacites of the Main Series, Santorini, Greece (o, Mann 1983) and Summer Coon, San Juan Mountains, Colorado (*, Zielinski & Lipman 1976). The highly altered sample 9 of Haukkamaa was omitted.

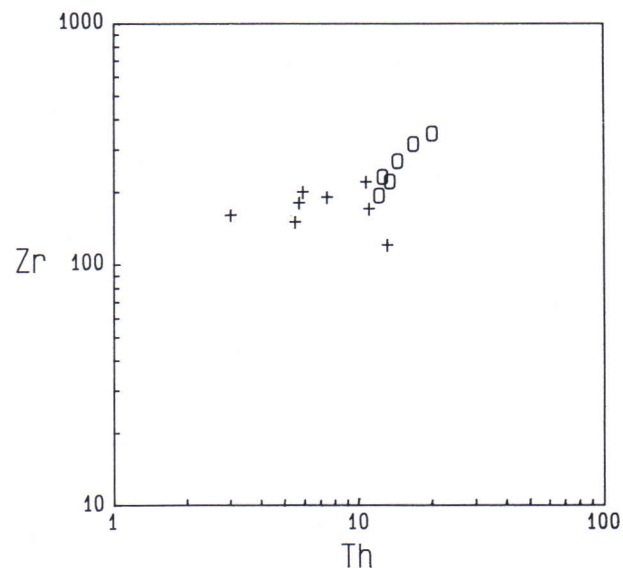


Fig. 14. Zr vs. Th diagram of the Haukkamaa volcanics (+) compared with that of the andesites - rhyodacites of the Main Series, Santorini (o, Mann 1983). The highly altered sample 9 of Haukkamaa was omitted.

served in the intermediate rocks.

Ba is relatively mobile during various alteration processes. However, as the Ba vs. SiO₂ and Ba vs. Th trends of the Haukkamaa rocks (Figs. 8 and 13) are rather coherent, they must be of significance. Because the Ba vs. Th and Zr vs. Th trends at Haukkamaa are markedly gentler than those in the Santorini and Summer Coon series (Figs. 13 and 14), the fractionated assemblage at Haukkamaa had higher solid/melt bulk distribution coefficient for Ba and Zr (D_{Ba} , D_{Zr}). The Santorini series is derived through fractionation of the assemblage plagioclase-augite-hypersthene-magnetite-apatite (Mann 1983), while the Summer Coon series is interpreted to be derived from fractionation of an assemblage dominated by plagioclase and hornblende (Zielinski & Lipman 1976). The assemblage at Haukkamaa probably contained phases with relatively high distribution coefficients for Ba and Zr. The distribution coefficients of Zr for hornblende and biotite (D_{Zr}^{hbl} and D_{Zr}^{bt}) are notably higher than those for olivine, plagioclase and pyroxenes (Pearce & Norry 1979). Further, D_{Ba}^{bt} is higher than D_{Ba}^{cpx} , D_{Ba}^{pl} and D_{Ba}^{hbl} (Arth 1976, Hanski 1983).

Fractionation of hornblende can explain the

Haukkamaa Zr vs. Th trend but it cannot explain the nearly horizontal Ba vs. Th trend which implies that the bulk D_{Ba} approached unity. A probable explanation is that the fractionated assemblage contained biotite. Because D_{Ba}^{bt} ranges from 5 to 20 (Hanski 1983), bulk D_{Ba} approaches unity if the assemblage has 5-20% biotite.

D_{HREE}^{hbl} values exceed unity in intermediate to felsic systems and are higher than D_{LREE}^{hbl} (Arth 1976). Consequently, the proportion of hornblende in the solid assemblage was probably not large since most of the Haukkamaa felsic rocks do not show a pronounced depletion in HREE. The relatively low HREE and Zr in sample 59 probably results from fractionation of both hornblende and zircon.

Many features of the Haukkamaa volcanics can be attributed to fractional crystallization dominated by plagioclase. It is not, however, implied that the rocks were necessarily derived from a single homogeneous source. This is because the Haukkamaa samples are from scattered localities and from different stratigraphic levels. Further, silicic magma chambers are often zoned and a part of the variation in composition may be attributable to process other than conventional fractional crystallization (Hildreth 1981).

DISCUSSION

Geochemical data and field studies suggest that calc-alkaline andesites-rhyolites, largely of pyroclastic origin, abound at Haukkamaa. A part of the volcanic activity may have been subaerial. Thus the Haukkamaa volcanics represent a relatively evolved stage of arc-type volcanism. In this context, the Haukkamaa belt resembles many parts of the coeval Tampere Schist Belt about 50 km to the south (Kähkönen 1987, 1989).

In the western CSS, i.e. west of the CFGC, the supracrustal rocks are dominated by turbiditic sedimentary rocks and the volcanics have largely non-arc affinities (Vaarma & Kähkönen this volume). In contrast, a significant proportion of the supracrustal belts of the eastern CSS, i.e. those within and near the CFGC, may comprise arc volcanics, since the

Haukkamaa belt and the volcanics of the Tampere Schist Belt (Kähkönen 1987), at the southern margin of the CFGC, are dominated by arc-type rocks. Thus the supracrustal belts in the eastern CSS comprise an arc-like realm which may be regarded as a continuation of the arc-like Northern Svecofennian Subprovince rather than as a part of the CSS proper which is dominated by sedimentary rocks. To the south this realm is separated from the arc-like Southern Svecofennian Subprovince by migmatites, i.e. by CSS sedimentary rocks. In conclusion, the turbidite-dominated CSS (or Bothnian Basin) between the volcanics-rich Northern and Southern Svecofennian Subprovinces seems to be a real feature but its areal extent may be smaller than suggested by Gaál and Gorbatshev (1987).

ACKNOWLEDGEMENTS

The REE analyses were financed by Research Project 24/001 of the Academy of Finland, led by Dr. Tapio Koljonen. The other trace element analyses were financed by an IGCP 217 - related Research Project 01/209 of the Academy of Finland. Dr. Olavi Kouvo kindly made the age determinations at the

Isotope Laboratory of the Geological Survey of Finland. This paper is contribution to IGCP Projects 179 and 217. The English language was revised by Paul Sjöblom. Figs. 8, 9, 11 and 12 were drawn by Mrs. Riitta Fagerström and Fig. 10 by Mrs. Tuju Pyykkö.

REFERENCES

- Arth, J.G. 1976.** Behaviour of trace elements during magmatic processes - A summary of theoretical models and their applications. *J. Res. U.S. Geol. Surv.* 4, 41-47.
- Bailey, J.C. 1981.** Geochemical criteria for a refined tectonic discrimination of orogenic andesites. *Chem. Geol.* 32, 139-154.
- Condie, K.C. 1986.** Geochemistry and tectonic setting of early Proterozoic supracrustal rocks in the southwestern United States. *J. Geol.* 94, 845-864.
- Condie, K.C., Viljoen, M.J. & Kable, E.J.D. 1977.** Effects of alteration on element distributions in Archean tholeiites from the Barberton Greenstone Belt, South Africa. *Contrib. Mineral. Petrol.* 64, 75-89.
- Ehlers, C., Lindroos, A. & Jaanus-Järkkälä, M. 1986.** Stratigraphy and geochemistry in the Proterozoic mafic volcanic rocks of the Nagu-Korpo area, SW Finland. *Precambrian Res.* 32, 297-315.
- Ewart, A. 1979.** A review of the mineralogy and chemistry of Tertiary-Recent dacitic, latitic, rhyolitic and related salic volcanic rocks. In: Barker, F. (ed.) *Trondhjemites, Dacites and Associated Rocks*. Amsterdam: Elsevier, 13-121.
- Ewart, A. 1982.** The mineralogy and petrology of Tertiary-Recent orogenic volcanic rocks: with special reference to the andesitic-basaltic compositional range. In: Thorpe, R.S. (ed.) *Andesites, Orogenic Andesites and Related Rocks*. Chichester: Wiley, 25-95.
- Fisher, R.V. 1979.** Models for pyroclastic surges and pyroclastic flows. *J. Volcanol. Geotherm. Res.* 6, 305-318.
- Front, K. & Nurmi, P. 1987.** Characteristics and geological setting of synkinematic Svecokarelian granitoids in southern Finland. *Precambrian Res.* 35, 207-224.
- Gaál, G. & Gorbatshev, R. 1987.** An outline of the Precambrian evolution of the Baltic Shield. *Precambrian Res.* 35, 15-52.
- Gill, J.B. 1981.** *Orogenic Andesites and Plate Tectonics*. Berlin; Springer-Verlag, 390 p.
- Hanski, E. 1983.** Alkuaineiden jakaantuminen mineraalien ja silikaattien kesken: Jakaantumiskertoimet. Arkeisten alu-eiden malmiprojekti, Raportti 15. Univ. Oulu, 179 p. (in Finnish)
- Hellman, P.L., Smith, R.E. & Henderson, P. 1979.** The mobility of the rare earth elements: evidence and implications from selected terrains affected by burial metamorphism. *Contrib. Mineral. Petrol.* 71, 23-44.
- Hietanen, A. 1975.** Generation of potassium-poor magmas in the northern Sierra Nevada and the Svecofennian of Finland. *J. Res. U.S. Geol. Surv.* 3, 631-645.
- Hildreth, W. 1981.** Gradients in silicic magma chambers: Implications for lithospheric magmatism. *J. Geophys. Res.* 86, 10153-10193.
- Hughes, C.J. 1973.** Spilites, keratophyres, and the igneous spectrum. *Geol. Mag.* 109, 513-527.
- Huhma, H. 1986.** Sm-Nd, U-Pb and Pb-Pb isotopic evidence for the origin of the early Proterozoic Svecokarelian crust in Finland. *Geol. Surv. Finland, Bull.* 337, 48 p.
- Huhma, H. 1987.** Provenance of Early Proterozoic and Archaean metasediments in Finland: a Sm-Nd isotopic study. *Precambrian Res.* 35, 127-143.
- Jahn, B.M., Auvrey, B., Blais, S., Capdevila, R., Cornichet, J., Vidal, F. & Hameurt, J. 1980.** Trace element geochemistry and petrogenesis of Finnish greenstone belts. *J. Petrol.* 21, 201-244.
- Kähkönen, Y. 1987.** Geochemistry and tectonomagmatic affinities of the metavolcanic rocks of the early Proterozoic Tampere Schist Belt, southern Finland. *Precambrian Res.* 35, 295-311.
- Kähkönen, Y. 1989.** Geochemistry and petrology of the metavolcanic rocks of the early Proterozoic Tampere Schist Belt, southern Finland. *Geol. Surv. Finland, Bull.* 345, 104 p.
- Kähkönen, Y., Huhma, H. & Aro, K. 1989.** U-Pb zircon ages and Rb-Sr whole-rock isotope studies of early Proterozoic volcanic and plutonic rocks near Tampere, southern Finland. *Precambrian Res.* 45, 27-43.
- Koljonen, T. & Rosenberg, R.J. 1975.** Rare earth elements in middle Precambrian volcanic rocks of Finland, with a discussion of the origin of the rocks. *Bull. Geol. Soc. Finland* 47, 127-138.
- Krogh, T.E. 1973.** A low-contamination method for hydrothermal decomposition of zircon and extraction of U and Pb for isotopic age determinations. *Geochim. Cosmochim. Acta* 37, 485-494.
- Lagerblad, B. & Gorbatshev, R. 1985.** Hydrothermal alteration as a control of regional geochemistry and ore formation in the central Baltic Shield. *Geol. Rundschau* 74, 33-49.
- Laitakari, I. 1980.** Vulkaanisista primäärirakenteista. *Geologi* 32, 124-125. (in Finnish)
- Latvalahti, U. 1979.** Cu-Zn-Pb ores in the Aijala-Orijärvi area, Southwest Finland. *Econ. Geol.* 74, 1035-1059.
- Le Bas, M.J., Le Maitre, R.W., Streckeisen, A. & Zanettin, B. 1986.** A chemical classification of volcanic rocks based on the total alkali-silica diagram. *J. Petrol.* 27, 745-750.
- Leeman, W.P. 1983.** The influence of crustal structure on compositions of subduction-related magmas. *J. Volcanol. Geotherm. Res.* 18, 561-588.
- Mäkelä, K. 1980.** Geochemistry and origin of Haveri and Kiiipu, Proterozoic strata-bound volcanogenic gold-copper and zinc mineralizations from southwestern Finland. *Geol. Surv. Finland, Bull.* 310, 79 p.
- Mann, A.C. 1983.** Trace element geochemistry of high alumina basalt - andesite - dacite - rhyodacite lavas of the Main Volcanic Series of Santorini Volcano, Greece. *Contrib. Mineral. Petrol.* 84, 43-57.
- Matisto, A. 1960.** Pre-Quaternary rocks, sheet 2213 Kuru. Geological map of Finland 1 : 100 000.
- Matisto, A. 1961.** Kallioperäkartan selitys. Summary: Explanation to the map of rocks, sheet 2213 Kuru. Geological map of Finland 1 : 100 000, 40 p.
- Miyashiro, A. 1974.** Volcanic rock series in island arcs and active continental margins. *Am. J. Sci.* 274, 321-355.
- Patchett, P. & Kouvo, O. 1986.** Origin of continental crust of 1.9-1.7 Ga age: Nd isotopes and U-Pb zircon ages in the Svecokarelian terrains of South Finland. *Contrib. Mineral. Petrol.* 92, 1-12.
- Pearce, J.A. 1982.** Trace element characteristics of lavas from destructive plate margins. In: Thorpe, R.S. (ed.), *Andesites, Orogenic Andesites and Related Rocks*. Chichester: Wiley & Sons, 525-548.
- Pearce, J.A. & Norry, M.J. 1979.** Petrogenetic implications of Ti, Zr, Y and Nb variations in volcanic rocks. *Contrib. Mineral. Petrol.* 69, 33-47.
- Rosenberg, R.J. 1977.** Instrumental neutron activation analysis as a routine method for rock analysis. Technical Research Centre of Finland. Electrical and Nuclear Technology, Publ. 19.
- Sederholm, J.J. 1903.** Pre-Quaternary rocks, sheet B2 Tampere. Geological map of Finland 1:400 000.
- Simonen, A. 1980.** The Precambrian in Finland. *Geol. Surv. Finland, Bull.* 304, 58 p.
- Sparks, R.S.J., Self, S. & Walker, G.P.L. 1973.** Products of ignimbrite eruptions. *Geology* 1, 115-118.

- Tiainen, M. 1983.** Kurun Haukkamaan intermediäärinen -felsisen liuskevyöhykkeen petrologiasta, geokemiasta ja rakenteesta. M.Sc. thesis, Univ. Helsinki, 123 p. (unpublished, in Finnish)
- Vaarma, M. & Kähkönen, Y. 1994.** Geochemistry of the Paleoproterozoic metavolcanics at Evijärvi, western Finland. Geol. Surv. Finland, Spec. Paper 19, 47-59.
- Vaasjoki, M. 1977.** Rapakivi granites and other postorogenic rocks in Finland: their age and the lead isotopic composition of certain associated galena mineralizations. Geol. Surv. Finland, Bull. 294, 71 p.
- Vivallo, W. & Rickard, D. 1984.** Early Proterozoic ensialic spreading-subsidence: evidence from the Garpenberg enclave, central Sweden. Precambrian Res. 26, 203-221.
- York, D. 1969.** Least squares fitting of a straight line with correlated errors. Earth Planet. Sci. Lett. 5, 320-324.
- Zielinski, R.A. & Lipman, P.W. 1976.** Trace element variations at Summer Coon volcano, San Juan Mountains, Colorado, and the origin of continental interior andesite. Geol. Soc. Am. Bull. 87, 1477-1485.

APPENDIX. Description of the samples. Grid coordinates by x and y. CAPITALS for major minerals. Min&acc: minor and accessory minerals. PL = plagioclase, HBL = hornblende, QTZ = quartz, BT = biotite, KFS = potassium feldspar, EP = epidote, MS = muscovite, SER = sericite, CHL = chlorite, ap = apatite, zirc = zircon, sph = sphene, op = opaque, crb = carbonate. Pc: the mineral occurs partly as phenocrysts; ϕ indicates the maximum diameter of the phenocrysts, and the percentages give the approximate amount of the phenocrysts in vol. %.

No. 4. x=6882.505, y=482.320. Pl-phyric crystal tuff. QTZ, PL (Pc, $\phi < 1$ mm, 10-20%), BT, HBL. Min&acc: Kfs, ap, ep, op, zirc. The sample is from a normally graded tuff. It contains about 20 vol.% felsic veins.

No. 9. x=6882.460, y=482.215. Silicified pl-phyric crystal tuff. QTZ, BT, PL (Pc, bytownite), KFS. Min&acc: ap, ep, ms, zirc, op. The rock is from a silicified sulfide-bearing crystal tuff in the same horizon as sample No. 4. It is rich in veins and patches of qtz. The few phenocrysts are poorly visible mosaic relicts.

No. 59. x=6884.150, y=481.690. Fine-grained felsic tuff. QTZ, KFS, BT, PL, MS. Min&acc: chl, ep, zirc.

No. 121. x=6883.620, y=483.770. Stratified pl-phyric crystal tuff. EP (30%), BT, PL (Pc, $\phi < 1$ mm, 30-40%), QTZ. Min&acc: Kfs, sph, ap, zirc, hbl, crb, op.

No. 178. x=6883.900, y=484.890. Qtz- and feldspar-phyric and clastic felsic schist. KFS (Pc, $\phi < 3$ mm, 20%), PL (Pc, $\phi < 2$ mm, 10%), QTZ (Pc, $\phi < 2,5$ mm, 5%), EP, BT. Min&acc: ms. The sample consists of even-grained and porphyritic rock fragments and it may be a lithic tuff in origin. The phenocrysts are in part embayed. Pressure shadows, epidotization and veinlets of qtz are common.

No. 180. x=6881.650, y=485.460. Bt- and pl-phyric massive andesite. QTZ (Pc), BT (Pc), PL (Pc, $\phi < 3$ mm, 30%, in part embayed). Min&acc: ap, ep, zirc. Pl altered to ep. Fine-grained bt-aggregates are often probably pseudomorphs after hbl or bt or both.

No. 205. x=6883.550, y=486.300. Porphyritic felsic rock. QTZ, EP, PL & KFS (Pc, $\phi < 0,5$ mm, rarely up to 3 mm, 30%), CHL, SER. Min&acc: ap, ep, op. The feldspar phenocrysts are mosaic relicts and the rock has been strongly epidotized and sericitized.

No. 226. x=6882.100, y=486.860. Qtz- and feldspar-phyric felsic rock. KFS (Pc, $\phi < 8$ mm, 20%), PL (Pc, $\phi < 2$ mm, 10-20%), QTZ (Pc, $\phi < 2$ mm, $< 5\%$), BT (Pc, $\phi < 2$ mm, $< 5\%$). Min&acc: ap, ep, ser, chl. It is a massive felsic rock and we have no conclusive evidence whether it is effusive or subvolcanic in origin. The phenocrysts of Kfs and qtz are in part embayed.

No. 249. x=6882.210, y=484.830. Uralite+pl-phyric massive intermediate rock. PL (Pc, $\phi < 3,5$ mm, 20-25%), Clinopyroxene (now hbl, Pc, $\phi < 1$ mm, 5-10%), HBL (Pc, $\phi < 0,5$ mm, $< 5\%$), BT (Pc, $\phi < 0,5$ mm, $< 5\%$), QTZ. Min&acc: ap, ep.

GEOCHEMISTRY OF THE PALEOPROTEROZOIC METAVOLCANIC ROCKS AT EVIJÄRVI, WESTERN FINLAND

by
Markus Vaarma and Yrjö Kähkönen

Vaarma, Markus & Kähkönen, Yrjö 1994. Geochemistry of the Paleoproterozoic metavolcanic rocks at Evijärvi, western Finland. *Geological Survey of Finland, Special Paper 19*, 47–59, 11 figures, one table and one appendix.

The Evijärvi area belongs to the Central Svecofennian Subprovince (CSS) of the Fennoscandian (or Baltic) Shield. The supracrustal rocks of this subprovince are dominated by turbiditic metagraywackes-metapelites. At Evijärvi, among the metasedimentary rocks, there are formations of metavolcanic rocks where pillow lavas are frequently met with. The metavolcanic rocks are mostly tholeiitic basalts and basaltic andesites, low in potassium and relatively high in sodium. These compositional features may in part be primary, but are in part caused by alteration. Most of the rocks show enrichments in LREE, but there are also flat and LREE-depleted chondrite-normalized patterns.

The metavolcanic rocks at Evijärvi show a variation in tectonomagmatic affinities from N-type mid-ocean ridge basalts (MORB) to alkaline within-plate basalts (WPB). Rocks plotting in arc fields in the discrimination diagrams are more frequent in the east (in the Isokylä and Patana formations) than in the west (in the Aho and Raisjoki formations) but, in general, arc affinities are not pronounced. Mafic volcanic rocks not showing chemical features typical of arc basalts seem to be common in the western part of the CSS. It is possible that these basalts and the Evijärvi mafic volcanic rocks were erupted in a marginal basin at an early stage of the ca. 1.9 Ga evolution of the Svecofennian crust.

Key words (GeoRef Thesaurus, AGI): metavolcanic rocks, pillow lava, basalts, geochemistry, rare earths, alteration, Proterozoic, Paleoproterozoic, Evijärvi Veteli, Finland

Markus Vaarma, Geological Survey of Finland, FIN-02150 Espoo, Finland
Yrjö Kähkönen, Department of Geology, P.O. Box 11 (Snellmaninkatu 3),
FIN -00014 University of Helsinki, Finland

INTRODUCTION

The Svecofennian Domain (Fig. 1) was generated from newly mantle-derived material some 1.9 Ga ago (Patchett et al. 1981, Huhma 1986, Patchett & Kouvo 1986). Similarities with the evolution of present-day convergent plate margins have been postulated for this process (Hietanen 1975, Gaál & Gorbatshev 1987).

The Svecofennian Domain is dominated by granitoids and, among the supracrustal rocks, by turbiditic metagraywackes-pelites and mafic to felsic metavolcanic rocks (Simonen 1980, Gaál & Gorbatshev 1987). The metamorphic conditions ranged from low grade to high grade but were regularly of a low-P type. The metavolcanic rocks (supracrustal rocks from here on without the prefix meta-) in many cases resemble those of young volcanic arcs but in places also show features not typical of arc volcanics (Latvalahti 1979, Mäkelä 1980, Ehlers et al. 1986, Kähkönen 1987, 1989). The

characteristic 1.90-1.86 Ga old igneous activity in the Svecofennian province was preceded by the formation of 1.96-1.97 Ga old ophiolite complexes (Koistinen 1981, Kontinen 1987) and 1.92-1.93 Ga old tonalitic gneisses (Helovuori 1979, Korsman et al. 1984) found near the Archean-Proterozoic boundary in eastern Finland (Fig. 1). A tonalite intruding mica gneisses and their S_2 -schistosity at Evijärvi has a pooled U-Pb zircon age of c. 1.91 Ga (Vaarma & Pipping in prep.). However, the zircon data seems to consist of two populations with ages of 1.883 Ga and c. 1.90 Ga. The younger population is interpreted to give the age of intrusion while the older yields the minimum age of the inherited component.

In this paper we will present petrographic and geochemical data and discuss the general geochemical features, effects of alteration, and tectonomagmatic affinities of the volcanic rocks at Evijärvi.

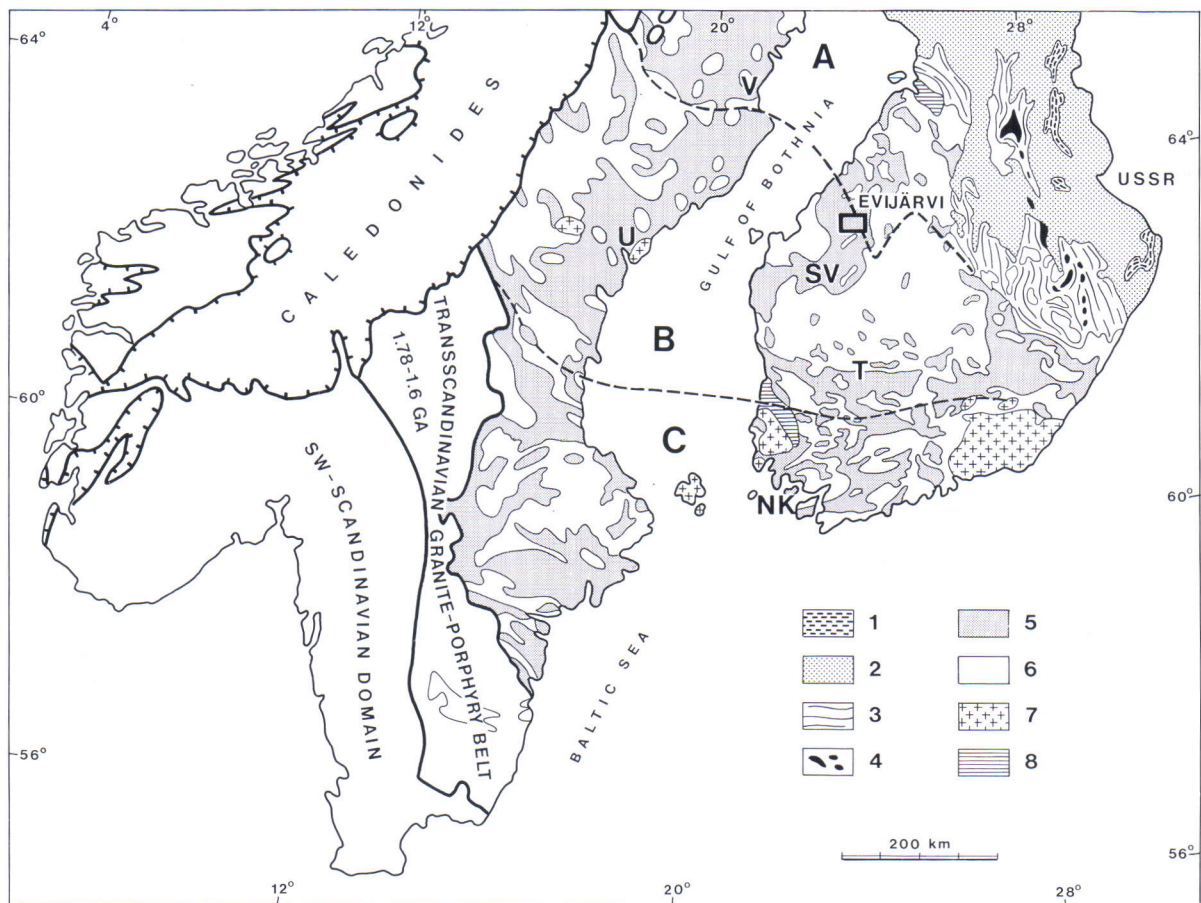


Fig. 1. Generalized geological map of central, western and southern Fennoscandian (or Baltic) Shield, after Simonen (1980), Papunen & Gorbunov (1985) and Gaál & Gorbatshev (1987). The inset shows the area of Fig. 2. 1 = Archean greenstone belts, 2 = Archean granitoids, 3 = Karelian schists, 4 = 1.96 - 1.97 Ga old ophiolite complexes, 5 = Svecofennian schists, gneisses and migmatites, 6 = Svecofennian plutonic rocks, 7 = Rapakivi granites, 8 = Jotnian sedimentary rocks. A = Northern Svecofennian Subprovince, B = Central Svecofennian Subprovince (or Bothnian Basin), C = Southern Svecofennian Subprovince, NK = Nagu-Korpo area, SV = Seinäjoki-Vittinki area, T = Tampere, U = Ullängar, V = Varuträsk.

GEOLOGY OF THE EVIJÄRVI AREA

Based on supracrustal lithologies, Gaál & Gorbatshev (1987) divided the Svecofennian Domain into the volcanic-rich Northern and Southern Svecofennian Subprovinces and the intervening Central Svecofennian Subprovince (CSS), which is characterized by metagraywackes and metapelites deposited in the so-called Bothnian Basin (Hietanen 1975). The Evijärvi area lies within the CSS, near the boundary to the Northern Svecofennian Subprovince.

The supracrustal rocks at Evijärvi (Fig. 2) are dominated by mica schists and gneisses that were originally turbiditic graywackes and mudstones. Staurolite and garnet are the characteristic porp-

hyroblasts in the metapelites of the easternmost parts of the study area. In the central parts, staurolite is absent but muscovite-rich pseudomorphs do occur. In the western parts, K-feldspar and knots of fibrolitic sillimanite occur as porphyroblasts. The climactic grade of metamorphism increased from medium grade in the east to high grade in the west.

Structurally, the rocks at Evijärvi show signs of polyphase deformation but gently to moderately dipping S_0/S_1 and S_2 planes in general have northeastern vergence (Vaarma 1984). The supracrustal rocks are not necessarily autochthonous and overthrusts to approximately northeast may be possible.

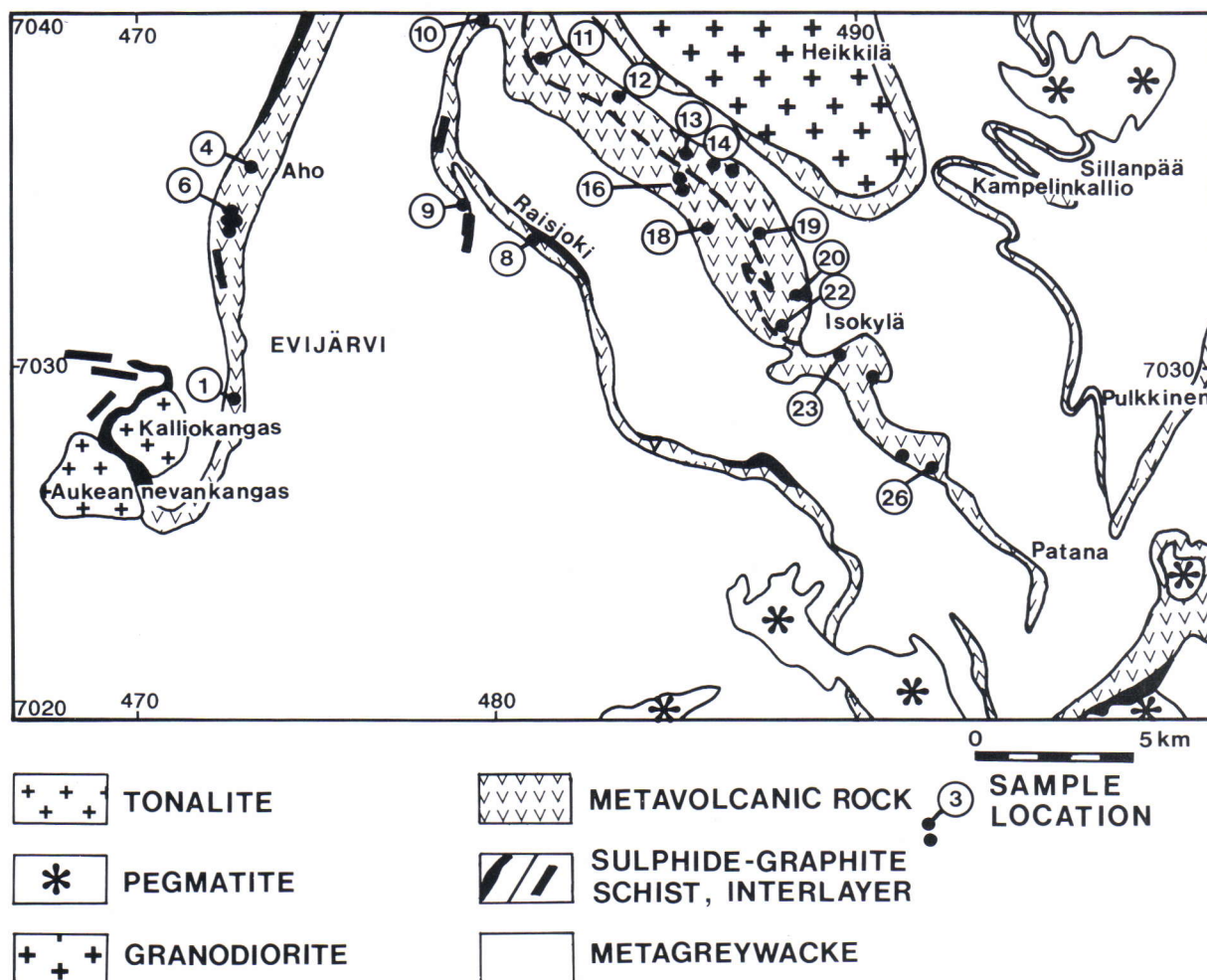


Fig. 2. Lithological map of the Evijärvi area. The dots indicate the sampling localities; the numbered ones are the samples analyzed for trace elements (Table 1). The dashed line marks the boundary between the Patana and Isokylä formations.

Volcanic formations at Evijärvi

The volcanics at Evijärvi are dominated by mafic rocks. They occur typically as narrow formations within sedimentary rocks. Because of the scarcity of outcrops, the volcanic formations are best traced on low-altitude airborne magnetic maps as belts of positive anomalies. Although the outcrops are scarce, various primary features are to be observed and pillow lavas occur in each of the formations now considered. The formations also contain sulfide-graphite schists, which indicate hydrothermal precipitation associated with the volcanic activity.

The volcanic rocks considered now are divided into four informally defined formations: the Aho and Raisjoki formations in the west and the Isokylä and Patana formations in the east. Because the volcanic rocks of the Aho formation resemble those of the Raisjoki formation in mode of occurrence, petrography and geochemistry, these two formations are discussed together. Although contacts were not observed, the volcanic formations seem to be underlain and overlain by sedimentary rocks. The stratigraphic relation of the Aho and Raisjoki formations to the Isokylä and Patana formations is not known with certainty but the Isokylä formation probably overlies the Patana formation.

The Raisjoki formation is in general less than 0.5 km wide across the strike in horizontal section while the Aho formation is up to 1.5 km wide. The S_0/S_1 and S_2 planes have gentle to moderate dips to the west or southwest. Based on airborne geophysical maps, we suggest that the Aho formation was tectonically shortened.

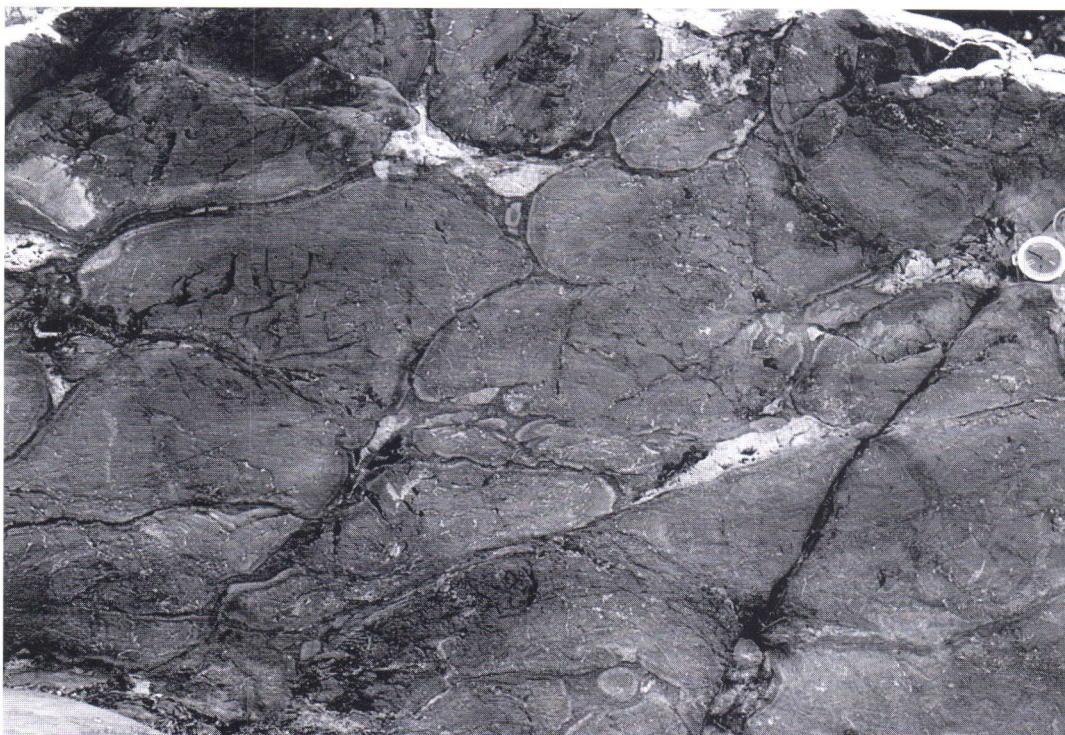
The volcanic rocks of the Aho and Raisjoki formations (Fig. 2) are characterized by fine- to medium-grained massive mafic lavas, but there are also pillow lavas. A few rocks with fragmental structures are thought to be hyaloclastic breccias, and some polymictic strata may be subaqueous mass flow deposits of volcanoclastic origin. The Aho formation comprises also fine-grained thinly bedded tuffs or tuffites. Black schist are frequent in both formations.

The Isokylä and Patana formations occur close to each other but they can be discerned based on petrography, lithology and geochemistry. In places, the boundary between these formations is marked by gently west to southwest dipping calcareous rocks.

In the Patana formation, the volcanics are characterized by massive fine- and even-grained mafic rocks. In places they show pillow (Fig. 3), hyaloclastic and agglomerate/lapilli structures. In general, the Patana volcanics are more mafic than those of the Isokylä formation. The Patana formation also comprises black schist horizons.

In the Isokylä formation, intermediate volcanics, in addition to mafic volcanics, are common. Contrary to those of the Patana formation, the volcanics typically are plagioclase-phyric with phenocrysts up to 5 mm in diameter. Volcanic breccias and pyroclastic rocks are relatively common near Isokylä but there are also lavas and sills. Pillow lavas and pillow breccias were observed, too (Fig. 3). Black schists are less frequent in the Isokylä formation than in the other volcanic formations now discussed.

3a)



3b)



3c)



Fig. 3. Pillow lavas of the Evijärvi area. **a.** Patana formation ($x = 7033.03$, $y = 2486.38$). **b.** Isokylä formation; note the overturned position indicated by the form of the pillows ($x = 7035.84$, $y = 2486.06$). **c.** Pillow breccia in the Isokylä formation ($x = 7032.26$, $y = 2488.54$).

GEOCHEMISTRY

The volcanic rocks at Evijärvi are dominated by low-K subalkaline basalts and basaltic andesites (Fig. 4). Most of the samples from the Aho and Raisjoki formations are basalts while those from the Isokylä and Patana formations are mainly basaltic andesites. Two samples from Aho have a trachybasaltic composition. Although high in K, they still are of the sodic type, or hawaiites, in that the $\text{Na}_2\text{O} - 2$ exceeds the K_2O content (cf. Le Bas et al. 1986). These two samples are fine-grained stratified tuffs or tuffites.

The Evijärvi volcanics plot mostly in the tholeiitic field in the FeO^*/MgO vs. SiO_2 diagram (Fig. 4). The Aho and Raisjoki basalts, in particular, show a wide variation in their FeO^*/MgO ratios. Their tendency to iron-enrichment is corroborated by the increase in Ti with increasing Zr (Fig. 10). The tholeiitic imprint of the Isokylä and Patana formations is less pro-

nounced than that of the Aho and Raisjoki formations.

The P_2O_5 content ranges between 0.05% and 0.8%, but is mostly below 0.4% (Fig. 5). The highest values are found in the Isokylä andesites. The samples of the Patana formation are lower in P than those of the other formations. Being also rather low in LREE and Zr (Figs. 6 and 10), they are relatively primitive.

The Evijärvi volcanics show mostly enrichment in light rare earth elements (LREE) over heavy rare earth elements (HREE) in that the chondrite-normalized ratios of La and Yb ($\text{La}_N:\text{Yb}_N$ ratio) frequently exceed unity (Fig. 6; Table 1). Sample 4 has, however, a flat REE pattern, and samples 18 and 26, from Patana, are depleted in LREE. The positive ϵ_{Nd} values of 2.9 - 4.5 determined by Huhma (1986) from samples 18 and 26 corroborated that these rocks

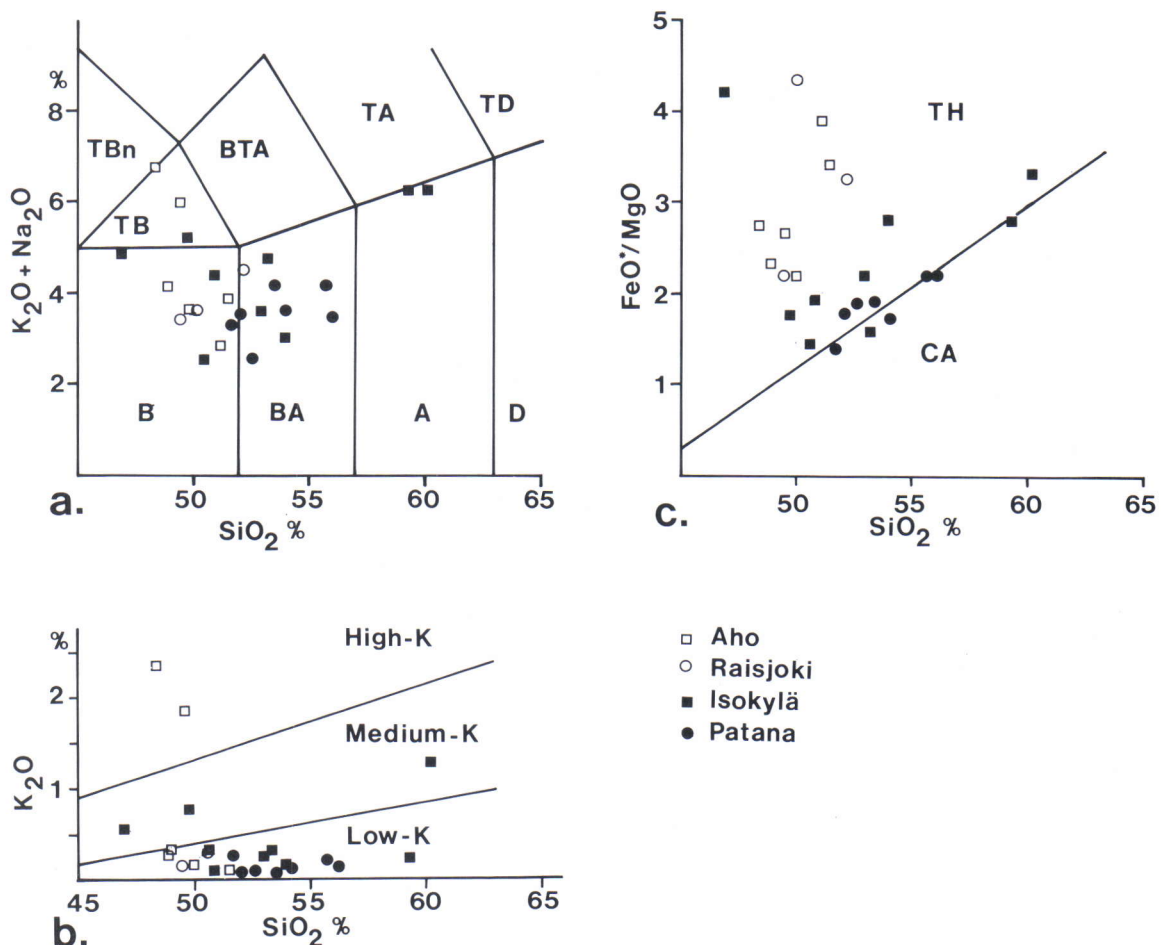


Fig. 4. Total alkali vs. silica (TAS), K_2O vs. SiO_2 and FeO^*/MgO vs. SiO_2 diagrams of the Evijärvi volcanics. Data from Table 1 and Vaarma (1984). Analyses were calculated to 100% with total Fe as FeO^* . a: The fields in the TAS diagram are from Le Bas et al. (1986); B = basalt; TB = trachybasalt; TBn = tephrite basanite; BA = basaltic andesite; BTA = basaltic trachyandesite; A = andesite; TA = trachyandesite; D = dacite; TD = trachyte and trachydacite. b: The lines giving the boundaries of the low-K, medium-K and high-K fields are from Gill (1981). c: The TH/CA (tholeiitic/calc-alkaline) boundary is drawn after Miyashiro (1974).

are derived from depleted mantle sources. The trachybasaltic tuff sample 6 from Aho has the highest $La_N:Yb_N$ value, 6.6. The REE patterns of the

subalkaline samples from Aho and Raisjoki are in many cases slightly convex and their $La_N:Sm_N$ ratios are below or near unity.

The problem of alteration

Sea-floor alteration and later metamorphism have possibly affected the composition of the Evijärvi volcanics. In general, low-T reactions between basalt and sea water cause enrichment in such elements as K, Rb, Sr, U and Cs, while greenschist to amphibolite facies hydrothermal alteration may result in leaching of these elements (Saunders & Tarney 1984). Granulitic or high-grade metamorphism possibly causes depletion of K, Rb, U, Th and

Cs (Tarney & Windley 1977).

The problem of alteration in the Evijärvi rocks is discussed by comparing the P and K contents with those of young mafic volcanic rocks. It is also illustrated by the $MgO/10 - CaO/Al_2O_3 - SiO_2/100$ and K_2O vs. Na_2O diagrams, and the igneous spectrum (Figs. 7-9). The essential questions are whether there are marked changes in alkali contents and whether the low-K character is a primary feature.

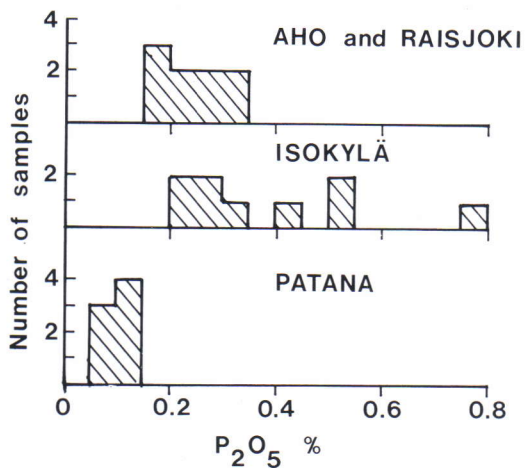


Fig. 5. P_2O_5 frequency diagram of the Evijärvi volcanics. Data from Table 1 and Vaarma (1984).

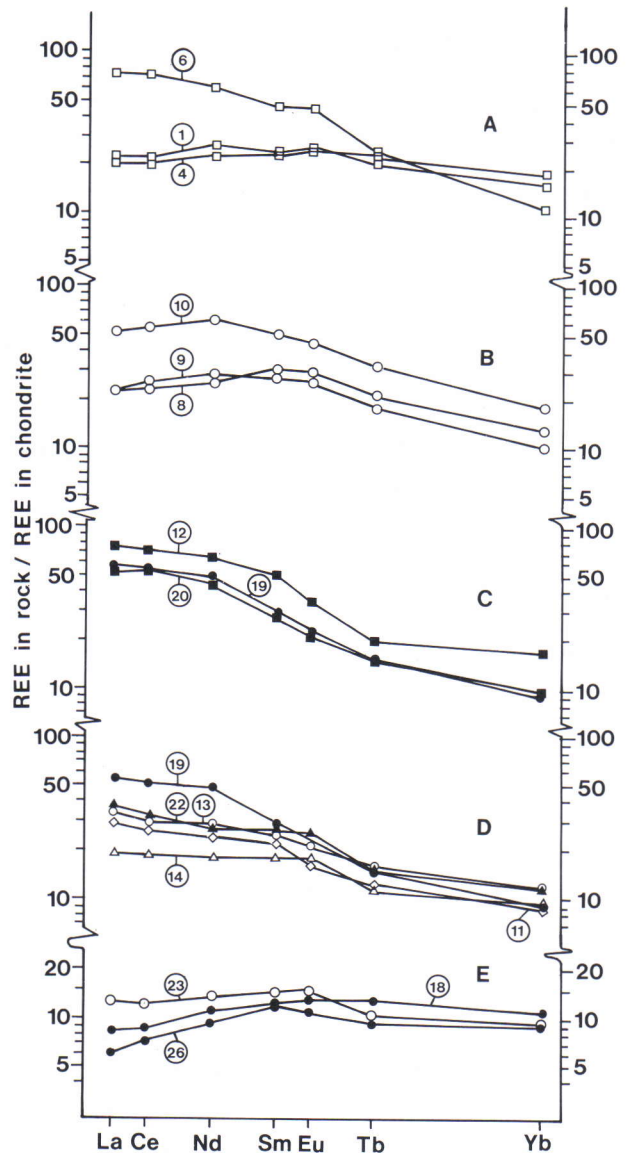


Fig. 6. Chondrite-normalized REE patterns of the Evijärvi volcanics. Data from Table 1. A. Aho formation; B. Raisjoki formation; C. and D. Isokylä formation; E. Patana formation. Chondrite values: Leedeey 6 divided by factor 1.2 (Jahn et al. 1980; Tb from Koljonen & Rosenberg 1975).

Table 1. Chemical composition of the metavolcanic rocks at Evijärvi. Total Fe as FeO*. Oxides and S in weight-%, other elements in ppm. Sample locations are given in Fig. 2 and petrography in Appendix. Major elements were analyzed at the Geological Survey of Finland from fused discs using a Philips 1410/AHP XRF instrument. S, Cr, Zn, Cu, Ni, V, Zr, Sr and Ba were determined from pressed rock powder briquettes with a Philips PW 1400/AHP XRF spectrometer at the Raahelaboratory of Rautaruukki Oy. The Th, U and REE determinations were carried out by instrumental neutron activation analysis at the Reactor Laboratory of the Technical Research Centre of Finland (Rosenberg 1977).

Sample	Aho			Raisjoki			Isokylä						Patana				
	1	4	6	8	9	10	11	12	13	14	19	20	22	16	18	23	26
SiO ₂	49.58	49.92	47.71	50.36	47.61	47.60	44.80	58.26	48.68	49.77	47.96	57.36	52.33	53.98	50.16	51.15	50.33
TiO ₂	2.31	2.54	3.67	2.56	1.89	3.16	1.15	1.52	1.55	1.26	1.25	1.65	0.73	1.07	1.04	1.02	
Al ₂ O ₃	13.27	15.29	13.81	13.27	12.01	12.83	14.17	16.72	17.40	13.88	14.97	17.30	17.05	15.98	13.86	13.91	14.44
FeO	15.31	14.69	14.26	13.83	13.87	15.47	6.54	3.89	7.80	7.24	9.36	5.80	9.65	9.81	11.04	11.96	10.01
MnO	0.23	0.20	0.14	0.19	0.19	0.25	0.15	0.05	0.09	0.14	0.12	0.04	0.15	0.16	0.19	0.21	0.17
MgO	3.94	4.29	5.36	4.26	6.33	3.54	3.70	1.17	5.39	4.55	4.88	2.07	3.45	4.49	6.20	6.48	7.12
CaO	9.23	6.02	5.36	7.34	10.87	8.46	14.60	8.39	12.55	11.98	11.30	6.33	9.47	7.67	10.23	9.97	10.90
Na ₂ O	2.58	3.64	3.98	4.31	3.17	3.30	4.03	4.81	2.21	4.24	3.98	5.83	2.77	3.82	3.37	2.39	3.01
K ₂ O	0.20	0.13	1.78	0.07	0.15	0.16	0.70	1.24	0.28	0.29	0.10	0.21	0.15	0.20	0.05	0.09	0.25
P ₂ O ₅	0.18	0.25	0.29	0.22	0.16	0.32	0.25	0.74	0.50	0.21	0.25	0.48	0.23	0.09	0.11	0.10	0.09
S	0.24	0.03	0.63	0.02	1.06	0.01	1.36	0.93		0.02	0.69	1.63	0.02	0.05	0.01	0.02	0.04
OX.SUM	96.83	96.97	96.36	96.41	96.25	95.09	90.09	96.79	96.45	93.56	94.17	96.67	96.90	96.93	96.28	97.30	97.34
Cr	30	50	870	100	510	80	80	0		230	120	190	0	120	250	200	260
Zn	140	160	160	140	190	160	80	100		70	80	70	140	60	90	100	110
Cu	160	220	210	70	190	90	60	10		20	80	60	10	90	10	60	20
Ni	60	60	430	100	250	90	60	10		120	150	70	30	40	110	100	130
V	620	650	520	520	470	590	210	140		250	240	250	359	290	370	380	370
Zr	150	180	260	190	120	240	130	170		110	120	130	130	60	60	60	60
Sr	110	130	230	130	150	200	200	290		120	220	190	260	260	110	100	110
Ba	60	30	510	80	30	30	220	260		90	70	120	680	90	40	20	230
Th	0.7	0.6	3.1	1.16	0.89	1.57	1.1	15	0.8	0.82	1.1	0.8	0.89			0.36	0.19
U	0.3	0.4	2.5	1.57	3.9	1.23	0.5	2.5	3.2	0.8	0.3	18.5	0.59		0.3		
La	6.9	6.3	23	7	7.3	16.6	9.2	23	10.5	6	17.2	16.9	11.6		2.6	3.9	1.88
Ce	18.1	16.2	59	18.8	21	46	21	58	24	15.2	42	42	27		7	9.9	6
Nd	16.2	13.3	36	15.3	16.9	38	14.5	38	16.9	10.8	28	27	16.3		6.4	8.1	5.6
Sm	4.7	4.5	9	5.9	5.2	9.7	4.2	9.5	4.7	3.5	5.6	5.2	5.3		2.4	2.8	2.3
Eu	1.84	1.84	3.3	2.1	1.82	3.2	1.18	2.5	1.54	1.27	1.66	1.52	1.83		0.93	1.06	0.79
Tb	0.96	1.07	1.14	0.98	0.86	1.51	0.56	0.93	0.75	0.55	0.7	0.71	0.69		0.62	0.5	0.45
Yb	3.2	3.8	2.3	2.7	2.2	3.9	1.84	3.6	2.5	1.93	1.9	1.98	2.5		2.3	2	1.9
FeO*/MgO	3.89	3.42	2.66	3.25	2.19	4.37	1.77	3.33	1.45	1.59	1.92	2.80	2.80	2.18	1.78	1.84	1.41
Ti/V	22.3	23.4	42.3	29.5	24.1	32.1	32.8	65.0		30.2	31.2	30.0	27.5	15.1	17.3	16.4	16.5
La _N /Yb _N	1.42	1.09	6.60	1.71	2.19	2.81	3.30	4.22	2.77	2.05	5.98	5.64	3.06		0.75	1.29	0.65
La _N */Sm _N	0.89	0.85	1.56	0.72	0.86	1.04	1.34	1.48	1.36	1.04	1.87	1.98	1.33		0.66	0.85	0.50

In young basalts, the P content tends to be higher in medium-K and high-K rocks than in low-K rocks (Ewart 1982, Pearce 1982). The P_2O_5 content in young basalts with K_2O content below 0.25% is frequently below 0.2% (Basaltic Volcanism Study Project 1981, references of Fig. 8 of this study). The K_2O content of the Evijärvi basalts and basaltic andesites is mostly below 0.25% (Fig. 4) whereas the P_2O_5 content, excluding those of the Patana formation, tends to exceed 0.2% (Fig. 5). The low-K character of the Evijärvi volcanics may in part be attributed to alteration.

Three samples from Isokylä plot well outside the field of unaltered rocks in Fig. 7. The symbol nearest the CaO/Al_2O_3 apex represents an amygdaloidal rock with about 20% CaO. This sample is the medium-K nearly trachybasaltic rock with a high FeO^*/MgO ratio and about 47% SiO_2 in Fig. 4. The other two Isokylä rocks plotting well outside the field of unaltered rocks are medium-K samples 11 and 12. They contain tremolite and diopside, respectively, as major minerals (Appendix). These features may indicate the addition of carbonate. Apparently, the three rocks have undergone marked changes in com-

position.

The metamorphic grade in the Evijärvi area increases from east to west so that the metamorphic conditions approach high grade around the Aho

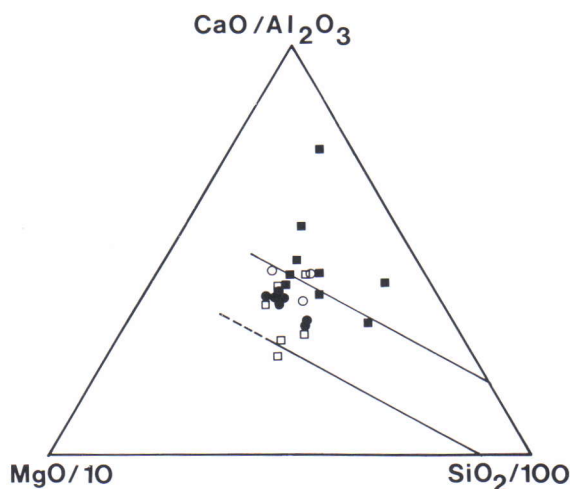


Fig. 7. $MgO/10 - CaO/Al_2O_3 - SiO_2/100$ diagram of the Evijärvi volcanics. Data and symbols as in Fig. 4. The lines define the field of unaltered rocks (Davis et al. 1978).

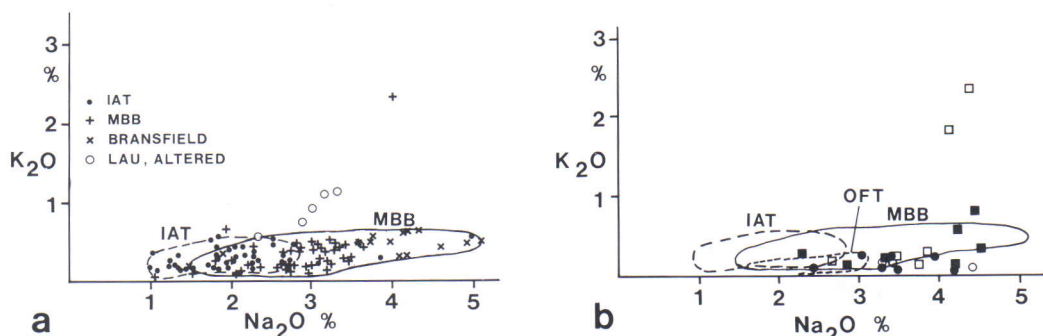


Fig. 8. K_2O vs. Na_2O diagram. **a:** Basalts from island arc tholeiitic series (IAT), marginal basins (MBB), Bransfield Strait marginal basin, and altered basalts from Lau Basin. Data from Ewart & Bryan (1972), Hart et al. (1972), Reay et al. (1974), Ridley et al. (1974), Hawkins (1976), Ewart et al. (1977), Tarney et al. (1977), Saunders & Tarney (1979), Baker (1978), Weaver et al. (1979), and Wood et al. (1980). The sample with about 2.3% K_2O is a genuine alkaline basalt from Shikoku Basin and shows that the MBB comprise rocks plotting above the drawn MBB field. The lower boundary of the MBB field therefore has more significance than the higher-K boundary. **b:** Evijärvi volcanics. Data and symbols as in Fig. 4. The IAT and MBB fields are based on typical island arc tholeiitic basalts and marginal basin basalts (including Bransfield Strait basalts) shown in Fig. 8a. The field of OFT (ocean floor tholeiites) is from Weaver et al. (1979).

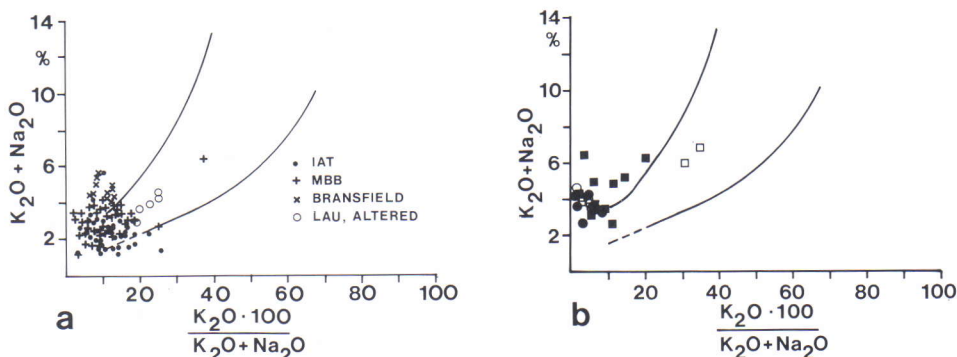


Fig. 9. K_2O+Na_2O vs. $(K_2O/(K_2O+Na_2O)) \cdot 100$ diagram. The continuous lines give the boundaries of the igneous spectrum (Hughes 1973). **a:** IAT and MBB basalts. Data as in Fig. 8a. **b:** Evijärvi volcanics. Data, data processing and symbols as in Fig. 4.

formation. However, because there are low-K rocks also in the east, where medium-grade conditions prevailed, the low K content is probably not attributed to the depletion in K during high-grade metamorphism.

Some marginal basin basalts (MBB) are higher in Na than typical low-K ocean-floor basalts (OFT) and island arc tholeiites (IAT), and they plot outside the igneous spectrum (Figs. 8 and 9). This might indicate alteration caused by sea water in the subaqueous volcanic rocks. However, since the Quaternary MBB of Bransfield Strait are subaerial, their composition (Figs. 8 and 9) cannot be attributed to subaqueous alteration. Thus the Na₂O contents of about 4-5% in basalts low in K do not necessarily indicate alteration

and the igneous spectrum of Hughes (1973) needs revision. Consequently, the relatively high Na content in the low-K Evijärvi volcanics may in part be a primary feature. Some samples, however, plot well below the field of MBB (Fig. 8) and alteration possibly affected these rocks.

The low-K basalts of Aho and Raisjoki show slightly convex LREE-enriched REE patterns. Although such features are not common in fresh basalts, they do exist (p. 174 in Basaltic Volcanism Study Project 1981, Saunders 1984). Thus the rocks were not necessarily affected by alteration.

The high K content in the two trachybasaltic tuffs or tuffites from Aho is petrographically explained by biotite occurring as a major constituent;

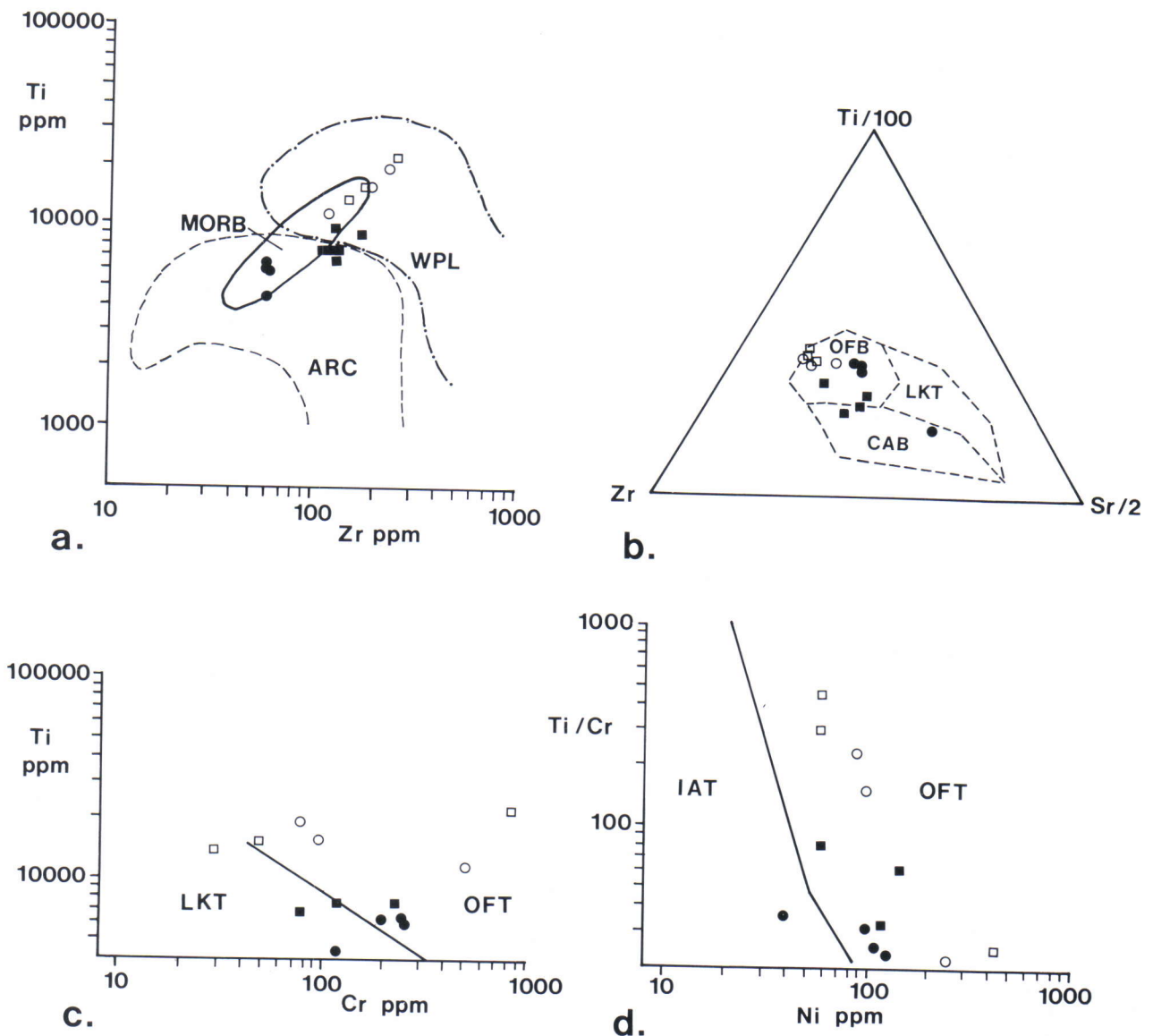


Fig. 10. Tectonomagmatic discrimination diagrams of the Evijärvi volcanics. Data from Table 1, symbols as in Fig. 4. a: MORB = mid-ocean ridge basalts, ARC = volcanic arc lavas, WPL = within plate lavas (Pearce 1982). b: basalts and basaltic andesites only; OFB = ocean-floor basalts, LKT = low-potassium tholeiites, CAB = calc-alkaline basalts (Pearce & Cann 1973). c: basalts and basaltic andesites only; LKT = island-arc low-K tholeiites, OFT = ocean-floor tholeiitic basalts (Pearce 1975). d: basalts and basaltic andesites only; IAT = island-arc tholeiites, OFT = ocean-floor tholeiites (Beccaluva et al. 1979).

these compositions are not caused by sericitization or K-feldspathization. The P_2O_5 content in these rocks is lower than in alkaline basalts on the average (Pearce 1982, Mullen 1983). This could indicate

mixing with pelites high in K and low in P. However, mixing with pelites cannot explain the high contents of Ti, Zr, Cr and Ni in sample 6. The two trachybasaltic rocks may represent primary igneous compositions.

TECTONOMAGMATIC AFFINITIES

Elements such as Ti, Zr, V, Ni, Th and REE are less mobile than, e.g., Si, K and Rb during alteration and metamorphism (Condie 1981, Pharaoh & Pearce 1984, Saunders & Tarney 1984). They are therefore of special interest in discussing the paleotectonic environment of metamorphosed volcanic rocks (e.g. Pearce & Cann 1973).

The basalts from the Aho and Raisjoki formations are relatively rich in Ti and Zr and plot partly in the common field of mid-ocean ridge basalts (MORB) and within-plate lavas (WPL) in the Ti vs. Zr diagram (Fig. 10). Two samples plot in the WPL field only. Also the Zr-Ti-Sr, Ti vs. Cr and Ti/Cr vs. Ni diagrams indicate non-arc affinities (Fig. 10). In the Ti vs. V diagram (Fig. 11), the rocks, with one exception, plot

outside all the fields shown. With Ti/V ratios ranging from 22 to 42 (Table 1), the rocks would resemble MORB or back-arc basin basalts (Ti/V is below 50) rather than oceanic within plate basalts (WPB) in which Ti/V exceeds 40 (Shervais 1982). It should be noted, however, that the WPB data of Shervais are scanty. The dominantly slight LREE enrichments in the Aho and Raisjoki basalts indicate similarities with T-type MORB or subalkaline (tholeiitic) WPB (Pearce 1982). The marked LREE enrichment in the trachybasaltic sample 6, together with the high contents of Ti and Zr, makes this sample resemble alkaline WPB, although it is, as discussed above, rather poor in P.

The volcanic rocks of the Patana formation are low in Zr and plot in the common field of MORB and arc lavas in the Ti vs. Zr diagram (Fig. 10). They are more like MORB than arc basalts in the Zr-Ti-Sr, Ti vs. Cr and Ti/Cr vs. Ni diagrams. In having Ti/V ratios between 15 and 20 (Table 1), they resemble arc tholeiites rather than MORB (Shervais 1982) but, in fact, also MORB comprise rocks with Ti/V ratios of between 15 and 20 (Fig. 11). The LREE depleted REE patterns of samples 18 and 26 resemble the REE patterns of N-type MORB or IAT.

The volcanic rocks of the Isokylä formation plot near the MORB/ARC/WPL triple point in the Ti vs. Zr diagram (Fig. 10). In the Zr-Ti-Sr, Ti/Cr vs. Ni and Ti vs. Cr diagrams, they plot in the fields of both MORB and arc lavas. The Ti/V ratios in the Isokylä basalts and basaltic andesites are 27-33 (Table 1), and in the Ti vs. V diagram the rocks plot outside the arc field (Fig. 11). With their consistent LREE enrichment, these rocks differ from IAT and N-type MORB. REE patterns such as these are found in E-type MORB, various WPB and calc-alkaline arc volcanics.

In conclusion, the Evijärvi volcanics show a variation in tectonomagmatic affinities. Some of the rocks resemble N-type MORB, some samples show similarities with arc volcanics, and some resemble WPB and T-type MORB. Rocks plotting in arc fields in the discrimination diagrams are more common at Patana and Isokylä than at Aho and Raisjoki. However, the arc affinities are not pronounced even at Patana and Isokylä.

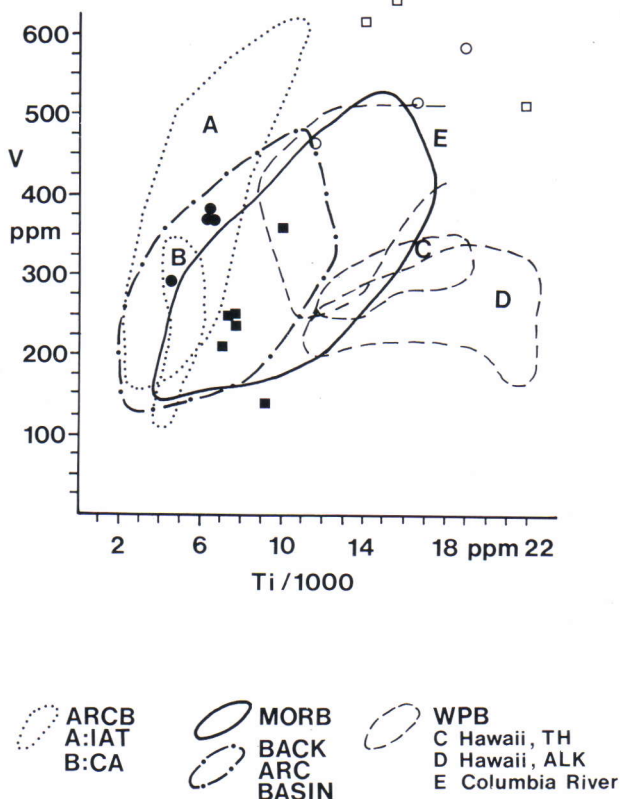


Fig. 11. Ti vs. V diagram of the Evijärvi basalts and basaltic andesites. Data from Table 1, symbols as in Fig. 4. Fields are based on Shervais (1982).

DISCUSSION

In addition to the Evijärvi area, mafic volcanic rocks not showing pronounced arc affinities are known in the western CSS. The Seinäjoki-Vittinki basalts (Fig. 1) have Ti and Zr contents resembling more those in MORB and WPL than those in arc basalts (see data in Mäkitie & Lahti 1992). In Sweden, the Ullånger and Varuträsk basalts (see Fig. 1), are similar to N-type MORB and tholeiitic WPB (Pharaoh & Pearce 1984). In addition, the Nagu-Korpo basalts in the Southern Svecofennian Subprovince (Fig. 1) resemble the CSS basalts considered; they occur as narrow horizons within a thick graywacke-mudstone sequence, they show frequently pillow structures and they do not have arc affinities (Ehlers et al. 1986). The non-arc affinity of the Ullånger, Varuträsk and Nagu-Korpo basalts is corroborated by the absence of Ta and Nb depletions in these rocks. We speculate that this may concern the Evijärvi and Seinäjoki-Vittinki basalts as well.

The abundance of turbiditic sedimentary rocks and the absence of oceanic crust indicate that the CSS was not a wide oceanic basin. Rather, it was a marginal basin between volcanic arcs (Hietanen 1975), between arc and continent, or between continental fragments. Marginal basin basalts display a wide variation in tectonomagmatic affinities. For

instance, young back-arc basalts range from those indistinguishable from N-type MORB to those resembling calc-alkaline basalts (Saunders & Tarney 1984). So, the character and compositional variation of the Evijärvi and the western CSS basalts might be attributed to the evolution in a marginal basin.

The Nagu-Korpo basalts seem to be older than the arc-type volcanic rocks nearby (Ehlers et al. 1986). Also the Evijärvi volcanic rocks and other western CSS basalts are possibly older than the Svecofennian arc-type volcanic rocks. In any case, the volcanics at Evijärvi are older than the 1883 Ma tonalite. The Ullånger and Varuträsk basalts might be younger; e.g. the Ullånger basalt seems to be stratigraphically above a 1874 Ma rhyolite (interpretation from Lundqvist 1987). However, considering the scarcity of the top of the strata observations (Lundqvist 1987) as well as the character of the rock type at Ullånger (amphibolitic inclusion in gneiss; Pharaoh & Pearce 1984), it is possible that the Swedish CSS basalts are rather contemporaneous with the Evijärvi basalts. Thus, the mafic volcanic rocks in the Swedish CSS, at Evijärvi and at Seinäjoki-Vittinki may represent the early stages of the evolution which led to the development of the ca. 1.9 Ga volcanic arcs of the Svecofennian Domain.

ACKNOWLEDGEMENTS

We thank Fredrik Pipping for his support during all the stages of this study. He, Asko Kontinen, Anu Karessuo and Leena-Marja Kokko critically read the manuscript. The Th, U and REE analyses were financed by Research Project 24/001 of the Academy of Finland, led by Tapio Koljonen. The other trace

element determinations were financed by the Academy of Finland via IGCP Project 179, led by Kauko Meriläinen. The figures were drawn by Minna Ahokas and Elsa Järvimäki. The English language was revised by Paul Sjöblom.

REFERENCES

- Baker, P. E. 1978.** The South Sandwich Islands: III Petrology of the volcanic rocks. Brit. Antarct. Surv. Sci. Rept. 93, 34 p.
- Basaltic Volcanism Study Project 1981.** Basaltic Volcanism on the Terrestrial Planets. Pergamon Press, New York, 1286 p.
- Beccaluva, L., Ohnenstetter, D. & Ohnenstetter, M. 1979.** Geochemical discrimination between ocean-floor and island-arc tholeiites - application to some ophiolites. Can. J. Earth Sci. 16, 1874-1882.
- Condie, K.C. 1981.** Archean Greenstone Belts. Amsterdam: Elsevier, 434 p.
- Davis, A., Blackburn, W. H., Brown, W. R. & Ehmann, W. D. 1978.** Trace element geochemistry and origin of late Precambrian-early Cambrian Catoctin greenstones of the Appalachian Mountains. Univ. California at Davies, Davies, Calif. Rep. (unpublished)
- Ehlers, C., Lindroos, A. & Jaanus-Järkkälä, M. 1986.** Stratigraphy and geochemistry in the Proterozoic mafic volcanic rocks of the Nagu-Korpo area, SW Finland. Precambrian Res. 32, 297-315.
- Ewart, A. 1982.** The mineralogy and petrology of Tertiary-Recent orogenic volcanic rocks: with special reference to the andesitic-basaltic compositional range. In: Thorpe, R.S. (ed.) Andesites, Orogenic Andesites and Related Rocks. Chichester: Wiley & Sons, 25-95.
- Ewart, A. & Bryan, W.B. 1972.** Petrography and geochemistry of the igneous rocks from Eua, Tongan islands. Geol. Soc. Am. Bull. 83, 3281-3298.
- Ewart, A., Brothers, R. N. & Mategan, A. 1977.** An outline of the geology and geochemistry, and the possible petrogenetic evolution of the volcanic rocks of the Tonga-Kermadec-New

- Zealand island arc. *J. Volcanol. Geotherm. Res.* 2, 205-250.
- Gaál, G. & Gorbatshev, R. 1987.** An outline of the Precambrian evolution of the Baltic Shield. *Precambrian Res.* 35, 15-52.
- Gill, J.B. 1981.** *Orogenic Andesites and Plate Tectonics*. Berlin: Springer-Verlag, 390 p.
- Helovuori, O. 1979.** Geology of the Pyhäsalmi ore deposit. *Econ. Geol.* 74, 1084-1101.
- Hietanen, A. 1975.** Generation of potassium-poor magmas in the northern Sierra Nevada and the Svecofennian of Finland. *J. Res. U.S. Geol. Surv.* 3, 631-645.
- Hughes, C. J. 1973.** Spilites, keratophyres, and the igneous spectrum. *Geol. Mag.* 109, 513-527.
- Huhma, H. 1986.** Sm-Nd, U-Pb and Pb-Pb isotopic evidence for the origin of the early Proterozoic Svecokarelian crust in Finland. *Geol. Surv. Finland, Bull.* 337, 48 p.
- Jahn, B.-M., Auvray, B., Blais, S., Capdevila, R., Cornichet, J., Vidal, F. & Hameurt, J. 1980.** Trace element geochemistry and petrogenesis of Finnish greenstone belts. *J. Petrol.* 21, 201-244.
- Kähkönen, Y. 1987.** Geochemistry and tectonomagmatic affinities of the metavolcanic rocks of the early Proterozoic Tampere Schist Belt, southern Finland. *Precambrian Res.* 35, 295-311.
- Kähkönen, Y. 1989.** Geochemistry and petrology of the metavolcanic rocks of the early Proterozoic Tampere Schist Belt, southern Finland. *Geol. Surv. Finland, Bull.* 345, 104 p.
- Koistinen, T.J. 1981.** Structural evolution of an early Proterozoic strata-bound Cu-Co-Zn deposit, Outokumpu, Finland. *Trans. R. Soc. Edinburgh Earth Sci.* 72, 115-158.
- Koljonen, T. & Rosenberg, R.J. 1975.** Rare earth elements in middle Precambrian volcanic rocks of Finland, with a discussion of the origin of the rocks. *Bull. Geol. Soc. Finland* 47, 127-138.
- Kontinen, A. 1987.** An early Proterozoic ophiolite -the Jormua mafic-ultramafic complex, northeastern Finland. *Precambrian Res.* 35, 313-341.
- Korsman, K., Hölttä, P., Hautala, T. & Wasenius, P. 1984.** Metamorphism as an indicator of evolution and structure of the crust in eastern Finland. *Geol. Surv. Finland, Bull.* 328, 40 p.
- Latvalahti, U. 1979.** Cu-Zn-Pb ores in the Aijala-Orijärvi area, Southwest Finland. *Econ. Geol.* 74, 1035-1059.
- Le Bas, M.J., Le Maitre, R.W., Streckeisen, A. & Zanettin, B. 1986.** A chemical classification of volcanic rocks based on the total alkali-silica diagram. *J. Petrol.* 27, 745-750.
- Lundqvist, Th. 1987.** Early Svecofennian stratigraphy of southern and central Norrland, Sweden and the possible existence of an Archean basement west of the Svecokareliides. *Precambrian Res.* 35, 343-352.
- Mäkelä, K. 1980.** Geochemistry and origin of Haveri and Kiipu, Proterozoic strata-bound volcanogenic gold-copper and zinc mineralizations from southwestern Finland. *Geol. Surv. Finland, Bull.* 310, 79 p.
- Mäkitie, H. & Lahti, S.I. 1992.** Seinäjoen kartta-alueen kallioperä. Summary: Pre-Quaternary rocks of the Seinäjoki map-sheet area. Geological map of Finland 1:100 000. Explanation to the maps of Pre-Quaternary Rocks, sheet 2222 Seinäjoki, 60 p.
- Miyashiro, A. 1974.** Volcanic rock series in island arcs and active continental margins. *Am. J. Sci.* 274, 321-355.
- Mullen, E.D. 1983.** MnO/TiO₂/P₂O₅: a minor element discriminant for basaltic rocks of oceanic environments and its implications for petrogenesis. *Earth Planet. Sci. Lett.* 62, 53-62.
- Patchett, J. & Kouvo, O. 1986.** Origin of continental crust of 1.9-1.7 Ga age: Nd isotopes and U-Pb zircon ages in the Svecokarelian terrains of South Finland. *Contrib. Mineral. Petrol.* 92, 1-12.
- Patchett, P.J., Kouvo, O., Hedge, C.J. & Tatsumoto, M. 1981.** Evolution of continental crust and mantle heterogeneity: evidence from Hf isotopes. *Contrib. Mineral. Petrol.* 78, 279-297.
- Pearce, J.A. 1975.** Basalt geochemistry used to investigate past tectonic environments on Cyprus. *Tectonophysics* 25, 41-67.
- Pearce, J.A. 1982.** Trace element characteristics of lavas from destructive plate margins. In: Thorpe, R.S. (ed.) *Andesites, Orogenic Andesites and Related Rocks*. Chichester: Wiley & Sons, 525-548.
- Pearce, J.A. & Cann, J.R. 1973.** Tectonic setting of basic volcanic rocks determined using trace element analyses. *Earth Planet. Sci. Lett.* 19, 290-300.
- Pharaoh, T.C. & Pearce, J.A. 1984.** Geochemical evidence for the geotectonic setting of early Proterozoic metavolcanic sequences in Lapland. *Precambrian Res.* 25, 283-308.
- Reay, A., Rooke, J.M., Wallace, R.C. & Whelan, P. 1974.** Lavas from Niuafou Island, Tonga, resemble ocean-floor basalts. *Geology* 2, 605-606.
- Ridley, W.I., Rhodes, J.M., Reid, A.M., Jakeš, P., Shis, C. & Bass, M.N. 1974.** Basalts from Leg 6 of the Deep-Sea Drilling Project. *J. Petrol.* 15, 140-159.
- Rosenberg, R. J. 1977.** Instrumental neutron activation analysis as a routine method for rock analysis. Technical Research Centre of Finland. Electrical and nuclear technology. Publication 19.
- Saunders, A.D. 1984.** The rare earth element characteristics of igneous rocks from the ocean basins. In: Henderson, P. (ed.) *Rare Earth Element Geochemistry*. Amsterdam: Elsevier, 205-236.
- Saunders, A.D. & Tarney, J. 1984.** Geochemical characteristics of basaltic volcanism within back-arc basins. In: Kokelaar, B.P. & Howells, M.F. (eds.) *Marginal Basin Geology*. Oxford: Blackwell, 59-76.
- Saunders, A.D. & Tarney, J. 1979.** The geochemistry of basalts from a back-arc spreading centre in the East Scotia Sea. *Geochim. Cosmochim. Acta* 43, 555-572.
- Shervais, J.W. 1982.** Ti-V plots and the petrogenesis of modern and ophiolitic lavas. *Earth and Planet. Sci. Lett.* 59, 101-118.
- Simonen, A. 1980.** The Precambrian in Finland. *Geol. Surv. Finland, Bull.* 304, 58 p.
- Tarney, J. & Windley, B.F. 1977.** Chemistry, thermal gradients and the evolution of the lower continental crust. *J. Geol. Soc. Lond.* 134, 153-172.
- Vaarma, M. 1984.** Pohjanmaan liuskeyvyöhykkeen geologia Evijärven alueella. M.Sc. thesis, Univ. Helsinki, 143 p. (unpublished, in Finnish)
- Vaarma, M. & Pipping, F. in prep.** Alajärven ja Evijärven kartta-alueiden kallioperä. Summary: Pre-Quaternary rocks of the Alajärvi and Evijärvi map-sheet areas. Explanation to the maps of Pre-Quaternary rocks, sheets 2313 and 2314. Geological map of Finland 1 : 100 000.
- Weaver, S.D., Saunders, A.D., Pankhurst, R.J. & Tarney, J. 1979.** A geochemical study of magmatism associated with the initial stages of back-arc spreading. The Quaternary volcanics of Bransfield Strait, from South Shetland Islands. *Contrib. Mineral. Petrol.* 68, 151-169.
- Wood, D.A., Joron, J.-L., Marsh, N.G., Tarney, J. & Treuil, M. 1980.** Major- and trace-element variations in basalts from the North Philippine Sea drilled during Deep Sea Drilling Project Leg 58: A comparative study of back-arc-basin basalts with lava series from Japan and mid-ocean ridges. In: deVries Klein, G. et al. (eds.) *Initial Reports of the Deep Sea Drilling Project, 58*. Washington D.C.: U.S. Government Printing Office, 873-894.

APPENDIX. Petrographic data of the Evijärvi metavolcanic rocks. Chemical compositions are given in the Table 1 and sample locations in Fig. 2. Major constituents are marked with capital initials, minor constituents and accessories with small ones. Qz = quartz, Pl = plagioclase (An_{x} = anorthite content), Kfp = potassium feldspar, Hb = hornblende, Tre = tremolite, Di = diopside, Bt = biotite, sph = sphene, opq = opaque, chl = chlorite, epid = epidote, carb = carbonate, seric = sericite, sauss = saussurite, zr = zircon.

No. of sample	Rock	Constituents	Texture	Sample location
1.	Mafic pillow lava	Hb, Pl(An_{42}), Qz, Opq, Tre, sph, zr.	Nematoblastic, fine to medium-grained, weakly oriented	Aho x=7029.30, y=472.62
4.	Mafic pillow lava	Hb, Tre, Qz, Pl(An_{39-54}), Opq, bt, sph, carb.	Nematoblastic, fine to medium-grained	x=7035.78, y=473.38
6.	Mafic stratified tuff	Hb, Qz, Bt, Pl, Opq, carb, sph, zr.	Nematoblastic, fine to medium-grained, oriented, rich in bt	x=7034.36, y=472.55
8.	Mafic pillow lava	Hb, Pl(An_{25}), Qz, Opq, carb.	Nematoblastic, fine-grained	Raisjoki x=7033.76, y=480.98
9.	Mafic hyalobreccia	Hb, Qz, Pl, Opq, bt, carb, sph.	Grano-nematoblastic, heterogeneous, fine to medium-grained	x=7034.52, y=479.12
10.	Massive basalt	Hb, Qz, Opq, carb.	Nematoblastic, oriented, fine-grained	x=7039.84, y=479.46
11.	Basalt	Hb, Tre, Qz, Bt, Opq, pl, chl, sph, zr.	Nematoblastic	Isokylä x=7038.74, y=481.17
12.	Andesite	Di, Qz, Pl(An_{63}), Kfp, Opq, chl, bt, sph, epid, seric.	Granoblastic, medium-grained, oriented	x=7037.67, y=483.68
13.	Basalt	Hb, Pl, Qz, bt, opq, carb, chl.	Nematoblastic, fine-grained	x=7036.03, y=485.29
14.	Plagioclase-phyric mafic pillow lava	Hb, Pl(An_{24-50}), Qz, Carb, opq, chl, sauss.	Blastoporphyritic, nematoblastic, fine to medium-grained	x=7036.84, y=486.06
19.	Plagioclase-phyric basalt	Hb, Pl(An_{42}), Qz, opq, carb, bt, sph, seric.	Blastoporphyritic, nematoblastic medium-grained, oriented	x=7033.91, y=487.34
20.	Plagioclase-phyric andesite	Hb, Pl, Qz, Chl, Opq, carb, sph.	Blastoporphyritic, nematoblastic, amygdaloidal, fine to medium-grained	x=7032.13, y=488.36
22.	Basaltic andesite	Hb, Pl, Qz, Opq, sph, chl, carb.	Nematoblastic, medium-grained, oriented	x=7031.34, y=487.95
16.	Basaltic andesite	Hb, Pl(An_{23}), Qz, Bt, Chl	Nematoblastic, medium-grained, oriented	Patana x=7035.18, y=485.35
18.	Mafic pillow lava	Hb, Pl(An_{35-40}), Qz, Opq, carb, seric.	Nematoblastic, fine-grained	x=7034.08, y=485.88
23.	Basaltic andesite	Hb, Pl(An_{40}), Qz, Opq.	Nematoblastic, fine to medium-grained	x=7030.56, y=489.65
26.	Basalt	Hb, Pl(An_{25}), Qz, Opq sph.	Nematoblastic, fine-grained	x=7027.45, y=492.14

GEOCHEMISTRY OF CALC-ALKALINE METAVOLCANIC ROCKS IN THE PARIKKALA-PUNKAHARJU AREA, SOUTHEASTERN FINLAND

by
Ahti Viluksela

Viluksela, Ahti 1994. Geochemistry of calc-alkaline metavolcanic rocks in the Parikkala-Punkaharju area, southeastern Finland. *Geological Survey of Finland, Special Paper 19*, 61–69, 7 figures and one table.

The Parikkala-Punkaharju area in southeastern Finland consists mostly of pelitic metasediments and intrusive rocks of granitic composition. Metavolcanic rocks occur as separate formations in a zone surrounded by the metasediments and the intrusions. The composition of the metavolcanic rocks varies from basaltic to rhyolitic with dacites being most common rocks. In some formations, trachytes and trachyandesites are also present. Geochemically the metavolcanic rocks are calc-alkaline. Basalts and basaltic andesites resemble the basalts of mature young volcanic arcs. The composition of the rocks, together with some of the tectonomagmatic diagrams and the trace-element pattern of basalts suggest that these rocks were erupted in a tectonic setting with characteristics very much similar to that of young active continental margins.

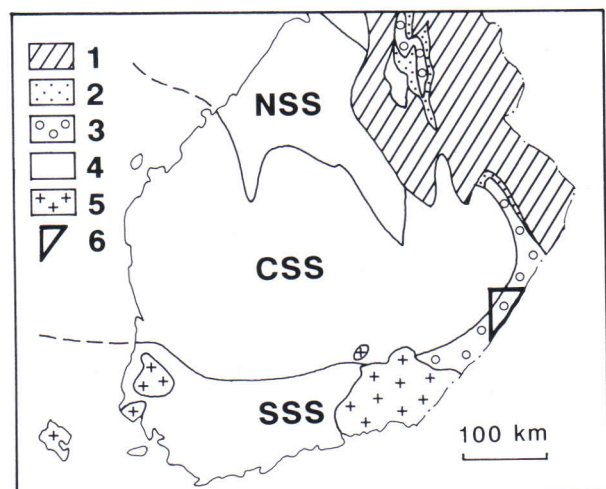
Key words (GeoRef Thesaurus, AGI): metavolcanic rocks, dacites, andesites, basalts, geochemistry, calc-alkalic composition, island arcs, Proterozoic, Paleoproterozoic, Parikkala, Uukuniemi, Punkaharju, Finland

Ahti Viluksela, Paikkalinnuntie 2, FIN- 02660 Espoo, Finland

INTRODUCTION

The Parikkala-Punkaharju area in southeastern Finland is part of the Paleoproterozoic Svecofennian Domain (Fig.1). This study deals with the geochemical features and tectonomagmatic affinities of acid, intermediate and basic metavolcanic rocks of the Parikkala-Punkaharju area, based on their major and trace-element compositions. Petrographical data and results of chemical analyses are available in detail in Nykänen (1983) and Viluksela (1988).

Fig. 1. Geological setting of the Parikkala-Punkaharju area (modified from Gaál & Gorbatshev 1987). 1 = Archean granitoids and gneisses, 2 = Jatulian Group (mostly quartzites). Svecofennian Domain: 3 = Kalevian Group (metasediments); 4 = Svecofennian granitoids and gneisses; NSS = Northern Svecofennian Subprovince; CSS = Central Svecofennian Subprovince; SSS = Southern Svecofennian Subprovince. 5 = rapakivi granite, 6 = study area.



GEOLOGICAL BACKGROUND AND SETTING

The prevailing rock units in the Parikkala-Punkaharju area are pelitic metasediments and large bodies of intrusive rocks (Fig. 2). The metasediments are mainly migmatitic garnet-cordierite gneisses metamorphosed under upper amphibolite or granulite facies conditions (Nykänen 1983). Most of the intrusive rocks are granitoids but there are also intrusions of diorite and gabbro with associated peridotitic portions. Gabbros, diorites, tonalites, quartz diorites and granodiorites belong to the Svecokarelian synorogenic group (1900-1860 Ma) and granites to

the late-orogenic group (1830-1800 Ma) (Nykänen 1983). The granitoids plot in the I-type field in the Na_2O vs. K_2O diagram (Viluksela 1988).

Between the metapelites and the intrusive rocks there is a narrow, discontinuous zone consisting of acid to basic metavolcanic rocks, often referred to as the leptite-amphibolite zone. According to Nykänen (1983), this zone forms the lowermost stratigraphic unit in the area and it is overlain by the metapelites. The intrusive rocks crosscut both the metavolcanic rocks and the metapelites.

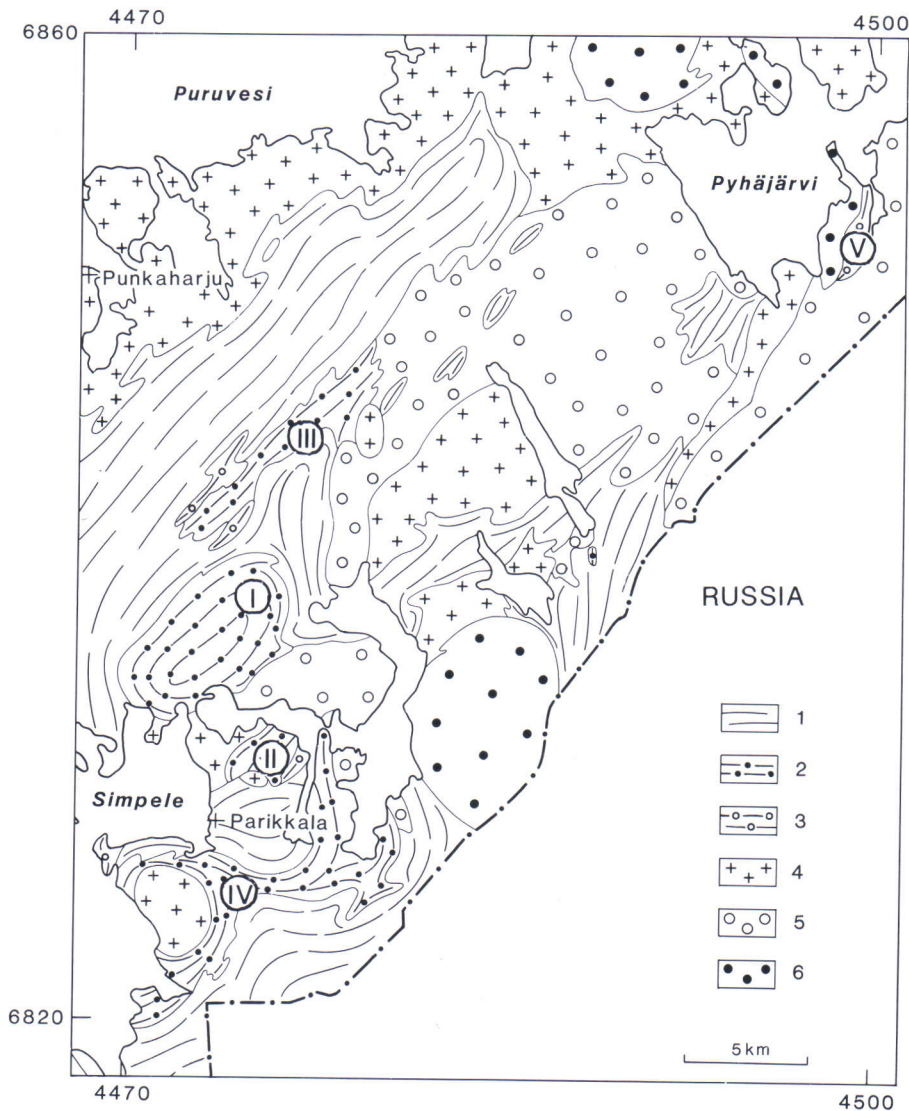


Fig. 2. Geology of the Parikkala-Punkaharju area. 1 = mica gneisses and schists, 2 = acid and intermediate metavolcanic rocks., 3 = basic metavolcanic rocks, 4 = granite, 5 = granodiorite, tonalite and quartz diorite, 6 = diorite, gabbro and peridotite. Simplified after Nykänen (1980, 1982). The Subareas examined in this study are: I = Savikumunsalo, II = Eskola, III = Matko, IV = Oravaniemi and V = Ukuniemi.

METAVOLCANIC ROCKS

The metavolcanic rocks occur in a zone about 30 km long, which comprises several separate formations. The paucity of basic rocks in comparison with acid and intermediate rocks is readily apparent from the lithological map (Fig. 2). According to the TAS diagram (Fig. 4 a) most of the metavolcanic rocks are dacites, with smaller amounts of rhyolites, andesites, basaltic andesites, basalts and more alkali-rich trachytes and trachyandesites. In the remainder of this text these rock names are used without the meta-prefix.

Within the metavolcanite zone, rhyolites and dacites of mainly pyroclastic origin form the stratigraphically lowermost unit. These are overlain by andesitic and basaltic lavas and volcanoclastic deposits, with a volcanic conglomerate being uppermost. Clastic sedimentary material is in places abundant in the metavolcanics. Metavolcanic rocks also occur as intercalations amongst the overlying metapelites.

Lithologies within the various formations show significant mutual variations in composition. In subarea I (Savikummunsalo; Fig. 2), the main rock type is dacite, although trachyandesitic rocks also occur in the marginal zone. Stratification and amygdaloidal, brecciated or fragmental features are sometimes present. Subarea II (Eskola) consists almost entirely of reddish, in places weakly stratified trachyte with intercalations of trachyandesite. In Subarea III (Matko), the rocks vary in composition from basalts to rhyolites, with dacites being the most abundant. In the southern end of the formation basalts and basaltic andesites form small, separate bodies around dacites and rhyolites. Basalts sometimes show

banding due to the presence of diopside. Andesites and basalts also occur as intercalations amongst the dacites. In addition, some picritic ultramafic intercalations are present. The latter probably represent the basal cumulus parts of basalt flows. Alternating layers of varying composition reflect changes in magma composition. Apparent lava beds can in some cases be distinguished from tuff-like, banded layers. Fragmental volcanic features such as agglomerate and lapilli as well as spherulites are visible in some places. In Subarea IV (Oravaniemi), the rock types vary from dacites in the west to trachytes in the east. Metasedimentary intercalations and sometimes gradational transitions into metasediments are common features. Subarea V (Uukuniemi) consists almost entirely of dark green basaltic uralite porphyrite with stratification and breccia and sometimes ellipsoidal orbicular fragments possibly representing volcanic ejecta.

The main minerals in the rhyolites and dacites are plagioclase (An_{20-30}), quartz, biotite and/or hornblende. They are usually light gray, fine-grained rocks, although they are locally coarser. Trachytes are reddish in color and contain K-feldspar as the main mineral, in addition to plagioclase (An_{25-30}), quartz and hornblende. Andesites, basaltic andesites and basalts consist of plagioclase (An_{40-60}) and hornblende with occasional biotite. The main minerals in the trachyandesites are plagioclase (An_{30}), hornblende, K-feldspar and sometimes sphene. Common accessory minerals occurring in variable amounts in different rock types include K-feldspar, apatite, chlorite, muscovite, carbonate, opaques, sphene and zircon.

GEOCHEMISTRY AND TECTONOMAGMATIC AFFINITIES

Effects due to the possible alteration of rocks can be avoided to some extent by selecting the samples carefully and by using "immobile" elements in the classification (e.g. Pearce and Cann 1973). The geochemical alteration of magmatic rocks can be examined by a ternary diagram proposed by Davis et al. (1978). Practically all the Parikkala-Punkaharju metavolcanic rocks plot in the field of unaltered rocks (Fig. 3).

Fig. 3. Diagram for assessing alteration of magmatic rocks of the Parikkala-Punkaharju area. Unaltered rocks plot between the lines (Davis et al. 1978). Symbols: filled circles = Subarea I, filled squares = Subarea II, open circles = Subarea III, open squares = Subarea IV, crosses = Subarea V.

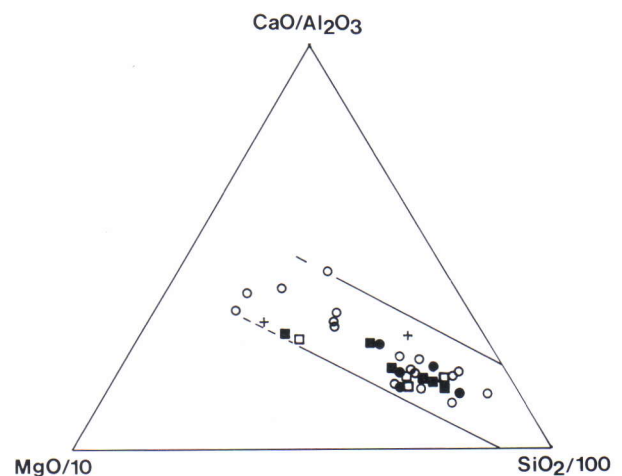


Table 1. Selected geochemical analyses of metavolcanic rocks from the Parikkala-Punkaharju area. Data from Viluksela (1988) and Nykänen (1983).

	1	2	3	4	5	6	7	8	9	10	11	12
SiO ₂	67.36	65.49	55.33	50.55	45.47	53.82	58.12	67.17	71.31	65.05	67.67	49.58
TiO ₂	0.53	0.37	1.44	1.36	1.77	1.51	0.90	0.71	0.67	0.62	0.32	1.16
Al ₂ O ₃	14.68	15.89	16.16	15.57	15.96	16.58	15.25	15.14	15.57	16.69	15.32	13.56
Fe ₂ O ₃ *	3.95	2.88	9.28	10.30	14.53	10.04	7.04	3.88	1.89	3.81	2.47	11.75
MnO	0.06	0.06	0.12	0.15	0.31	0.17	0.11	0.05	0.03	0.03	0.05	0.21
MgO	1.50	1.82	2.71	4.01	7.04	3.93	4.40	2.36	0.60	2.20	1.32	9.10
CaO	2.97	2.80	4.78	11.24	12.41	7.87	6.89	4.09	1.89	3.30	2.66	8.79
Na ₂ O	3.76	5.83	5.52	3.05	0.83	3.46	3.08	3.82	6.18	4.61	5.25	1.67
K ₂ O	3.05	3.00	1.91	1.19	0.32	0.74	0.73	1.62	1.32	2.10	2.94	2.06
P ₂ O ₅	0.17	0.25	0.40	0.58	0.31	0.26	0.23	0.23	0.01	0.12	0.17	0.41
	-----	-----	-----	-----	-----	-----	-----	-----	-----	-----	-----	-----
Total	98.03	98.39	97.65	98.00	98.95	98.38	96.75	99.07	99.47	98.53	98.17	98.21
Sr	270	1540		490	334	290	503	230	230	370	1310	320
Rb	100	50		80		30		120	40	90	60	80
Ba	600	1740		380		300		410	230	780	1490	390
Th	10	10				10		10	10	20	10	
Nb	10	10		20	770	10		20	10	10	10	20
Zr	250	160		200	153	210	133	310	360	190	130	110
Y				23	34		17		6			
Cr	110	80		230		180	123	90	90	230	90	470
Ni	20	30		90		90	76	20	10	50	20	130
Co	10	10		30	174	40		10		10		50
V	60	50		190		210	133	90	30	120	30	230
La	35	44				16.8		45		39	33	17.7
Ce	53	74				27.5		76		61	51	31
Nd	20	30				14.9		36		29	20	21
Sm	4.1	5.0				5.2		6.7		5.1	3.5	4.5
Eu	0.92	1.33				2.13		1.17		1.04	0.93	1.23
Tb	0.43	0.33				0.70		0.78		0.51	0.26	0.47
Yb	1.68	0.64				2.2		2.7		1.91	0.54	1.02
Lu	0.29	0.16				0.52		0.43		0.36	0.12	0.19

- 1 = Dacite (I), x = 6834200, y = 4470350
 2 = Trachyte (II), x = 6829300, y = 4475970
 3 = Trachyandesite (II), x = 6830960, y = 4475600
 4 = Basalt (III), x = 6840230, y = 4472080
 5 = Basalt (III), x = 6844920, y = 4477940
 6 = Basaltic andesite (III), x = 6839200, y = 4473550
 7 = Andesite (III), x = 6840940, y = 4472730
 8 = Dacite (III), x = 6839840, y = 4472710
 9 = Rhyolite (III), x = 6842180, y = 4475090
 10 = Dacite (IV), x = 6821870, y = 4473210
 11 = Trachyte (IV), x = 6825710, y = 4477080
 12 = Basalt (V), x = 6853540, y = 4499620

Selected geochemical analyses of the metavolcanic rocks of the Parikkala-Punkaharju area are presented in Table 1. All analyzed samples have been plotted in various geochemical diagrams (Fig. 4). TAS and AFM diagrams (Figs. 4a and 4b) show that the samples fall into three separate groups. Basalts, basaltic andesites and andesites form one group that is clearly distinct from acid and alkali-rich rocks, particularly in regard to alkali contents. Three picritic

rocks differ from other basalts by their very low alkali contents. Andesitic rocks are rather rare. The metavolcanic rocks form a calc-alkaline trend on the AFM diagram, a feature which is characteristic to acid-intermediate rocks of island arc suites. The basic rocks instead mostly fall within the tholeiitic field. This is a common feature of basalts in calc-alkaline suites such as the Aijala-Orijärvi area in the South Svecofennian Subprovince (Latvalahti 1979). The

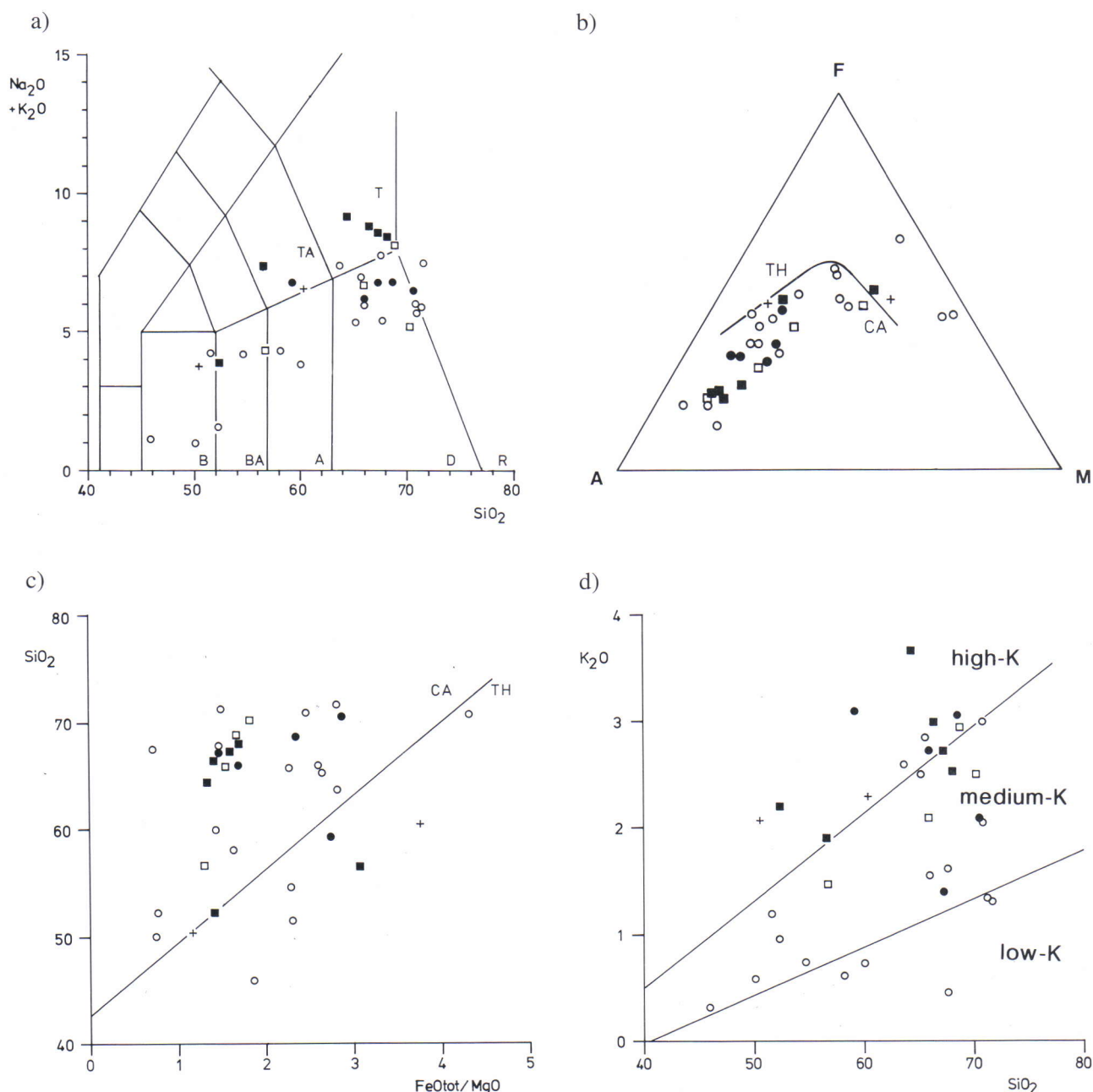


Fig. 4. Diagrams for evaluating the geochemical nature of metavolcanics of the Parikkala-Punkaharju area. **a.** TAS diagram. Fields: B = basalt, BA = basaltic andesite, A = andesite, D = dacite, R = rhyolite, TA = trachyandesite, T = trachyte (Le Bas et al. 1986). **b.** AFM diagram. The line separating tholeiitic (TH) and calc-alkaline (CA) rocks is after Irvine and Baragar (1971). **c.** SiO_2 - $\text{FeO}^{\text{tot}}/\text{MgO}$ diagram (Miyashiro 1975) CA = calc-alkaline rocks, TH = tholeiitic rocks. **d.** K_2O vs. SiO_2 diagram. High-K, medium-K and low-K fields after Gill (1981). Symbols as in Fig. 3.

SiO₂ vs. FeO^{tot}/MgO diagram (Fig. 4c) shows dispersion of the samples, with basic samples plotting again in the tholeiitic field. In the K₂O vs. SiO₂ diagram (Fig. 4d), the samples chiefly lie within the medium-K and high-K fields of Gill (1981). These fields correspond approximately to the fields of calc-alkaline series rocks and K-rich calc-alkaline series rocks, respectively, of Peccerillo and Taylor (1976).

The REE patterns of the Parikkala-Punkaharju metavolcanic rocks show distinct enrichment in light REE (LREE). Fig. 5 shows REE patterns for selected samples representing four rock types. The LREE enrichment is strongest in trachyte (La_N:Yb_N 42) and dacite (La_N:Yb_N 13.5) both of which show mutually similar LREE patterns. Basalts (La_N:Yb_N 11.4) and basaltic andesites (La_N:Yb_N 5.0) show weaker LREE enrichments. The patterns for basaltic andesite differ from the others in showing a positive Eu anomaly.

Fig. 6 shows the metavolcanic rocks of Parikkala-Punkaharju area plotted on different tectonomagmatic diagrams. Because most of the diagrams were devised for basaltic rocks, only basalts and basaltic andesites have been included. In spite of the geochemical heterogeneity of basalts and basaltic andesites in the area, the diagrams reveal the volcanic arc affinities of these rocks. However, on the Ti-

Zr-Y diagram (Fig. 6b), all samples plot quite close to the within-plate basalt field. All of the metavolcanic rocks have been plotted on the Ti vs. Zr diagram (Fig. 6d), because this diagram is also appropriate for acid rocks (Pearce 1982). Some basaltic samples plot in the WPL-field due to their higher Ti content. On the Zr/Y vs. Zr diagram (Fig. 6e), which shows the fields for oceanic and volcanic arc basalts, the basalts and basaltic andesites plot in the field of continental arcs.

Pearce (1983) presents MORB-normalized trace-element patterns for basalts from different tectonic settings and distinguishes different source components that affect the level and shape of the patterns. The average pattern of five basalts and basaltic andesites from the Parikkala-Punkaharju area (Fig. 7) shows an apparent subduction zone component with high values of Sr, K, Rb, Ba and Th. Compared to island arc basalts, the pattern also has higher values of Nb, Zr, Ti and Y, consistent with the presence of a within-plate component. This kind of pattern is characteristic of active continental margin calc-alkaline basalts that contain a considerable proportion of sub-continental lithosphere in their source (Pearce 1983). Similar features can be seen in the pattern of a basalt from central Chile, which is presented in Fig. 7 as an example of such a setting.

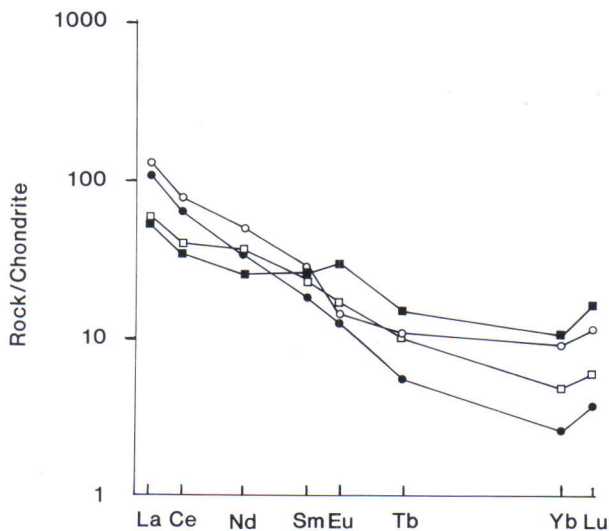


Fig. 5. Chondrite-normalized REE-patterns for the Parikkala-Punkaharju metavolcanics. Symbols: open circle = dacite (Nr. 10 in Table 1), filled circle = trachyte (Nr. 11), open square = basalt (Nr. 12), filled square = basaltic andesite (Nr. 6). Normalizing values from Hickey and Frey (1982).

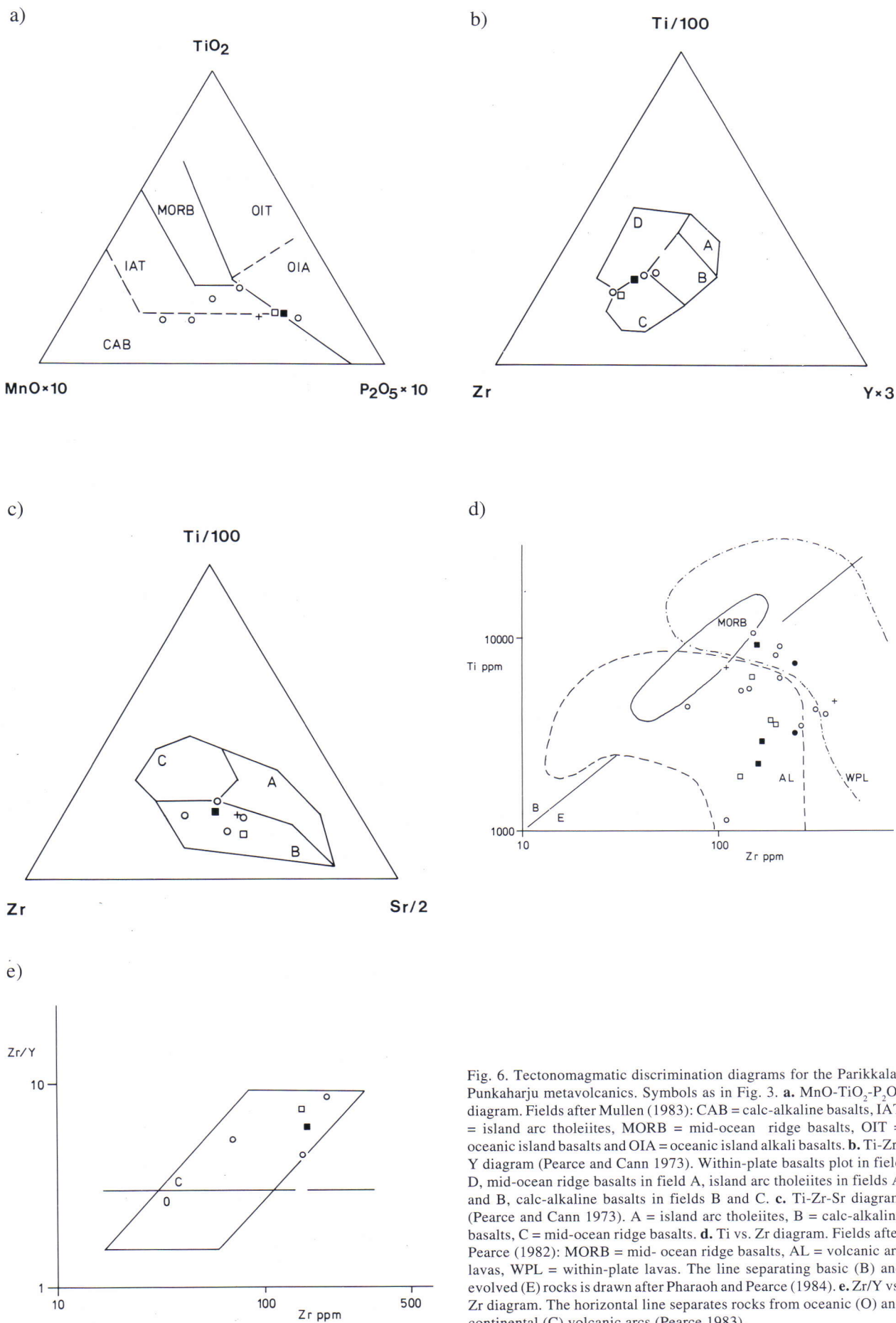


Fig. 6. Tectonomagmatic discrimination diagrams for the Parikkala-Punkaharju metavolcanics. Symbols as in Fig. 3. **a.** MnO-TiO₂-P₂O₅ diagram. Fields after Mullen (1983): CAB = calc-alkaline basalts, IAT = island arc tholeiites, MORB = mid-ocean ridge basalts, OIT = oceanic island basalts and OIA = oceanic island alkali basalts. **b.** Ti-Zr-Y diagram (Pearce and Cann 1973). Within-plate basalts plot in field D, mid-ocean ridge basalts in field A, island arc tholeiites in fields A and B, calc-alkaline basalts in fields B and C. **c.** Ti-Zr-Sr diagram (Pearce and Cann 1973). A = island arc tholeiites, B = calc-alkaline basalts, C = mid-ocean ridge basalts. **d.** Ti vs. Zr diagram. Fields after Pearce (1982): MORB = mid-ocean ridge basalts, AL = volcanic arc lavas, WPL = within-plate lavas. The line separating basic (B) and evolved (E) rocks is drawn after Pharaoh and Pearce (1984). **e.** Zr/Y vs. Zr diagram. The horizontal line separates rocks from oceanic (O) and continental (C) volcanic arcs (Pearce 1983).

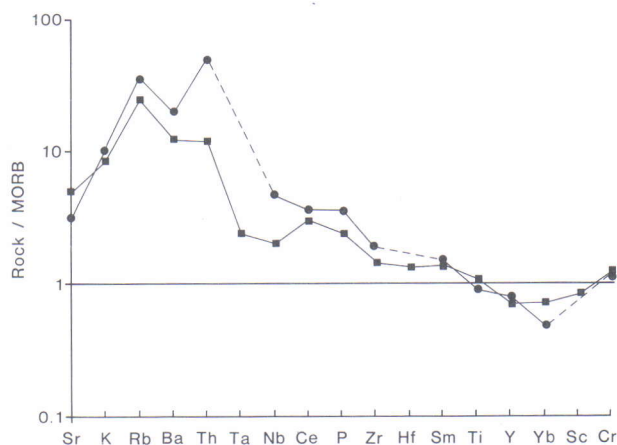


Fig. 7. MORB-normalized geochemical patterns of basalts of the Parikkala-Punkaharju area. Symbols: filled circle = average of five basalts and basaltic andesites; filled box = calc-alkaline basalt from central Chile (Pharaoh & Pearce 1984). Normalizing values from Pearce (1982).

DISCUSSION

The metavolcanic rocks of the Parikkala-Punkaharju area resemble in many respects metavolcanic rocks in other parts of the Southern Svecofennian Subprovince. This area has been considered to constitute an island arc (Hietanen 1975). The metavolcanic rocks of this Subprovince are mostly calc-alkaline and the acid rocks tend to predominate (e.g. Latvalahti 1979, Löfgren 1979). Young calc-alkaline volcanic rocks occur in island arcs and at active continental margins (e.g. Miyashiro 1975, Condie 1982) and the volcanic arc model is widely accepted for the leptite belts in Finland and Sweden. In Sweden, some debate has occurred between the advocates of island arc models (Löfgren 1979, Loberg 1980) and the more complicated subduction-related Andino-type continental arc model (Vivallo and Rickard 1984, Kresten 1986).

The tectonomagmatic diagrams, as well as other geochemical criteria, suggest a volcanic arc environment for the basaltic rocks of the Parikkala-Punkaharju area. However, some high Ti contents in the basic rocks of the area contrast with the Ti contents of young volcanic arc basalts. Svecofennian basaltic rocks in general show a wide variation in Ti contents (Kähkönen 1981). The metavolcanic rocks in the Tampere Schist Belt resemble the rocks of

young, mature island arcs, but there also some basaltic rocks have high Ti contents. This feature has been attributed to a temporary extensional stage during the geological evolution of the area (Kähkönen 1987).

Leeman (1983) postulated a connection between the thickness of the crust and the composition of volcanic rocks erupted in the volcanic arc. Tholeiitic basalts and basaltic andesites are common in volcanic arcs overlying thin, oceanic crust, whereas more acid calc-alkaline volcanics are dominant in mature island arcs and active continental margins overlying thick, continental crust. The greater the proportion of andesites, dacites and rhyolites of all volcanic rocks, the thicker is the crust under the arc (Leeman, op. cit.). In the Parikkala-Punkaharju area, about 75 % of the metavolcanic rocks are andesites, dacites or rhyolites. This suggests that the volcanic arc was underlain by a thick crust during the extrusion of these rocks. The effect of a within-plate component in the trace element pattern suggests the influence of the sub-continental lithosphere in magma genesis. In conclusion, the tectonic environment of the metavolcanic rocks of the Parikkala-Punkaharju area has characteristics similar to those of young active continental margins.

ACKNOWLEDGEMENTS

I want to thank Kauko Meriläinen, Jukka Kousa, Yrjö Kähkönen, Mikko Nironen, Markus Vaarma, the late Osmo Nykänen, and Liisa Sirén, who all

contributed to this work in different ways. The English language was revised by Peter Sorjonen-Ward.

REFERENCES

- Condie, K.C. 1982.** Plate Tectonics and Crustal Evolution, 2nd ed. New York: Pergamon Press, 310 p.
- Davis, A., Blackburn, W.H., Brown, W.R. & Ehmann, W.D. 1978.** Trace element geochemistry and origin of late Precambrian-early Cambrian Catocin greenstones of the Appalachian Mountains. Univ. California at Davies, Davies, Calif., Rep. (unpublished)
- Gaál, G. & Gorbatshev, R. 1987.** An outline of the Precambrian evolution of the Baltic Shield. *Precambrian Res.* 35, 15-52.
- Gill, J.B. 1981.** Orogenic Andesites and Plate Tectonics. Berlin: Springer-Verlag, 390 p.
- Hickey, R.L. & Frey, F.A. 1982.** Geochemical characteristics of boninite series volcanics: implications for their source. *Geochim. Cosmochim. Acta* 46, 2099-2115.
- Hietanen, A. 1975.** Generation of potassium-poor magmas in the northern Sierra Nevada and the Svecofennian of Finland. *J. Res. U.S. Geol. Surv.* 3, 631-645.
- Irvine, T.N. & Baragar, W.R.A. 1971.** A guide to the chemical classification of the common volcanic rocks. *Can. J. Earth. Sci.* 8, 523-548.
- Kähkönen, Y. 1981.** Oriveden ja Ylöjärven vulkaaniset vyöhykkeet; erityisesti niiden geokemia. Phil. lic. thesis, Univ. Helsinki, 210 p. (unpublished, in Finnish)
- Kähkönen, Y. 1987.** Geochemistry and tectonomagmatic affinities of the metavolcanic rocks of the early Proterozoic Tampere Schist Belt, southern Finland. *Precambrian Res.* 35, 295-311.
- Kresten, P. 1986.** Geochemistry and tectonic setting of metavolcanics and granitoids from the Falun area, south central Sweden. *Geol. Fören. Stockholm Förh.* 107, 275-285.
- Latvalahti, U. 1979.** Cu-Zn-Pb ores in the Aijala-Orijärvi area, southwest Finland. *Econ. Geol.* 74, 1035-1059.
- Le Bas, M.J., Le Maitre, R.W., Streckeisen, A. & Zanettin, B. 1986.** A chemical classification of volcanic rocks based on total alkali-silica diagram. *J. Petrol.* 27, 745-750.
- Leeman, W.P. 1983.** The influence of crustal structure on compositions of subduction-related magmas. *J. Volcanol. Geotherm. Res.* 18, 561-588.
- Loberg, B.E.H. 1980.** A Proterozoic subduction zone in southern Sweden. *Earth Planet. Sci. Lett.* 46, 287-294.
- Löfgren, C. 1979.** Do leptites represent Precambrian island arc rocks? *Lithos* 12, 159-165.
- Miyashiro, A. 1975.** Volcanic rock series and tectonic setting. *Ann. Rev. Earth Planet. Sci.* 3, 251-269.
- Mullen, E.D. 1983.** MnO/TiO₂/P₂O₅: a minor element discriminant for basaltic rocks of oceanic environments and its implications for petrogenesis. *Earth Planet. Sci. Lett.* 62, 53-62.
- Nykänen, O. 1980.** Pre-Quaternary rocks, sheet 4124+4142 Punkaharju. Geological map of Finland 1 : 100 000.
- Nykänen, O. 1982.** Pre-Quaternary rocks, sheet 4123+4114 Parikkala. Geological map of Finland 1 : 100 000.
- Nykänen, O. 1983.** Punkaharjun ja Parikkalan kartta-alueiden kallioperä. Summary: Pre-Quaternary rocks of the Punkaharju and Parikkala map-sheet areas. Explanation to the maps of pre-Quaternary rocks, sheets 4124+4142 and 4123+4114. Geological map of Finland 1:100 000. 81 p.
- Pearce, J.A. 1982.** Trace element characteristics of lavas from destructive plate boundaries. In: Thorpe, R.S. (ed.) *Andesites. Orogenic Andesites and Related Rocks*. Chichester: Wiley, 525-548.
- Pearce, J.A. 1983.** Role of subcontinental lithosphere in magma genesis at active continental margins. In: Hawkesworth, C.J. & Norry, M.J. (eds.) *Continental Basalts and Mantle Xenoliths*. Cheshire: Shiva, 230-249.
- Pearce, J.A. & Cann, J.R. 1973.** Tectonic setting of basic volcanic rocks determined using trace element analyses. *Earth Planet. Sci. Lett.* 19, 290-300.
- Peccerillo, A. & Taylor, S.R. 1976.** Geochemistry of Eocene calc-alkaline volcanic rocks from the Kastamonu area, northern Turkey. *Contrib. Mineral. Petrol.* 58, 63-81.
- Pharaoh, T.C. & Pearce, J.A. 1984.** Geochemical evidence for the tectonic setting of early Proterozoic metavolcanic sequences in Lapland. *Precambrian Res.* 25, 283-308.
- Viluksela, A. 1988.** Rantasalmen ja Parikkalan-Punkaharjun vulkaniittien petrografia, geokemia ja tektonomagmaattinen luonne. M.Sc. thesis, Univ. Helsinki, 96 p. (unpublished, in Finnish)
- Vivallo, W. & Rickard, D. 1984.** Early Proterozoic ensialic spreading-subsidence: evidence from the Garpenberg enclave, central Sweden. *Precambrian Res.* 26, 203-221.

REE DISTRIBUTION IN THE PHOSPHORITE BANDS WITHIN THE PALEOPROTEROZOIC TUOMIVAARA AND PAHTAVAARA IRON-FORMATIONS, CENTRAL AND NORTHERN FINLAND

by
Seppo Gehör

Gehör, Seppo 1994. REE distribution in the phosphorite bands within the Paleoproterozoic Tuomivaara and Pahtavaara iron-formations, central and northern Finland. *Geological Survey of Finland, Special Paper 19*, 71–83, 8 figures, two tables and one appendix.

The Paleoproterozoic quartz-banded iron-formations (IF) in Tuomivaara in the Kainuu Schist Belt, central Finland and in Pahtavaara in the Kittilä Greenstone Belt, northern Finland are characterized by exceptionally high phosphorus content. Phosphorus is concentrated in phosphorite bands varying in thickness from millimeters to 2 cm. The bands are mainly composed of fluorapatite, and the amount of quartz, calcite, chlorite, micas, Fe sulfides and graphite is variable.

The REE abundances are significantly higher in the phosphorite bands than in the IF proper (29x at max.) and in the coeval metapelites. In comparison to the other Paleoproterozoic IF, the REE contents of both the IF studied are higher due to their apatite dissemination.

On the basis of their chondrite-normalized REE patterns the IF and phosphorite samples fall into two types: 1) Samples with Ce-depleted LREE-enriched patterns are similar in their REE signature to the chemical sediments of mid-ocean ridges and some of them nearly equal with the marine phosphorites. This type is characteristic especially of the oxide-silicate IF at Tuomivaara. 2) Samples with Ce-depleted, nearly flat REE patterns resemble closely the patterns of seawater. This type contains samples from both IF of the study.

Eu behaves variably within the Tuomivaara IF, varying in chondrite-normalized patterns from slightly depleted in phosphorites and IF to slightly positive in the black schist. In the chemical sediments of the Tuomivaara IF, the magnitude of Ce depletions increases with the decrease in the magnitude of Eu depletions and the greatest Ce depletions are found in the oxide-silicate IF. The samples from the Pahtavaara IF do not show any Eu anomalies. The negative Ce anomalies suggest the predominance of oxidizing conditions during the precipitation and diagenesis of the IF studied. Consequently, the precipitation of the chemical sediments took place within a depositional environment consistent with those of recent phosphorites which accumulate in relatively shallow, upwelling oceanic water.

Key words (GeoRef Thesaurus, AGI): iron formations, metapelite, geochemistry, phosphorus, rare earths, precipitation, Proterozoic, Paleoproterozoic, Pahtavaara, Kittilä, Tuomivaara, Sotkamo, Finland

Seppo Gehör, Department of Geology, University of Oulu, Linnanmaa
FIN-90570 Oulu, Finland

INTRODUCTION

The rare earth element (REE) concentrations in chemical sediments, especially in limestones, banded iron-formations (IF) and phosphorites, provide information about the conditions of the sedimentary environment and of the seawater from which they were precipitated. Due to their specific chemical properties, these elements are resistant to later geochemical reactions. In particular the fractionation of REE during postdepositional geochemical processes is thought to be insignificant.

The behavior of Ce and Eu in chemical sediments has been discussed extensively since the first REE analyses were documented for these materials. The evidence of their valence states (Ce^{3+} vs. Ce^{4+} and Eu^{2+} vs. Eu^{3+}) is widely applied to evaluate the oxidation-reduction conditions of the depositional environment.

The positive Eu anomaly, so typical of Archean IF, was considered by Fryer (1977) to reflect the reducing seawater conditions at that time. He suggested that the disappearance of the Eu anomaly and the generation of relative Ce depletion, characteristic for modern seawater, began during Proterozoic time. The negative Ce anomaly in modern seawater is considered to be due to the oxidation of Ce^{3+} to Ce^{4+} (Barret et al. 1988, Fleet 1983). Since the Fe-Mn nodules in oceans are usually characterized by positive Ce anomaly, Ce^{4+} is considered to preferentially have removed into nodules in connection with precipitation of hydrous Mn oxides. As the precipitation of Fe-Mn nodules resulted in Ce-depleted seawater, the marine phosphorites, which were precipitated from seawater, are Ce-depleted (Goldberg et al 1963, Fleischer and Altschuler 1969, Piper 1974). Based on the chemical properties of Ce and Eu, McArthur and Walsh (1984) suggested that the phosphorites which obtain their REE under reducing conditions should not show the negative Ce anomalies but may show a positive Eu anomaly. Those phosphorites which gain their REE in oxic conditions may show

negative Ce anomalies.

The application of Eu and Ce anomalies to demonstrate the oxidation-reduction conditions is called into question by several authors. The Ordovician IF in New Brunswick (Graf 1978) revealed a positive Eu anomaly similar to that found in Archean IF. The present-day hydrothermal solutions are LREE-enriched and have a significant positive Eu anomaly (Michard et al. 1983). The positive Eu anomaly in the Archean Isua IF was considered by Dymek and Klein (1988) to be derived from hydrothermal solutions. Similarly, Derry and Jacobsen (1990) suggested that the positive Eu anomalies in the Hamersley and Michipoten IF indicate submarine hydrothermal circulation of seawater through a mid-ocean ridge. The Ce anomalies, if present, are suggested to reflect the composition of seawater. On the other hand, Bau (1991) has shown that the Eu behavior of hydrothermal or metamorphic fluids is also dependent on pH conditions.

In Paleoproterozoic and Archean IF, the REE abundances are typically low in comparison with their coeval shales or with the crustal averages. However, Laajoki (1975) documented exceptionally high REE contents for an IF, rich in apatite, at Puolanka, central Finland. As shown in the present study, the other Paleoproterozoic IF in central and northern Finland also have this same feature.

The attention of the present study is directed to the REE compositions of the phosphorites of the IF proper and of the coeval metapelites. The samples analyzed for REE, 13 in total, were collected from two IF from dissimilar depositional environments. Eleven of the samples are from the Tuomivaara IF, a part of the Kainuu Schist Belt in central Finland (Fig. 1). Two samples are from the Pahtavaara IF in the Kittilä Greenstone Belt in northern Finland. Both IF are rich in phosphorus, which is mainly concentrated in fluorapatite, found in millimeter to 2 cm thick phosphorite bands (Fig. 2).

GEOLOGICAL SETTING

The metasedimentary rocks in the Tuomivaara area (Fig. 1b) are composed of two major units. The lower unit, the Jatuli tectofacies, is comprised mainly of conglomerates and quartzites and lies non-conformably on the Archean basement. The upper unit, the Kaleva tectofacies, in turn lies unconformably on the Jatulian metasediments. Sedimentological studies at the Tuomivaara IF indicate depositional setting

of a submarine-fan system within the flyschoidal Kaleva tectofacies (Gehör & Havola 1988).

Based on the prevailing Fe mineralogy, the Tuomivaara IF is divided into silicate, silicate-oxide and sulfide IF types. In comparison to the conventional IF facies classification of James (1954), the silicate, oxide and sulfide "facies" at the Tuomivaara IF are intermixed with each other in a millimeter

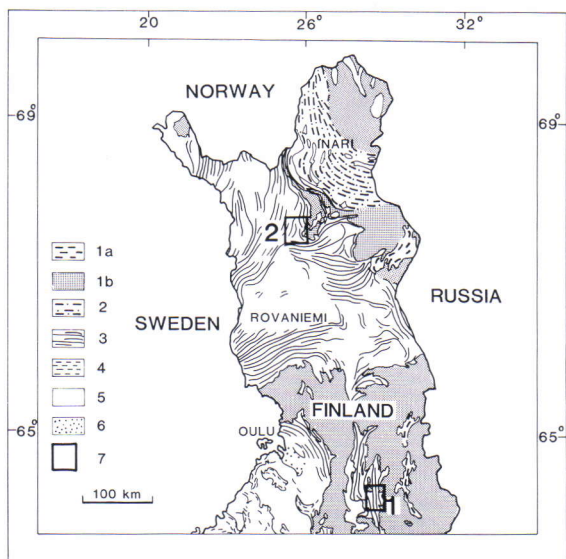


Fig. 1a. Main structural units of the Precambrian of Finland, modified after Simonen (1980). Archean: 1a = schists and paragneisses; 1b = orthogneisses. Proterozoic: 2 = granulites; 3 = Karelidic schists; 4 = Svecofenidic schists; 5 = orogenic plutonic rocks. Postsvecokarelian: 6 = Jotnian sediments. 7 = Study areas: 1 = Tuomivaara; 2 = Pahtavaara.

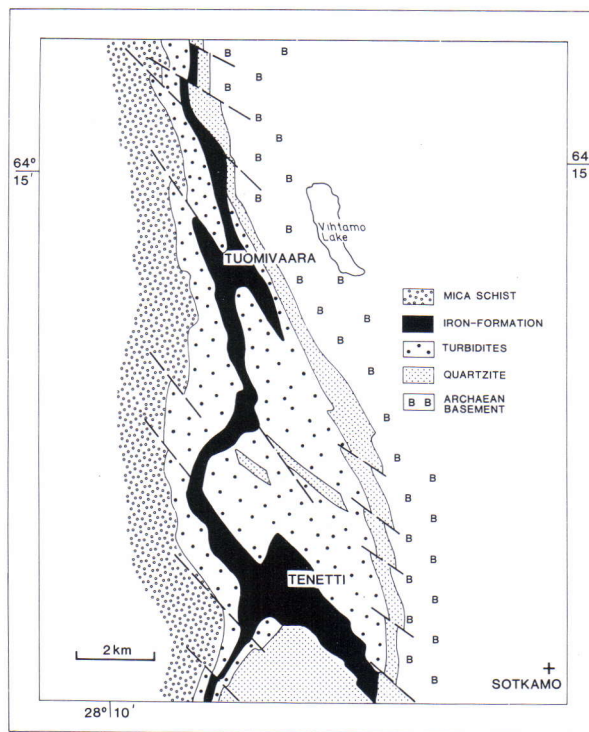


Fig. 1b. General geological map of the Tuomivaara area (modified from Gehör & Havola 1988).

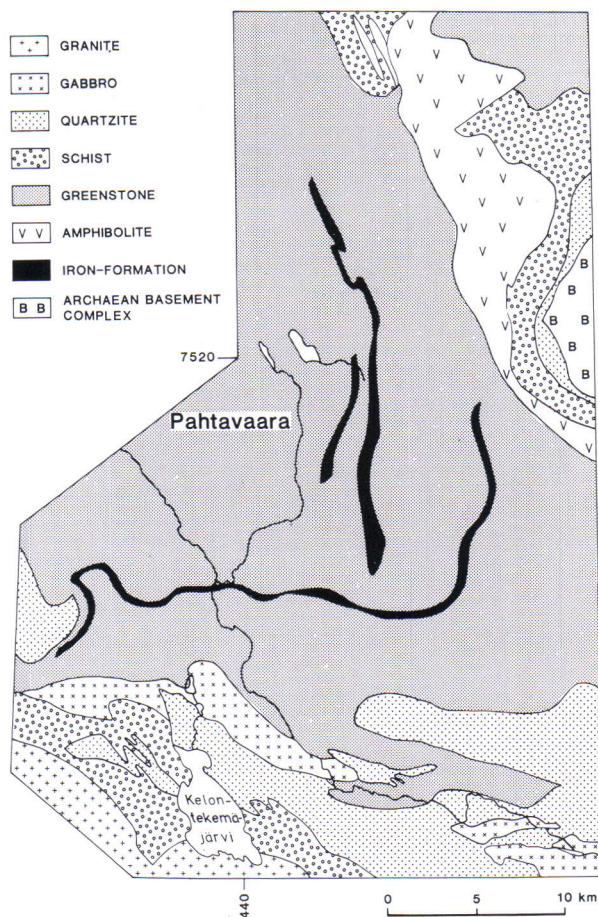
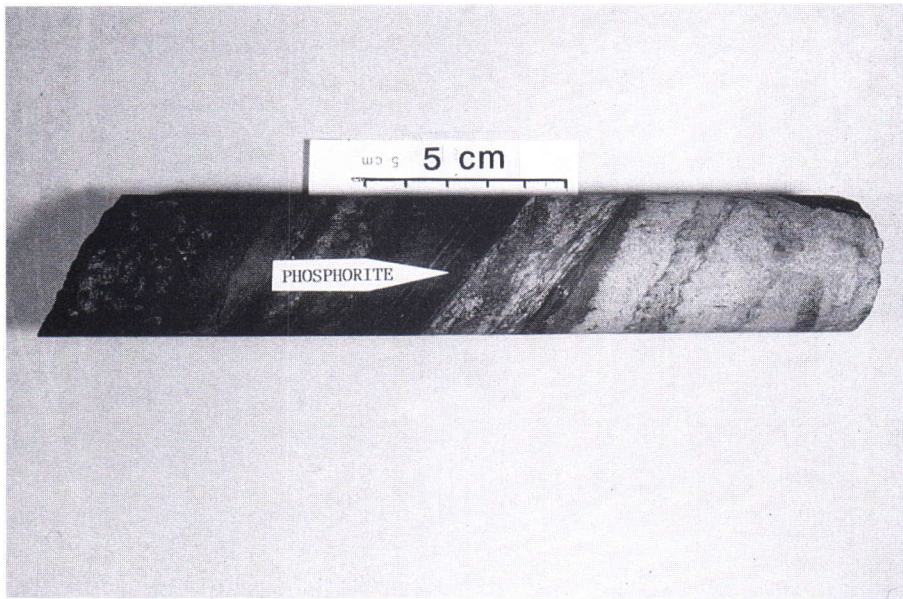
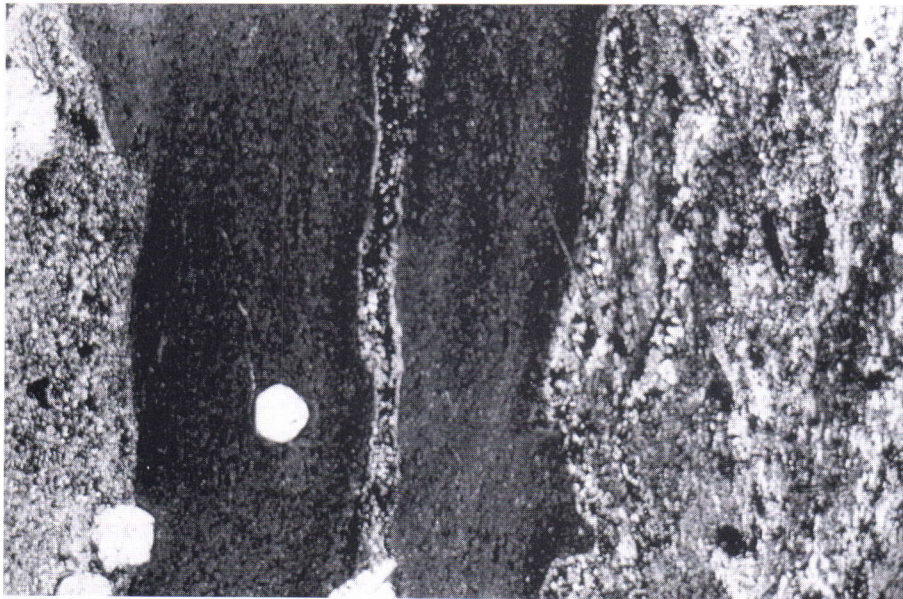


Fig. 1c. General geological map of the Porkonen-Pahtavaara area (modified from Kallio et al. 1980 and Gehör 1982).

2a)



2b)



2c)

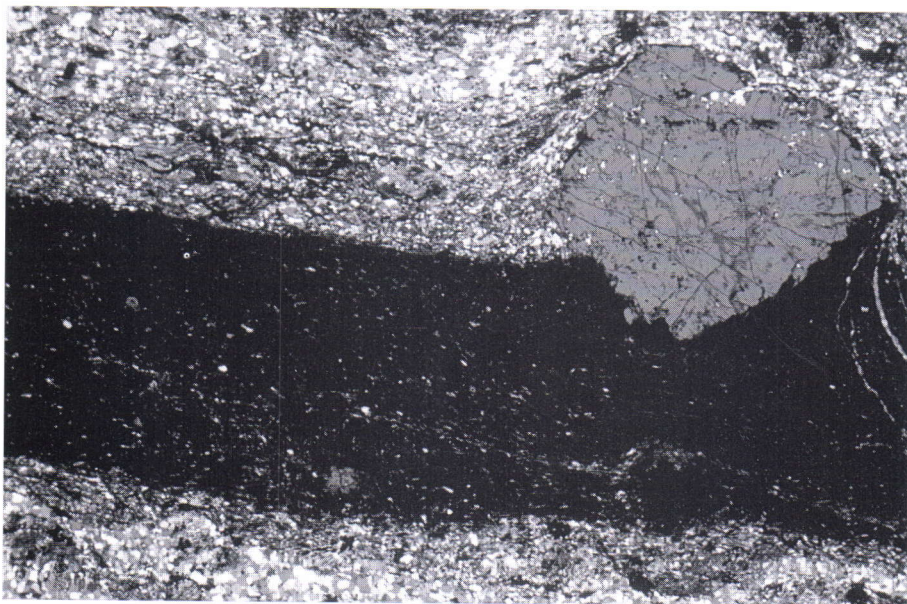


Fig. 2. Examples of the phosphorite bands in the Tuomi-vaara iron-formation. **a)** Drill core, silicate IF. The bands left of the phosphorite band are composed of alternating bands rich in grunerite, garnet, biotite and quartz. The grayish bands right of the phosphorite band are chert. **b)** Photomicrograph (parallel polarizer) of oxide-silicate IF. The thickness of the two graphitic phosphorite bands (black) are 4 and 6 mm. The porphyroblasts within the phosphorite bands are almandine. **c)** Photomicrograph of silicate IF, the thickness of the phosphorite band is 3 mm. The porphyroblast above the band is almandine and the small white grains inside the band are quartz. The host in the immediate vicinity of the phosphorite band is chert with biotite-grunerite spots.

Table 1. Whole rock chemical data for the samples from Tuomivaara (drill hole 2; Nos 1-13) and Tenetti (No 14).

	1	2	3	4	5	6	7
SiO ₂	52.20	56.80	38.10	51.10	45.40	60.60	64.60
TiO ₂	0.26	0.23	0.31	0.27	0.32	0.32	0.26
Al ₂ O ₃	5.30	4.00	5.50	3.50	5.90	4.30	3.60
Fe ₂ O ₃	27.20	31.80	24.60	34.40	41.20	26.40	28.00
MnO	0.21	0.23	0.06	0.07	0.11	0.07	0.12
MgO	3.20	2.40	1.90	1.60	2.10	1.40	1.50
CaO	6.56	2.28	14.50	4.85	2.18	3.96	1.38
Na ₂ O	0.20	0.00	1.00	0.00	0.20	0.50	0.00
K ₂ O	0.86	1.36	1.81	1.07	1.39	1.33	1.03
P ₂ O ₅	2.13	1.23	13.70	3.19	0.58	2.36	0.69
Tot	98.12	100.33	101.48	100.05	99.38	101.24	101.18
BaO	0.02	0.01	0.01	0.01	0.01	0.02	0.02
Co	40	50	30	40	40	30	30
Cu	40	100	50	70	120	50	70
Ni	60	50	40	110	90	50	50
Zn	90	60	70	60	70	50	60
Pb	50	40	100	40	110	40	30
	8	9	10	11	12	13	14
SiO ₂	34.10	52.20	54.80	47.70	35.70	27.50	44.00
TiO ₂	0.08	0.08	0.21	0.08	0.43	0.10	0.71
Al ₂ O ₃	4.20	5.20	3.40	2.60	9.90	1.80	9.70
Fe ₂ O ₃	50.50	40.30	29.80	43.00	49.30	63.10	26.80
MnO	0.19	0.25	0.05	0.12	0.13	0.37	2.73
MgO	3.10	1.80	1.70	1.60	1.60	2.90	5.70
CaO	8.85	1.24	5.10	3.03	1.72	2.92	8.07
Na ₂ O	1.30	0.00	0.00	0.00	0.00	0.00	0.00
K ₂ O	0.50	0.12	1.10	0.43	2.68	0.70	0.05
P ₂ O ₅	7.24	0.15	3.75	1.76	0.11	1.39	0.24
Tot	101.2	101.34	99.91	100.32	101.57	100.78	98.00
BaO	0.0	0.0	0.03	0.00	n.d.	0.00	n.d.
Co	30	40	30	40	40	60	n.d.
Cu	50	30	70	60	40	160	n.d.
Ni	30	50	70	60	50	110	n.d.
Zn	60	50	70	50	80	110	n.d.
Pb	70	20	40	40	60	50	n.d.

1 = Depth 21.4 m, Silicate IF

2 = 23.15, Silicate IF

 3 = 26.8, Silicate IF
 phosphorite banded

4 = 34.6, Silicate-oxide IF

5 = 34.9, Silicate-oxide IF

6 = 37.2, Silicate IF

 7 = 40.3, (*Sample No. 5*
in Appendix I), Oxide-
 Silicate IF

 8 = 45.40 Oxide-silicate IF,
 phosphorite banded

9 = 53.45, Oxide-silicate IF

 10 = 54.50, Oxide silicate IF
 phosphorite banded

11 = 63.50, Oxide silicate IF

12 = 78.10, Silicate-sulphide IF

13 = 80.50, Sulphide IF

Outcrop

 14 = Tenetti (*Sample No. 11 in*
Appendix I), Silicate IF

scale and locally with the surrounding lithologies. At least part of the oxide "facies" has textural and mineralogical features that are secondary in origin and obviously were generated during late metamorphic, oxidizing events. The sulfide "facies", on the other hand, is difficult to distinguish from the fine-grained black schists. The silicate-oxide and silicate IF occur mainly in the lower part of the formation. Most of the sulfide IF occurs in the upper part of the sequence where it is intercalated with turbiditic beds.

The Tuomivaara IF has not been dated but the whole-rock Pb-Pb age determinations from phosphorus-rich metasediments elsewhere in the Kainuu Schist Belt, which according to their sedimentological character are analogous with the Tuomivaara IF, yielded an upper limit of 2080±45 Ma (Sakko & Laajoki 1975). An age of 1897±7 was obtained by U-Pb-methods as the lower limit (Vaasjoki et al. 1980) from thucolite in the U-rich black schist at Nuottijärvi, Paltamo.

At Tuomivaara, phosphorite interbands are found throughout the sequence and the oxide-silicate IF are especially phosphorus-rich (Table 1). In drill core No. 1 the average P_2O_5 content of the whole rock analyses, containing all IF types, is 1.89 % (length of the analyzed core is 129 m), while it is 2.36 % in the oxide-silicate IF (length 23 m), and 2.03 % in the sulfide IF (length 38 m). Besides fluorapatite, the phosphorite bands are composed of quartz, albite, garnet, calcite, chlorite, biotite, pyrrhotite and graphite.

The Pahtavaara IF belongs to the Kittilä Greenstone Belt, which consists mainly of komatiites, tholeiites, tuffaceous schists, phyllites and dolomites (Paakkola 1971, Lehtonen & Rastas 1986, Paakkola & Gehör 1988). The belt is divided into two lithostratigraphic units: 1) the (lower) Lapponi Group, consisting mainly of quartzites, mica schists, and metavolcanics; and 2) the (upper) Kumpu Group, consisting of coarse clastics, quartzites and conglomerates (Mikkola 1941). The amount of chert is

locally large in comparison to other chemical precipitates.

All the IF facies described by James (1954) are found in the Porkonen-Pahtavaara area. Manganoan silicate-carbonate facies dominates, while the oxide and sulfide facies are more restricted and located in the upper part of the sequence (Paakkola 1971). Phosphorite bands occur in all these facies types and the P_2O_5 content ranges up to 4.07 % (Paakkola 1971). The phosphorite bands consist of fluorapatite, quartz, chlorite, carbonates, biotite and stilpnomelane. The amount of other constituents besides fluorapatite is typically negligible. The precipitation of the IF was interrupted by periods of volcanic activity, as is demonstrated by the intense intermixing of chemical precipitates with tuffites. Based on the lithological and environmental character, together with the major and trace element compositions, the Pahtavaara IF is classified as an Algoma type (Gehör 1982), using the criteria outlined by Gross (1980).

SAMPLES AND ANALYTICAL TECHNIQUES

All but one sample (No. 11) of this study are from drill cores (see Appendix). The phosphorite samples were cut from the drill cores and they contain, besides fluorapatite, varying amounts of other minerals. Especially quartz is present in considerable quantities. The high quartz content decreases the REE concentrations but it is unlikely to have any significant bearing on the patterns.

The REE analyses were performed by instrumental neutron activation analysis (INAA) at the Reactor Laboratory of the Technical Research Centre (STRC) of Finland (Rosenberg et al. 1982). The bulk chemical analyses were carried out at the Department of Geology, University of Oulu. The major elements and barium were analyzed by XRF and the trace elements by AAS.

ANALYTICAL RESULTS

The REE contents of the samples are listed in Table 2. The chondrite-normalized patterns are shown in Fig. 3 for the Tuomivaara IF, and in Fig. 4 for the Pahtavaara IF.

The ability of phosphorites to incorporate REE during precipitation and diagenesis is considerable in comparison to IF in which the REE abundances are generally low. Consequently, the REE abundances in the analyzed phosphorite bands are significantly higher than those in the associated sediments and in

the IF proper. This is demonstrated by the samples taken from adjacent bands. The difference in the REE contents between a phosphorite and its host is highest in samples 12 and 13 from Pahtavaara (Fig. 4). The REE concentration (8 elements) of the sulfide facies host (sample 12) is 25 ppm while it is 687 ppm in sample 13, a 4 mm thick phosphorite band (Table 2). The same phenomenon also characterizes the samples from the Tuomivaara IF, although the differences are smaller (Figs. 3a and 3b, Table 2).

REE in the chemical sediments at the Tuomivaara IF

The typical features of the chondrite-normalized patterns of the chemical sediments at Tuomivaara are LREE enrichments (Figs. 3 and 4) and Ce depletions. Most of them are also characterized by Eu depletions. The LREE enrichments are prominent in most cases ((La/Yb)_N values range from 8 to 24) but phosphorite samples 7 and 8 have low (La/Yb)_N values (2.7 and 4.6). In the chemical sediments the magnitude of Ce depletions increases with the decrease in the magnitude of Eu depletions (Fig. 5). The greatest Ce depletions are found in oxide IF and in

phosphorite interbedded in oxide IF.

The REE patterns of the chemical sediments with pronounced LREE enrichment are similar to those reported by Fleischer (1983) (Table 2, Fig. 3b). Especially the pattern of sample 2 from Tuomivaara, representing silicate IF, and pattern of the average of 13 marine phosphorites in the data of Fleischer are nearly identical.

As is shown in Fig. 6, the present REE data are similar also to those of the phosphorites in Chateman Rise, Blake Plateu and Phosphoria. The main differ-

Table 2. REE concentration (ppm) in the Tuomivaara and Pahtavaara iron-formations, phosphorites and coeval metasediments.

	1	2	3	4	5	6	7		
La	34	32	155	70	157	25	42		
Ce	37	44	157	71	246	44	76		
Nd	32	25	167	73	223	50	87		
Sm	7.2	5.6	43	17.5	43	18.1	29		
Eu	1.7	0.94	14.5	5	12.7	5.4	8.3		
Tb	1.1	0.55	6.9	2.5	8.1	1.01	7.9		
Yb	2.7	1.75	12	4	4.5	1.01	10.4		
Lu	0.3	0.27	1.1	0.4	0.26	0.07	0.76		
Total	116.03	110.11	556.47	243.41	694.56	144.59	261.36		
Ce/Ce*	0.54	0.72	0.47	0.49	0.67	0.66	0.67		
Eu/Eu*	0.76	0.60	1.06	0.90	0.79	1.28	0.72		
(La/Yb) _N	8.50	12.35	8.72	11.82	23.56	16.71	2.73		
(La/Lu) _N	11.59	12.12	14.7	17.45	61.71	36.5	5.54		
1= Sulphide IF with apatite dissemination, Tuomivaara 2= Silicate IF, Tuomivaara 3= Phosphorite band in Oxide-Silicate IF, Tuomivaara 4= Oxide silicate IF(host to sample 3), Tuomivaara 5= Phosphorite band in Oxide-Silicate IF, Tuomivaara 6= Phosphorite band in black Schist, Tuomivaara 7= Phosphorite band in Sulphide IF, Tuomivaara									
	8	9	10	11	12	13	*	#	
La	165	23	26	27	7	131	0.31	31	
Ce	246	33	40	59	9	191	0.808	67.03	
Nd	154	18.5	28	25	< 630	195	0.600	30.4	
Sm	42.0	3.7	5.8	5.5	1.2	59	0.195	5.98	
Eu	11.3	1.4	1.3	1.5	0.5	22	0.0735	1.253	
Tb	7.7	0.46	0.73	0.75	0.35	14.2	0.0474	0.85	
Yb	24.0	2.10	3.10	2.50	0.80	67.0	0.209	3.11	
Lu	2.7	0.32	0.43	0.30	0.11	8.0	0.0322	0.456	
Total	517.20	82.52	105.35	102.07	25.51	687.2	-	-	
Ce/Ce*	0.74	0.62	0.72	1.15	0.62	0.60			
Eu/Eu*	0.79	1.33	0.74	0.90	1.06	1.00			
(La/Yb) _N	4.64	7.40	5.66	7.29	6.08	1.32			
(La/Lu) _N	6.24	7.3	6.18	9.20	6.70	1.67			
8 = Phosphorite band in Sulphide IF, Tuomivaara 9 = Black Schist, Tuomivaara (host to Sample 8) 10 = Metapelite, Tuomivaara 11 = Aluminous silicate IF, Tenetti/Tuomivaara (Major elem. in Col. 14 in Table 1) 12 = Sulphide IF, Pahtavaara (host to sample 13) 13 = Phosphorite band, Pahtavaara * = Chondrite REE concentrations used in normalization. Data from Boynton (1984), Table 3.3/recommended chondrite # = North American Shale Composite (NASC) from Gromet et al. 1984 (Table 2; average from col. 5, 6 and 7)									

ences concern the REE abundances which are higher in the phosphorite bands of Tuomivaara. The magnitude of the Ce depletion is extremely high in the Blake Plateau and Phosphoria phosphorites in comparison to the samples from Tuomivaara.

The REE patterns of oceanic chemical sediments in three different depositional settings are illustrated in Fig. 7. These patterns have similarities with the REE

patterns from Tuomivaara in relation to LREE/HREE ratios and Ce behavior.

The phosphorite samples 7 and 8 with relatively low $(La/Yb)_N$ values are hosted by a sulfide IF. In general, according to their LREE/HREE ratio and their Ce and Eu behavior, the REE patterns of these samples resemble the REE patterns of seawater.

REE in aluminous silicate IF at Tenetti

One sample comes from the silicate IF at Tenetti (Fig. 3b), in the southern part of the Tuomivaara IF. This sample (No. 11) represents an aluminous IF (a garnet-amphibolite schist), which consists of alter-

nating chert, amphibole-garnet and biotite bands. Based on its whole rock chemistry (Table 1), this sample and the other garnet-amphibolites in the area fulfill the definition of IF ($Fe > 15\%$).

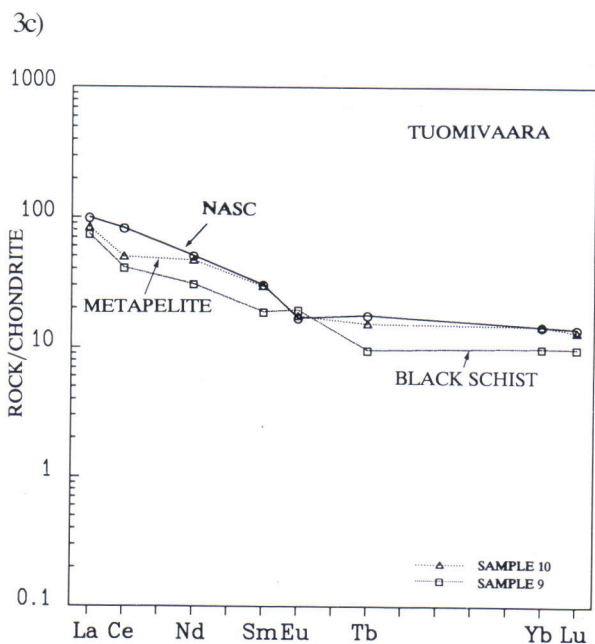
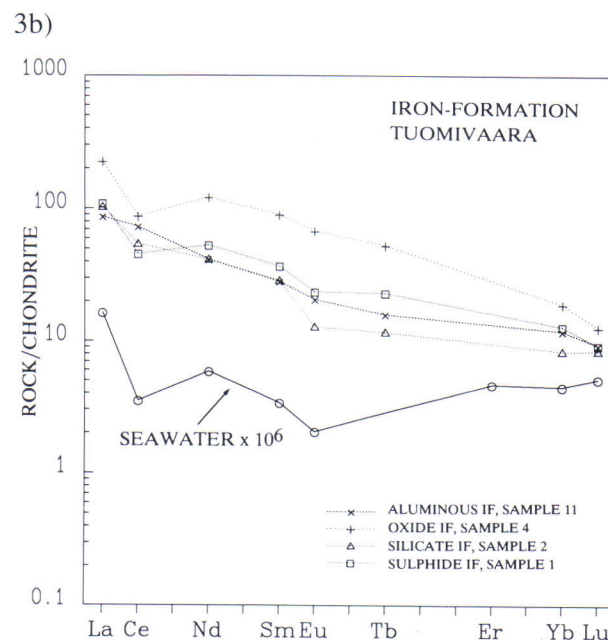
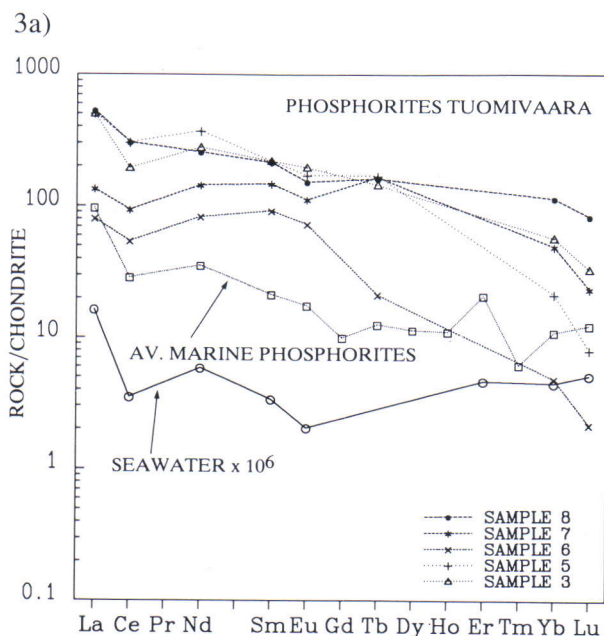


Fig. 3. Chondrite-normalized REE patterns in the Tuomivaara IF: **a)** phosphorite bands; **b)** iron-formation; **c)** coeval metapelite and black schist. Numbers refer to samples in Appendix. The REE patterns of Pacific Ocean seawater ($\times 10^6$) from Masuda & Ikeuchi (1979), for North American shale composite (NASC) from Gromet et al. (1984; Table 2; average from columns 5, 6 and 7) and for average phosphorites from Fleischer (1983, Table 1, No. 3). The chondritic REE concentrations for normalization of the REE values for Figs. 3-8 were obtained from the data published in Boynton (1984, Table 3.3; "recommended values").

The REE pattern of sample 11 differs from those of the other samples from Tuomivaara by its lack of a negative Ce anomaly ($Ce/Ce^* 1.15$; Table 2). On the Ce/Ce^* vs. Eu/Eu^* plot (Fig. 5) this sample plots

separately from the other samples of the Tuomivaara IF. The REE pattern is quite similar to that of NASC (Fig 3c), which may imply an admixture of detrital material among the Fe precipitates.

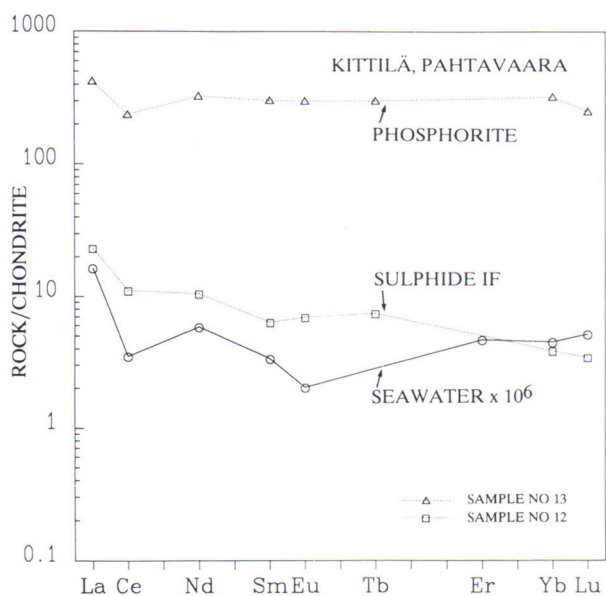


Fig. 4. Chondrite-normalized REE patterns in the Pahtavaara IF. The REE pattern of Pacific Ocean seawater ($\times 10^6$) from Masuda & Ikeuchi (1979). Numbers refer to samples in Appendix.

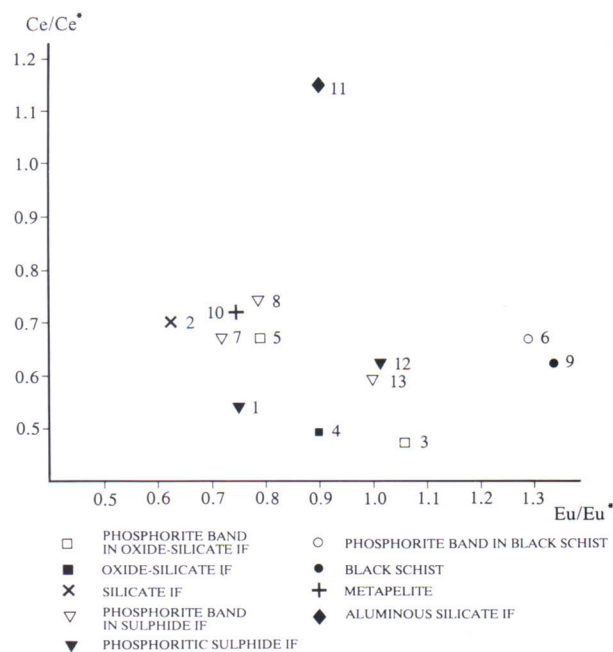


Fig. 5. Ce/Ce^* vs. Eu/Eu^* plots for the Tuomivaara and Pahtavaara IF. Samples (numbers as in Appendix) No. 1-11 from the Tuomivaara IF and No. 12-13 from the Pahtavaara IF.

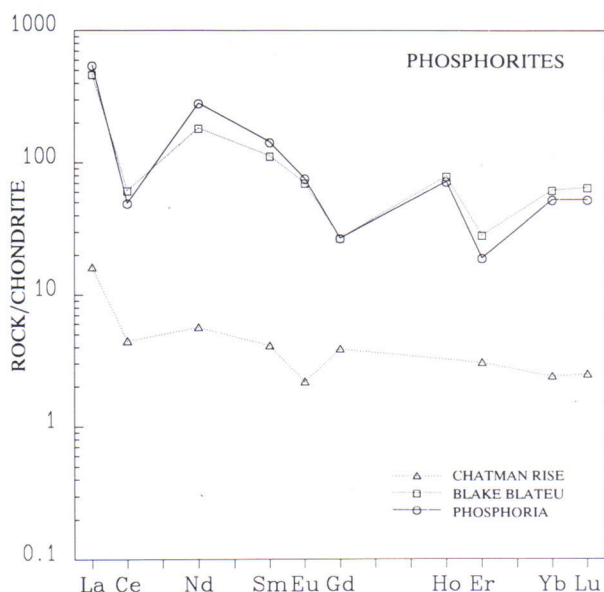


Fig. 6. Chondrite-normalized REE for phosphorites in Chatman Rise, Blake Plateau and Phosphoria. Data from McArthur & Walsh (1984, Table 3, samples GMI-C-46B, BP1¹¹ and U.S.G.S.47, respectively). Pacific Ocean seawater ($\times 10^6$) from Masuda & Ikeuchi (1979).

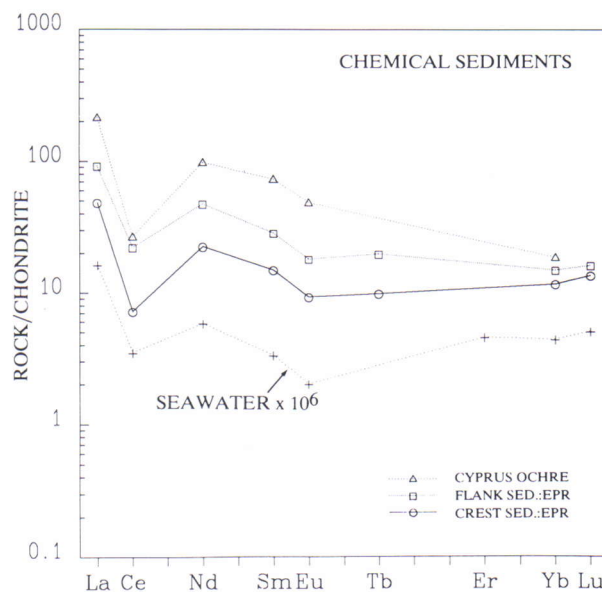


Fig. 7. Chondrite-normalized REE patterns for three types of chemical sediments: Cyprus ochre; flank sediment at East Pacific Rise (EPR) and crest sediment of EPR. Data from Fryer (1977, Table 1, analyses 3, 1 and 2, respectively). Pacific Ocean seawater ($\times 10^6$) from Masuda & Ikeuchi (1979).

REE in black schist and metapelite of the Tuomivaara sequence

The REE patterns of the two samples from detrital sediments, black schist (No. 9) and metapelite (No. 10), are shown in Fig. 3c. These samples have small depletions in Ce (Ce/Ce^* 0.62 and 0.72), which is probably due to fluorapatite dissemination. The metapelite sample No. 10 is slightly depleted in Eu

(Fig. 3c) and its REE pattern is similar to that of NASC, whereas the black schist sample No. 9 has a positive Eu anomaly (Eu/Eu^* 1.33). On the Ce/Ce^* vs. Eu/Eu^* plot (Fig. 5) this sample, together with sample No. 6, is separated from the others.

REE in the Pahtavaara IF

The two analyses from Pahtavaara (Table 2, Fig. 4) come from adjacent sulfide and phosphorite bands. The great difference in the REE abundances between these bands implies that during the precipitation of the IF and phosphorite, REE were precipitated with the phosphate compounds.

The REE patterns of the two samples from the Pahtavaara IF are similar to those of the Tuomivaara chemical sediments that have relatively flat REE

patterns. The $(La/Yb)_N$ values differ in the sulfidic host (6.08) and phosphorite interband (1.32), while Ce and Eu have a similar behavior (Figs. 3a and 4, Table 2). As a part of the samples in the Tuomivaara IF, both the samples from Pahtavaara have a "seawater-type" REE-pattern, in the sense that they are depleted in Ce, with Ce/Ce^* values of 0.60 and 0.62.

The role of secondary modification of REE

The effect of metamorphism on the REE patterns of IF and phosphorites is debatable. Bliskovisky et al. (1969) reported that the REE abundances in phosphorites are insensitive to weathering and metamorphism. Appel (1983), based on the assumption that REE are equally immobile during diagenesis and metamorphism, considered that the REE patterns of the Isua IF were all pre-diagenetic and pre-metamorphic. In contrast, Fryer (1983) suggested that the negative Eu anomalies of the Isua IF were caused by high grade metamorphism. However,

Dymek & Klein (1988), who reported positive Eu anomalies from graphitic samples of the Isua IF, preferred the REE to reflect the composition of the precipitating solutions. They did not find any Eu removal as Eu^{2+} even though the conditions during precipitation were reducing.

With few exceptions the REE data of marine phosphorites and the phosphorites of the present data are analogous. Based on this evidence, the role of metamorphism and diagenesis on the REE patterns is thought to be of minor importance.

DISCUSSION

The REE patterns of the Tuomivaara and Pahtavaara IF largely reflect the varying amounts of the fractions of the phosphorites and disseminated fluorapatite. At the same time they shed complex evidence on the contribution from the solutions which precipitated phosphorites and IF minerals and on the contribution from the detrital sources.

Both IF of the present study are contaminated by external sources, as is revealed by the interbedding of the chemical precipitates and other lithologies. The effect of the external sources on the REE is obviously masked by the fluorapatite dissemination. This is

demonstrated by the relatively similar REE patterns in all the IF types and associated metasediments.

Since the samples from the oxide-silicate IF at Tuomivaara are fairly LREE-enriched, a more detailed review is required for considering if the IF type or, especially, the oxidizing environment had an influence on the REE behavior. A direct comparison of the present data with the REE data from oxide, silicate and sulfide facies IF in the literature may be misleading because of the high phosphorus contents in the IF studied.

There are only few examples in the literature

which document the differences in the REE distribution among the different IF types. No reports exist of differences in Ce and Eu concentrations in oxidizing vs. reducing environments. The pattern types for oxide, sulfide and silicate facies are similar (e.g. Laajoki 1975, Fryer 1977, Appel 1983, Dymek & Klein 1988). Instead, there are considerable differences even within each facies.

The flat REE patterns documented for the oxide facies by Fryer (1977, 1983) prove to be different from the samples from the oxide-silicate IF of the present study. Fryer found that the REE patterns in the oxide facies are widely variable, which he interpreted to reflect absorption processes and complex diagenetic changes. The silicate-carbonate IF facies reported by Fryer show REE distributions compatible with an origin as crystalline precipitates in equilibrium with seawater.

Similarly, the data for the oxide-silicate facies presented here contrast with the data reported by Derry and Jacobsen (1990) from the Sokoman and Gunflint IF (Fig. 8). These authors found that the NASC-normalized oxide facies samples are typically HREE-enriched, being slightly less HREE-enriched than modern seawater but indistinguishable from modern metal oxy-hydroxides precipitated from seawater. As is shown in Figs. 3a and 3b, there is not a distinct correspondence in the present oxide facies REE data with REE in modern seawater. Instead, the REE patterns of the sulfidic schists of the Tuomivaara and Pahtavaara IF are similar to the patterns of seawater and these flat patterns are similar to those of the oxide facies in the Sokoman and Gunflint IF.

The REE data of the present study shows closer similarity with the data from phosphorites, chemical sediments of mid-ocean ridges and seawater than with the Paleoproterozoic IF in general. There are differences in the magnitudes of Eu and Ce anomalies, but as is shown in numerous studies these elements vary widely in their abundance in phosphorites, in chemical sediments and in seawater. This is demonstrated by De Baar et al. (1985), who found that Ce depletion was smaller in Pacific surface seawater than at a depth of 3250 m. Elderfield and Greaves (1982) observed that Eastern Atlantic surface seawater has a pronounced negative Eu anomaly, while Eu is normal at a depth of 100 m. Similarly, the phosphorites (McArthur & Walsh 1984, Piper et al. 1988) and chemical sediments at mid-ocean ridges (Fryer 1977) have a variety of pattern types, with Ce and Eu depletions present or absent.

The Tuomivaara and Pahtavaara IF, regardless of their different depositional environments, display similar Ce behavior. Of these two IF, Eu is slightly depleted in the Tuomivaara IF only. From the several

theories concerning the behavior of Ce and Eu in IF, a special interest is focused to the following two:

1) Fluctuations of fO_2 during deposition and diagenesis.

Negative Ce anomalies are widely considered to be related to oxidizing conditions (see p. 72). For example, McArthur and Walsh (1984) suggested that in reducing conditions phosphorites do not show a negative Ce anomaly but may show a positive Eu anomaly.

All except one sample (No 11) of the present study display a slight negative Ce anomaly. According to the above theory, the change in redox conditions from oxidizing to highly reducing should be combined with the disappearance of Ce anomaly, which, however, is not true in these samples. Even the two black schist samples from Tuomivaara, which could be expected to have deposited within reducing conditions, have Ce depletions accompanied by positive Eu anomalies. The negative correlation between Ce/Ce* and Eu/Eu* (Fig. 5) may imply a modest variation in redox conditions during precipitation but, nevertheless, all the samples from the chemical sediments (excluding No. 11) are Ce-depleted.

2) Influence of hydrothermal and metamorphic fluids.

Hydrothermal fluids are interpreted to be responsible for positive Eu anomalies of IF (Dymek & Klein 1988, Fralick et al. 1989, Derry & Jacobsen 1990). The volcanic affinity of some of the amphibolitic interbands within the Tuomivaara IF is established

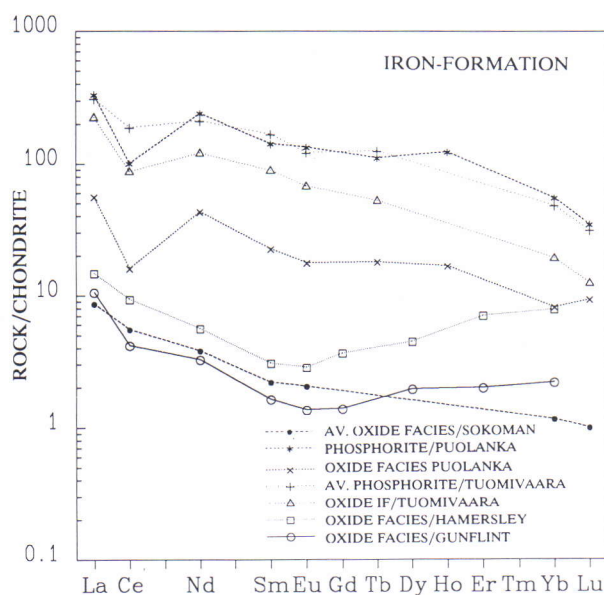


Fig. 8. Chondrite-normalized REE patterns for average oxide facies in the Sokoman IF, oxide facies in Hamersley and Gunflint (Derry & Jacobsen, 1990; Table 1, analyses 28, 1A and 30, respectively), oxide facies and phosphorite in Värylänkylä, Puolanka (Laajoki 1975; Table 2, analyses 2 and 8), average phosphorites from Tuomivaara (samples 3,5,6,7 and 8), and oxide IF (sample 4) from Tuomivaara.

by the whole rock compositions of the silicate IF at Tenetti. The exceptional sample No. 11, with a slightly positive Ce anomaly, however, has a negative Eu anomaly just like the majority of the samples from Tuomivaara. Neither does the Pahtavaara IF have positive Eu anomalies, which would be expected for rocks deposited in association of volcanism and hydrothermal activity.

Bau (1991) has shown that the hydrothermal-metamorphic fluids in reducing, mildly acidic conditions show positive Eu anomalies and $(La/Lu)_N > 1$. If these observations are applicable to natural systems, the positive Eu anomalies in the two black schists could be attributed to hydrothermal-metamorphic fluids. However, any special difference in the $(La/Lu)_N$ values (36.5 and 7.35; Table 3) in comparison to the other samples cannot be distinguished as all the analyzed samples have $(La/Lu)_N$ values > 1 with an average of 17.8.

Consequently, the precipitation of the Tuomivaara IF took place in an environment similar to those of

marine phosphorites in which oceanic upwelling carries oxic seawater in. Although the fine-scale lithological variation within the IF sequence would be indicative of fluctuations in fO_2 during precipitation, the evidence given by the Eu and Ce behavior do not support those kind of changes. Based on these data, the precipitation of IF and phosphorite was controlled by dominantly oxidizing conditions. However, a certain amount of evidence exists that in the chemical sediments of the Tuomivaara IF the magnitude of Ce depletion increases with the decrease in the magnitude of Eu depletion, and the greatest Ce depletions are found in the oxide-silicate IF. The appropriate depths for the precipitation of the Tuomivaara IF correspond to those of phosphorites; less than 1000 m (Cook 1976). The participation of hydrothermal fluids in the precipitation of chemical sediments is not reflected in the Eu behavior; instead the positive Eu anomalies in the two black schists may be related to injection of hydrothermal fluids into the sedimentary basin.

CONCLUSIONS

The REE data of the Paleoproterozoic Tuomivaara and Pahtavaara IF show that:

1) The phosphorite bands are enriched in REE in comparison to their host IF and schists. The general shape of the chondrite-normalized REE pattern in the Pahtavaara IF corresponds to that of seawater and marine phosphorites. The Tuomivaara IF resembles the former data in HREE composition. However, it includes samples which are enriched of LREE relative to HREE, thus having a similarity to the chemical sediments of mid-ocean ridges. The moderately small deviations of the REE patterns of the phosphorites of the present study from those of the recent marine phosphorites suggest that modification of the REE compositions during metamorphism was not remarkable.

2) The REE patterns of the phosphorites and most of the iron-formations display a minor depletion in

Ce, reflecting the compositions of seawater from which they were precipitated. This suggests that oxidizing conditions predominated during the precipitation of the chemical sediments of the Tuomivaara and Pahtavaara IF. In the chemical sediments of the Tuomivaara IF the magnitude of Ce depletions increases with the decrease in the magnitude of Eu depletions and the greatest Ce depletions are found in the oxide-silicate IF.

3) The rocks of the turbidite-hosted Tuomivaara IF are characterized by a variable Eu behavior with Eu/Eu^* values ranging from 0.60-1.23. The Pahtavaara IF, which is found in a volcanic association, lacks Eu anomalies.

4) The IF, both in Pahtavaara and Tuomivaara, precipitated in conditions which resembled those of recent marine phosphorites; oxic upwelling oceanic water and depths evidently no more than 1000 m.

ACKNOWLEDGEMENTS

The author wishes to thank Prof. Robert F. Dymek, Dr. Hannu Huhma and Dr. Yrjö Kähkönen for the helpful reviews which led to substantial improvements of the earlier versions of the manuscript. Thanks are also expressed to Ms. Kristiina Karja-

lainen, who drafted the maps. This study was supported by a grant from the Academy of Finland in contribution to the IGCP Project 217 "Proterozoic Geochemistry". The English language was revised by Christopher Cunliffe.

REFERENCES

- Appel, P. W. U. 1983.** Rare earth elements in the early Archean Isua iron-formation, West Greenland. *Precambrian Res.* 20, 243-258.
- Barrett, T. J., Fralick, P. W. & Jarvis, I. 1988.** Rare-earth-element geochemistry of some Archean iron formations north of Lake Superior, Ontario. *Can. J. Earth Sci.* 25, 570-580.
- Bau, M. 1991.** Rare earth element mobility during hydrothermal and metamorphic fluid-rock interaction and the significance of the oxidation state of europium. *Chem. Geol.* 93, 219-230.
- Bliskovskiy, V. Z., Mineyev, D. A. & Kholodov, V. N. 1969.** Accessory lanthanides in phosphorites. *Geochem. Int.* 6, 1055-1069.
- Boynton, W. V. 1984.** Cosmochemistry of the rare earth elements: Meteorite studies. In: Henderson, P.J. (ed.) *Rare Earth Element Geochemistry; Developments in geochemistry 2*, Amsterdam: Elsevier, 63-114.
- Cook, P. J. 1976.** Sedimentary phosphate deposits. In: Wolf, K.H. (ed.) *Handbook of strata-bound and stratiform ore deposits*, Amsterdam: Elsevier, 505-535.
- De Baar, H. J. W., Bacon, M. P., Brewer, P. G. & Bruland, K. W. 1985.** Rare-earth elements in the Pacific and Atlantic Oceans. *Geochim. Cosmochim. Acta* 49, 1943-1959.
- Derry, L. A. & Jacobsen, S. B. 1990.** The chemical evolution of Precambrian seawater: Evidence from REEs in banded iron formations. *Geochim. Cosmochim. Acta* 54, 2965-2977.
- Dymek, R. F. & Klein, C. 1988.** Chemistry, petrology and origin of banded iron-formation lithologies from the 3800 Ma Isua Supracrustal Belt, West Greenland. *Precambrian Res.* 39, 247-302.
- Elderfield, H. & Greaves, M. J. 1982.** The rare earth elements in seawater. *Nature* 296, 214-219.
- Fleet, A. J. 1983.** Hydrothermal and hydrogenous ferro-manganese deposits: Do they form a continuum? The rare earth element evidence. In: Rona, P.A., Boström, K., Laubier, L. & Smith, K.L. (eds.) *Hydrothermal Processes at Seafloor Spreading Centers*. New York: Plenum Press, 535-555.
- Fleischer, M. 1983.** Distribution of the lanthanides and yttrium in apatites from iron ores and its bearing on the genesis of ores of the Kiruna type. *Econ. Geol.* 78, 1007-1010.
- Fleischer, M. & Altschuler, Z. S. 1969.** Relation of the rare earth composition of minerals to geological environment. *Geochim. Cosmochim. Acta* 33, 725-732.
- Fralick, P., Barret, T., Jarvis, K., Jarvis, I., Schnieders, B. & Kemp, R. 1989.** Sulfide-facies iron formation at the Archean Morley occurrence, Northwestern Ontario: Contrasts with oceanic hydrothermal deposits. *Can. Mineral.* 27, 601-616.
- Fryer, B. J. 1977.** Rare earth evidence in iron formations for changing Precambrian oxidation states. *Geochim. Cosmochim. Acta* 41, 361-367.
- Fryer, B. J. 1983.** Rare-earth elements in iron-formation. In: Trendall, A.F. & Morris, R.C. (eds.) *Facts and Problems. Developments in Precambrian Geology 6*. Amsterdam: Elsevier, 345-358.
- Gehör, S. 1982.** Kittilän manganosideriittiliuskeiden petrografia, mineralogia ja geokemia. M.Sc. thesis, Univ. Oulu, 112 p. (unpublished, in Finnish)
- Gehör, S. & Havola, M. 1988.** The depositional environment of the early Proterozoic Tuomivaara iron-formation and associated metasediments, eastern Finland. *Geol. Surv. Finland, Spec. Paper 5*, 109-133.
- Goldberg, E. D., Koidie, M., Schmitt, R. A. & Smith, R. H. 1963.** Rare-earth distributions in the marine environment. *J. Geophys. Res.* 68, 4209-4217.
- Graf, I. L. 1977.** Rare earth elements as hydrothermal tracers during the formation of massive sulphide deposits in volcanic rocks. *Econ. Geol.* 72, 527-548.
- Graf, I. L. 1978.** Rare earth elements, iron-formations and seawater. *Geochim. Cosmochim. Acta* 42, 1845-1850.
- Gromet, L. P., Dymek, R. F., Haskin, L. A. & Korotev, R. L. 1984.** The "North American shale composite": Its compilation, major and trace element characteristics. *Geochim. Cosmochim. Acta* 48, 2469-2482.
- Gross, G. A. 1980.** A classification of iron formations based on depositional environments. *Can. Mineral.* 18, 215-222.
- James, H. L. 1954.** Sedimentary facies of iron formation. *Econ. Geol.* 49, 235-291.
- Kallio, M., Kärkkäinen, N., Sarapää, O. 1980.** Keski-Lapin liuskealue Itä-Kittilän ja Länsi-Sodankylän osalta. Osa I: Petrografinen kuvaus ja kallioperäkartta. Kuhmon ja Kittilän malmiprojektit, Univ. Oulu, Rep. 28, 134 p. (in Finnish)
- Laajoki, K. 1975.** Rare earth elements in Precambrian iron-formations in Väyrylänkylä, South Puolanka area, Finland. *Bull. Geol. Soc. Finland* 47, 93-107.
- Lehtonen, M. & Rastas, P. 1986.** Aluetutkimukset / Keski-Lappi. Lapin vulkaniittiprojektin vuosikertomus 1986, 4-15. (in Finnish)
- Masuda, A. & Ikeuchi, Y. 1979.** Lanthanide tetrad effect observed in marine environment. *Geochem. J.* 13, 19-22.
- McArthur, J. M. & Walsh, J. N. 1984.** Rare-earth geochemistry of phosphorites. *Chem. Geol.* 47, 191-220.
- Michard, A., Albarede, F., Michard, G., Minster, J. F. & Harlou, J. L. 1983.** Rare-earth elements and uranium in high-temperature solutions from East Pacific Rise hydrothermal vent field (13N). *Nature* 303, 795-797.
- Mikkola, E. 1941.** Muonion, Sodankylän ja Tuontsajoen kallioperä. Pre-Quaternary rocks of Muonio, Sodankylä and Tuontsajoki. Explanation to the maps of rocks, sheets B7, C7 and D7. Geological map of Finland 1:400 000, 286 p.
- Paakkola, J. 1971.** The volcanic complex and associated manganiferous iron formation of the Porkonen-Pahtavaara area in Finnish Lapland. *Bull. Comm. géol. Finlande* 247, 83 p.
- Paakkola, J. & Gehör, S. 1988.** The lithofacies associations and sedimentary structures of the iron-formations in the early Proterozoic Kittilä greenstone belt, northern Finland. *Geol. Surv. Finland, Spec. Paper 5*, 213-238.
- Piper, D. Z. 1974.** Rare earth elements in ferromanganese nodules and other marine phases. *Geochim. Cosmochim. Acta* 38, 1007-1022.
- Piper, D.Z., Baedeker, P.A., Crock, J.G., Burnett, W. & Loebner, B.J. 1988.** Rare earth elements in the phosphatic-enriched sediment of the Peru shelf. *Marine Geol.* 80, 269-285.
- Rosenberg, R. J., Kaistila, M. & Zilliacus, R. 1982.** Instrumental epithermal neutron activation analysis of solid geochemical samples. *J. Radioanal. Chem.* 71, 419-428.
- Sakko, M. & Laajoki, K. 1975.** Whole rock Pb-Pb isochron age for the Pääkkö iron formation in Väyrylänkylä, South Puolanka area, Finland. *Bull. Geol. Soc. Finland* 47, 113-117.
- Simonen, A. 1980.** The Precambrian in Finland. *Geol. Surv. Finland Bull.* 304, 58 p.
- Vaasjoki, M., Äikäs, O. & Rehtijärvi, P. 1980.** The age of mid-Proterozoic phosphatic metasediments in Finland as indicated by radiometric U-Pb dates. *Lithos* 13, 257-262.

Appendix. Sample description.

No	Depth (m)	Description
Sotkamo, Tuomivaara / drill hole 1		
1	15.80	Sulfide IF, with apatite dissemination
2	43.40	Silicate IF
3	48.80	Phosphorite band in oxide-silicate IF
4	48.85	Oxide-silicate IF (host to sample 3)
Sotkamo, Tuomivaara / drill hole 2		
5	40.30	Phosphorite band in oxide-silicate IF
6	137.17	Phosphorite band in black schist
7	150.30	Phosphorite band in sulfide (-carbonate) IF
8	202.74	Phosphorite band in sulfide (-carbonate) IF
9	202.80	Black schist
Sotkamo, Tuomivaara / drill hole 3		
10	16.40	Metapelite
Sotkamo, Tenetti		
11	Outcrop	Aluminous silicate IF
Kittilä, Pahtavaara / drill hole 2		
12	325.05	Sulfide IF (host to sample 13)
13	325.10	Phosphorite band in sulfide IF

GEOLOGY AND GEOCHEMISTRY OF THE HÄMEENLINNA-SOMERO VOLCANIC BELT, SOUTHWESTERN FINLAND: A PALEOPROTEROZOIC ISLAND ARC

by
Gerhard Hakkarainen

Hakkarainen, Gerhard 1994. Geology and geochemistry of the Hämeenlinna-Somero Volcanic Belt, southwestern Finland: a Paleoproterozoic island arc. *Geological Survey of Finland, Special Paper 19*, 85–100, 7 figures and 3 tables.

The Paleoproterozoic Hämeenlinna-Somero Volcanic Belt is situated south of the Bothnian basin in southern Finland, within the South Svecofennian Subprovince. Chemically and lithologically the belt resembles modern island arc environments. Three deformational events were recognized in the area. The dominant D₁ phase folded the supracrustal rocks isoclinally with E-W trending axial planes. The NE trending D₂ and SSE trending D₃ phases vary locally in intensity. Two large steeply dipping shear complexes of different ages are met within the area. The older, W-SW trending Hämeenlinna shear zone predates the intrusion of late-kinematic potassium granites but postdates the synkinematic granodiorite emplacement. The younger, NW trending Painio-Hirsjärvi fault zone shows a sinistral sense of shear and postdates the emplacement of potassium granites.

The belt is subdivided into two groups. (1) The (lower) Forssa group comprises calc-alkaline metavolcanics and metasediments. The metavolcanic rocks range from basaltic to rhyolitic in composition, with abundant andesites. The area was originally a complex of stratovolcanoes with high erosion rates, producing large amounts of reworked volcanic material. (2) The (upper) Häme group is characterized by an association of basaltic to andesitic lava flows with interlayered pyroclastics, erupted in an E-W trending fissure system. The volcanics are layered upon pelitic sediments and graywackes. The earliest extrusives in the Forssa group are rhyolites to dacites followed by andesites and basalts. Volcanism in the Häme group began with basalt eruptions and contemporaneous precipitation of Fe-sulfide formations at the base of the pile, and volcanism subsequently changed into andesitic.

Major and trace element geochemistry of the volcanic rocks resembles that in modern mature arcs. In general the volcanics are of medium-K type, with relatively high abundances of LILE. The Forssa group volcanics show a calc-alkaline fractionation trend. The Häme group rocks have more tholeiitic affinities, with Fe enrichment relative to Mg. The P₂O₅ content is slightly higher in the basalts of the Häme group than in those of the Forssa group. The Mg numbers in the basalts are moderate (40–52) and the Ni content low (20–50 ppm).

Key words (GeoRef Thesaurus, AGI): volcanic belts, metavolcanic rocks, basalts, andesites, deformation, geochemistry, stratigraphy, island arcs, Proterozoic, Paleoproterozoic, Hämeenlinna, Forssa, Somero, Finland

*Gerhard Hakkarainen, Department of Geology and Mineralogy, Åbo Akademi University, Domkyrkotorget 1, FIN-20500 Turku, Finland
Present address: Boliden Mineral AB, S-77698 Garpenberg, Sweden*

INTRODUCTION

The Fennoscandian Shield is divided into three parts, the oldest being the Archean craton (3.1-2.7 Ga) in the east (Fig. 1). It is bordered to the west by the Paleoproterozoic Karelian and Svecofennian terrains (2.5-1.7 Ga). The youngest region of Proterozoic age is the Southwestern Gneiss Complex or the Southwest Scandinavian Domain (0.9-1.75 Ga) (Gaál & Gorbatshev, 1987). No Archean components have been found in the central part of the Svecofennides. The Svecofennian supracrustal rocks were syntectonically intruded by granodiorites, tonalites and quartz diorites, and minor ultramafic and gabbroic bodies. The cessation of the Svecofennian orogeny is postulated from the large scale anatexis of the supracrustals and the emplacement of the late-kinematic K-rich granites.

The Svecofennian volcanic rocks in Finland yield ages of 1.91 to 1.89 Ga (Patchett & Kouvo 1986, Gaál & Gorbatshev 1987, Kähkönen et. al. 1989)

and plutonism was almost contemporaneous with volcanism (1.89-1.83 Ga; Patchett & Kouvo 1986). The estimated 30-40 Ma duration of volcanic activity in the Svecofennian resulted in volcanic belts of different chemical and lithological characteristics. They vary from bimodal suites in southern Finland (Ehlers & Lindroos 1990) to calc-alkaline and alkaline suites to the north (Kähkönen 1989), which indicates a complex development.

The Hämeenlinna-Somero Volcanic Belt (HSB) is part of the South Svecofennian Subprovince in southwestern Finland and forms a large arc-like structure striking E-W. It is one of the largest exposed coherent volcanic belts in the Finnish part of the Svecofennides. The lateral extent of the belt is 100 km in the E-W direction and 60 km in the N-S direction. This study focuses on the central parts of the belt.

Simonen (1953, 1980) divided the Svecofennian supracrustal rocks into three major categories. The

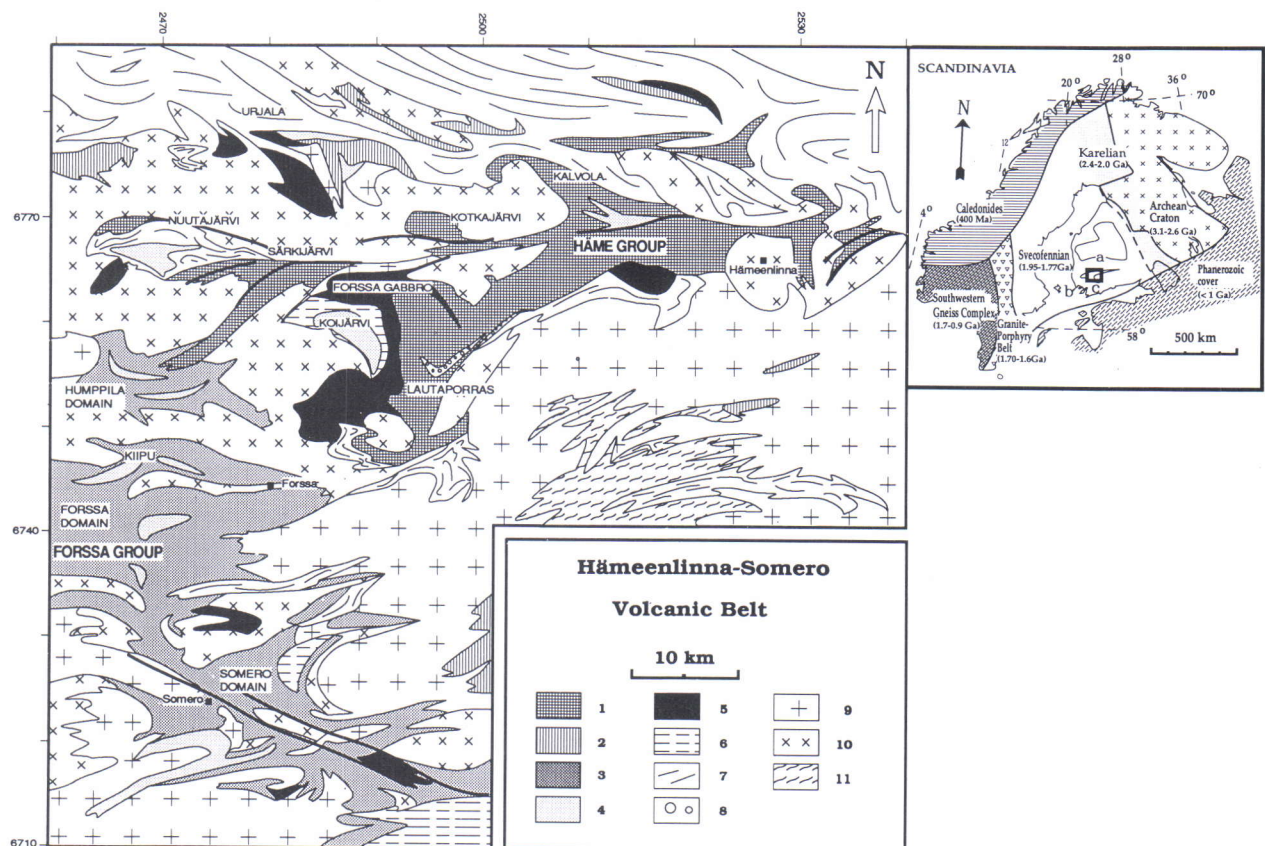


Fig. 1. Geological map of the central parts of the Hämeenlinna-Somero Volcanic Belt. The thick lines in the upper part represent the Hämeenlinna Shear Zone and those in the southern part the Painio Shear Zone. 1 = Häme group basalts and andesites, 2 = basalts and andesites (relationship to the Forssa and Häme groups unknown), 3 = Forssa group andesites and basalts, 4 = dacites and rhyolites, 5 = gabbros and ultramafic rocks, 6 = intercalations of quartz-feldspar gneisses and mica gneisses or schists, 7 = mica schists and gneisses (originally graywackes and pelites), 8 = volcanic conglomerates, 9 = late-kinematic K-granites, partly migmatitic, 10 = synkinematic granodiorites, tonalites and quartz diorites, 11 = migmatitic granodiorites and tonalites. The inset shows the major provinces (domains) of the Fennoscandian Shield. The dashed line represents the Ladoga - Bothnian Bay zone. The study area is shown by the square. a = Tampere, b = Enklinge, c = Orijärvi-Lohja.

Lower Svecofennian subgroup consists of immature graywacke-slates and quartz-feldspar rocks. The Middle Svecofennian subgroup consists of basic and intermediate volcanics and intercalated sedimentary

rocks, while the Upper Svecofennian subgroup comprises argillaceous sediments. Roughly, the HSB corresponds to the Middle Svecofennian subgroup of Simonen (1980).

METAMORPHISM

The study area was metamorphosed to amphibolite facies but the original volcanic textures are still preserved. Common mineral assemblages in the mafic rocks are plagioclase and hornblende. Some of the hornblende phenocrysts are augite pseudomorphs and relict zonation in plagioclase is common. The sedimentary rocks contain assemblages of biotite, garnet and cordierite.

The metamorphic grade in the northern part of the study area is slightly lower than in the south. This is shown by locally persisting assemblages of cordierite-andalusite-chlorite-white mica in the northern pelitic schists. Retrograde reactions are manifested in the alteration of Ca-rich plagioclase to Na-rich plagioclase, zoisite and epidote and in alteration of hornblende to biotite. Mäkelä (1980) estimated the pressure and temperature to be 3-4 kbar and 600°C at Kiipu in the Forssa area. In the northern part of the

study area the intrusive rocks comprise granodiorites and quartz diorites.

The higher metamorphic grade in the southern part is shown by a higher degree of melting of the supracrustal rocks and formation of migmatites. Still, the volcanic and sedimentary rocks in the southern part, situated in a depression adjoined by migmatite rocks, show lower-grade metamorphic features such as stable muscovite-cordierite assemblages. The boundary between the migmatite zone and the less metamorphosed northern zone with granodiorites and quartz diorites runs in a WSW-ENE direction near Forssa (Fig. 1). Further southwards, the amphibolite facies rocks in Orijärvi-Lohja yield temperatures and pressures of about 650° and 3 to 5 kbar (Schreurs & Westra 1986) and the grade of metamorphism was highest in the West-Uusimaa thermal dome.

SUBDIVISION OF THE STUDY AREA

The volcanic belts in southwestern Finland are characterized by various lithologies. The unique characteristic features of different belts are summarized below. The Orijärvi-Lohja area (Schreurs & Westra 1986, Colley & Westra 1987, Mäkelä 1989, Väisänen 1991) 50 km south of the study area (Fig. 1) consists of bimodal volcanic rocks, and abundant limestones and iron formations. The present study area is composed of tholeiitic to calc-alkaline rhyolitic to basaltic volcanic rocks, containing few Fe-oxide formations and limestones. The Tampere volcanics, 70 km north of Hämeenlinna, consist mainly of calc-alkaline high-K dacites and andesites and shoshonitic rocks associated with conglomerates (Kähkönen 1989). The Haveri tholeiitic basalt formation also occurs in this area (Mäkelä 1980, Kähkönen & Nironen, this volume).

Based on lithological differences (Table 1, Fig. 2), the belt is divided into two groups: (1) the Forssa group is dominated by andesites and (2) the Häme group by basalts. Furthermore, there are two domains whose relationship to these two groups is uncertain, the Nuutajärvi and Koijärvi domains.

Northwards the Häme group is in contact with migmatites and gneisses. The basalts rest on pelites, and in addition some of the extrusives in the upper part of the group occur as massive interlayers in the sedimentogenic migmatites and gneisses to the north. Within the Forssa group no basement below the volcanic rocks has been found (Table 1). Since both of the groups are embraced by large granitoid batholiths the only areas where they actually are in mutual contact are the Humppila and Nuutajärvi domains (Fig. 1).

Table 1. Lithological differences between the Häme and Forssa groups.

Forssa group	Häme group
No clearly discernible sedimentary basement.	Basement of pelitic schists and volcanogenic conglomerates.
The most abundant rock type is andesite.	The most abundant rock type is basalt.
Acid volcanic rocks are abundant.	Acid volcanic rocks are sparse.
Both uralite- and plagioclase-porphyritic rocks.	Mostly uralite-porphyritic rocks.
Intermediate and mafic lavas with pillow structures and autobrecciation.	The main part consists of massive lava flows, the offshoots (Kalvola) are autobrecciated and pillowed.
Sedimentary (pelitic) intercalations in the volcanic formations.	No pelitic intercalations in the volcanic formations.

FORSSA GROUP

The Forssa group includes three synformal E-W trending structures, which in order from south to north are the Somero, Forssa and Humpvila domains. The volcanic rocks range from uralite- and

plagioclase-porphyritic basalts and andesites to various plagioclase-porphyritic dacitic and rhyolitic lavas and pyroclastic rocks, andesite being the most abundant rock type.

Humpvila domain

Here the Forssa group consists of basaltic uralite-porphyritic agglomerates and lavas, and of thick andesitic to dacitic tuffs in the southern part. In the northern part there is a heterogeneous association of laminated intermediate and acid tuffs, tuffites, agglomerates, lavas and minor pelitic interlayers. The Häme group basalts lie in a NE trending syncline, and the basalts are exposed on the present erosion surface in the eastern part of the domain only. At Humpvila Fe-sulfide formations are as intercalations in the

Häme group basalts close to the depositional contact with the Forssa group. The Fe-formations occur as 3-4 m thick disseminated layers between basalt units or as more dispersed in bodies of mica-rich altered basalt. Dacitic to rhyolitic pyroclastic interlayers or fragments are also found in the basalts. The relationship between the two groups is based on the fact that the Fe-formations elsewhere also occupy a stratigraphical position in the lowest part of the Häme group.

Forssa domain

In the Forssa domain several different lithological entities can be distinguished. Successions of thick andesitic lava flows and agglomerates are the most abundant ones. The lavas are partly pillowed and autobrecciated. Several acid eruptive centers with rhyolitic and dacitic lava domes, enclosed in agglomerates and laminated tuffs, occur within the andesites. The Kiipu area in the northern part of the Forssa domain contains a succession with reworked acid volcanic rocks, sulfide mineralizations and sparse

limestone layers (Lindroos 1980, Mäkelä 1980).

In the area south of Forssa grading into distal facies volcanic and volcanoclastic rocks indicates increasing distance from the volcanic centers. The central vents were identified by successions of thick lavas, coarse agglomerates and poorly sorted tuffs. At the western margin of the Forssa domain, lavas are rare and laminated fine-grained tuffites are abundant. Accordingly, the volcanic centers were situated in the central part of the Forssa domain, where the

largest sheets of basalt and andesite lavas occur and where the rhyolite domes are found. The narrow neck between the Somero and the Forssa domains comprises

relatively mafic rocks with basaltic autobrecciated and partly pillowed lavas, lapilli tuffs and agglomerates interlayered with sparse andesitic tuff horizons.

Somero domain

The Somero domain was described by Mäkelä (1989) and Stel et al. (1989). The geology is controlled by a synformal depressional structure oriented subparallel with the Painio shear zone, also called the

Hirsjärvi fault by Mäkelä (1989). The WNW to ESE trending shear complex divides the area into two lithologically different parts (Fig. 1). South of the shear complex the rocks consist mostly of andesites

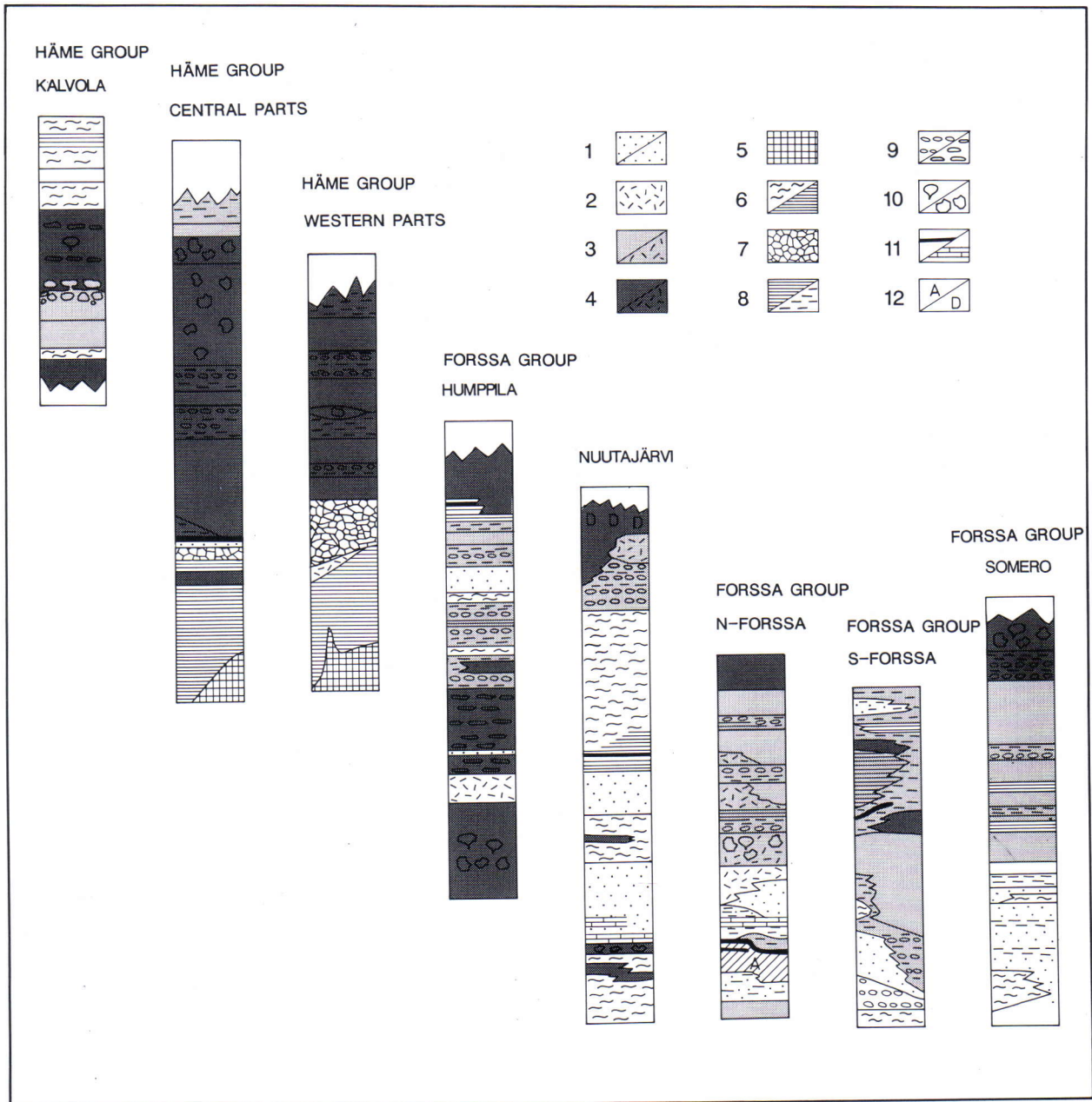


Fig. 2. Stratigraphic columns from the Forssa and the Häme groups. Kalvola represents an offshoot in the gneisses and schists to the north. The western parts of the Häme group constitute the Lautaporras area (Fig. 1). The central parts of the Häme group constitute the areas east of Lautaporras. The intermediate and mafic volcanic rocks in the uppermost part of the Nuutajärvi column belong to the Häme group. 1 = rhyolite, 2 = dacitic feldspar porphyry, 3 = andesitic uralite/plagioclase porphyry, 4 = basaltic uralite/plagioclase porphyry, 5 = gabbro, 6 = graywacke/pelite, 7 = conglomerate, 8 = tuffite/tuff, 9 = agglomerate, 10 = pillow lava/autobrecciated lava, 11 = Fe-sulfide formation/limestone, 12A = Mg-metasomatic rock, 12D = diopside-bearing rock.

and these belong to the Forssa group. This sequence contains a Zn-Ag sulfide mineralization described by Mäkelä (1989). In addition, a 300 m thick rhyolitic to dacitic plagioclase-quartz-porphyritic stratified

tuff formation lies south of the Somero town. The successions north of the shear complex show a wider range of rocks including basalts, quartz-feldspar gneisses, and turbiditic pelitic schists and gneisses.

HÄME GROUP

The Häme group consists of tholeiitic plagioclase- and uralite-porphyritic basalts grading into even-grained or plagioclase-porphyritic andesites. In its present outline it is a 5 km wide irregular zone striking E-W for approximately 100 km. At Lautaporras the volcanic rocks are folded into a large northeastwardly plunging synform, which is partly intruded and split by the Forssa gabbro (Figs. 1 and 2). East of Lautaporras, in the central part, the belt bends from NE towards E. The group is built up of thick lava flows and interlayered basaltic pyroclastics. The most abundant rock type is a uralite porphyritic rock with 2-3 mm hornblende phenocrysts and smaller plagioclase phenocrysts which occasionally show oscillatory zoning. However, some of the andesitic end members contain only plagioclase phenocrysts. Augite is seldom found as phenocrysts due to the strong uralitization. The pyroclastic rocks are mostly poorly sorted, although some reworked tuffs in the upper part of the volcanic pile are graded.

Deformed basaltic feeder dikes occur throughout the Häme group. Most of them are fine-grained with small- or medium-sized hornblende phenocrysts, but coarse-grained porphyritic hornblenditic dikes and sills, containing more than 50% phenocrysts, also occur in the volcanic pile and in the underlying pelitic schists.

Several branches of the upper part of the Häme group extend into the gneissose sediments to north. At Kalvola they consist of several generations of autobrecciated and pillowed uralite-porphyritic basalts. Stratigraphically these rocks are succeeded

by plagioclase-porphyritic andesites, which in turn are cut and brecciated by younger uralite-porphyritic basalt dikes.

On the southern margin of the group the basalts rest upon a 100-200 m thick sequence of volcanic conglomerates and interlayered tuffs. The conglomerates are poorly sorted and contain subrounded clasts of plagioclase- and uralite-porphyritic and even-grained basalts. They have a matrix-supported fabric and resemble debris flow deposits. Carbonate breccia pipes and a 1-2 m thick banded Fe-oxide-chert layer occur in the lowermost part of the conglomerates. Also in the lowermost part of the conglomerates at Lautaporras dacitic feldspar-porphyritic fragments are common, and their shapes vary from angular to well rounded. Similar rocks are found in the Forssa group. The conglomerates are located between two basalt formations but this arrangement is not depositional, rather it is caused by folding. (see page 92.)

Approximately 2-5 m thick laminated Fe-sulfide formations occur in connection with the basal conglomerates. Their occurrence is not restricted to the depositional level of the conglomerates, but they are partly interlayered with basalts higher in stratigraphy.

South of the volcanics and conglomerates there are pelitic and laminated schists containing corroded cordierite pseudomorphs and a metamorphic differential banding. Top of strata directions were determined from scour surfaces, graded bedding, slumping and load casts in several locations along the contact between the pelites and the basalts.

KOIJÄRVI AND NUUTAJÄRVI DOMAINS

The Kojjärvi domain divides the Häme group into two parts. The NW corner of the domain consists of a syncline containing graded cordierite-mica schists, interlayered with rhyolitic lava flows and basaltic tuffs. The gradation between mica schists and volcanoclastics suggests a local origin for the sediments. The SE part consists of a thick sequence of rhyolitic lava flows, reworked pyroclastics and a banded chert-Fe-sulfide formation. The domain is bounded by the Kojjärvi shear zone in the west and

by the Forssa gabbro in the east. The observations of Neuvonen (1954) suggest that the Kojjärvi domain was uplifted relative to the Häme group. It seems appropriate to infer that the Kojjärvi domain represents a block that was juxtaposed vertically by faults to the same level as the Häme group.

The Nuutajärvi area forms an ellipsoid-shaped anticline. The internal stratigraphy is deduced from structural criteria and top of strata determinations. According to Neuvonen (1954), the supracrustal

rocks can be divided into three major units. The author's observations are broadly compatible with those of Neuvonen, with slight modifications. (1) The oldest unit consists, from the lowermost member upwards, of basaltic pillow lavas, mudstones with interlayers of basaltic and rhyolitic to rhyodacitic tuffs, calcareous precipitates, and rhyodacitic lavas and reworked tuffs. (2) The middle unit consists of

graywackes and pelites with minor basaltic to dacitic tuffs. Its lowermost part is dominated by pelites with local sulfide-rich intercalations. (3) The uppermost unit comprises basaltic to intermediate pyroclastics and lavas, which belong to the Häme group. It starts with andesitic agglomerates and lavas, which are succeeded by basaltic tuffs and lavas.

DEFORMATION

The structural styles of the Orijärvi-Lohja area and the Tampere Schist Belt have been investigated by several authors. The HSB is situated between these two areas.

Nironen (1989) proposed for the central parts of the Tampere Schist Belt an initial deformation D_1 with subvertical axial planes and horizontal fold axes. D_2 and D_3 are non-penetrative low-angle shears in relation to D_1 with dextral and sinistral asymmetric folding, respectively. Ploegsma and Westra (1990) described in the Orijärvi area a recumbent D_1 folding event with subhorizontal E-W trending axial planes that could be correlated with the D_1 event near Tampere. The NE-SW oriented D_2 dominates the tectonic style. The locally occurring D_3 consists of open folds with axial planes in NW-SE to NE-SW directions.

The deformational styles in the northern part of the HSB, which comprises all domains except Somero, are illustrated in Fig. 3 and listed in Table 2. The D_1

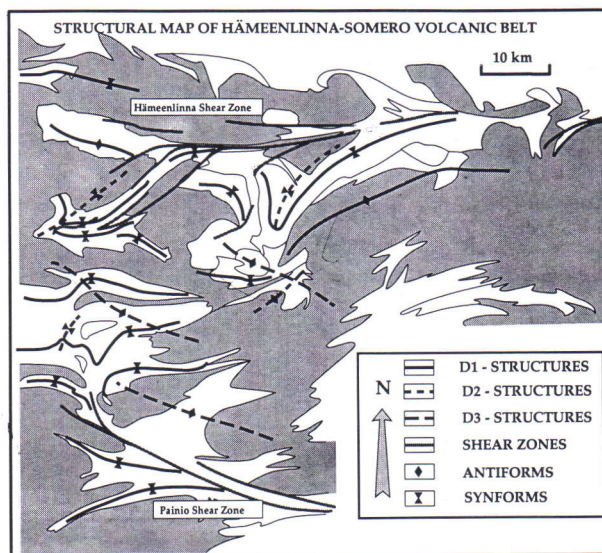


Fig. 3. Structural map of the Hämeenlinna-Somero Volcanic Belt. Only the major tectonic features are illustrated. Plutonic rocks are shown as shaded areas.

Table 2. Record of the deformational history in the Hämeenlinna-Somero Volcanic Belt.

pre- D_1	S_0	Slumpings, load casts, sedimentary dykes, ripple marks
D_1	F_1	Tight to open folding with subhorizontal fold axes.
	S_1	Dominant penetrative axial-plane schistosity, usually oriented E-W. Metamorphic differentiation.
D_2	F_2	Small-scale asymmetric drag folds to large-scale open folds with dominantly dextral sense of shear. Steeply plunging fold axes ($> 60^\circ$).
	S_2	Axial-plane crenulation cleavage deforming S_0 and S_1 , oriented $20-60^\circ$ with subvertical axial planes.
D_3	F_3	Local large-scale undulatory uplifting associated with plutonic emplacement. Open folds with steep axial planes striking $115-130^\circ$.
	S_3	Weakly developed axial plane schistosity.
D_4	F_4	Non-penetrative brittle to plastic shear deformation.
	S_4	NW-SE to NE-SW oriented shear zones locally bending the earlier S-planes.

event was an E-W oriented isoclinal to open folding, with initially subhorizontal fold axes. The D_2 event was regionally a non-penetrative asymmetrical shear folding, predominantly dextral with subvertical axial planes oriented 40° to 60° . D_2 developed locally a penetrative S_2 cleavage, which overprints the S_0 bedding and the S_1 axial plane schistosity. S_2 is markedly well-developed in the western part of the Häme group and in the northern part of the Humppila domain. At Lautaporras the basal conglomerates of the Häme group are structurally between thick basalt formations. They are exposed in the core of a D_1 anticline. During D_2 the S_1 and S_0 structures were folded into a large-scale open synform plunging towards the NE.

The D_3 event is observed locally and it is also recorded by Stel et al. (1989) in Somero. D_3 is defined by large subhorizontal open folds and the associated schistosity is developed only in narrow zones on the fold limbs. A prominent D_3 feature occurs in the migmatized gneisses east of Forssa, where S_2 and small-scale asymmetric folds of D_2 are folded by F_3 . S_1 is here expressed as a metamorphic segregation in 0.5-1 mm thick mafic and felsic laminae or as a strong planar fabric in the aluminous mica gneiss layers. The regional consistency of S_2 implies that the D_3 event was not regionally prominent.

D_4 comprises narrow N-S oriented brittle shears with local folding of the earlier schistosities and the bedding around the fracture planes.

The southern migmatite zone and the northern part, dominated by granodiorites, show slightly different deformational patterns. The lineations are generally steep in the granodiorite zone. In contrast, the lineations in the migmatite zone tend to be subhorizontal plunging less than 45° . This may be explained by subparallelism of S_1 and S_2 , resulting in type 0 fold patterns of Ramsay & Huber (1987). Transposition of S_1 towards S_2 causes the intersection lineations to be subhorizontal when corresponding axial planes have different dips. No observations of recumbent folding during D_1 were made in the northern parts, but in Somero the S_1 axial planes tend to be more horizontal, causing the differences in lineations mentioned above. Generally, the deformational styles of the HSB resemble those

found in the Tampere Schist Belt, but the more flat-lying S_1 planes in Somero may reflect the regional change from recumbent folding in Orijärvi to more upright folding northwards to the Forssa-Hämeenlinna area.

Several complexes of megashears transect the Svecofennian bedrock in southern Finland. Two large shear complexes are detected in the study area, the Painio shear zone in Somero (Mäkelä 1989, Stel et al. 1989) and the Hämeenlinna shear zone (Fig. 3). The rocks in the shear zones vary from protomylonites and mylonites to pseudotachylytes. Usually a mylonitic foliation developed around the crushed clasts and changed them to resemble protomylonites.

The Hämeenlinna shear zone trends E-W and forms an incoherent lineament with irregular boundaries and consisting of several branches. At Humppila it branches out in a duplex which comprises the Nuutajärvi and Humppila domains. Observations on both dextral and sinistral sense of shear have been made. The Kojjärvi sedimentary-acid volcanogenic basin was juxtaposed against the Häme group during this faulting. The diversity of movement directions indicates that the shear zone was affected by displacements both horizontally and vertically.

In the northern part of the Humppila domain the extremely well-developed S_2 is the dominant schistosity. The areas where S_2 dominates over S_1 and where the shears of the Hämeenlinna shear zone form duplex structures coincide fairly well with each other. In these areas both structures are oriented NE and hence these structures may have a genetic relationship.

The Hämeenlinna shear zone cross-cuts and deforms the intermediate synkinematic granitoids. However, within this zone there is a totally undeformed late kinematic K-granite. In contrast, the Painio shear zone regularly deforms the late kinematic pegmatitic and granitic veins. Hence the NW-SE trending lineaments tend to be younger and the E-W to NE-SW trending zones, like the Hämeenlinna shear zone, are slightly older. The movements in the Hämeenlinna and the Painio shear zones are of different ages and they are closely related to the emplacement of the plutonic rocks in respective areas.

GEOCHEMISTRY OF THE VOLCANIC ROCKS

In general, the rocks of the Forssa group range from basalts to rhyolites, but intermediate rocks are the most common ones. The Häme volcanics, in contrast, are dominated by basalts and basaltic andesites, while dacites and rhyolites are scarce.

Representative analyses of the HSB volcanics are in Table 3. The classification based on alkalis is questionable to some degree since these elements are sensitive to alteration. However, the K_2O+Na_2O vs. SiO_2 diagram shows that the rocks of the Forssa and

Table 3. Representative analyses of the volcanic rocks from the Häme group (H) and the Forssa group (F).

Numb	1.	2.	3.	4.	5.	6.	7.	8.	9.	10.	11.
Label	459.2	109	215	65	144.2	323	48	459.1	338	121	37
Group	H	H	H	F	H	F	F	H	F	F	F
SiO ₂	45.95	48.30	49.90	50.40	53.90	54.90	58.50	59.20	59.26	61.50	70.90
TiO ₂	1.61	1.12	0.83	1.11	1.09	1.63	1.01	0.86	0.84	0.55	0.30
Al ₂ O ₃	17.45	15.30	18.30	15.70	15.70	14.40	15.60	15.10	17.69	17.50	14.70
FeO*	11.60	11.36	9.81	11.23	10.44	11.27	8.69	6.33	8.71	6.14	3.25
MnO	0.18	0.20	0.17	0.20	0.17	0.18	0.17	0.13	0.07	0.12	0.06
MgO	6.67	6.74	5.62	4.67	3.97	3.18	2.96	2.87	2.17	2.67	0.64
CaO	8.43	10.20	8.59	8.79	7.36	7.37	6.30	9.48	4.39	5.66	1.77
Na ₂ O	2.17	2.91	2.84	2.31	2.74	3.25	2.81	3.30	3.79	3.77	4.02
K ₂ O	2.83	0.73	0.75	1.40	1.80	1.39	1.83	1.24	2.68	0.91	3.45
P ₂ O ₅	0.17	0.30	0.30	0.24	0.37	0.27	0.25	0.20	0.19	0.18	0.09
Sum	97.06	97.16	97.11	96.05	97.54	97.84	98.12	98.71	99.79	99.00	99.18
Cr (ppm)	42	240	167	50	70	20	<10	-	-	-	-
Ni	70	90	32	30	30	10	14	20	26	24	16
Co	-	-	-	-	-	-	-	-	23	-	11
V	165	290	224	270	220	320	188	180	316	103	39
Cu	20	60	320	190	60	150	38	20	8	93	13
Zn	150	110	117	140	120	140	95	90	63	73	59
S	90	60	220	170	80	190	79	50	420	1330	90
Rb	-	-	<20	-	-	-	71	-	<20	27	90
Ba	353	192	225	242	373	393	234	343	272	297	729
Sr	270	530	576	316	470	290	214	440	163	217	194
Zr	90	60	91	90	130	150	144	150	149	113	244
Mg-value (%)	50.60	51.39	50.51	42.56	40.39	33.45	37.77	44.68	30.74	43.65	25.97
Sum of alkalis	5.00	3.64	3.59	3.71	4.54	4.64	4.64	4.54	6.47	4.68	7.47
CIPW Normative composition (wt%), Fe calculated as 0.85% FeO and 0.15% Fe ₂ O ₃											
Q	0.00	0.00	0.00	2.81	6.20	7.71	13.48	12.58	10.58	16.89	27.90
Or	16.73	4.31	4.44	8.27	10.64	8.22	10.84	7.33	15.84	5.39	20.43
Ab	14.76	24.62	24.03	19.54	23.18	27.5	23.78	27.92	30.53	31.9	33.84
An	26.13	26.56	35.01	28.36	25.26	20.63	24.56	22.76	20.66	27.07	8.49
Ne	1.95	00.0	00.0	00.0	00.0	00.0	00.0	00.0	00.0	00.0	00.0
Di	12.17	18.57	4.81	11.56	7.61	12.13	4.36	19.28	0.00	0.00	0.00
Hy	0.00	5.72	24.01	20.35	19.44	15.45	16.18	5.39	16.42	14.39	5.77
Ol	18.29	12.24	0.31	0.00	0.00	0.00	0.00	0.00	0.00	0.00	0.00
Il	2.91	2.13	1.58	2.11	2.07	3.1	1.42	1.63	1.60	1.04	0.58
Mt	2.80	2.75	2.37	2.71	2.52	2.72	2.10	1.53	2.11	1.48	0.79
Sum	96.19	97.51	97.44	96.35	97.87	98.06	98.36	98.96	99.99	99.34	99.45

1. Uralite-porphyrific basalt dyke, Häme group, Kalvola (x=6775.18,y=2505.08).
2. Uralite-porphyrific lava, Häme group, Lautaporras (x=6754.37, y=2494.20).
3. Even-grained metabasalt, Häme group, Särkijärvi (x=6764.45, y=2478.15).
4. Metabasalt, Forssa group, Forssa domain (x= 6735.80, y=2467.89).
5. Uralite-plagioclase-porphyrific lava, Häme group, Kotkajärvi (x=6767.53, y=2499.77).
6. Meta-andesite, Forssa group, Forssa-Somero domain (x= 6727.93, y=2470.60).
7. Even-grained andesitic metalava, Forssa group, Forssa domain (x=6738.20, y=2469.82).
8. Plagioclase-porphyrific andesite metalava, Häme group, Kalvola (x=6775.19, y=2505.08).
9. Uralite-plagioclase-porphyrific andesite, Forssa group, Forssa domain, Kiipu (x=6747.07, y=2467.06).
10. Andesitic metalava, Forssa group, Forssa domain (x=6737.82, y=2465.82).
11. Rhyolitic metalava, Forssa group, Humppila domain (x=6755.43, y=2469.24).

Analytical equipment: Philips PW 1400 XRF-spectrometer (powder briquettes).
 Laboratories: Outokumpu Oy and Rautaruukki Oy

the Häme groups represent mostly subalkaline types. In the K_2O vs. SiO_2 diagram, they vary from low-K to high-K rocks but are dominated by medium-K types. The scatter in the total alkalis relative to silica is mainly due to variation in the potassium content and less dependent on the variation of sodium (Fig. 4b-c).

The rocks of the Forssa group show a general calc-alkaline fractionation trend in the AFM and SiO_2 vs. FeO^*/MgO diagrams (Figs. 4a and 5b), but the basalts and a few andesites show a diversified trend with tholeiitic affinities. With a few exceptions, the rocks of the Häme group have tholeiitic rather than calc-alkaline affinities. However, the tholeiitic affinities are not pronounced in either group and in the TiO_2 vs. FeO^*/MgO diagram (Fig. 5a) the basalts are transitional between tholeiitic and calc-alkaline rocks. The general trend is an enrichment in Fe relative to Mg in the early stages of crystallization in both the Häme and the Forssa groups. During progressive crystallization of dacites, rhyodacites and rhyolites in the

Forssa group constant FeO^*/MgO ratios were maintained. According to Miyashiro (1974), TiO_2 decreases in calc-alkaline series and increases in tholeiitic series during fractionation. The TiO_2 contents in the HSB basalts show a decrease with increasing silica content, and in andesites ($SiO_2 = 55-60\%$) titanium decreases less rapidly than for the other silica values (Fig. 6a). Also P_2O_5 values decrease with increasing silica in both groups. The P_2O_5 contents in the basalts of the Häme group (0.27-0.41%) are slightly higher than in those of the Forssa group (0.13-0.31%; Fig. 6b).

The trace elements Ni, Cr, Co, Zr, Sr and Ba distinguish to a lesser extent the two groups and the distribution fields overlap. The Ni content in the basalts and basaltic andesites are low, ranging between 20 and 60 ppm; nevertheless in the Häme group two samples contain 90 ppm Ni (Fig. 6d). The Häme basalts show slightly elevated Sr values compared to the Forssa basalts (Fig. 6c). The Häme basalts are mostly olivine-normative in contrast to

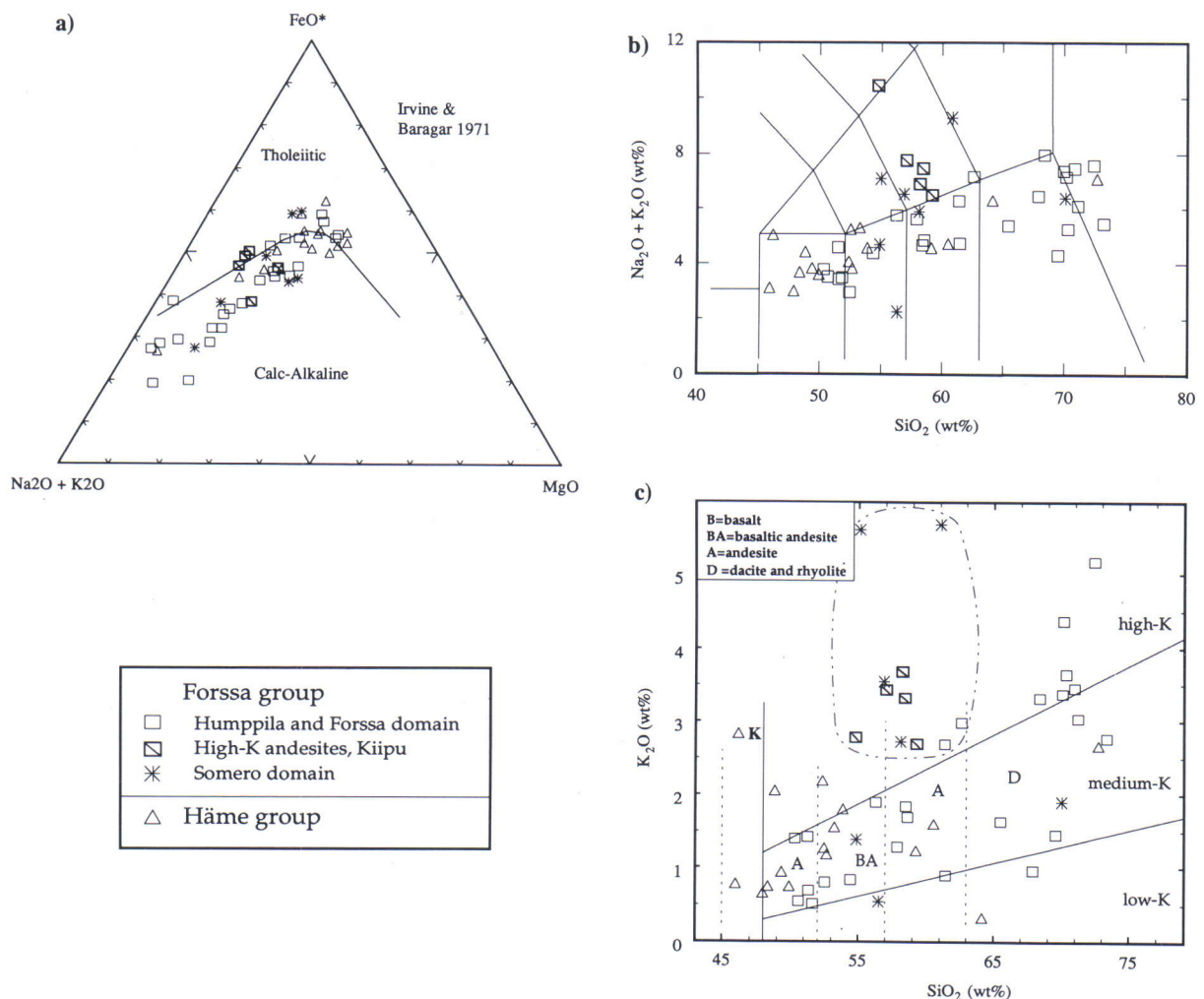


Fig. 4. Geochemical characteristics of the Hämeenlinna-Somero Volcanic Belt. AFM diagram after Irvine & Baragar (1971); K_2O vs. SiO_2 and total alkalis vs. SiO_2 diagrams after Le Maitre (1989). The point marked with "K" is a TiO_2 - and K_2O -rich basalt from Kälvola. The dash-dotted line in Fig. 4c delineates the high-K andesites.

those of the Forssa group, which are quartz-normative. The normative An content ranges between 50 and 60% (see Table 3).

There are some exceptions to the summary given above. The andesites at Kiipu and partly those in Somero are high-K rocks (trachyandesites). Recent orogenic high-K andesites are relatively rich in P_2O_5 , ranging from 0.32-0.54% (Baker 1982). Since the high-K andesites in Somero and Kiipu have low P_2O_5 contents of ca. 0.2%, their high K contents are probably due to alteration. At Kiipu also the FeO^*/MgO ratios and the V contents are high (Figs. 5b and 7b). In the V vs. MnO plot (Fig. 7b) the Kiipu trachyandesites deflect from the general differentiation trend. Both in Somero and Kiipu the high-K rocks are located close to sulfide mineralizations. Thus pre-metamorphic redistribution of alkalis and partly of ferromagnesian elements by ore-forming fluids is suggested to explain the deviations. The Ti-Zr relations in Fig. 7a show that these rocks do not differ from the main trend on behalf of these incom-

patible elements, which are stable during metasomatic alteration.

Some of the basalts in Kalvola, which form an offshoot from the Häme group, are fairly rich in TiO_2 and K_2O and poor in SiO_2 and P_2O_5 (Table 3, Number 1). The sample is taken from a 10 m thick dyke which is situated in an unaltered andesite. In most of the diagrams the sample deviates markedly from the general fractionation trend of the HSB. The high alkali content is due to K-enrichment, while the Na-content is similar to that of the other basalts of the area. The Kalvola basalts contain normative nepheline but the content of Ba and Sr is lower than in average high-K rocks with similar alkali contents from convergent plate boundaries (see Baker 1982). The high K and low P contents suggest that the elevated K-values are caused by metasomatic processes. The Kalvola basalts are interpreted, due to their stratigraphic position, as magmas that erupted during a late stage in the evolution of the Häme group, possibly from a different magmatic source.

The low Mg and Ni values indicate that the HSB volcanics underwent significant fractionation during ascent to the surface. The fast decrease in the Ni contents suggests an early olivine removal (Fig. 6d). The abundance of plagioclase phenocrysts indicates low-pressure fractionation conditions and the lower Sr content in the Forssa group basalts reflects a greater involvement of plagioclase precipitation. Also, the abundance of uraltite shows that clinopyroxene was a major crystallizing phase.

The HSB volcanics are compared to Japanese volcanoes in Fig. 5. The Amagi volcano belongs to the Izu-Bonin arc and the Asama volcano belongs to the Northeast Japan arc. The chemistry of each of them represents a single trend calc-alkaline compositional variation. The single trend variation reflects a magmatic evolution from a single magmatic source, hence these volcanoes should be good for comparison purposes. The Forssa group displays two different trends; one follows the calc-alkaline Amagi trend and the other follows the more tholeiitic Hachijojima trend in the Miyashiro's (1974) FeO^*/MgO vs. TiO_2 diagram. In the FeO^*/MgO vs. SiO_2 diagram the Forssa group also displays two different trends. Some of the samples defining the subhorizontal trend are altered, but this trend also embraces unaltered samples. Wilson (1991, p. 181) reports relatively high Fe_2O_3/FeO -ratios in recent island arcs. High oxygen fugacities in magmas imply that magnetite would be a near liquidus phase. Varying oxidation conditions during low-pressure fractionation play a fundamental role in determining whether the magmas fractionate along the tholeiitic or the calc-alkaline path. In Fig. 5b, the steep trend of the Forssa group is caused by magnetite/ilmenite precipitation during high oxygen

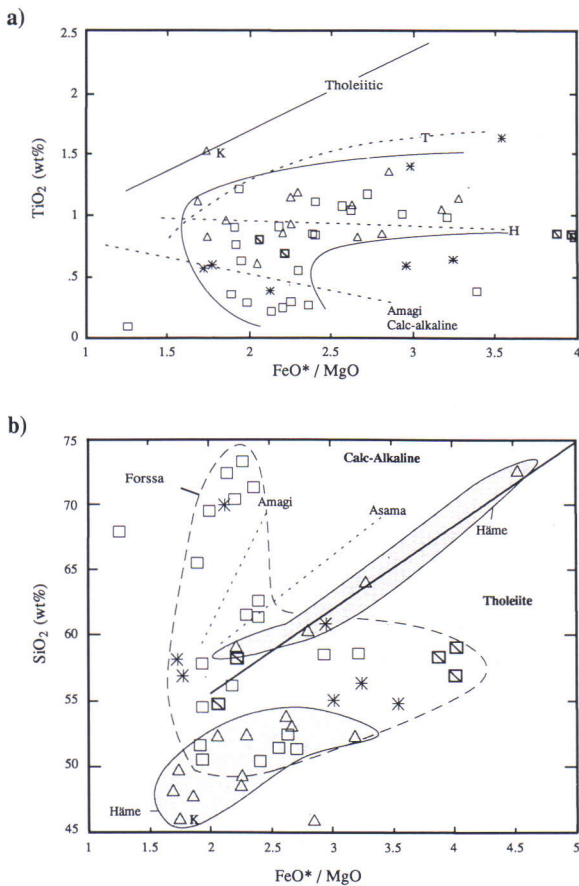


Fig.5. Geochemical variation diagrams for the rocks of the Hämeenlinna-Somero Volcanic Belt (after Miyashiro 1974). a) TiO_2 vs. FeO^*/MgO . b) SiO_2 vs. FeO^*/MgO . Symbols as in Fig. 4. The shaded fields outline the rocks of the Häme group and the dashed line outlines rocks of the Forssa group. Light dotted lines are fractionation trends. Lines in Fig. a: T= Hachijojima tholeiites; H= Hachijojima less typical tholeiites.

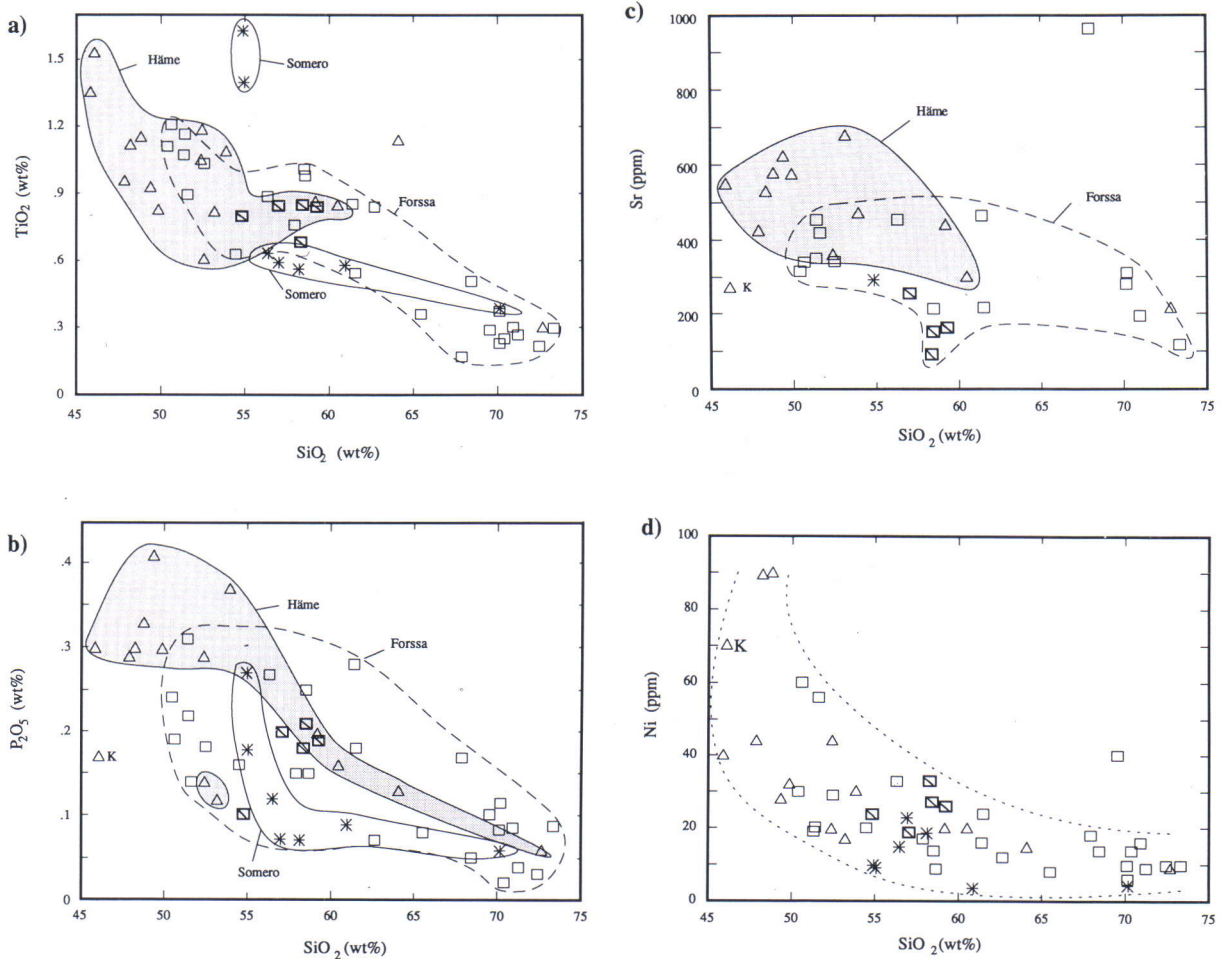


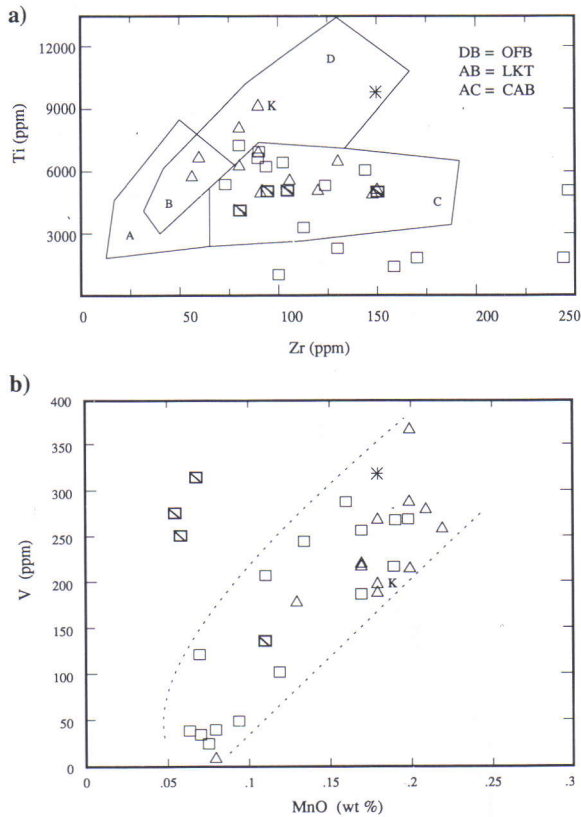
Fig. 6. Harker-type variation diagrams for the rocks of the Hämeenlinna-Somero Volcanic Belt. Symbols as in Fig. 4. The lines define the fields for the Häme and Forssa groups and the Somero domain.

fugacities. In Fig. 5a most of the intermediate rocks of the Forssa group follow a trend which is intermediate between the tholeiitic and calc-alkaline trend. This trend may be caused by less magnetite/ilmenite precipitation during lower oxygen fugacities. Amagite-type fractionation depletes the liquids from titanium more rapidly. The scatter of the samples and the deviating trends in the $\text{FeO}^*/\text{MgO}-\text{SiO}_2-\text{TiO}_2$ plots reflect interaction of replenishment, eruption and extensive differentiation, which resulted in variations of the oxygen fugacities in the magma chambers.

Variable conditions of low-pressure fractionation may occur in individual arc segments. For example, in the South Sandwich arc the volcanic rocks vary, in terms of their potassium content, from low-K to calc-alkaline types, but in terms of their FeO^*/MgO -ratios they can be classified as tholeiites (Wilson 1991, p. 173). The HSB volcanics are mostly calc-alkaline, but the FeO^*/MgO characteristics show that part of the basalts are tholeiitic. This diversity could be explained by similar variation in the

fractionation conditions as in the South Sandwich arc.

In recent orogenic belts, occurrence of andesites is mainly restricted to subduction settings. In mature arcs, like Japan, the andesite/basalt ratios tend to be greater than 2 (Gill 1981, p. 95, Aramaki & Ui 1982, Hall 1989, p. 391). The Forssa group has a high andesite/basalt ratio (estimated ratio = 2-4), while in the Häme group the andesite/basalt ratio is similar to that in primitive arcs (<1). Also, the TiO_2 content in the HSB is typical for recent volcanic arcs. The high Zr/Ti-ratios, low Ni and high LILE concentrations classify the HSB as a calc-alkaline island arc complex. Due to the monogenetic rock association in the Häme group the magmatic evolution may there be different from that in the Forssa group. Since basalts dominate in the Häme group, it could be regarded as a tholeiitic trench-side assemblage, but the relatively high Zr, LILE and P_2O_5 values discriminate the Häme group basalts from primitive arc tholeiites. Some of the basalts lack normative quartz. According to Miyashiro (1974), this is unusual even for



basalts of the inner volcanic zones in island arcs.

The chemical characteristics of arc volcanics vary in space and time. The alkalinity of arcs is regarded as an indicator of their maturity. Studies from the mature arcs in Japan suggest an increase in alkalinity away from the trench and several investigations show that a significant change in the geochemistry may also occur along the arcs (Gill 1981, p. 213). Based on the geochemical similarities between the volcanic rocks of the HSB and evolved, mature island arc rocks, such as those in the Honshu and Sunda arcs, it appears feasible to suggest that the formation of the HSB volcanics was preceded by crustal thickening.

Fig. 7. **a)** Ti vs. Zr diagram for the rocks of the Hämeenlinna-Somero Volcanic Belt (after Pearce & Cann 1973). Rhyolites and dacites are also plotted. CAB = calc-alkaline basalts, LKT = low-K tholeiites, OFB = ocean floor basalts, D = within plate basalts. **b)** V vs. MnO diagram. Symbols as in Fig. 4.

STRATIGRAPHY AND EVOLUTION

The complexity of the volcanic and sedimentary successions in the Forssa domain makes it difficult to establish a common stratigraphic record. The complexities may be explained by contemporaneous eruptions of different types of magmas from different volcanic centers or different magma batches from one center.

In the southern Forssa domain, andesites brecciated rhyolitic tuffs, and in the Somero domain andesitic fragments have been encountered in basalt lavas. In the Forssa domain basaltic to andesitic uralite-porphyr dikes cross-cut or are emplaced as sills in andesitic and dacitic plagioclase-porphyr dikes. Furthermore, there are two thick coarsely plagioclase-porphyr dikes containing fragments of intermediate volcanic rocks. Evidently the volcanic activity started with acid eruptions, which were succeeded by intermediate and finally, by basaltic eruptions. The Häme group volcanics were deposited on sedimentary rocks, which may partly represent erosion products from the Forssa group. The wide distribution of basaltic feeder dikes suggests that the Häme group basalts were not erupted through a central vent; rather the eruptions took place along a

fissure system. Volcanism started with explosive shallow-water eruptions that formed volcanic breccias and local pillow lavas. Contemporaneous erosion resulted in the development of debris flows, which formed volcanic conglomerates at the base of the Häme group. The lavas in the central parts of the Häme group do not exhibit pillow structures, and the poor stratification of the pyroclastics suggests that the central parts were formed partly in subaerial conditions. The Fe-sulfide formations at the base of the volcanic pile suggest that extension of the crust caused fissures which provided pathways for magmas. During the extensional period small anoxic basins were formed which favored the precipitation of strata rich in Fe-sulfides.

From the above data, a complex magmatic evolution can be deduced. The lowermost exposed sequences comprise the Forssa group rhyolitic to basaltic volcanics. They were followed by the extrusion of the Häme group basalts. The relatively K- and Ti-rich basalts of Kalvola cross-cut the intermediate end members of the Häme group and they commenced the latest extrusional event in the area.

DISCUSSION

The lithostratigraphic correlation and the tectonic setting of the volcanic-sedimentary sequences in southern Finland is principally unresolved. Interpretation of the Svecofennian stratigraphy has been done in some key areas; however the relationships between different belts is obscure and the tectonostratigraphic relationship between, for example, the supracrustals of the Hämeenlinna-Somero (this study), Tampere (Kähkönen 1987, 1989) and Orijärvi-Kemiö (Colley & Westra 1987, Mäkelä 1989) (Fig. 1) areas is yet to be solved. Most of the volcanics in the Svecofennides are calc-alkaline with arc affinities (Gaál & Gorbatshev 1987). In general, the volcanic belts in southwestern Finland show a northward transition from bimodal sequences in Enklinge-Orijärvi (Ehlers & Lindroos 1990, Lindroos 1990) through calc-alkaline associations (Hämeenlinna-Somero; Hakkarainen 1989, this study) to more alkaline volcanics in Tampere (Kähkönen 1987). The tholeiitic Haveri basalts in the Tampere region are considered to represent an initial-stage island arc environment (Mäkelä 1980). The concept that the southern Svecofennian volcanic belts were formed in an oceanic environment (Gaál 1990) was mainly based on the absence of evidence of an older continental basement. Huhma et al. (1991) concluded that many of the zircons in the graywackes at Tampere are older (2.0-1.9 Ga) than the volcanic rocks (1.904-1.89 Ga) from the same area. This implies the existence of an earlier crust predating the formation of the arc volcanics.

If the abundances of LIL-elements in the HSB basalts are primary, an enrichment process in the mantle would be indicated. This could not likely take place in larger extents in a thin oceanic plate. For example, the Mariana-Izu arcs, with a 20-30 km thick crust, are primitive and dominated by tholeiitic low-K basalts. K-rich lavas occur in the Mariana arc (Lin et al. 1989), but volumetrically in smaller amounts, relative to the bulk volume, than the medium-K lavas in the HSB. Furthermore, in the HSB calc-alkaline rocks are more abundant than tholeiitic rocks. Miyashiro (1974) stressed that the ratio of calc-alkaline/tholeiitic rocks tends to increase with increasing thickness of the crust. Crustal thickening restrains primitive magmas from ascending to the surface. They are collected in shallow magma chambers where they evolve to calc-alkaline successions. Hence, the HSB volcanics were probably formed in a mature arc milieu.

Although the high andesite/basalt ratio is a general feature in the HSB, the Häme group volcanic rocks show a monotonous evolution with mainly basaltic

derivatives. This kind of monogenetic volcanism can be ascribed to tensional stress fields (Nakamura & Uyeda 1980), which are found in the rear of subduction zones. The tholeiitic Häme group could have been produced at a short stage of tension (decoupling) during the generally compressional arc volcanism. Cyclic variation between plate decoupling and coupling in oceanic island arcs is described by Hawkins et al. (1984).

The Japanese and Izu-Mariana arcs have high convergence rates of 7-9 cm/yr and together they form one of the fastest consuming plate margins active today. Japan represents an evolved stage of arc volcanism. The existence of several volcanic zones with geochemical island arc affinities in the Svecofennian Domain and their formation within a few tens of millions of years suggests fast movement rates in the pre-Svecofennian plate collage. Therefore, the magma generation in the HSB may show similarities to the magmatic evolution of the Japan-Mariana arcs. The volcanic rocks in the HSB show both tholeiitic and calc-alkaline affinities. Andesites, dacites and rhyolites are abundant and the basalts have higher potassium contents than the basalts in primitive island arcs. These characteristics suggest a subduction site like that of Group II in Gill (1981, p. 220), with relatively high convergence rates. The magmas in the HSB are chemically more diverse compared to the primitive, more depleted and iron-enriched magmas of Group I formed in arcs with thin crust. More than 80% of the erupted magmas in Group I are tholeiitic, which is not the case in the HSB.

More precise geochronological data are needed to establish a detailed and accurate model for the evolution of the Svecofennian crust, and the discussion presented below should be seen as tentative. The complex tectonostratigraphic relations of the volcanic belts at Orijärvi, Tampere and Hämeenlinna could be consistent with a model with several small tectonic entities. They vary in size from small microcontinents to accretionary prisms, and interact with each other through thrusting, subduction, docking etc. The amalgamation of primitive arcs, fore-arc basins, back-arc basins, and rifts upon each other provides material for crustal thickening and evolution to mature calc-alkaline volcanism. The formation of arc volcanics in southern Finland could have been predated by a rift-related bimodal magmatism, such as in Orijärvi (Colley & Westra 1987, Väisänen 1991) and Enklinge (Ehlers & Lindroos 1990, Lindroos 1990). A similar type of bimodal magmatism may have contributed to the crustal thickening that

preceded the arc volcanism and the thickening resulted in a continental geochemical signature of the arc magmas.

Generation of oceanic subduction zones involves earlier imbrication and fracturing of the lithosphere. Early fractures and faults form zones of weakness in the lithosphere and these zones are apt to develop into new subduction zones when the plate margins are subjected to compressional stress (Hawkins et al. 1984). The bimodal magmatism in southern Finland could be a result of an early imbrication and extension of the oceanic crust. Some of the fractures could later have developed into arcs in southern Finland, when the stress field changed to compressional. The assumed subduction zone on the border to the Archean craton is earlier or of the same age with the earliest phases of the Svecofennides (Park 1985, Gaál & Gorbatshev 1987). A plausible explanation could be that a NE movement of the "proto-Svecofennian

plate" caused a consuming subductional event on the border to the Archean craton. Continental margins tend to have slower closing rates than intra-oceanic margins (Sugisaki 1976). Therefore, fast movement of the "proto-Svecofennides" northeastwards could have exceeded the consumption of the oceanic plate at the Ladoga-Bothnian Bay zone. The compression caused by the onpushing plate would have been released in migration or formation of new subduction zones further away from the craton. If the motion of the Svecofennian collage was in a NE-ESE-direction (Gaál & Gorbatshev 1987), the angle between the movement direction and the orientation of the Bothnian-Ladoga arc (NNW-SSE) supports the interpretation of the conversion of the Bothnian-Ladoga arc into a dextral strike slip complex. This concept is favored by the locking event of the Bothnian-Ladoga arc described by Park (1985).

ACKNOWLEDGEMENTS

The author is grateful to Dr. Y. Kähkönen, Dr. T. Brewer, Prof. C. Ehlers and Dr. M. Nironen for critically reading and thereby greatly improving the

manuscript. The English language was revised by Christopher Cunliffe.

REFERENCES

- Aramaki, S. & Ui, T. 1982. Japan. In: Thorpe, R.S. (ed.) *Andesites. Orogenic Andesites and Related Rocks*. Chichester: John Wiley & Sons, 259-292.
- Baker, P.E. 1982. Evolution and classification of orogenic volcanic rocks. In: Thorpe, R.S. (ed.) *Andesites. Orogenic Andesites and Related Rocks*. Chichester: John Wiley & Sons, 11-23.
- Colley, H. & Westra, L. 1987. The volcano-tectonic setting and mineralization of the early Proterozoic Kemiö-Orijärvi-Lohja belt, SW Finland. In: Pharao, T.C., Beckinsdale, R.D. & Rickard, D. (eds.) *Geochemistry and Mineralization of the Proterozoic Volcanic Suites*. Geol. Soc. Spec. Publ. 33, 95-107.
- Ehlers, C. & Lindroos, A. 1989. Early Proterozoic Svecofennian volcanism and associated plutonism in Enklinge, SW Finland. *Precambrian Res.* 47, 307-318.
- Gaál, G. & Gorbatshev, R. 1987. An outline of the Precambrian evolution of the Baltic Shield. *Precambrian Res.* 35, 15-52.
- Gaál, G. 1990. Tectonic styles of Early Proterozoic ore deposition in the Fennoscandian Shield. *Precambrian Res.* 46, 83-114.
- Gill, J. 1981. *Orogenic Andesites and Plate Tectonics*. Heidelberg: Springer Verlag, 390 p.
- Hakkarainen, G. 1989. Lahden-Someron vulkaniittimuodostuman stratigrafia. *Inst. Geol. Miner. Univ. Turku*, Publ. 20, 59 p. (in Finnish)
- Hall, A. 1989. *Igneous Petrology*. 2. edition. Harlow: Longman Scientific & Technical, 573 p.
- Hawkins, J.W., Bloomer, S.H., Evans, C.A. & Melchior, J.T. 1984. Evolution of intraoceanic arc-trench systems. *Tectonophysics* 102, 174-205.
- Huhma, H., Claesson, S., Kinny, P.D. & Williams, I.S. 1991. The growth of Early Proterozoic crust: new evidence from Svecofennian detrital zircons. *Terra Nova* 3, 175-179.
- Irvine, T.N. & Baragar, W.R.A. 1971. A guide to classification of the common volcanic rocks. *Can. J. Earth Sci.* 8, 523-548.
- Kähkönen, Y. 1987. Geochemistry and tectonomagmatic affinities of the metavolcanic rocks of the early Proterozoic Tampere Schist Belt, southern Finland. *Precambrian Res.* 35, 295-312.
- Kähkönen, Y. 1989. Geochemistry and petrology of the metavolcanic rocks of the early Proterozoic Tampere Schist Belt, southern Finland. *Geol. Surv. Finland, Bull.* 345, 107 p.
- Kähkönen, Y., Huhma, H. & Aro, K. 1989. U-Pb zircon ages and Rb-Sr whole-rock isotope studies of early Proterozoic volcanic and plutonic rocks near Tampere, southern Finland. *Precambrian Res.* 45, 27-43.
- Le Maitre, R.W. (ed.) 1989. *A Classification of Igneous Rocks and Glossary of Terms*. Oxford: Blackwell, 193 p.
- Lin, P.-N., & Stern, R.J. & Bloomer, S.H. 1989. Shoshonitic volcanism in the northern Mariana arc 2. Large-ion lithophile and rare earth element abundances: evidence for the source of incompatible element enrichments in intraoceanic arcs. *J. Geophys. Res.* 94, 4497-4514.
- Lindroos, A. 1980. En zinkmineraliserings relation till metamorfa och hydrotermalt omvandlade vulkaniska bergarter i Ypäjä och Jockis, sydvästra Finland. M. Sc. thesis, Åbo Akademi Univ. 89 p. (unpublished, in Swedish)
- Lindroos, A. 1990. De tidiga Svecofenniska vulkaniterna i SW Finland, deras stratigrafi och geokemi. Ph. Lic. thesis, Åbo

- Akademi Univ. 52 p. (unpublished, in Swedish)
- Miyashiro, A. 1974.** Volcanic rock series in island arcs and active continental margins. *Am. J. Sci.* 274, 321-355.
- Mäkelä, K. 1980.** Geochemistry and origin of Haveri and Kiipu, Proterozoic stratabound volcanogenic gold-copper and zinc mineralizations from southwestern Finland. *Geol. Surv. Finland, Bull.* 310, 79 p.
- Mäkelä, U. 1989.** Geological and geochemical environments of Precambrian sulphide deposits in southwestern Finland. *Ann. Acad. Sci. Fennicae A.III.151*, 102 p.
- Nakamura, K. & Uyeda, S. 1980.** Stress gradient in arc - back arc regions and plate subduction. *J. Geophys. Res.* 85, 6419-6428.
- Neuvonen, K.J. 1954.** Stratigraphy of the schists of the Tammela-Kalvola area, Southwestern Finland. *Bull. Comm. géol. Finlande* 27, 84-95.
- Nironen, M. 1989.** The Tampere Schist Belt: Structural style within an early Proterozoic volcanic arc system in southern Finland. *Precambrian Res.* 43, 23-40.
- Park, A. 1985.** Accretion tectonism in the Proterozoic Svecokareliides of the Baltic Shield. *Geology* 13, 725-729.
- Patchett, P.J. & Kouvo, O. 1986.** Origin of continental crust of 1.9-1.7 Ga age: Nd isotopes and U-Pb zircon ages in the Svecokarelian terrain of South Finland. *Contrib. Mineral. Petrol.* 78, 279-297.
- Pearce, J.A. & Cann, J.R. 1973.** Tectonic setting of basic volcanic rocks determined using trace element analyses. *Earth Planet. Sci. Lett.* 19, 290-300.
- Ploegsma, M. & Westra, L. 1990.** The Early Proterozoic Orijärvi triangle (southwest Finland): a key area on the tectonic evolution of the Svecofennides. *Precambrian Res.* 47, 51-69.
- Ramsay, J.G. & Huber, M.I. 1987.** *The Techniques of Modern Structural Geology, Volume 2: Folds and Fractures.* London: Academic Press, 309-695.
- Schreurs, J. & Westra, L. 1986.** Thermotectonic evolution of a Proterozoic, low pressure granulite dome, west Uusimaa, SW Finland. *Contrib. Mineral. Petrol.* 93, 236-250.
- Simonen, A. 1953.** Stratigraphy and sedimentation of the Svecofennidic, early Archean supracrustal rocks in Southwestern Finland. *Bull. Comm. géol. Finlande* 160, 64 p.
- Simonen, A. 1980.** The Precambrian in Finland. *Geol. Surv. Finland, Bull.* 304, 58 p.
- Stel, H., Veenhof, R., Huizenga, J.M., Timmerman, M. & Hartsink, J.M.H. 1989.** Infra-supra structure relations of microcline-granite domes in the Somero area, Svecofennides, SW Finland. *Bull. Geol. Soc. Finland* 61, 131-141.
- Sugisaki, R. 1976.** Chemical characteristics of volcanic rocks: Relation to plate movements. *Lithos* 9, 17-30.
- Väisänen, M. 1991.** *Strukturgeologi i Orijärviområdet, SW Finland: Iilijärvi och Orijärvi malmförekomsternas strukturella lägen.* M.Sc. thesis, Åbo Akademi Univ., 65 p. (unpublished, in Swedish)
- Wilson, M. 1991.** *Igneous Petrogenesis.* London: HarperCollins Academic, 466 p.

SHOSHONITIC AND HIGH-K METAVOLCANIC ROCKS IN THE SOUTHERN PARTS OF THE PALEOPROTEROZOIC TAMPERE SCHIST BELT, SOUTHERN FINLAND: EVIDENCE FOR AN EVOLVED ARC-TYPE SETTING

by
Yrjö Kähkönen

Kähkönen, Yrjö 1994. Shoshonitic and high-K metavolcanic rocks in the southern parts of the Paleoproterozoic Tampere Schist Belt, southern Finland: evidence for an evolved arc-type setting. *Geological Survey of Finland, Special Paper 19*, 101–115, 11 figures, two tables and one appendix.

The southern part of the E-W striking synclinal Tampere Schist Belt (TSB) near Tampere is dominated by metasedimentary rocks, characterized by the turbidites of Myllyniemi formation. However, the southernmost parts of the belt are relatively rich in metavolcanic rocks.

This study presents data on the southern metavolcanics of the TSB at six localities. The Tohloppi, Kiviranta and Sorila successions probably comprise a single horizon. Although they lie in the southernmost part of the TSB, their stratigraphic position is not definite. The metavolcanics at Viinaränninnotko and Pohjala possibly interfinger or underlie the Myllyniemi turbidites and the Teacher's metavolcanics occur among the turbidites above these volcanic successions. The proportions and stratigraphic relations of lavas, pyroclastic rocks and sills vary from section to section. Most of the sections studied represent subaqueous environments of deposition but at Tohloppi there may be shallow-water or fluvial/alluvial deposits of an emergent volcanic island.

The southern metavolcanics of the TSB range from basalts to trachytes/rhyolites in composition but they are mostly trachyandesites or basaltic trachyandesites with shoshonitic affinity. The alkali-rich character agrees with the fairly high contents of P and LREE. In general, significant metasomatism is not evident. The most pronounced shoshonitic affinities are observed at Tohloppi, Kiviranta and Sorila.

Based on the Ti vs. Zr diagram and the high Th/Ta ratios, the southern metavolcanics of the TSB were formed in an arc-type setting. The shoshonitic to high-K character indicates an environment of an evolved arc.

Key words (GeoRef Thesaurus, AGI): metavolcanic rocks, shoshonite, stratigraphy, geochemistry, tectonics, island arcs, Proterozoic, Paleoproterozoic, Tampere, Orivesi, Finland

*Yrjö Kähkönen, Department of Geology, P.O. Box 11 (Snellmaninkatu 3),
FIN-00014 University of Helsinki, Finland*

INTRODUCTION

The volcanic-sedimentary Tampere Schist Belt (TSB, Fig. 1) is situated near the center of the Paleoproterozoic Svecofennian Domain which was formed by rapid mantle-derived crustal growth some 1.9 Ga ago (Huhma 1986, Patchett & Kouvo 1986). The TSB is characterized by turbiditic meta-graywackes-mudstones and predominantly intermediate arc-type pyroclastic metavolcanic rocks (Ojakangas 1986, Kähkönen 1987, 1989). The metavolcanic rocks are ca. 1905-1890 Ma in U-Pb zircon age (Kähkönen et al. 1989) and a meta-graywacke sample has detrital zircons with ages ranging from 1907±15 Ma to Archean (Huhma et al. 1991). The supracrustal rocks were metamorphosed at low-P conditions near the greenschist-amphibolite facies transition. Structurally, the TSB comprises an E-W striking major isoclinal F_1 syncline with subhorizontal fold axes and subvertical axial plane schistosity (Kähkönen 1989, Nironen 1989). The northern limb of the major syncline near Tampere is dominated by metavolcanic rocks while meta-graywackes and metamudstones characterize the

southern limb (Table 1 in Kähkönen & Leveinen, this volume). The southernmost parts of the TSB are, however, rich in metavolcanic rocks. Minor synclines and anticlines as well as local zones of pronounced deformation complicate the interpretation. According to the general structural concept the southern TSB metavolcanics should lie low in the succession of the southern limb. This may be true for some of the metavolcanic units studied but U-Pb zircon ages of the volcanics in the Tohloppi - Kalkku area (Fig. 1; H. Huhma, personal communication; see also Kähkönen et al. 1989) make this concept in part problematic.

The main purpose of this study is to present new data on the metavolcanic rocks of the southern parts of the TSB and to discuss their mutual correlation. Tentative interpretations of depositional environments are also presented. In addition to those in the text, petrographic data are given in Appendix. Since all the rocks studied are metamorphic the prefix meta- is omitted from here on.

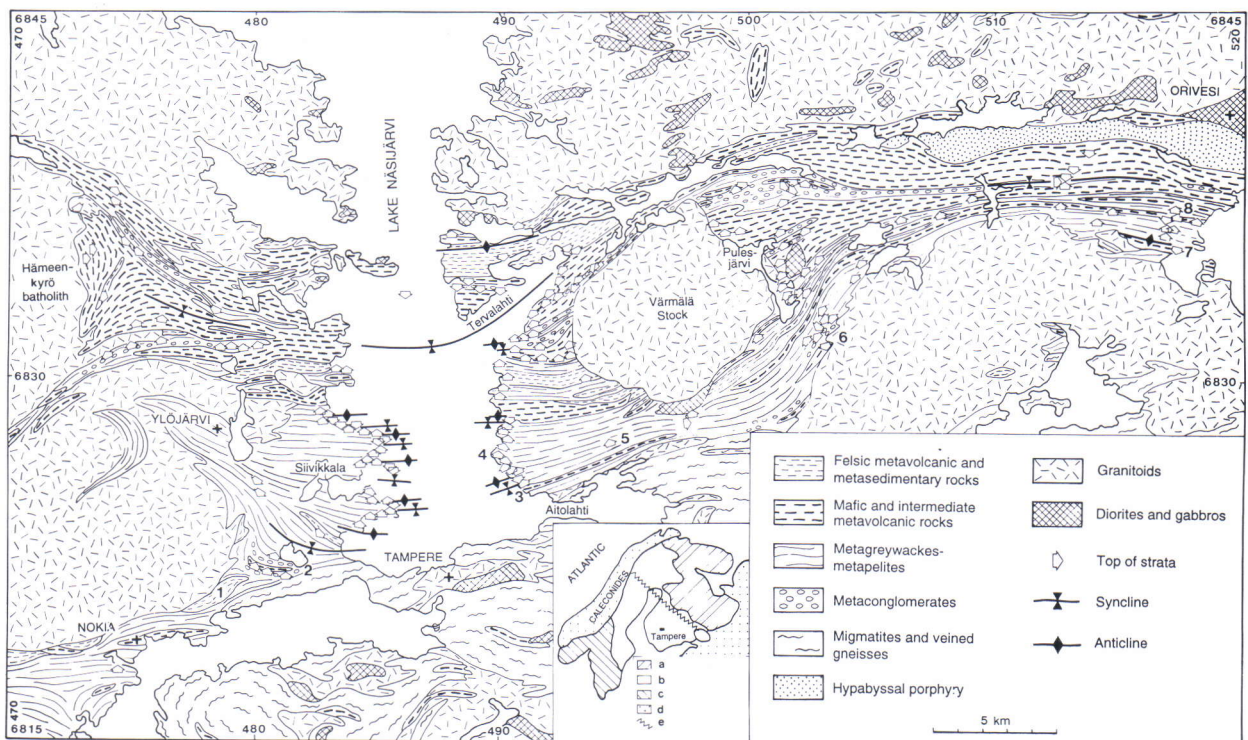


Fig. 1. Lithological map of the Tampere Schist Belt with top of strata observations and a simplified structural interpretation. Slightly modified from Kähkönen (1989) and Luukkonen et al. (1992). Numbers 1-8 indicate localities mentioned the text: 1 = Kalkku, 2 = Tohloppi, 3 = Kiviranta, 4 = Myllyniemi, 5 = Sorila, 6 = Viinaränninnotko, 7 = Pohjala, 8 = Teacher's. The inset shows the location of the Tampere Schist Belt in the Svecofennian Domain: a = Archean, b = Svecokarelian, c = Post-Svecokarelian (Precambrian), d = Phanerozoic, e = boundary between the Svecofennian and Karelian Domains.

STRATIGRAPHY AND LITHOLOGY OF THE STUDIED SECTIONS

This study presents data from six localities: Tohloppi, Kiviranta, Sorila, Viinaränninnotko, Pohjala and Teacher's (Fig. 1). The Tohloppi succession displays northern younging directions. It lies at the southern limb of a minor syncline, and the Kiviranta and Sorila successions probably have a similar structural position. The author has suggested that the three successions underlie the Myllyniemi turbidites to the north (e.g. Kähkönen 1993) but the situation does not seem to be that simple. A new U-Pb age determination from a rhyolite close to Tohloppi (H. Huhma, personal communication), supported by the 1891 ± 16 Ma U-Pb zircon age of the nearby Kalkku porphyry (Kähkönen et al. 1989), suggests that the Tohloppi-Kiviranta-Sorila succession has an age close to the volcanics above the Myllyniemi turbidites. The problems might be due to early thrusts (cf. Ayres & Corfu 1991).

The correlation of the Tohloppi-Kiviranta-Sorila horizon with the succession at Viinaränninnotko is problematic since the structure between Sorila and Viinaränninnotko is not well known. The Viinaränninnotko succession is, however, tentatively classified either as a member/tongue of the Myllyniemi

formation or as a separate formation interfingering with the turbidites.

The Viinaränninnotko and Pohjala successions are similar in that they have top of strata to the south. They lie at the southern limb of a minor anticline and may represent the same horizon rich in volcanics. The lithologies in the northern and southern limbs of this minor anticline contrast near the hinge zone; the rocks at the southern limb are rich in volcanics while those at the northern limb consist of turbidites, in particular of quartz-rich graywackes and conglomerates. This might be explained by rapid facies changes in a volcanic-sedimentary basin but the contrast is so strong that it is probable that faults exist in the hinge zone. The transition zone between the TSB and the veined gneisses to the south is a subvertical south-dipping thrust or reverse fault (Nironen 1989). Assuming similar sense of movement for the suggested faults near Viinaränninnotko and Pohjala it is probable that the volcanic-rich successions of the southern limb are stratigraphically below the turbidites of the northern limb. Since the Teacher's volcanics occur among the latter turbidites they are above the Pohjala volcanics in the stratigraphic column.

Tohloppi

The succession at Tohloppi is divided here into four units which comprise, from bottom to top, (1) lower graywackes, mudstones and tuffs (at least 200 m), (2) lower conglomerates (160 m), (3) Pl+Ur -phyric lava (280 m), and (4) upper conglomerates (up to 200-250 m). Crossbedding in sandstones and graded bedding in graywackes indicate northern younging directions. The conglomerates are polymictic and overwhelmingly dominated by volcanic clasts.

(1) The original thickness of the lower graywackes, mudstones and tuffs is unknown since there is a fault between the schists and the veined gneisses to the south. The graywackes and mudstones are partly tuffaceous. The tuffs comprise fine-grained tuffs, lithic and crystal tuffs as well as lapilli tuffs.

(2) The lower Tohloppi conglomerates are mostly clast-supported cobbly to pebbly rocks. The clasts are rounded to subrounded but there are also angular to subangular pebbles. The lowest 100 m are poorly exposed but there seem to occur interbeds of sandstone. The conglomerates grade upwards into strata dominated by trough cross-bedded sandstones and pebbly sandstones (Fig. 2a). The cross-bedded sets

are up to 10 cm high. The paleocurrents seem to be dominantly in the SW-NE sector. The sandstones are overlain by a 10-20 m thick stratum of partly tuffaceous mudstones.

(3) The Pl+Ur -phyric lava at Tohloppi is mostly massive, with polygonal fractures giving a blocky impression (Fig. 2b). The fragments are mostly closely spaced but there are also loosely packed structures (Fig. 2c). Fractures are not prominent in the lowermost parts of the lava. The uppermost parts are characterized by large quartz-filled amygdules (diameter up to 5 cm) and lobate or tongue-like features with sparse fine-grained matrix. In places the uppermost parts are massive with no polygonal fractures or lobate structures. Contacts indicative of separate flows were not observed (cf. Mueller 1991), and there seems to be only a single thick flow which may have formed a lava dome. The polygonal fractures probably result from in situ brecciation in a rather viscous, slowly moving lava and the loosely packed structures indicate local mechanical attrition of adjacent blocks.

(4) The upper Tohloppi conglomerates are characteristically clast-supported cobbly to pebbly rocks

with rounded to subrounded clasts. Several interbeds of sandstone occur within the conglomerate. The uppermost sandstone strata comprise an up to ca. 25 cm high cross-bedded set with paleocurrent to the western sector (Fig. 2d).

The succession at Tohloppi is interpreted as an upward shoaling sequence of a partly emergent volcano. Based on the criteria of Dimroth et al. (1982), the conglomerates and related sandstones

are fluvial rather than submarine fan deposits, and they were probably deposited from tractional currents in shallow-water or fluvial/alluvial environments. The occurrence of angular to subangular clasts indicates short transportation. The large amygdules in the lava are also suggestive of a shallow-water or subaerial environment. The absence of pillow lavas may indicate similar environments but it may also be a function of high viscosity of lava (cf. Mueller 1991).

2a)



2b)



2c)



2d)



Fig. 2. Structures of the sedimentary and volcanic rocks at Tohloppi. Length of compass 12 cm. **a.** Trough cross-bedded sandstones and pebbly sandstones in the uppermost part of the lower conglomerates. Top of strata to the north. **b.** Lava with closely spaced polygonal fractures. **c.** Lava with loosely packed fragments. **d.** Cross-bedded sandstone among the uppermost parts of the upper conglomerates. Top of strata to the north, paleocurrent to the western sector.

Kiviranta

No top of strata evidence exists in the succession at Kiviranta but based on graded bedding 100-200 m to the north, the succession has northern younging directions. The lowest part of the succession comprises mica schists and tuffaceous(?) chlorite schists. These rocks are overlain by (1) a feldspar porphyry (ca. 50 m), (2) Pl±Ur -phyric volcanics (20 m), (3) conglomerates (20-25 m), and (4) a heterogeneous unit (10-20 m) of lapilli tuffs, massive tuffs/tuffites and mafic to intermediate graywackes and mudstones. The rocks in the transition zone to the Myllyniemi turbidites show prominent deformation but, in general, they were originally mudstones.

(1) The feldspar porphyry is mostly massive but the southernmost parts show prominent banding, possibly due to deformation. In places lapilli-sized felsic fragments are poorly distinguishable. The porphyry is probably not a dyke because clasts with a similar composition are common in the conglomer-

ates at Kiviranta (Table 1).

(2) The Pl±Ur -phyric rocks are dominated by a massive Ur+Pl -porphyry which may be a lava flow. In addition, lapilli tuffs and tuff breccias occur stratigraphically below the porphyry.

(3) The Kiviranta conglomerates are polymictic, clast-supported and massive cobbly to pebbly rocks, and they contain at least one 20 cm thick interbed of sandstone. The clasts are dominated by volcanic rocks. They show pronounced flattening but were originally rounded to subrounded. The gradation into the overlying volcanic and sedimentary rocks (4) is obscure. The sedimentary rocks at Kiviranta are probably mass-flow deposits.

The succession at Kiviranta probably represents a deeper-water environment than the conglomerates and lava at Tohloppi. The relative abundance of pyroclastic rocks could be the result of hydroclastic or hydrovolcanic explosive eruptions.

Sorila

At Sorila, only a 15-20 m thick sequence of highly strained Pl±Ur -phyric rocks was studied. In the south, the porphyritic rocks are massive but to the north there are also 5-20 cm thick intermediate to

felsic interbeds. Intermediate tuffs or tuffaceous sedimentary rocks dominate the northernmost part of the section.

Viinaränninnotko

The 250-300 m thick south-younging Viinaränninnotko succession comprises, from the bottom to the top, turbidites (100-150 m), volcanic rocks (ca. 70 m), and conglomerates, graywackes and mudstones (ca. 100 m, bounded to the south by granitoids).

The turbiditic mudstones and graywackes below the volcanic unit are mostly thinly bedded to very thinly bedded and seem to thicken upward. The rocks are in part tuffaceous (hornblende-bearing), and the uppermost strata contain volcanoclastic fallout deposits. The volcanic unit at Viinaränninnotko is divided here into three parts:

(1) The lowermost part is 35 m thick and it is characterized by very thickly bedded massive lithics-bearing crystal tuffs (Fig. 3a). In places the rocks display stratification without sharp bedding plane boundaries (Fig. 3b), and rarely they are lapilli tuffs (Fig. 3c). The contact with the underlying thinly bedded strata is erosional (Fig. 3d). Phenocrysts of plagioclase and clinopyroxene (now actinolite/hornblende) amount to 10-50% in total (Appendix). The

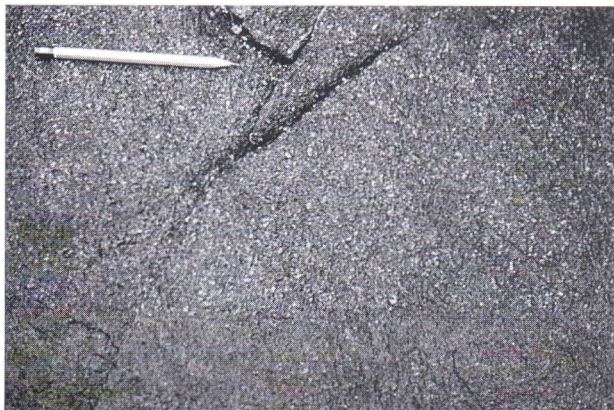
rocks are subaqueous volcanoclastic tuff flow deposits (see Fisher 1984, Cas & Wright 1991).

(2) The tuffs are overlain by 25-30 m of Pl±Ur -phyric lavas. In places the plagioclase phenocrysts display flow texture (Fig. 3e). The lavas are largely massive but there are finer-grained enclaves (Fig. 3e), and under the microscope the lavas seem to contain two different porphyritic components (Appendix). In part the lavas are fragmental and in places they show tongue-like features which are lava toes rather than true pillows (Fig. 3f).

(3) The lavas grade into a 7-8 m thick horizon of non-porphyritic stratified mafic tuffs.

The volcanic unit is overlain by conglomerates (ca. 5 m) which grade upward into graywackes and mudstones. The conglomerates are characteristically clast-supported, cobbly and massive but the uppermost 0.5 m seem to comprise a finer-grained part. The clasts are mostly rounded to subrounded and in part subangular. They are polymictic but overwhelmingly dominated by volcanic rocks. One non-contin-

3a)



3b)



3c)



3d)



3e)



3f)



Fig. 3. Structures of the volcanic rocks at Viinaränninnotko. Length of pen and pencil 13 cm. **a.** Contact of two massive lithics-bearing crystal tuff beds. **b.** Medium to thinly bedded tuffs. **c.** Weathered patches, poorly discernible lapillis in lapilli tuff. **d.** Erosional base of the crystal tuffs. Top of strata to S. **e.** Flow line orientation of plagioclase phenocrysts in lava. Note also the enclaves. **f.** Lava toes (in the centre) at the contact to the underlying pyroclastic rocks (to the left).

uous interbed of sandstone was observed. The conglomerates are thought to be mass flow deposits.

The succession at Viinaränninnotko, from thinly bedded turbidites via tuff flows to lavas, and finally to conglomerates and graywackes-mudstones, probably represents subaqueous deposits on an upper

slope of a volcanic apron. In general, the deposition occurred in deeper water than the deposition of the Tohloppi conglomerates and lava but the Viinaränninnotko lavas may represent a stage at which the pile had grown close to the surface of water.

Pohjala

The 300-400 m thick Pohjala succession is composed of graywackes and mudstones, fallout tuffs, conglomerates, lithics-bearing crystal tuffs, and massive Pl- and Pl+Ur -phyric rocks which are probably sills. To the south the rocks change into gneisses. An erosional base of a mass flow conglomerate (with predominantly volcanic clasts) indicates that the top

of strata is to the south (Fig. 4a). The crystal tuffs are mostly massive but in part stratified, and there are also pebble/cobble-bearing interbeds. The graywackes are partly tuffaceous (hornblende-bearing) and some strata contain pebbles. The probable depositional environment was subaqueous on the slope of a volcanic apron.

Teacher's

The Teacher's volcanics constitute an interbed among turbidites that have northern younging directions. The turbidites stratigraphically below contain graywackes and mudstones while those immediately above are mudstones only.

The total thickness of the Teacher's volcanics does not exceed 50 m and the studied part is ca. 20 m thick. The lower 10 m comprise stratified crystal tuffs which may in part contain lithic or vitric clasts (Appendix). The lowermost 6 m are thinly to medium bedded tuffs (Fig. 4b) while the overlying 4 m are medium to thickly bedded tuffs. The upper 10 m of

the section consist of pyroclastic rocks with poorly distinguishable lapilli- to block-sized fragments. Similar fragmental rocks are found stratigraphically below the studied section in a separate outcrop.

The Teacher's volcanics are pyroclastic deposits which, based on the character of the associated sedimentary rocks, are subaqueous. The stratified tuffs were deposited as the fallout debris from the umbrella region of submarine eruption columns and the fragmental rocks represent the associated debris flows (see Cashman & Fiske 1991).

4a)



4b)



Fig. 4. **a.** Erosional base of a volcanic conglomerate at Pohjala. Top of strata to the south. Length of pen 13 cm. **b.** Thinly bedded tuff, probably fallout debris from submarine pyroclastic eruptions, Teacher's volcanics. Length of compass 12 cm.

GEOCHEMISTRY

Analytical methods

Most of the major element and Zr, Cr, Ni, Sr, Ba, V, Zn and Cu determinations were made with a Philips PW 1400/AHP XRF instrument at the Raahe laboratory of Rautaruukki Oy (Ala-Vainio 1986). Some of the determinations were made by Dr. A. Vuorinen with a ICP-AES instrument at the Department of Geology,

University of Helsinki. Rare earth elements, Rb, Ta, Hf, Th and Sc were analysed by instrumental neutron activation method at the Technical Research Centre of Finland (Rosenberg et al. 1982). The results are given in Table 1.

Results

The southern volcanics of the TSB range from basalts to trachytes/rhyolites in composition but they are mostly trachyandesites and basaltic trachyandesites in the TAS diagram (Fig. 5). According to the K_2O vs. SiO_2 diagram, high-K and shoshonitic rocks dominate. Mobility of alkalis may be a problem in these classifications but the SiO_2 vs. Zr/TiO_2 diagram (Fig. 6) also indicates a trachyandesitic affinity for most of the southern TSB volcanics. The trachyandesites and basaltic trachyandesites are shoshonites and latites in the classification of Le Maitre (1989) since their K_2O contents exceed the value of Na_2O-2 (Table 1). In general, there is no prominent iron enrichment with increasing silica.

The rocks are mostly within the igneous spectrum (Fig. 7a) and thorough alteration is not evident. Since the spectrum needs revision (Fig. 7b), most of the

rocks which fall outside the conventional spectrum may also represent primary compositions.

The La contents are mostly 30-35 ppm, the P_2O_5 contents mostly 0.35-0.55%, the Zr contents 130-220 ppm, and the Sr contents 400-900 ppm (Table 1, Fig. 5). The Cr contents (mostly 200-500 ppm) and Ni contents (mostly 90-150 ppm) are fairly high. The enrichments of LREE over HREE are pronounced (Fig. 8); $La_N:Yb_N$ ranges from 7 to 14, typically from 10 to 14 (Table 1). Most of the HREE patterns slope moderately ($Tb_N:Yb_N$ ranges from 1.1 to 1.6, typically from 1.4 to 1.6; Table 1). Except for the feldsparphyric sample 1-Kiv/86, there are no prominent Eu depletions. The non-smooth LREE patterns of samples 5-C-Viina and 2-B-YKÄ/86 are possibly attributed to analytical uncertainties.

Individual characteristics and mutual correlations

The $Pl\pm Ur$ -phyric rocks at Tohloppi and Kiviranta comprise a coherent group in their alkali, P (P_2O_5 0.36-0.46%) and REE characteristics ($La_N:Yb_N$ 11-14, $Tb_N:Yb_N$ 1.4-1.6), although the Zr contents at Kiviranta are relatively low. The rather high K_2O/Na_2O ratios of the Sorila volcanics might be attributed to alteration but, in general, these rocks share most of the features of the Tohloppi and Kiviranta volcanics. It is probable that the volcanics of the three localities represent the same horizon.

The tuffs and lavas at Viinaränninnotko display some mutual differences as well as some differences from the generalizations presented above. The lavas are relatively low in K and they are subalkaline rocks in the TAS diagram but, based on the SiO_2 vs. Zr/TiO_2 diagram and the P_2O_5 contents, both subalkaline and alkali-rich affinities may be deduced. The discrepancies are attributed to the occurrence of enclaves and heterogeneous porphyritic components which could indicate mingling of magmas. Instead, the Viinaränninnotko tuffs have alkali and P_2O_5 contents

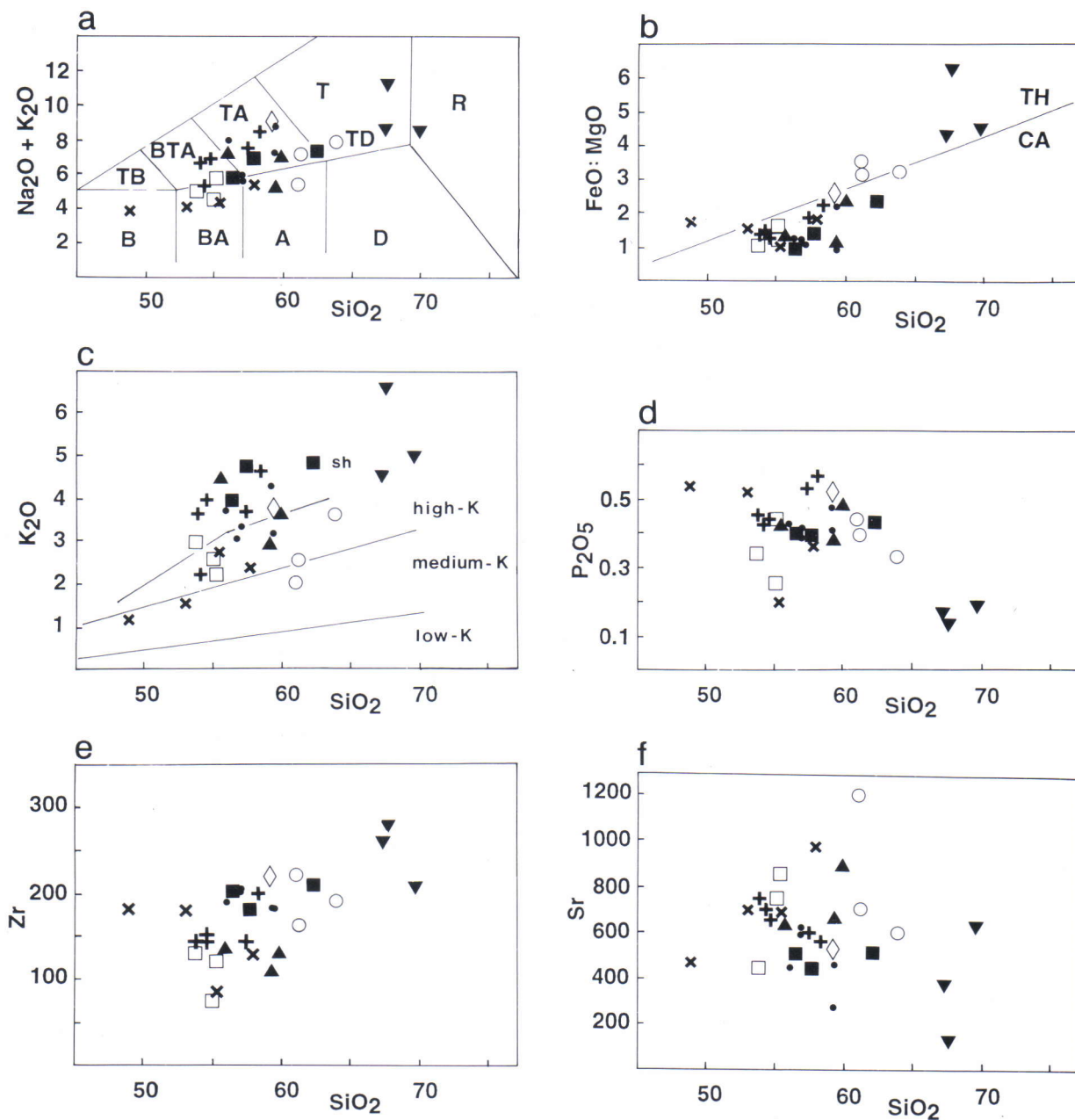
like those in alkali-rich rocks. They have considerably lower REE contents than the Viinaränninoja lava analyzed for REE, and the latter rock is not parental to them. The Viinaränninnotko tuffs largely resemble the $Pl\pm Ur$ -phyric rocks at Tohloppi, Kiviranta and Sorila in chemical composition but their LREE contents tend to be lower.

The Pohjala tuffs are basaltic andesites rather than trachybasaltic andesites. On average, they tend to be lower in K, P and Zr than the Viinaränninnotko tuffs and the $Pl\pm Ur$ -phyric rocks at Tohloppi, Kiviranta and Sorila. The differences may indicate that the Pohjala and Viinaränninnotko tuffs do not represent the same volcanic strata although they structurally may belong to the same horizon. More data are needed for final conclusions. The Pohjala sill is higher in alkalis, Al, P and Zr, and lower in Cr and Ni than the Pohjala tuffs. It seems to be more fractionated than the latter rocks.

The Teacher's tuffs are distinguishable from the other Pl -phyric rocks studied here in many respects. They tend to be relatively low in K and straddle the

Table 1. Major and trace element data for the southern volcanics of the TSB. Major elements and Zr, Ni, Sr, Ba, V, Zn and Cu by XRF but for samples V-2D/90, V-2E/90, 15-D/Pohj and 15-I-Pohj by ICP-AES. REE, Sc, Rb, Ta, Th and Hf by INAA. Oxides in weight%, trace elements in ppm. Total Fe as FeO.

sample	TOHLOPPI					KIVIRANTA					SORILA					
	4- YKÄ/83	7- YKÄ/83	8-1- YKÄ/83	13-1- YKÄ/83	34-1- YKÄ/83	1- Kiv/86	2- Kiv/89	3- Kiv/89	4- Kiv/89	5- Kiv/89	6- Kiv/89	6-A- YKÄ/86	6-B- YKÄ/86	6-C- YKÄ/86		
SiO ₂	54.50	56.59	53.90	54.49	58.48	65.39	64.90	52.30	68.70	57.20	56.70	54.69	55.52	60.51		
TiO ₂	0.61	0.67	0.69	0.61	0.61	0.54	0.58	0.68	0.53	0.75	0.61	0.63	0.61	0.69		
Al ₂ O ₃	13.60	13.99	15.48	14.25	15.18	15.71	16.30	14.10	14.70	14.80	13.20	13.77	13.35	14.27		
FeO	7.55	5.78	6.28	7.45	7.36	3.02	3.19	7.53	3.10	6.99	6.69	7.82	7.94	7.04		
MnO	0.13	0.09	0.13	0.11	0.09	0.07	0.08	0.15	0.05	0.16	0.14	0.15	0.14	0.11		
MgO	6.93	6.41	5.29	6.72	3.42	0.48	0.74	6.24	0.70	2.98	6.98	7.51	5.67	3.05		
CaO	6.87	4.96	6.76	6.58	4.84	1.02	2.68	6.16	2.74	6.13	6.33	6.49	6.23	4.20		
Na ₂ O	2.13	3.80	4.05	2.64	4.38	4.48	3.92	2.65	3.49	3.21	2.31	1.82	2.25	2.51		
K ₂ O	3.12	2.96	3.50	2.87	4.13	6.38	4.36	4.17	4.92	3.44	2.75	3.76	4.50	4.64		
P ₂ O ₅	0.36	0.45	0.40	0.39	0.39	0.14	0.16	0.40	0.18	0.46	0.37	0.39	0.37	0.41		
sum	95.80	95.70	96.47	96.12	98.89	97.23	96.91	94.38	99.11	96.12	96.08	97.04	96.58	97.43		
Zr	200	180	190	200	180	280	260	130	210	130	110	200	180	210		
Cr	480	530	530	460	510			530		260	470	490	460	160		
Ni	130	90	170	130	120	20	10	140	10	50	110	140	120	70		
Sr	590	260	430	610	450	120	370	620	620	880	650	500	440	500		
Ba	880	1090	1370	910	1030	910	920	1190	1930	960	770	860	860	1270		
V	160	140	160	170	160	30	20	180	50	190	140	160	160	160		
Zn	80	70	90	80	70	50	80	100	20	80	90	100	90	90		
Cu	90	60	30	130	20	30	20	90	20	100	130	70	50	70		
La	31.4				31.3	26					32.4	30		31		
Ce	49.6				45.9	49					49.6	54		56		
Nd	21.9				21.2	26					20.7	29		27		
Sm	4.78				4.86	5.6					4.79	4.9		4.9		
Eu	1.29				1.26	1.05					1.33	1.22		1.32		
Tb	0.546				0.547	0.59					0.556	0.57		0.53		
Yb	1.54				1.56	2.4					1.53	1.76		1.47		
Sc	30.7				32.3						30.5					
Rb	72.3				52.3						76.9					
Ta	0.724				0.687						0.662					
Th	6.23				5.94						6.11					
Hf	3.84				3.73						3.47					
K ₂ O:Na ₂ O	1.46	0.78	0.86	1.09	0.94	1.42	1.11	1.57	1.41	1.07	1.19	2.07	2.00	1.85		
La _N /Yb _N	13.43				13.22	7.14					13.95	11.23		13.89		
Tb _N /Yb _N	1.55				1.54	1.08					1.59	1.42		1.58		
sample	VIINARÄNNINNOTKO					POHJALA					TEACHER'S					
	1- Viina	2- Viina	3- Viina	5-B- Viina	5-C- Viina	11- Viina	12- Viina	V-2D /90	V-2E /90	2-A- YKÄ/86	2-B- YKÄ/86	15-I- Pohj	15-D- Pohj	3-A- YKÄ/86	3-B- YKÄ/86	3-C- YKÄ/86
SiO ₂	52.40	51.96	51.32	55.04	56.33	49.57	45.59	57.33	53.80	57.26	51.55	54.04	54.14	58.84	58.15	61.85
TiO ₂	0.62	0.61	0.57	0.56	0.76	0.69	0.78	0.70	0.53	0.63	0.56	0.70	0.62	0.53	0.60	0.41
Al ₂ O ₃	16.64	16.64	15.81	17.32	17.49	14.63	16.38	15.37	12.48	19.06	13.47	15.21	13.19	17.32	16.34	17.17
FeO	7.44	7.95	7.76	5.84	6.20	7.79	11.43	7.48	9.19	5.03	9.00	7.97	9.39	5.93	6.82	4.54
MnO	0.14	0.11	0.14	0.09	0.07	0.15	0.18	0.13	0.17	0.10	0.17	0.10	0.16	0.17	0.19	0.12
MgO	5.89	5.89	5.49	3.21	2.80	5.02	6.75	4.25	9.31	1.98	8.78	5.43	8.1	1.90	1.96	1.42
CaO	6.22	6.76	8.40	6.44	4.51	11.64	8.54	8.41	7.63	3.86	7.45	8.56	8.29	4.47	5.89	3.62
Na ₂ O	2.79	2.92	2.96	3.66	3.75	2.44	2.41	2.93	1.62	5.20	2.00	3.39	1.91	4.37	3.20	4.13
K ₂ O	3.80	3.48	2.05	3.47	4.42	1.42	1.09	2.32	2.55	3.46	2.78	2.15	2.42	2.42	1.92	3.45
P ₂ O ₅	0.42	0.43	0.40	0.50	0.55	0.49	0.49	0.36	0.19	0.50	0.32	0.42	0.24	0.37	0.41	0.31
sum	96.35	96.75	94.90	96.13	96.88	93.83	93.65	99.28	97.47	97.09	96.08	97.97	98.46	96.33	95.48	97.03
Zr	150	140	140	140	200	180	180	130	82	220	130	122	75	160	220	190
Cr	380	340	360	200	130	330	370	320	600	60	640	295	500	20	20	20
Ni	100	100	130	50	40	90	90		150	20	170		10	10	10	10
Sr	650	730	700	590	560	690	460	970	680	520	430	842	729	700	1190	590
Ba	1140	1400	960	1320	1750	1030	150	1223	605	850	1100	1068	793	1320	1070	1560
V	180	190	190	160	170	190	210	180	178	140	180	2	205	80	100	60
Zn	80	100	80	70	80	90	180	75	99	80	100	82	92	100	110	80
Cu	70	60	150	40	120	60	10	140			70			30	30	20
La	18.9				21	34					22			29		35
Ce	32				51	63					41			52		57
Nd	15.9				23	31					26			25		26
Sm	3.7				4.5	5.9					4.6			4.9		4.8
Eu	1.09				1.34	1.6					1.18			1.78		1.61
Tb	0.42				0.54	0.63					0.51			0.43		0.45
Yb	1.25				1.7	1.8					1.49			1.49		1.69
K ₂ O:Na ₂ O	1.36	1.19	0.69	0.95	1.18	0.58	0.45	0.79	1.57	0.67	1.39	0.63	1.27	0.55	0.60	0.84
La _N /Yb _N	9.96				8.14	12.44					9.73			12.82		13.64
Tb _N /Yb _N	1.47				1.39	1.53					1.50			1.27		1.17



- Tohloppi
- ▲ Kiviranta, PLG+UR-phyric rocks
- ▼ Kiviranta, feldspar porphyries
- Sorila
- + Viinaränninnotko, tuffs
- × Viinaränninnotko, lavas
- Pohjala, tuffs
- ◇ Pohjala, PLG-phyric sill
- Teacher's

Fig. 5. SiO_2 variation diagrams of the southern volcanic rocks of the Tampere Schist Belt. Data from Table 1. The total of oxides was calculated to 100%. Zr and Sr in ppm, others in weight%. **a.** Total alkali vs. SiO_2 (TAS) diagram. Fields after Le Maitre (1989): B = basalt; BA = basaltic andesite; A = andesite; D = dacite; BTA = basaltic trachyandesite; TA = trachyandesite; T&TD = trachyte and trachydacite; R=rhyolite. **b.** $\text{FeO}^{\text{tot}}/\text{MgO}$ vs. SiO_2 diagram. TH (tholeiitic) and CA (calcalkaline) fields after Miyashiro (1974). **c.** K_2O vs. SiO_2 diagram. Low-K, medium-K and high-K fields after Le Maitre (1989), the boundary between the high-K and sh (shoshonitic) fields after Ewart (1982). **d.** P_2O_5 vs. SiO_2 diagram. **e.** Zr vs. SiO_2 diagram. **f.** Sr vs. SiO_2 diagram.

andesite/trachyandesite boundary in the TAS and the SiO_2 vs. Zr/TiO_2 diagrams. A minor iron enrichment might be deduced in the FeO/MgO vs. SiO_2 diagram. The Cr and Ni contents are notably low, and the Sr contents are relatively high. The REE patterns are distinguished since the HREE slope gently ($\text{Tb}_N:\text{Yb}_N$ ca. 1.2) and since there are minor positive Eu anomalies.

The feldspar porphyries of Kiviranta are classified as trachytes, trachydacites and rhyolites. They are rather rich in Zr, low in P, and tend to show an

iron enrichment in the FeO/MgO vs. SiO_2 diagram. The pebble from the Kiviranta conglomerate resembles the feldspar porphyry samples. Sample 1-Kiv/86 has a nearly flat HREE pattern (Fig. 8). The prominent Eu minimum indicates fractionation of plagioclase during fractional crystallization, or occurrence of plagioclase in the solid residue if partial melting is invoked. Since this sample is lower in LREE but higher in HREE than the $\text{Pl}\pm\text{Ur}$ -phyric volcanics of Kiviranta, Tohloppi and Sorila the latter rocks are not parental to it.

Comparison with young shoshonites and high-K andesites

The P_2O_5 , REE, Sr and Zr contents of young shoshonitic (trachy)andesites range widely (Table 2) but, in general, they exceed those in the spatially associated medium-K (or calc-alkaline) and high-K andesites (e.g. Ewart 1982). The (trachy)andesites also tend to be higher in LREE and Zr than the associated shoshonitic basaltic (trachy)andesites (Table 2). Some shoshonitic (trachy)andesites have nearly flat HREE patterns but in most cases they have moderately sloping HREE patterns with $\text{Tb}_N:\text{Yb}_N$ ca. 1.4 or more (see data in Gorton 1977,

Meen & Eggler 1987, Francalanci et al. 1989).

Most of the southern volcanics of the TSB resemble young shoshonites in their alkali contents (Fig. 5, Table 2). The $\text{Pl}\pm\text{Ur}$ -phyric rocks at Tohloppi, Kiviranta and Sorila, in particular, are similar to young shoshonitic andesites since they have relatively high LREE, P, Zr and Sr contents and since their HREE patterns slope moderately. These rocks were no doubt originally shoshonitic because REE, P and Zr are relatively resistant to alteration. Their Cr and Ni contents are higher than those in young shoshonites

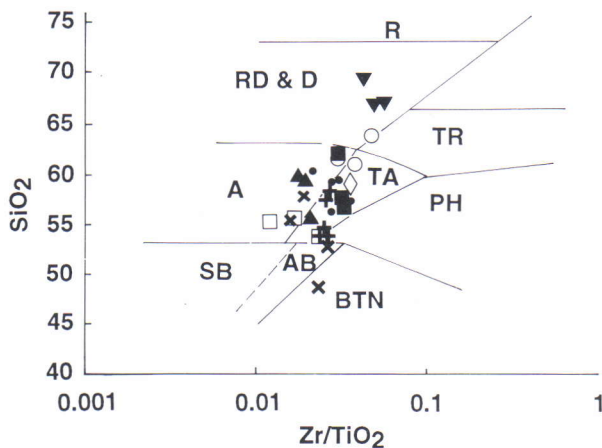
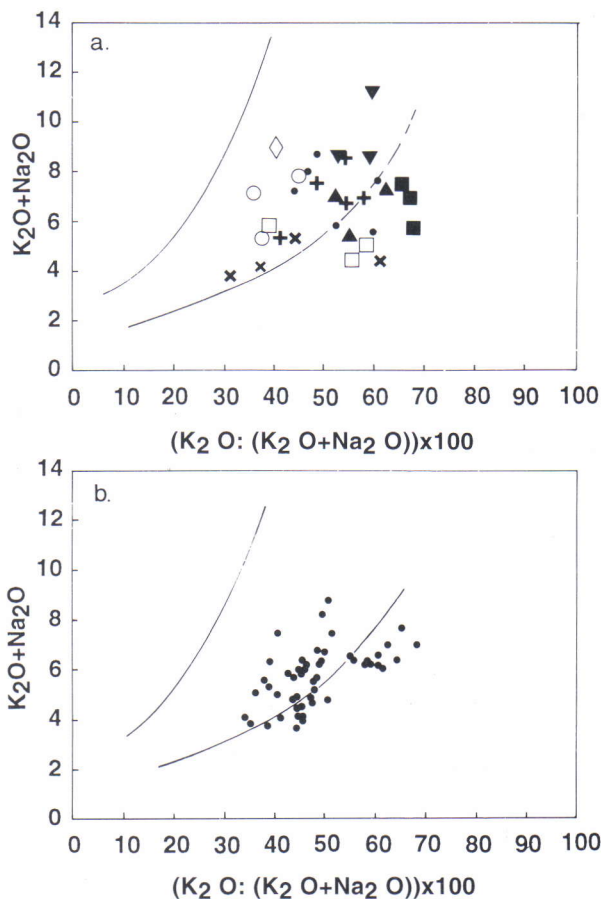


Fig. 6. The southern volcanic rocks of the Tampere Schist Belt in the SiO_2 vs. Zr/TiO_2 diagram of Winchester and Floyd (1977). Fields: SB = sub-alkaline basalt; AB = alkali basalt; BTN = basanite, trachybasanite and nephelinite, A = andesite, RD & D = rhyodacite and dacite, TA = trachyandesite, PH = phonolite, TR = trachyte, R = rhyolite. Data from Table 1., symbols as in Fig. 5.

Fig. 7.a. The southern volcanic rocks of the Tampere Schist Belt in the igneous spectrum of Hughes (1973). The lines delimit the field of relatively unaltered volcanic rocks according to Hughes. Data from Table 1, symbols as in Fig. 5. b. Young calc-alkaline, high-K calc-alkaline, shoshonitic and potassic volcanics from Stromboli in the igneous spectrum of Hughes (1973). Data from Francalanci et al. (1989).



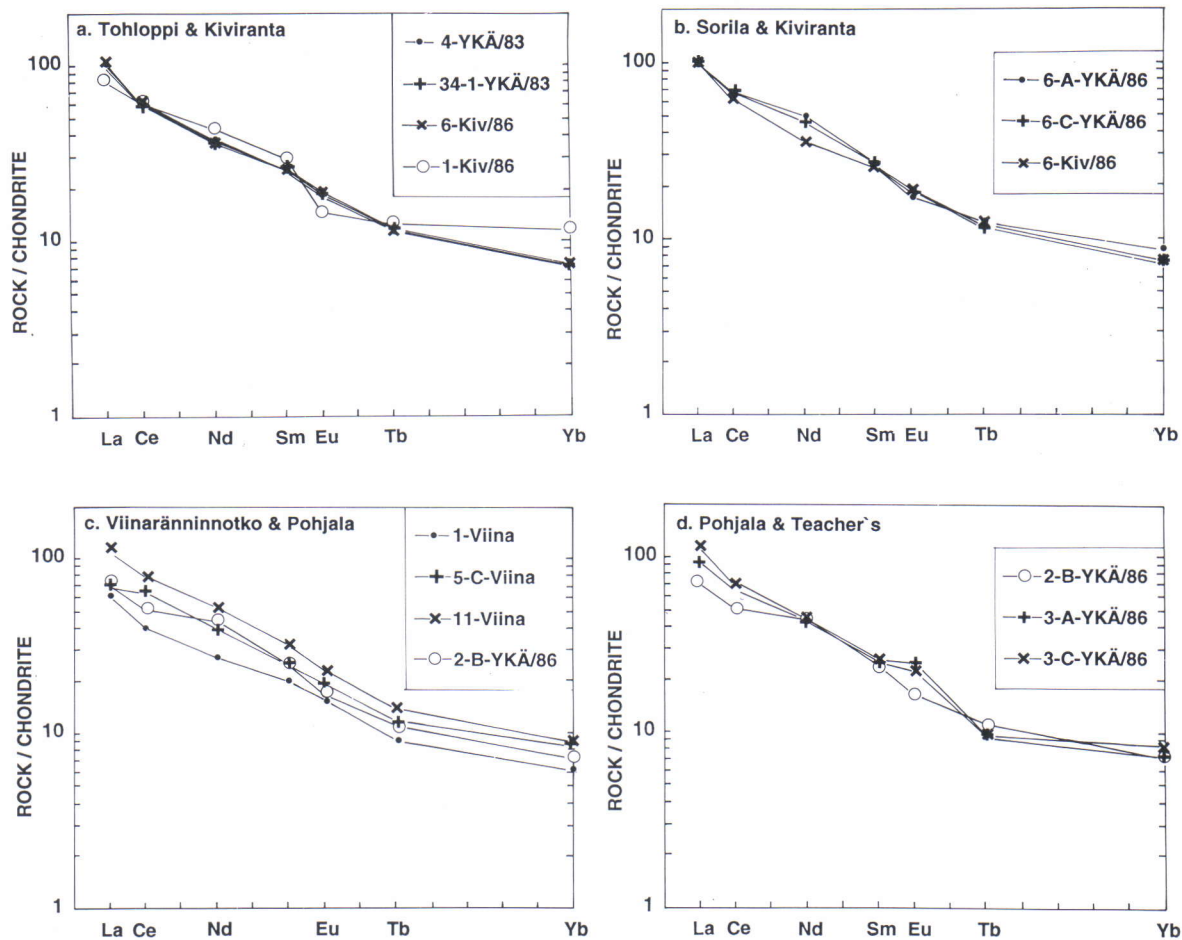


Fig. 8. Chondrite-normalized REE patterns of the southern volcanic rocks of the Tampere Schist Belt. Data from Table 1. Chondrite values: Leedeey-6 divided by factor 1.2 (Jahn et al. 1980, Tb from Koljonen & Rosenberg 1975).

Table 2. Averages and representative values of selected young shoshonitic basaltic andesites and andesites compared with the averages of the southern metavolcanics of the TSB. SiO₂, TiO₂, Na₂O, K₂O and P₂O₅ in weight%; Zr, Sr, La and Cr in ppm.

	1.	2.	3.	4.	5.	6.	7.	8.	9.	10.	11.	12.	13.	14.	15.	16.	17.	18.	19.
SiO ₂	54.37	54.18	54.35	53.42	52.76	60.88	58.68	56.5	54.94	59.64	60.24	59.27	55.59	55.40	56.91	53.41	51.57	53.24	59.61
TiO ₂	1.60	1.12	0.87	1.00	0.93	0.83	0.75	0.92	0.90	1.01	0.79	0.56	0.64	0.68	0.64	0.62	0.68	0.63	0.52
Na ₂ O	3.78	3.57	2.91	3.42	3.44	3.56	3.55	4.00	4.19	4.06	3.07	2.67	3.40	2.72	2.19	3.22	2.35	2.43	3.90
K ₂ O	3.45	3.75	4.02	3.47	2.53	3.57	3.73	3.43	3.45	4.25	5.15	2.68	3.32	3.45	4.30	3.44	1.84	2.45	2.60
P ₂ O ₅	0.74	0.68	0.42	0.62	0.46	0.46	0.40	0.60	0.41	0.46	0.37	0.41	0.40	0.41	0.39	0.46	0.38	0.33	0.36
Zr	328	226	159	137	133	184	275	140	132	394	277	150	190	123	197	154	143	109	190
Sr	1071	1043	773	1030	1145	434	595	733	547	902	752	850	468	717	480	646	700	667	827
La	89	70	47	38	77	30	68	42	57	150	58	18	31	32	31	20	34	22	32
Cr	172	196	27	85	112	19	12	71	8	66	20		502	420	370	282	405	478	20
Ni	75	63	17	35	60	6	16	32	3	59	14		128	100	110	84	110	170	10

1. Average of shoshonitic basaltic andesites, western South America (Ewart 1982)
2. Average of shoshonitic basaltic andesites, western USA - Eastern Zone (Ewart 1982)
3. Average of shoshonitic basaltic andesites, Mediterranean (Ewart 1982)
4. Average of shoshonitic basaltic andesites, Southwestern Pacific (Ewart 1982)
5. Average of shoshonites, Yellowstone National Park, USA. Data from Nicholls & Carmichael (1969)
6. Average of shoshonitic andesites, Vanuatu (New Hebrides). Data from Gorton (1977)
7. Average of shoshonitic andesites, Stromboli, Italy. Data from Francalanci et al. (1989)
8. Average of the Cretaceous Independence HATS andesites. Data from Meen & Eggler (1987)
9. Shoshonitic andesite, South Hiyoshi, Marianas (Bloomer et al. 1989, Lin et al. 1989)
10. Average of shoshonitic andesites, Western USA, Eastern Zone (Ewart 1982)
11. Average of shoshonitic andesites, Mediterranean (Ewart 1982)
12. Representative and preferred values of shoshonitic andesites (Jakeš & White 1972)
13. Average of the Tohloppi lavas
14. Average of the PLG+ -UR-phyric volcanic rocks at Kiviranta
15. Average of the PLG+ -UR-phyric volcanic rocks at Sorila
16. Average of the Viinaränninnotko tuffs
17. Average of the Viinaränninnotko lavas
18. Average of the Pohjala tuffs
19. Average of the Teacher's volcanics

(Table 2). As prominent accumulation of mafic phenocrysts is not evident (Appendix), the shoshonites of the southern TSB are less fractionated than young shoshonites typically.

The Viinaränninnotko tuffs comprise another group which has prominent shoshonitic affinities according to the alkali contents. The LREE evidence for their

shoshonitic character is less unanimous than for the rocks discussed above but the P_2O_5 , Sr and Zr contents are relatively high, the HREE patterns slope moderately ($Tb_N:Yb_N$ are 1.4-1.5) and, in fact, also their La contents of ca. 20 ppm are close to the La value given by Jakeš and White (1972) for a typical shoshonitic andesite (Table 2).

TECTONIC SETTING

The southern volcanics of the TSB display pronounced arc affinities since most of them have intermediate silica contents, since they fall in the arc field in the Ti vs. Zr diagram (Fig. 9), and since their

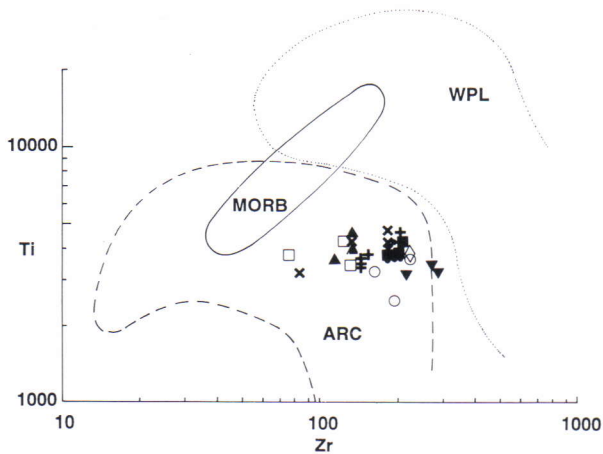


Fig. 9. Ti vs. Zr diagram of the volcanic rocks of the southern parts of the Tampere Schist Belt. Data from Table 1, symbols as in Fig. 5. ARC = arc lavas, MORB = mid-ocean ridge basalts, WPL = within plate lavas (Pearce 1982).

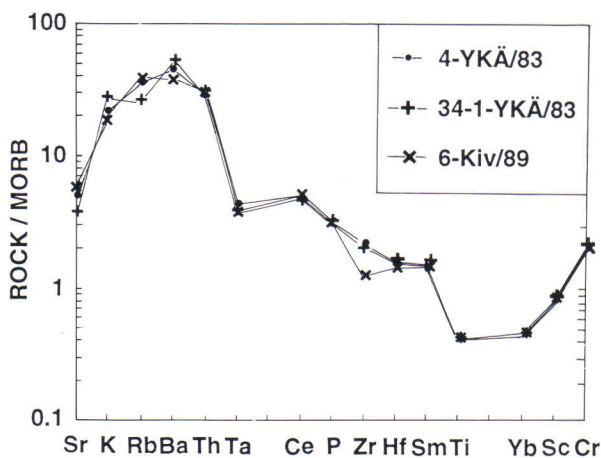


Fig. 10. Mid-ocean ridge basalt (MORB) -normalised trace element patterns of the volcanic rocks from Tohloppi and Kiviranta. MORB values from Pearce (1982). Data from Table 1.

MORB-normalized spidergrams have prominent Ta depletions (Fig. 10). Some continental flood basalts show Ta and Nb depletions (Holm 1985, Duncan 1987) but the rocks studied here are distinguished from them as intermediate and largely pyroclastic rocks.

Jakeš and White (1972) suggested a generalized temporal sequence from low-K rocks to calc-alkaline and finally to shoshonitic ones in volcanic arcs. There are exceptions like the unusual shoshonites in the primitive Marianas arc (Stern et al. 1988). However, although Arculus and Johnson (1978) presented criticism against the generalized model, they agreed that shoshonites most commonly occur in regions of long history of plate interactions and that shoshonites do not appear to erupt in most young arcs. Evidently, the alkali-rich southern volcanics of the TSB, particularly the shoshonitic volcanics at Tohloppi, Kiviranta and Sorila, indicate a setting of an evolved arc.

The shoshonites of oceanic island arcs tend to have lower La (and other LREE) contents than the shoshonites of active continental margins (Morrison 1980; Table 2). The southern volcanics of the TSB

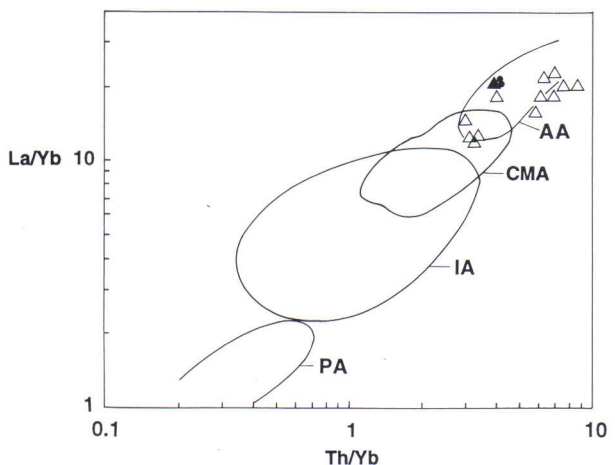


Fig. 11. La/Yb vs. Th/Yb diagram of the trachyandesites from Tohloppi and Kiviranta, and of calc-alkaline, high-K calc-alkaline and shoshonitic andesites and basaltic andesites (SiO_2 exceeds 54%) on Stromboli (triangles). Symbols for Tohloppi and Kiviranta as in Fig. 5. Data from Table 1 and Francalanci et al. (1989). Fields from Condie (1989): PA = primitive arc; IA = island arc; CMA = continental margin arc; AA = Andean arc.

would thus resemble oceanic shoshonites more than those of continental margins but the groups are overlapping and the data are not sufficient. On the other hand, the volcanics of Tohloppi and Kiviranta fall in the field of Andean andesites in the La/Yb vs. Th/Yb diagram (Fig. 11). However, the significance of this diagram is questionable as the subalkaline to

shoshonitic lavas from Stromboli also fall in the field of Andean andesites. Stromboli is located in a region with a long history of plate interactions but the crust beneath Stromboli is thin (18 km; Francalanci et al. 1989). Therefore, thick Andean-type crust is not necessarily implied by the composition of the southern volcanics of the TSB.

ACKNOWLEDGMENTS

This study is part of the project 1011197 "Geology and geochemistry of the supracrustal rocks of the early Proterozoic Tampere Schist Belt" of the Academy of Finland. Financial support was also received from the Wilhelm Ramsay and Th. G. Sahama Memorial Foundation. The comments by Kent Condie

and Raimo Lahtinen greatly improved the paper. I also appreciate the stimulating discussions with Richard Ojakangas. The figures were drawn by Riitta Fagerström. The English language was revised by Christopher Cunliffe. The paper is a contribution to the IGCP project 217 "Proterozoic Geochemistry".

REFERENCES

- Ala-Vainio, I. 1986.** XRF routine analysis by the fundamental parameter method. Proceedings of the Thirty-ninth Chemist's Conference. Scarborough, June 17-19, 1986. Research and Development, British Steel Corporation, 51-54.
- Arculus, R. J. & Johnson, R. W. 1978.** Criticism of generalised models for the magmatic evolution of arc-trench systems. *Earth Planet. Sci. Lett.* 39, 118-126.
- Ayres, L. D. & Corfu, F. 1991.** Stacking of disparate volcanic and sedimentary units by thrusting in the Archean Favourable Lake greenstone belt, central Canada. *Precambrian Res.* 50, 221-238.
- Bloomer, S. H., Stern, R. J., Fisk, E. & Geschwind, C. H. 1989.** Shoshonitic volcanism in the northern Mariana arc I. Mineralogical and major and trace element characteristics. *J. Geophys. Res.* 94, 4469-4494.
- Cas, R. A. F. & Wright, J. V. 1991.** Subaqueous pyroclastic flows and ignimbrites: an assessment. *Bull. Volcanol.* 53, 357-380.
- Cashman, K. V. & Fiske, R. S. 1991.** Fallout of pyroclastic debris from submarine volcanic eruptions. *Science* 253, 275-280.
- Condie, K. C. 1989.** Geochemical changes in basalts and andesites across the Archean-Proterozoic boundary: Identification and significance. *Lithos* 23, 1-18.
- Dimroth, E., Imreh, L., Rocheleau, M. & Goulet, N. 1982.** Evolution of the south-central part of the Archean Abitibi Belt, Quebec. Part I: Stratigraphy and paleogeographic model. *Can. J. Earth Sci.* 19, 1729-1758.
- Duncan, A. R. 1987.** The Karoo igneous province - a problem area for inferring tectonic setting from basalt geochemistry. *J. Volcanol. Geotherm. Res.* 32, 13-34.
- Ewart, A. 1982.** The mineralogy and petrology of Tertiary-Recent orogenic volcanic rocks: with special reference to the andesitic-basaltic compositional range. In: Thorpe, R.S. (ed.) *Andesites. Orogenic Andesites and Related Rocks*. Chichester: Wiley, 25-95.
- Fisher, R. V. 1984.** Submarine volcanoclastic rocks. In: Kokelaar, B.P. & Howells, M.F. (eds.) *Marginal Basin Geology*. Oxford: Blackwell, 5-27.
- Francalanci, L., Manetti, P. & Peccerillo, A. 1989.** Volcanological and magmatological evolution of Stromboli volcano (Aeolian Islands): the roles of fractional crystallization, magma mixing, crustal contamination and source heterogeneity. *Bull. Volcanol.* 51, 355-378.
- Gorton, M. P. 1977.** The geochemistry and origin of Quaternary volcanism in the New Hebrides. *Geochim. Cosmochim. Acta* 41, 1257-1270.
- Holm, P. E. 1985.** The geochemical fingerprints of different tectonomagmatic environments using hygromagmatic elements abundances of tholeiitic basalts and basaltic andesites. *Chem. Geol.* 51, 303-323.
- Hughes, C. J. 1973.** Spilites, keratophyres, and the igneous spectrum. *Geol. Mag.* 109, 513-527.
- Huhma, H. 1986.** Sm-Nd, U-Pb and Pb-Pb isotopic evidence for the origin of the early Proterozoic Svecokarelian crust in Finland. *Geol. Surv. Finland, Bull.* 337, 48 p.
- Huhma, H., Claesson, S., Kinny, P. D. & Williams, I. S. 1991.** The growth of Early Proterozoic crust: new evidence from Svecofennian detrital zircons. *Terra Nova* 3, 175-179.
- Jahn, B. M., Auvray, B., Blais, S., Capdevila, R., Cornichet, J., Vidal, P. & Hameurt, J. 1980.** Trace element geochemistry and petrogenesis of Finnish greenstone belts. *J. Petrol.* 21, 201-244.
- Jakeš, P. & White, A. J. R. 1972.** Major and trace element abundances in volcanic rocks of orogenic areas. *Geol. Soc. Am. Bull.* 83, 29-40.

- Kähkönen, Y. 1987.** Geochemistry and tectonomagmatic affinities of the metavolcanic rocks of the early Proterozoic Tampere Schist Belt, southern Finland. *Precambrian Res.* 35, 295-311.
- Kähkönen, Y. 1989.** Geochemistry and petrology of the metavolcanic rocks of the early Proterozoic Tampere Schist Belt, southern Finland. *Geol. Surv. Finland, Bull.* 345, 104 p.
- Kähkönen, Y. 1993.** Stratigraphy and evolution of the Palaeoproterozoic supracrustal rocks in the Tampere area, southern Finland: a preliminary review. *GGT/SVEKA, Työkokous Kuopiossa* 25. - 26.11.1993.
- Kähkönen, Y., Huhma, H. & Aro, K. 1989.** U-Pb zircon ages and Rb-Sr whole-rock isotope studies of early Proterozoic volcanic and plutonic rocks near Tampere, southern Finland. *Precambrian Res.* 45, 27-43.
- Kähkönen, Y. & Leveinen, J. 1994.** Geochemistry of metasedimentary rocks of the Paleoproterozoic Tampere Schist Belt, southern Finland. *Geol. Surv. Finland, Spec. Paper* 19, 117-136.
- Koljonen, T. & Rosenberg, R. 1975.** Rare earth elements in Middle Precambrian volcanic rocks of Finland, with a discussion of the origin of the rocks. *Bull. Geol. Soc. Finland* 47, 127-138.
- Le Maitre, R.W. (ed.) 1989.** A Classification of Igneous Rocks and Glossary of Terms: Recommendations of the International Union of Geological Sciences Subcommittee on the Systematics of Igneous Rocks. Blackwell: Oxford, 193 p.
- Lin, P.-N., Stern, R.J. & Bloomer, S.H. 1989.** Shoshonitic volcanism in the northern Mariana arc 2. Large-ion lithophile and rare earth element abundances: evidence for the source of incompatible element enrichments in intraoceanic arcs. *J. Geophys. Res.* 94, 4497-4514.
- Luukkonen, A., Grönholm, P. & Hannila, T. 1992.** Eräiden Etelä-Suomen kulta- ja sen seuralaismetalliesiintymien geologiset pääpiirteet. Summary: Main geological features of certain gold and tungsten-tin-gold prospects in southern Finland. *Geol. Surv. Finland, Rep. Invest.* 113, 90 p.
- Meen, J. K. & Egglar, D. H. 1987.** Petrology and geochemistry of the Cretaceous Independence volcanic suite, Absaroka Mountains, Montana: clues to the composition of the Archean sub-Montanan mantle. *Geol. Soc. Am. Bull.* 98, 238-247.
- Miyashiro, A. 1974.** Volcanic rock series in island arcs and active continental margins. *Am. J. Sci.* 274, 321-355.
- Morrison, G. W. 1980.** Characteristics and tectonic setting of the shoshonite rock association. *Lithos* 13, 97-108.
- Mueller, W. 1991.** Volcanism and related slope to shallow-marine volcanoclastic sedimentation: an Archean example near Chibougamau, Quebec, Canada. *Precambrian Res.* 49, 1-22.
- Nicholls, J. & Carmichael, I. S. E. 1969.** A commentary on the absarokite-shoshonite-banakite series of Wyoming, U.S.A. *Schweiz. Mineral. Petrogr. Mitt.* 49, 47-64.
- Ojakangas, R. W. 1986.** An early Proterozoic metagraywacke-slate turbidite sequence: The Tampere schist belt, southwestern Finland. *Bull. Geol. Soc. Finland* 58, 241-261.
- Patchett, J. & Kouvo, O. 1986.** Origin of continental crust of 1.9-1.7 Ga age: Nd isotopes and U-Pb zircon ages in the Svecokarelian terrain of South Finland. *Contrib. Mineral. Petrol.* 92, 1-12.
- Nironen, M. 1989.** The Tampere Schist Belt: structural style within an early Proterozoic volcanic arc system in southern Finland. *Precambrian Res.* 43, 23-40.
- Pearce, J. A. 1982.** Trace element characteristics of lavas from destructive plate margins. In: Thorpe, R.S. (ed.), *Andesites. Orogenic Andesites and Related Rocks*. Chichester: Wiley, 525-548.
- Rosenberg, R. J., Kaistila, M. & Zilliacus, R. 1982.** Instrumental epithermal neutron activation analysis of solid geochemical samples. *J. Radioanal. Chem.* 71, 419-428.
- Stern, R.J., Bloomer, S.H., Lin, P.-N., Ito, E. & Morris, J. 1988.** Shoshonitic volcanism in nascent arcs: New evidence from submarine volcanoes in the northern Marianas. *Geology* 16, 426-430.
- Winchester, J.A. & Floyd, P.A. 1977.** Geochemical discrimination of different magma series and their differentiation products using immobile elements. *Chem. Geol.* 20, 325-343.

APPENDIX. Sample description. Capitals for major minerals, ϕ = maximum diameters, xx% = amount, pc = partly as phenocrysts; ps = pseudomorph, gm = groundmass. Pl = plagioclase, Hbl = hornblende, Act = actinolite, Qtz = quartz, Bt = biotite, Kfs = K-feldspar, Ep = epidote, Ur = uralite (pseudomorphous after clinopyroxene), Crb = carbonate, Op = opaques, Cpx = clinopyroxene, Ab = albite, Olg = oligoclase, Ans = andesine. x and y give grid coordinates.

TOHLOPPI

- 4-YKÄ/83. Lava with polygonal fractures. PL (pc ϕ to 2.5x5 mm, 10%, Olg, often mosaic), ACT/HBL (pc Cpx-ps ϕ to 2x2 mm, 15%), BT (pc Hbl-ps), QTZ (largely as amygdules), KFS. Poorly oriented, gm in places shows flow texture. x = 6822.25, y = 2479.98.
- 7-YKÄ/83. Lava with polygonal fractures. PL (pc, ϕ to 1.5x4 mm, 10%), ACT (pc Cpx-ps ϕ to 1.5 mm, 10%), BT (pc Hbl-ps ϕ to 1.5 mm, 5-10%), QTZ (partly as amygdules). x = 6822.80, y = 2480.16.
- 8-1-YKÄ/83. Massive lava, 30 cm below the contact to the overlying sedimentary rocks. PL (Pc ϕ to 1x4.5 mm, 10-15%, Ab), ACT/HBL (pc Cpx-ps ϕ to 2x3 mm, 10%), BT (Hbl-ps are rare), EP. Homogenous, rather oriented gm. Amygdules of Qtz small and rare. x = 6822.40, y = 2480.10.
- 13-1-YKÄ/83. Massive lava, ca. 10 m below the contact to the overlying sedimentary rocks. PL (pc ϕ to 3 mm, 10-15%), ACT (pc Cpx-ps ϕ to 4 mm, 15-20%), BT (aggregates strongly oriented), QTZ (amygdules ϕ to 4 mm, 5%), EP. x = 6822.25, y = 2480.39.
- 34-1-YKÄ/83. Lava, ca. 20 m below the contact to the overlying sedimentary rocks. PL (pc ϕ to 2.5 mm, 10%), ACT (pc Cpx-ps ϕ to 3 mm, 15-20%), BT, EP, KFS. Homogeneous and very fine-grained gm. x = 6822.18, y = 2481.03.

KIVIRANTA

- 1-Kiv/86. Massive feldspar porphyry. PL (pc ϕ to 2x2 mm, 5%, Ab, seriate), BT, KFS, QTZ. x = 6825.37, y = 2490.95.
- 2-Kiv/89. Massive feldspar porphyry. PL (pc, Ab), KFS (pc, ϕ of the feldspars to 2x2 mm, 5%), QTZ, BT. x = 6825.37, y = 2490.79.
- 3-Kiv/89. Lapilli tuff between the feldspar phyric stratum and the massive Pl+Ur -porphyry. PL (pc ϕ to 1x1.5 mm, 20%), BT (Pc Hbl-ps), HBL, EP, QTZ, CRB. x = 6825.38, y = 2490.75.
- 4-Kiv/89. Feldspar-phyric pebble in conglomerate. PL (pc), KFS (pc, ϕ of the feldspars to 1x2 mm, 5%), QTZ, BT, OP. x = 6825.40, y = 2490.76.
- 5-Kiv/89. Matrix-supported lapilli tuff above the conglomerate. PL (pc ϕ to 1.5x3.5 mm, 5-10%, Ab-Olg), ACT/HBL (pc Cpx-ps ϕ to 1.5x3 mm, 10-15%), BT (mostly aggregates with a prominent orientation), EP, QTZ. x = 6825.45, y = 2490.82.
- 6-Kiv/89. Massive Pl+Ur -porphyry. PL (pc ϕ to 2x3 mm, 15-20%, prominent epidotization, Ab), ACT/HBL (pc Cpx-ps ϕ to 4x4 mm, 15-20%), BT, QTZ, CRB, EP. Pronounced schistosity. x = 6825.40, y = 2490.88.

SORILA (x = 6827.56, y = 2496.65)

- 6-A-YKÄ/86. Ur+Pl -porphyry. PL (pc ϕ to 2x5 mm, 10-15%, strongly altered), ACT (pc Cpx-ps ϕ to 2.5x3 mm, 20%), BT, QTZ, EP. Pronounced schistosity.
- 6-B-YKÄ/86. Ur+Pl -porphyry. PL (pc ϕ to 1.5-2 mm, 5-10%), ACT/HBL (pc Cpx-ps ϕ to 2x3 mm, 10%), BT, QTZ, EP. Pronounced schistosity.
- 6-C-YKÄ/86. Stratified crystal or lithic tuff, 4 cm thick. PL (pc ϕ to 1 mm, 1-10%), QTZ, BT, EP. In part rich in KFS.

VIINARÄNNINNOTKO

Tuffs

- 1-Viina. Lithics-bearing crystal tuff from a faintly stratified 3 m thick stratum which has an erosional base, 20 cm from the base. PL (pc ϕ to 1x3 mm, 20-30%, Olg), QTZ, ACT, BT (some aggregates may be relicts of vitric clasts). x = 6831.30, y = 2503.01.
- 2-Viina. Lithics-bearing crystal tuff from the base of a non-stratified 4.5 m thick stratum, ca. 15 m above sample 1-Viina. PL (pc ϕ to 1.5x3 mm, 30-35%, partly in porphyritic rock fragments, Olg-Ans), ACT/HBL (pc Cpx-ps ϕ to 1x2 mm, 10-15%), BT (some aggregates may be

relicts of vitric clasts), QTZ. x = 6831.28, y = 2503.00.

3-Viina. Lithics-bearing crystal tuff 3 m above sample 2-Viina. PL (pc ϕ to 2.5x4.8 mm, 25-30%, Olg-Ans), ACT/HBL (pc Cpx-ps ϕ to 1x1 mm, 10-15%), QTZ, BT. x = 6831.28, y = 2503.00.

5-C-Viina. Crystal-bearing lithic tuff from a 2.7 m thick thickly to thinly bedded graded stratum, ca. 6 m above sample 3-Viina. PL (pc ϕ to 1.2x2 mm, 10%, olg), ACT/HBL, BT (pc Hbl-ps), QTZ. x = 6831.27, y = 2503.00.

5-B-Viina. Lithics-bearing crystal tuff which represents the matrix of a lapilli tuff. About 0.5 m from the base of a 4.5 m thick graded pyroclastic flow deposit, 1-2 m above sample 5-C-Viina. PL (pc ϕ to 2x3 mm, 25%), ACT/HBL (pc Cpx-ps ϕ to 1 mm, rare; pc Hbl-ps ϕ to 0.5x1 mm, 5%), QTZ, BT. x = 6831.27, y = 2503.00.

Lavas

11-Viina. Fragmental to lobate lava, ca. 1 m above the lower contact of lavas. PL (Pc ϕ to 4x5 mm, 10%, Ans), HBL (pc Cpx-ps ϕ to 2x3 mm, 10-15%), QTZ. In addition to two porphyritic components, there are also fine-grained shards. x = 6831.26, y = 2503.00.

12-Viina. Fragmental lava, ca. 20 m above the lower contact of lavas. PL (pc ϕ to 2x5 mm, 20-25%), ACT/HBL (pc Cpx-ps ϕ to 2x3 mm, 15-20%, Ans). Elongate PL-phenocrysts display flow texture. x = 6831.24, y = 2502.99.

V-2D/90. Massive lava, ca. 9 m thick, about 12 m above the lower contact of lavas. PL (pc ϕ to 1.5x3.5 mm, 15%, Olg-Ans), ACT/HBL (pc Cpx-ps ϕ to 3x3 mm, 20%). Felsic veinlets 2-4%. x = 6831.25, y = 2502.97.

V-2E/90. Lava which in places displays hazy fragmental structure, ca. 7-8 m thick, about 20 m above the lower contact of lavas. PL (pc ϕ to 1x4.5 mm, 15%, Olg-Ans), ACT/HBL (pc Cpx-ps ϕ to 2x3 mm, 15%), BT (ca. 5%, aggregates and one Cpx-ps). The sample comprises two porphyritic components. x = 6831.24, y = 2502.97.

POHJALA

2-A-YKÄ/86. Massive Pl-phyric rock, probably a sill. PL (pc ϕ to 2x4 mm, 20-25%), QTZ, BT (pc Hbl-ps, rare). KFS is fairly abundant in the Pl-pc. x = 6835.54, y = 2516.24.

2-B-YKÄ/86. Massive lithics-bearing crystal tuff. ACT/HBL (pc Cpx- & Hbl-ps ϕ to 1x1 mm, 30-40%), PL (pc ϕ to 0.5x1 mm, 10%, Ans), BT (10-15%, some aggregates may be relicts of vitric fragments), QTZ. x = 6835.58, y = 2516.26.

15-D-Pohj/90. From a 7 m thick lithics-bearing crystal tuff which is massive but contains a few pebbles and rarely shows hazy stratification. ACT/HBL (pc Cpx- & Hbl-ps ϕ to 1x1 mm, 30-40%), PL (pc ϕ to 1x1 mm, 10-15%, Ans), BT (15%, some aggregates may be relicts of vitric fragments), QTZ. x = 6835.38, y = 2516.99.

15-I-Pohj/90. From a 2.5 m thick massive lithics-bearing crystal tuff, 10 m above the former. ACT/HBL (pc Cpx- & Hbl-ps ϕ to 1x1 mm, 30%), PL (pc ϕ to 1x2.5 mm, 10-15%), BT (10-20%, some aggregates may be relicts of vitric fragments), QTZ. x = 6835.37, y = 2516.99.

TEACHER'S

3-A-YKÄ/86. Crystal tuff from a 6 m thick very thinly to thinly bedded unit. Possibly rich in poorly discernible relicts of lithic and vitric clasts. PL (pc ϕ to 1x1.5 mm, 20-25%), BT, QTZ, HBL (5%). Garnet is a minor mineral. x = 6836.72, y = 2517.59.

3-B-YKÄ/86. Stratified lithics-bearing crystal tuff above the former, from a 4 m thick medium to thickly bedded unit. Lithic clasts are poorly discernible. PL (pc ϕ to 0.5x1 mm, 20-25%), HBL, BT, QTZ. Garnet is a minor mineral. x = 6836.72, y = 2517.59.

3-C-YKÄ/86. From a 10 m thick lapilli tuff above the former. PL (pc ϕ to 2x4 mm, 20-30%), BT, QTZ. Lapilli are poorly discernible. x = 6836.73, y = 2517.59.

GEOCHEMISTRY OF METASEDIMENTARY ROCKS OF THE PALEOPROTEROZOIC TAMPERE SCHIST BELT, SOUTHERN FINLAND

by
Yrjö Kähkönen and Jussi Leveinen

Kähkönen, Yrjö & Leveinen, Jussi 1994. Geochemistry of metasedimentary rocks of the Paleoproterozoic Tampere Schist Belt, southern Finland. *Geological Survey of Finland, Special Paper 19*, 117–136, 10 figures, 3 tables and one appendix.

This study is based on major and trace element analyses on 90 samples mainly from two profiles in the metaturbidite-dominated southern limb of the E-W trending major syncline of the ca. 1.9 Ga volcanic-sedimentary Tampere Schist Belt (TSB). The chemical compositions of the TSB graywackes resemble those of recent turbidite sands from “pooled active margins” (PAM), i.e., from continental arc basins, back-arc basins, strike-slip basins, continental collision basins and forearc basins of mature arcs.

The composition of the TSB metasedimentary rocks shows variation according to stratigraphic position. The stratigraphically lowermost graywackes have 60–68% SiO₂. The overlying graywackes are first fairly silicic (ca. 73–80% SiO₂), but upward in the succession the SiO₂ contents decrease until the uppermost graywackes (in part fluvial) of the study profiles have 53–60% SiO₂. The mudstones associated with the uppermost graywackes tend to have higher P₂O₅, CaO, Sr and LREE contents, and their chemical index of alteration (CIA) and K₂O/Na₂O ratios are lower than those typical in the lower mudstones. Mudstones with low CIA values also occur in the lowermost stratigraphic levels. The above features reflect variations in the character of provenance and in the activity of volcanism. Even the lowermost turbidites are derived from an evolved volcanic arc rather than from an immature arc. Upward in the succession, the proportion of volcanic material in the sedimentary rocks first decreases, but increases again higher in the succession. The increased volcanic activity resulted in steeper relief, rapid accumulation and limited chemical weathering.

In general, the TSB metasedimentary rocks have prominent LREE enrichments and they mostly do not display significant Eu depletions. The bulk of their Paleoproterozoic source rocks were fairly evolved, but intracrustally differentiated rocks were not important components in the source areas. Turbidites with these characteristic are possibly more common among post-Archean siliciclastic metasedimentary rocks than has been reported previously.

Key words (GeoRef Thesaurus, AGI): schist belts, metasedimentary rocks, turbidite, graywacke, mudstone, stratigraphy, geochemistry, rare earths, Proterozoic, Paleoproterozoic, Tampere, Finland

Yrjö Kähkönen and Jussi Leveinen, Department of Geology, P.O. Box 11 (Snellmaninkatu 3), FIN-00014 University of Helsinki, Finland

INTRODUCTION

The composition of sedimentary rocks is controlled by tectonism, provenance, weathering, transportation, sorting and diagenesis. Sorting is important since muds tend to show more severe weathering and are commonly higher in most trace elements than their associated sands (e.g. Sawyer 1986, McLennan et al. 1990). Evolution and progressive erosion of the source areas is visible in the upward variation of individual successions (Ojakangas 1968, van de Kamp & Leake 1985). Tectonism is a fundamental control of sedimentation and, accordingly, the compositions of modern graywackes are strongly influenced by the tectonic setting of depositional basin and provenance (Dickinson & Suczek 1979, Valloni & Maynard 1981, McLennan et al. 1990). Compositional characteristics can therefore be used to infer the tectonic setting and provenance of ancient sedimentary rocks (e.g. Bhatia

1983, Bhatia & Crook 1986, Roser & Korsch 1986) and they are also useful in constraining the evolution of continental crust through geological time.

The main purpose of this study is to present the compositional characteristics and variation of the predominantly turbiditic metasedimentary rocks of the Paleoproterozoic Tampere Schist Belt (TSB). In addition, we examine geochemical methods for discrimination of tectonic setting of young turbidite sands and sandstones, and apply them to the TSB graywackes. In our data, 72 samples are from two profiles: the Näsijärvi profile on the eastern shore of Lake Näsijärvi and the Pulesjärvi profile 10-15 km east of the former. In addition, 18 samples from dispersed localities in the TSB are compared with the data from these profiles.

TAMPERE SCHIST BELT

The Tampere Schist Belt (Fig. 1) is a Paleoproterozoic volcanic-sedimentary belt mainly com-

posed of turbidite metasedimentary and mafic to felsic arc-type metavolcanic rocks (Ojakangas 1986,

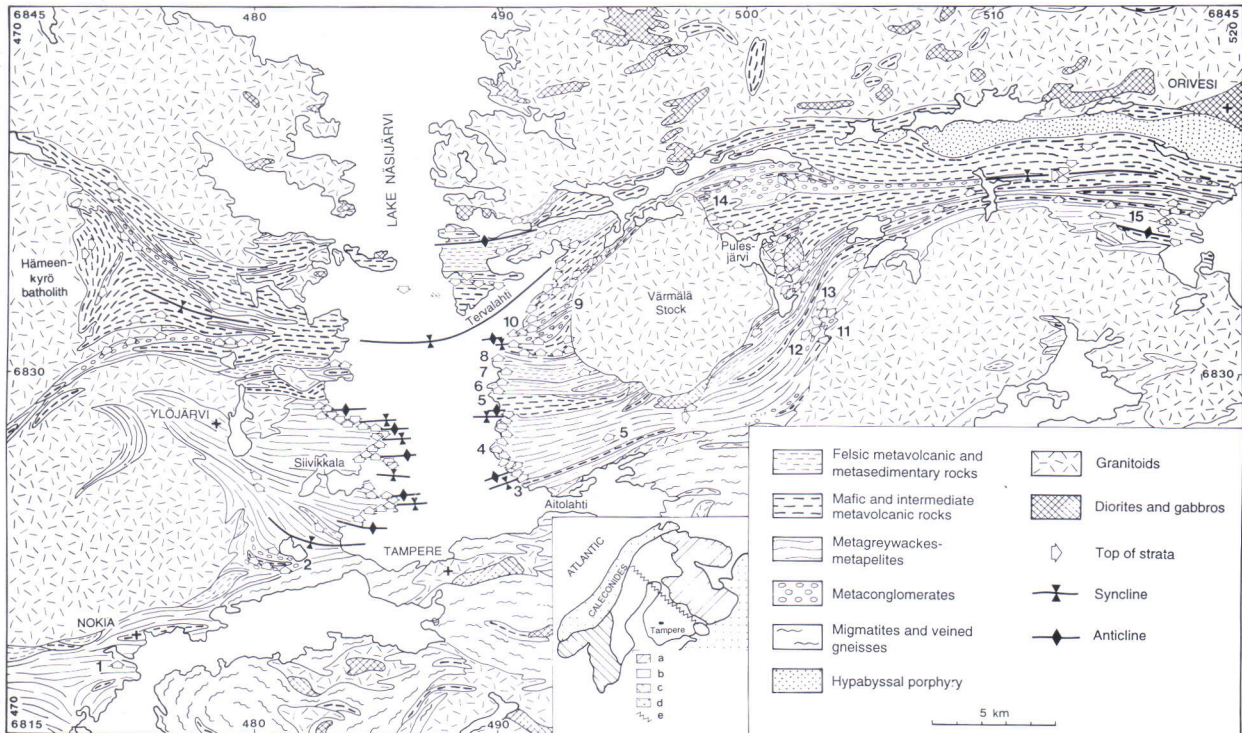


Fig. 1. Lithological map of the Tampere Schist Belt with top of strata observations and a simplified structural interpretation. Numbers 1-15 indicate important localities referred in the text: 1 = Vihola, 2 = Tohloppi, 3 = Kiviranta, 4 = Myllyniemi, 5 = Pirttiniemi, 6 = Tuuliniemi, 7 = Pylsynlahti, 8 = Tervakivi, 9 = Kolunkylä, 10 = Kisala, 11 = Viinaränninnotko, 12 = Ahvenlammi, 13 = Talvineva, Pynnölänkangas and Multivuori, 14 = Pohtola, 15 = Karppi. Puolamäki is situated ca. 1 km N of Multivuori. Slightly modified from Kähkönen (1989). The inset shows the location of the Tampere Schist Belt in the Svecofennian Domain: a = Archean, b = Svecokarelian, c = Post-Svecokarelian (Precambrian), d = Phanerozoic, e = boundary between the Svecofennian and Karelian Domains.

Kähkönen 1987, 1989). Metamorphism in the TSB culminated in low pressure conditions near the amphibolite-greenschist facies transition. (Since this study is concerned with the primary composition of supracrustal rocks, the names of the rock types are written from here on without the prefix meta-.) The volcanic rocks of the TSB have U-Pb zircon ages of 1.905-1.89 Ga (Kähkönen et al. 1989). The detrital zircons in the graywackes are mostly slightly older, ca. 1.91-2.0 Ga, and partly Archean (Huhma et al. 1991). Near Tampere, the TSB comprises a large F_1 syncline with an E-W trending subvertical axial

plane and subhorizontal axis (Kähkönen 1989, Nironen 1989). According to Simonen (1953), the lowermost unit consists of more than 3 km of graywackes and mudstones. It is overlain by felsic volcanic and sedimentary rocks and then by intermediate to mafic volcanic rocks. Conglomerates characterize the next unit and are overlain by mafic volcanic rocks. In addition, the Osara turbidites at Viljakkala, 35 km NW of Tampere, are underlain by the pillow-basalt bearing Haveri Formation (Mäkelä 1980, Kähkönen & Nironen, this volume).

STRATIGRAPHY OF THE NÄSIJÄRVI AND PULESJÄRVI PROFILES

A tentative stratigraphic division of the Näsijärvi and Pulesjärvi profiles is given in Table 1. Deformation and faults make the interpretation in places problematic. The pronounced deformation at Kiviranta, Pylsynlahti, Multivuori and Rukoijylhänotko (a valley southeast of Multivuori) are attributable to faults and shear zones, and they cause breaks in the succession. In the southernmost part of the Näsijärvi profile, the stratigraphic position of the Kiviranta succession is problematic (see Kähkönen, this volume). The structure is complex in the southern part of the Pulesjärvi profile but a minor anticline is present near Viinaränninnotko. Since the lithologies of the southern and northern limbs of this anticline are contrasting, faults in the hinge zone are implied. South-dipping subvertical reverse faults are suggested by Kähkönen (this volume). This would mean that the Viinaränninnotko volcanic and sedimentary rocks in the southern limb of the minor anticline are stratigraphically below the Ahvenlammi member of the Myllyniemi formation in the northern limb. The exact boundary between the Viinaränninnotko succession and the Ahvenlammi member is obscure.

The deformation also makes the estimation of the unit thickness difficult in certain locations. This

concerns particularly the Kupinniemi and Pynönlänkangas members and the Tuuliniemi formation (Table 1) which are dominated by mudstones. However, the 2-2.5 km estimated thicknesses for the Pulesjärvi and Kolunkylä successions are not complicated by deformation. The total thickness of the succession in the Näsijärvi profile is approximated to be close to 7 km (see also Simonen 1953). Pronounced deformation and intrusions make the succession considerably thinner in the Pulesjärvi profile.

Most of the sediment-dominated southern part of the Pulesjärvi profile is included into the Myllyniemi formation. The successions at Tervakivi and Puolamäki are similar since they, at both localities, comprise the lower volcanic member with feldsparphyric high-K rhyolite and the upper, graywacke-dominated sedimentary member in which the graywackes become more mafic upward (Appendix). Therefore, the strata at Puolamäki are included in the Tervakivi formation. The lower parts of the Pulesjärvi volcanic and sedimentary rocks are probably lateral equivalents of the lower parts of the Kolunkylä volcanic and sedimentary rocks but the upper parts of these successions are more difficult to correlate at the moment.

Table 1. Tentative stratigraphic division of the Näsijärvi and Pulesjärvi profiles. Based on Seitsaari (1951), Simonen and Kouvo (1951), Ojakangas (1986), Rautio (1987), Leveinen (1990), and data of Y. Kähkönen. The predominating rock types are given for each unit. The Kiviranta succession, south of Myllyniemi, is not included because of the problems discussed in Kähkönen (this volume).

NÄSIJÄRVI PROFILE

Kolunkylä sedimentary and volcanic rocks (2 - 2.5 km)
- conglomerates, graywackes, mudstones and various volcanic rocks

Tervakivi formation (ca. 300 m)
- thinly to medium bedded graded graywackes (ca. 250 m)
- volcanics with a feldspar-phyric high-K rhyolite (ca. 20 m)

Pylsynlahti schists (ca. 800 m, pronounced deformation)

Tuuliniemi formation (400 - 700 m, folding)
- mudstones

Pirttiniemi formation (ca. 400 m)
- intermediate volcanic rocks

Myllyniemi formation (1.5 - 2 km)
- **Kupinniemi** member (0.5 - 1 km, folding)
mudstones, few thinly to medium bedded graywackes
rare volcanic rocks
- **Jukonniemi** member (500 - 600 m)
medium to thickly bedded graywackes, and mudstones
- **Alasenlahti** member (ca. 200 m)
medium to thickly bedded graywackes, and mudstones
- **Vaarinniemi** member (ca. 150 m)
mudstones and thinly to medium bedded graywackes

--- pronounced deformation

PULESJÄRVI PROFILE

Pohtola volcanic and sedimentary rocks (mostly gentle dips)
- volcanic rocks, conglomerates, graywackes and mudstones

--- profile continues ca. 2 km west, at Pohtola

Pulesjärvi volcanic and sedimentary rocks (2 - 2.5 km)
- mafic to intermediate Pl±Ur-phyric volcanic rocks
separated by five 10 - 70 m thick sedimentary units of graywackes
and conglomerates

Tervakivi formation at Puolamäki (ca. 0.5 km)
- thinly to medium bedded graded graywackes (ca. 400 m)
- feldspar-phyric high-K rhyolite (50 m)

--- 200 - 300 m with poor exposure

Multivuori schists (ca. 400 m, noncoherent)
- mudstones and intermediate volcanic rocks, divided
into two parts by felsic schists and mylonite

--- fault at Rukojiyhännotko

Myllyniemi formation in the Pulesjärvi profile
(ca. 1 km, folding, tops mostly to the northwest)
- **Pynnölänkangas** member (0.5 - 0.7 km, folding)
mudstones and fine-grained graywackes
- **Talvineva** member (ca. 200 m)
very thickly to medium bedded graywackes
- **Ahvenlammi** member (ca. 100 m)
non-stratified or graded clast-supported pebbly gravels

--- break due to folding and faulting

Viinaränninnotko volcanic and sedimentary rocks
(200 - 300 m, top of strata to the south)
- mudstones
- mafic volcanic rocks (ca. 35 m)
- very thickly bedded pyroclastic rocks (ca. 35 m)
- mudstones and thinly bedded graywackes, in part tuffaceous

SEDIMENTARY ENVIRONMENTS

According to Ojakangas (1986), the TSB sedimentary rocks are mostly mid-fan turbidites of a submarine fan deposited in a forearc basin. Paleocurrent data suggest that the dominant sources were located to the east and southeast (Ojakangas 1986, Rautio 1987, Leveinen 1990). The conglomerate-dominated strata of the Ahvenlammi member are submarine channel or canyon deposits (Leveinen 1990). They represent more proximal environments than the other parts of the Myllyniemi formation.

Rautio (1987) interpreted the Kolunkylä sedimentary rocks as submarine mid-fan, upper fan and channel deposits. Since the Pulesjärvi sedimentary rocks are characterized by well-rounded, clast-supported, strongly channelized conglomerates and cross-bedded graywackes they probably resulted from tractional processes (Leveinen 1990). This Pulesjärvi succession, 2-2.5 km thick, contains a possible welded ignimbrite but no pillow lavas. The depositional environment of the Pulesjärvi sedimentary rocks was

probably fluvial. Together, the volcanic-rich uppermost parts of the study profiles represent a change from submarine to partly subaerial environments on the slopes of a volcanic apron. Considering the interpreted fluvial (at Pulesjärvi) vs. submarine (at Kolunkylä) environments and the observed paleocurrent trends, it is evident that the succession at

Pulesjärvi was deposited higher on the apron than the succession at Kolunkylä.

We also present data from the Mauri arkose, 25-40 km west of Tampere. Matisto (1968) suggested a fluvial-deltaic environment for this unit, but its stratigraphic position is not well known.

ANALYTICAL METHODS

Most of the analyses were carried out on pressed rock powder briquettes with a Philips PW 1400/AHP XRF instrument at the Research Centre of Rautaruukki Company (Ala-Vainio 1986). Two samples were analyzed with a Philips 1480 XRF instrument at the Geological Survey of Finland. For five samples the determinations, including La, were made by Dr. Antti Vuorinen with a Jobin Yvon 70+ ICP-AES

instrument at the Department of Geology, University of Helsinki. Three samples were checked by Dr. Tim Brewer with a XRF instrument at the University of Nottingham. Rare earth elements, Ta, Hf and Th were determined by the instrumental neutron activation method at the Technical Research Centre of Finland (Rosenberg et al. 1982). The results are given in Tables 2 and 3.

RESULTS

The TSB sedimentary rocks vary widely in their chemical composition. This is in part attributed to sorting and grain-size effects, but there is also significant variation according to the stratigraphic position. This variation reflects differences in the character of source areas.

The SiO₂ contents of the TSB graywackes vary from 53% to 80% (Fig. 2, Table 2). The CIA values (chemical index of alteration, Nesbitt & Young 1982) range between 33 and 61, mostly between 50 and 60. Note that the lowest CIA values are not due to carbonate but come from mafic graywackes rich in pseudomorphs after clinopyroxene clasts. The conglomerate samples (526a-YK/89, 21-22-Ahv/85) are largely similar to their associated graywackes. In general, the mudstones are lower in SiO₂ and Na₂O than the graywackes (the mafic graywackes excluded), and their Al₂O₃, TiO₂, FeO, K₂O, Ni and Zn contents and CIA values are mostly higher. When compared with rocks with similar SiO₂ contents, the mudstones tend to have higher Al₂O₃, K₂O and CIA, and lower MnO, CaO, P₂O₅, Sr and Zr than the graywackes. The effects of grain size and sorting are also shown by the siltstones and mudstone-graywacke mixtures; these rocks are intermediate between the clayey mudstones and high-Si graywackes. On the other hand, the graywackes with ca. 60-68% SiO₂ tend to comprise a group between the mafic graywackes and high-Si graywackes.

Pronounced recrystallization in the Pulesjärvi profile makes it difficult to petrographically distinguish between clayey and silty mudstones, but the clayey mudstones proper from the Näsijärvi profile have SiO₂ of ca. 60-64% (volatile-free basis), Al₂O₃ of 17 to 21%, K₂O:Na₂O ratios of 1.5 to 5, and CIA values of 59 to 69. Among the mudstones, the sensitivity of CIA indices, of K₂O/Na₂O ratios and of SiO₂ contents, to grain size is shown by the Jukonniemi and Tuuliniemi siltstones. These siltstones tend to have lower Al₂O₃, CIA and K₂O/Na₂O, and higher SiO₂ than the associated clayey mudstones (Table 2).

Some of the rocks studied which are mudstones in grain size are tuffs rather than epiclastic rocks. In the Näsijärvi profile, sample 532-YK/89 (poor in micas, contains possible shards and a few oversized Pl-clasts) is a good example. It is higher in silica (73% SiO₂) and has a CIA value of 52, lower than the distinctly epiclastic mudstones which typically have ca. 60% SiO₂ and CIA values of ca. 56-68. In the Pulesjärvi profile, the fine-grained felsic sample Tre 85 is also considered tuff rather than epiclastic according to its petrography, high silica contents and low CIA value (Table 2).

The chondrite-normalized REE patterns of the TSB sedimentary rocks show enrichments of LREE over HREE (La_N:Yb_N mostly 8-14) and the HREE patterns are flat or gently sloping (Tb_N:Yb_N mostly 1.1-1.5; Fig. 3; Table 3). The Eu/Eu* values range

Table 2. Major and trace element data for the sedimentary rocks of the Tampere Schist Belt. Rock types: cgl = conglomerate, cgr = coarse-grained graywacke, gr = graywacke, fgr = fine-grained graywacke, am-gr = amphibole-bearing graywacke, sm = silty mudstone, m = mudstone, cm = clayed mudstone, ftm = felsic tuffaceous mudstone. Oxides in weight%, trace elements in ppm. Total Fe as FeO. XRF analyses mostly by Rautaruukki, (GSF) by Geological Survey of Finland, (Br) by Tim Brewer. (UH) indicates analyses made by ICP-AES at the Department of Geology, University of Helsinki. In the Näsijärvi and Pulesjärvi profiles, the samples are arranged according the stratigraphic position from the bottom to the top.

NÄSIJÄRVI PROFILE												
MYLLYNIEMI FORMATION												
rock type	Vaarinniemi				Alasenlahti							
	1-B- YK/91 (UH)	1-Bm- YK/91 (UH)	4- YK/91 (UH)	46- RWO/82 gr	10- YK/91 (UH)	11- YK/91 (UH)	1- YKÄ/84 gr	1- YKÄ/84 gr	525- YK/89 cm (GSF)	2- YKÄ/84 gr	501- YKÄ/88 gr	501- YKÄ/88 gr (Br)
SiO ₂	60.81	65.43	61.65	63.90	75.17	73.96	74.76	76.37	58.89	79.16	76.90	76.46
TiO ₂	0.71	0.63	0.80	0.57	0.56	0.46	0.43	0.35	0.77	0.24	0.32	0.42
Al ₂ O ₃	20.39	15.61	15.15	14.20	11.28	12.30	12.68	11.56	18.54	9.93	10.30	11.10
FeO	3.94	5.76	8.04	5.05	4.51	3.69	3.06	2.44	6.73	2.23	2.23	3.46
MnO	0.07	0.08	0.10	0.06	0.04	0.03	0.04	0.03	0.05	0.03	0.03	0.03
MgO	1.59	2.30	3.09	2.05	1.40	1.40	1.32	1.05	2.65	0.94	0.84	1.41
CaO	4.21	1.47	2.00	1.68	1.42	0.77	0.72	0.81	0.70	0.93	0.96	0.71
Na ₂ O	5.18	2.29	2.82	3.40	2.95	2.45	2.32	2.73	1.62	2.66	2.88	2.42
K ₂ O	1.69	3.17	3.38	2.51	1.58	2.74	2.76	2.27	5.34	1.62	1.63	2.44
P ₂ O ₅	0.24	0.10	0.17	0.20	0.01	0.11	0.14	0.12	0.15	0.09	0.14	0.07
sum	98.83	96.84	97.20	93.62	98.92	97.91	98.23	97.73	95.44	97.83	96.23	98.52
S							0.02		0.27		0.01	
C												
CIA	53.08	61.23	55.90	55.52	55.20	59.40	60.95	57.83	65.57	55.92	55.51	58.35
K ₂ O:Na ₂ O	0.33	1.38	1.20	0.74	0.54	1.12	1.19	0.83	3.30	0.61	0.57	0.74
Zr	232	163	283	180	272		210	200	192	150	200	213
Ni				20			30	30	40	20	20	25
Sr	440	169	244	210	174	96	100	110	115	120	200	147
Ba	374	944	750	450	2350	530	640	520	1093	330	290	490
V	72	86	166	100	99		80	60	186	40	50	55
Zn	68	92	122	80	79	64	40	40	126	40	50	64
Cu				30			10	10	80	20	0	6
Y									23			16

NÄSIJÄRVI PROFILE																	
MYLLYNIEMI FORMATION																	
rock type	Jukonniemi												Kupinniemi				
	502- YKÄ/88 gr (GSF)	503- YKÄ/88 gr	504- YKÄ/88 gr	526a- YK/89 cgl/cgr	524- YK/89 cm	527- YK/89 cm	528- YK/89 sm/fgr	531- YK/89 gr	531- YK/89 gr (Br)	505- YKÄ/88 gr	506- YKÄ/88 gr	533- YK/89 fgr	532- YK/89 ftm	507- YKÄ/88 gr	508- YKÄ/88 gr	509- YKÄ/88 gr	534- YK/89 cm
SiO ₂	65.54	71.30	67.80	75.30	61.70	61.60	68.00	69.10	70.69	70.90	68.00	71.10	70.30	71.70	64.80	68.50	57.50
TiO ₂	0.64	0.48	0.49	0.31	0.71	0.71	0.58	0.57	0.60	0.57	0.66	0.62	0.44	0.52	0.71	0.59	0.75
Al ₂ O ₃	16.42	13.90	14.40	11.90	18.70	19.40	16.10	13.90	13.02	12.50	12.20	13.60	13.10	13.20	15.60	14.90	20.90
FeO	4.71	3.82	3.63	2.16	5.84	5.96	4.50	4.39	4.73	4.67	5.20	3.33	4.00	3.35	5.75	4.38	6.74
MnO	0.06	0.04	0.06	0.05	0.05	0.05	0.04	0.06	0.04	0.03	0.06	0.05	0.07	0.04	0.06	0.06	0.05
MgO	1.89	1.43	1.40	0.78	2.84	2.07	1.70	1.89	2.05	1.44	2.08	0.93	1.30	1.17	1.68	1.56	2.60
CaO	1.02	1.08	1.85	2.52	0.45	0.93	1.20	1.10	1.16	1.79	1.40	2.31	2.63	1.26	3.06	2.67	0.81
Na ₂ O	2.71	2.37	4.14	3.26	1.38	1.24	1.48	2.88	2.81	3.34	3.03	3.99	3.12	2.46	3.88	3.50	1.43
K ₂ O	4.02	3.30	2.05	0.85	5.15	5.91	4.33	3.17	2.97	1.94	2.41	1.58	1.66	2.53	2.12	2.12	5.44
P ₂ O ₅	0.17	0.16	0.19	0.21	0.16	0.11	0.14	0.18	0.14	0.28	0.20	0.28	0.11	0.17	0.26	0.23	0.10
sum	97.18	97.89	96.02	97.35	96.98	97.98	98.07	97.23	98.21	97.47	95.23	97.80	96.72	96.40	97.92	98.52	96.33
S	0.03	0.10		0.07	0.08	0.01	0.01	0.03	0.05	0.02		0.00	0.19		0.37	0.04	0.04
C				0.45	0.38		0.48			0.51	0.59						
CIA	60.59	59.54	53.72	52.25	68.30	65.66	63.34	57.72	56.66	53.51	54.59	52.13	52.77	59.23	52.25	53.56	68.23
K ₂ O:Na ₂ O	1.48	1.39	0.50	0.26	3.73	4.77	2.93	1.10	1.06	0.58	0.80	0.40	0.53	1.03	0.55	0.61	3.80
Zr	281	180	200	170	150	160	170	210	211	260	320	230	130	230	270	190	160
Ni	31	30	30	20	70	50	40	40	28	20	30	20	30	30	30	20	40
Sr	211	190	400	400	100	150	190	230	233	280	270	360	290	290	620	430	200
Ba	1144	670	410	370	1150	850	580	750	812	210	360	310	270	580	300	290	880
V	119	70	80	50	150	150	90	90	89	100	140	80	80	90	140	100	160
Zn	87	80	70	50	130	80	70	70	65	70	100	70	90	80	110	60	110
Cu	13	2	0	10	60	30	10	20	23	30	10	0	40	0	80	40	100
Y	26								22								

Table 2. (cont.)

NÄSIJÄRVI PROFILE															
rock type	TUULINIEMI FORMATION			TERVAKIVI FORMATION									KOLUNKYLÄ		
	535- YK/89 sm	537- YK/89 cm	540- YK/89 sm	541- YK/89 m	511- YK/89 gr	513- YK/89 gr	514- YK/89 gr	514- YK/89 gr (Br)	515- YK/89 gr	517- YK/89 gr	518- YK/89 gr	519- YK/89 gr	520- YK/89 am-gr	2- Kisala m	1- Kisala m
SiO ₂	65.10	60.50	60.00	62.90	67.20	64.60	65.40	66.94	67.40	67.50	65.80	65.50	61.90	60.30	61.30
TiO ₂	0.57	0.69	0.63	0.64	0.59	0.71	0.68	0.80	0.60	0.52	0.63	0.62	0.73	0.68	0.68
Al ₂ O ₃	16.80	20.30	16.70	16.80	14.80	14.40	14.40	13.91	14.50	14.40	15.60	15.10	14.00	18.30	17.80
FeO	4.89	5.80	6.78	5.83	4.95	5.80	5.43	6.11	4.93	4.26	5.24	5.06	7.08	6.45	6.07
MnO	0.06	0.06	0.10	0.06	0.05	0.07	0.07	0.18	0.05	0.07	0.06	0.05	0.10	0.06	0.06
MgO	2.07	2.34	2.85	2.56	2.00	2.25	1.94	2.13	1.88	1.47	1.98	2.04	4.02	2.65	2.56
CaO	1.48	1.46	2.58	1.44	1.81	3.30	2.99	2.82	1.27	2.91	1.47	1.93	3.58	1.73	1.85
Na ₂ O	2.92	2.45	3.31	1.99	2.40	2.88	3.44	3.17	2.03	3.48	2.29	2.84	2.58	2.27	2.60
K ₂ O	3.54	4.15	3.10	4.72	3.30	2.39	2.43	2.49	3.75	2.04	3.88	3.13	2.12	4.71	4.26
P ₂ O ₅	0.13	0.12	0.16	0.26	0.22	0.24	0.24	0.18	0.20	0.23	0.22	0.24	0.26	0.25	0.28
sum	97.56	97.88	96.21	97.20	97.33	96.65	97.02	98.73	96.60	96.89	97.18	96.51	96.37	97.39	97.46
S	0.01	0.01	0.00	0.01	0.01	0.01	0.01	0.01	0.01	0.05	0.01	0.00	0.00	0.04	0.07
C															
ClA	59.70	64.46	55.28	60.39	57.75	51.91	51.17	51.59	59.86	52.10	59.42	56.59	51.73	60.40	59.20
K ₂ O:Na ₂ O	1.21	1.69	0.94	2.37	1.38	0.83	0.71	0.79	1.85	0.59	1.69	1.10	0.82	2.07	1.64
Zr	180	130	160	150	170	180	180	201	160	140	170	170	140	160	160
Ni	40	50	50	50	30	30	30	26	20	20	30	30	40	50	50
Sr	230	250	310	300	340	460	420	410	270	470	290	380	500	320	380
Ba	810	900	350	920	670	620	540	621	870	410	1050	740	470	1060	1000
V	80	130	100	110	110	140	120	112	110	100	120	100	180	130	140
Zn	90	110	120	120	90	90	100	94	90	70	90	80	110	120	120
Cu	10	30	10	10	60	20	20	23	30	50	10	20	40	50	70
Y								20							

PULESJÄRVI PROFILE																					
rock type	MYLLYNIEMI FORMATION								Talvineva				Pynnölänkangas								
	Viinaränninnotko		Ahvenlammi		14- Ahv/85	16- Ahv/85	1- Ahv/84	21- Ahv/85	22- Ahv/85	23- Ahv/85	24- Ahv/85	Tre 53	Tre 59	Tre 60	Tre 61	Tre 62	Tre 77H	Tre 77S	Tre 76H	Tre 76S	
	gr	gr	gr	cgl	cgl/cgr	cgr	gr	gr	gr	gr	gr	cgr	gr	gr	sm	gr	m+fgr	gr	m		
SiO ₂	69.57	70.32	73.72	74.54	74.84	72.63	73.93	71.50	70.60	70.00	70.00	63.10	74.00	66.90	67.10	56.30					
TiO ₂	0.46	0.57	0.42	0.37	0.36	0.36	0.45	0.45	0.51	0.45	0.41	0.61	0.47	0.55	0.67	0.71					
Al ₂ O ₃	14.58	13.33	11.49	11.11	11.10	12.00	11.78	11.20	11.30	12.80	12.80	15.00	11.30	14.90	13.00	18.30					
FeO	3.57	4.77	3.61	3.97	3.49	3.58	3.96	3.42	3.91	3.84	3.19	4.92	2.82	3.98	4.84	5.98					
MnO	0.07	0.09	0.04	0.08	0.07	0.06	0.07	0.06	0.06	0.07	0.06	0.07	0.03	0.04	0.06	0.07					
MgO	0.99	1.24	1.41	1.24	1.21	1.55	1.65	1.58	1.79	1.79	1.71	2.72	1.16	1.78	1.99	2.48					
CaO	1.90	2.10	1.14	1.92	1.25	1.67	1.76	1.96	2.00	1.36	2.12	1.73	1.57	1.24	1.97	2.55					
Na ₂ O	3.87	3.36	3.00	2.31	2.39	2.68	2.29	2.77	2.85	2.28	3.73	2.86	2.56	1.91	2.88	3.50					
K ₂ O	2.43	2.21	2.38	2.65	3.55	3.22	3.17	2.18	1.91	2.97	1.66	3.39	1.85	3.52	2.40	3.47					
P ₂ O ₅	0.17	0.18	0.14	0.25	0.23	0.17	0.15	0.16	0.20	0.18	0.18	0.25	0.13	0.12	0.19	0.13					
sum	97.61	98.17	97.35	98.44	98.49	97.92	99.21	95.28	95.14	95.73	95.86	94.65	95.90	94.94	95.09	93.49					
S							0.01	0.05	0.01	0.01	0.01	0.00	0.00								
C																					
ClA	53.91	53.15	54.50	52.20	52.46	52.30	53.08	51.63	52.06	57.53	52.03	56.53	55.45	61.77	54.32	56.36					
K ₂ O:Na ₂ O	0.63	0.66	0.79	1.15	1.49	1.20	1.38	0.79	0.67	1.30	0.45	1.19	0.72	1.84	0.83	0.99					
Zr	160	190	200	150	170	180	240	260	250	180	170	160	230	180	350	200					
Ni	0	10	20	20	20	30	30	30	20	30	30	30	30	40	30	40					
Sr	380	370	130	160	140	160	140	170	250	180	260	240	280	220	340	450					
Ba	1040	550	510	880	770	720	750	440	310	920	290	730	390	890	440	760					
V	90	120	70	70	70	70	90	80	80	80	70	90	80	90	120	140					
Zn	70	90	50	40	40	50	40	40	60	60	50	80	60	90	110	130					
Cu	10	10	0	30	10	20	0	0	20	0	0	0	0	0	0	0					

Table 2. (cont.)

PULESJÄRVI PROFILE																
rock type	MULTIVUORI			TERVAKIVI FORMATION at Puolamäki						PULESJÄRVI						
	Tre 82 fgr+m	51-JEL/86 sm/fgr	Tre 85 ftm	Tre 103 gr	79-IV- JEL/86 gr	80-III-A- JEL/86 gr	80-III-B- JEL/86 gr	80-V- JEL/86 gr	81- JEL/86 am-gr	Tre 112 am-gr	Tre 149 am-gr	Tre 149B am-gr	Tre 192 am-gr	Tre 217 am-gr	Tre 262 am-gr	Tre 266 am-gr
SiO ₂	66.50	63.15	70.90	65.50	64.28	63.98	65.08	62.34	58.86	51.80	51.60	50.90	53.30	50.20	58.10	50.80
TiO ₂	0.48	0.54	0.12	0.51	0.69	0.68	0.66	0.67	0.90	0.90	0.62	0.70	0.44	0.61	0.63	0.61
Al ₂ O ₃	14.00	15.97	13.60	14.90	14.44	15.82	13.56	15.20	14.51	14.60	10.50	13.50	17.50	15.10	15.30	13.00
FeO	4.05	5.27	1.43	4.56	6.40	5.92	6.08	6.52	8.44	9.24	9.29	9.24	5.93	8.46	6.91	9.67
MnO	0.05	0.06	0.07	0.05	0.08	0.07	0.08	0.09	0.12	0.15	0.21	0.18	0.11	0.20	0.13	0.20
MgO	1.81	2.53	0.23	1.68	2.33	2.19	2.23	3.00	4.23	5.73	9.03	6.79	6.08	7.08	5.42	8.38
CaO	1.99	1.48	1.78	3.44	3.72	1.73	4.39	3.92	4.79	4.96	9.41	6.78	6.50	8.02	4.54	6.77
Na ₂ O	3.70	4.56	2.46	2.27	2.95	1.51	2.28	2.71	2.34	2.28	1.41	3.51	2.98	2.32	3.65	1.74
K ₂ O	2.11	2.79	5.18	2.44	2.78	4.95	2.59	2.86	2.78	3.36	1.72	2.12	1.79	2.19	1.93	3.48
P ₂ O ₅	0.19	0.17	0.03	0.24	0.27	0.24	0.26	0.33	0.33	0.36	0.23	0.35	0.31	0.51	0.43	0.34
sum	94.89	96.52	95.80	95.59	97.94	97.09	97.21	97.64	97.30	93.38	94.02	94.07	94.93	94.69	97.04	94.98
S	0.00	0.00	0.02	0.06					0.01	0.01	0.00	0.01	0.00	0.00	0.00	
C																
ClA	53.84	54.70	51.30	54.09	49.65	58.97	48.23	50.83	48.20	47.05	32.99	39.79	48.36	42.06	48.31	40.66
K ₂ O:Na ₂ O	0.57	0.61	2.11	1.07	0.94	3.28	1.14	1.06	1.19	1.47	1.22	0.60	0.60	0.94	0.53	2.00
Zr	200	190	170	150	210	200	230	190	220	100	100	100	80	70	110	60
Ni	30	40	10	30	30	40	40	30	30	40	100	70	70	80	60	90
Sr	270	220	290	600	400	120	220	450	270	640	890	880	1350	1230	1030	830
Ba	290	860	720	310	710	1460	490	660	720	920	410	790	1240	700	680	750
V	70	100	10	90	160	140	130	150	220	230	230	250	130	190	160	210
Zn	80	100	40	80	100	100	100	100	120	140	100	100	80	100	100	120
Cu	0	20	0	30	30	20	20	40	50	20	40	10	20	30	0	20

DATA OUTSIDE THE STUDY PROFILES																		
rock type	Pohtola			Vihola		Karpپی			Osara					Tohloppi		Mauri		
	Tre 350 am-gr	Tre 351 m	Tre 352 sm	61-A- RWO/82 gr	2-Vih/84 cgr	1- Karp/84 cgr	2- Karp/84 cgr	4- YKÄ/86 gr	11- YKÄ/86 gr	12-B- YKÄ/86 gr	13-A- YKÄ/86 gr	13-B- YKÄ/86 gr	13-C- YKÄ/86 gr	18- YKÄ/83 gr	5-3- YKÄ/83 m	10-A- YKÄ/86 arkose	10-B- YKÄ/86 arkose	10-C- YKÄ/86 arkose
SiO ₂	54.90	56.20	61.90	71.50	71.06	77.07	75.37	57.78	65.62	69.59	69.08	69.98	71.34	59.94	55.77	74.28	75.93	76.31
TiO ₂	0.77	0.69	0.53	0.50	0.57	0.36	0.40	0.90	0.58	0.45	0.56	0.45	0.41	0.54	0.87	0.37	0.30	0.41
Al ₂ O ₃	14.60	17.70	15.80	12.90	12.64	10.38	10.77	14.59	15.62	13.90	12.82	13.38	13.22	17.60	18.76	13.24	12.97	11.97
FeO	7.86	6.27	5.24	4.16	4.92	3.22	3.19	8.85	5.39	4.04	5.57	3.70	3.45	5.10	7.05	2.86	2.47	2.45
MnO	0.13	0.07	0.06	0.06	0.07	0.07	0.06	0.15	0.06	0.05	0.07	0.05	0.06	0.09	0.06	0.02	0.01	0.02
MgO	4.40	3.16	2.61	1.56	2.06	1.15	1.30	3.46	2.39	1.88	2.47	1.91	1.69	1.85	3.54	0.32	0.29	0.24
CaO	5.19	2.74	1.56	1.84	2.47	1.24	1.70	3.10	1.73	1.75	1.54	2.09	1.67	4.09	2.02	0.37	0.37	0.37
Na ₂ O	3.20	2.60	2.31	3.05	2.64	2.18	3.05	2.16	3.13	2.72	2.78	3.51	2.64	3.70	1.46	1.93	1.95	2.09
K ₂ O	2.06	3.94	4.14	2.39	2.27	2.96	1.63	4.01	3.53	2.97	2.93	2.16	3.52	4.70	6.91	5.54	5.22	4.36
P ₂ O ₅	0.26	0.36	0.29	0.17	0.37	0.11	0.11	0.34	0.19	0.16	0.17	0.18	0.17	0.45	0.48	0.04	0.04	0.04
sum	93.37	93.74	94.44	98.13	99.07	98.74	97.58	95.35	98.24	97.51	97.99	97.41	98.17	98.06	96.92	98.97	99.55	98.26
S	0.01	0.00	0.00	0.13			0.01											
C																		
ClA	46.27	56.65	58.66	54.06	52.79	53.40	52.15	51.85	56.29	56.08	54.84	52.87	54.13	48.57	58.01	57.31	57.60	57.51
K ₂ O:Na ₂ O	0.64	1.52	1.79	0.78	0.86	1.36	0.53	1.86	1.13	1.09	1.05	0.62	1.33	1.27	4.73	2.87	2.68	2.09
Zr	120	170	140	180	240	220	280	250	180	180	220	190	180	220	270	200	200	210
Ni	40	40	30	40	40	20	30	20	50	40	30	20	20	30	50	10	10	10
Sr	770	440	310	240	170	140	140	330	190	180	150	180	150	670	260	80	80	70
Ba	760	830	770	510	370	1020	200	1040	710	670	390	390	970	1140	820	1240	1060	
V	220	140	100	90	110	70	70	180	120	80	120	80	80	100	130	50	50	50
Zn	100	110	90	70	90	50	80	120	90	60	60	60	40	70	110	60	40	40
Cu	50	50	20	30	90	0	0	40	40	30	30	30	20	90	70	10	10	0

Table 3. REE and other trace element data (in ppm) for the sedimentary rocks of the Tampere Schist Belt. Analyses mostly by INAA, La by ICP for the Vaarinniemi samples. Eu* is an approximation based on the Sm-Tb trend of the chondrite-normalized patterns. Rock types as in Table 2.

rock type	MYLLYNIEMI FORMATION										TUULINIEMI FORMATION		
	Vaarinniemi			Alasenlahti		Jukonniemi		Kupinniemi					
	1-B- YK/91 gr	1-Bm- YK/91 sm	10- YK/91 gr	1- YKÄ/84 gr	525- YK/89 cm	502- YKÄ/88 gr	524- YK/89 cm	531- YK/89 gr	508- YKÄ/88 gr	534- YK/89 cm	537- YK/89 cm		
La	32	32	26	18.8	14.6	27.6	24.1	35.6	42.7	26.1	35.4		
Ce				34	25.6	47.2	40.3	51.1	66.6	38.1	50.2		
Nd				17.7	13.7	21.4	20	23.9	33	18.9	21.4		
Sm				3.4	4.17	5.86	4.75	5.3	7.15	4.06	4.69		
Eu				0.76	1.09	1.67	1.04	1.08	1.78	1.1	0.945		
Tb				0.31	0.578	0.615	0.612	0.491	0.734	0.546	0.552		
Yb				1.47	1.88	2.14	2.02	1.68	2.28	2.14	2.03		
La _N :Yb _N				8.42	5.12	8.50	7.86	13.96	12.34	8.03	11.49		
Tb _N :Yb _N				0.92	1.35	1.26	1.33	1.28	1.41	1.12	1.19		
Eu:Eu*				0.81	0.84	1.01	0.72	0.75	0.88	0.91	0.69		
Ta				0.67	1.21	0.968	1.16	0.778	0.92	1.23	1.43		
Hf				5.4	5.2	7.16	4.63	7.17	7.89	4.98	4.26		
Th				9.4	12.9	12	13.6	8.7	11.1	14.1	16.6		

rock type	TERVAKIVI FORMATION				KOLUN- KYLÄ	MYLLYNIEMI FM. at Ahvenlammi and Talvineva		TERVAKIVI FM. at Puolamäki		PULESJÄRVI			OSARA
	541- YK/89 m	513- YK/89 gr	518- YK/89 gr	520- YK/89 am-gr	2- Kisala m	1- Ahv/84 gr	Tre 60 gr	79-IV- JEL/86 gr	81- JEL/86 am-gr	Tre 149 am-gr	Tre 217 am-gr	Tre 262 am-gr	13-A- YKÄ/86 gr
	La	38.4	34	30.6	24.6	38.6	49	8.17	31	30	22.1	22	31.3
Ce	58.4	61	46	40.1	55.9	63	18.2	57	53	35.4	36.7	49.3	107
Nd	27.5	27.8	22.7	18.4	27	15	6.59	29	28	18.7	18.5	23.5	43
Sm	5.65	4.86	5.55	4.27	5.9	2.6	1.23	5.4	5.2	3.69	3.81	5.2	7.5
Eu	1.32	1.21	1.11	1.12	1.28	0.91	0.55	1.33	1.35	1.18	1.36	1.53	1.26
Tb	0.57	0.577	0.53	0.51	0.589	0.28	0.4	0.55	0.57	0.518	0.445	0.569	0.6
Yb	1.83	1.85	1.82	1.62	1.93	1.68	2.16	1.95	1.86	1.34	1.14	1.78	2.4
La _N :Yb _N	13.82	12.11	11.08	10.00	13.17	19.21	2.49	10.47	10.62	10.86	12.71	11.58	18.66
Tb _N :Yb _N	1.37	1.37	1.28	1.38	1.34	0.73	0.81	1.24	1.34	1.69	1.71	1.40	1.10
Eu:Eu*	0.83	0.84	0.72	0.87	0.79	1.12	1.09	0.89	0.92	1.01	1.23	1.03	0.65
Ta	0.908	0.823	0.817	0.718	1.02	0.77	0.866			0.533	0.36	0.67	1.07
Hf	5.78	6.68	5.39	4.48	5.18	3.9	5.28			2.55	1.76	3.2	5.7
Th	8.78	9.95	8.16	6.91	10.7	11.5	18.3			3.47	2.93	4.39	22

mostly from 0.7 to 1.1, but, since the non-smooth patterns may indicate analytical uncertainties, some of these values should be discussed with caution (see p. 134).

We do not have data from true graywacke-mudstone pairs, but the Tervakivi mudstone tends to be higher in REE than the associated graywackes, and the Kisala mudstone from Kolunkylä is higher in most REE than the Pulesjärvi graywackes. This agrees with the typical turbidites in which muds are mostly enriched in REE relative to the associated sands (McLennan et al. 1990). In contrast, the mudstones of the Myllyniemi formation tend to be lower in REE than the associated graywackes. Data from true graywacke-mudstone pairs are needed for further discussion.

The differences and variation trends in Fig. 2 can largely be explained by leaching during weathering, and by mixing and sorting during transportation and deposition. During weathering, Ca, Sr and Mn are

leached into the solutions while Al and K are retained in the clayey products of weathering. The difference in Zr is attributed to detrital zircon in the graywackes. A part of the variation is controlled by stratigraphic position. For instance, the mudstones and graywackes of the Tervakivi formation are higher in P₂O₅ than the typical mudstones and graywackes of the Myllyniemi formation (Figs. 4 and 5). It is also evident that the variation trends in Fig. 2 can largely be explained by the mixing of four major components during sedimentation: (1) clays, (2) a silica- and quartz-rich sand-sized component, (3) an intermediate volcanic component, and (4) a component derived from fairly mafic volcanic rocks. Based on petrography, the silica-rich component comprises felsic volcanics, granitoids, vein quartz, and quartz arenites (Ojakangas 1986, observations by the authors). The mafic volcanic component, prominent in the Pulesjärvi graywackes, is rich in K₂O and Sr and thus has shoshonitic characteristics.

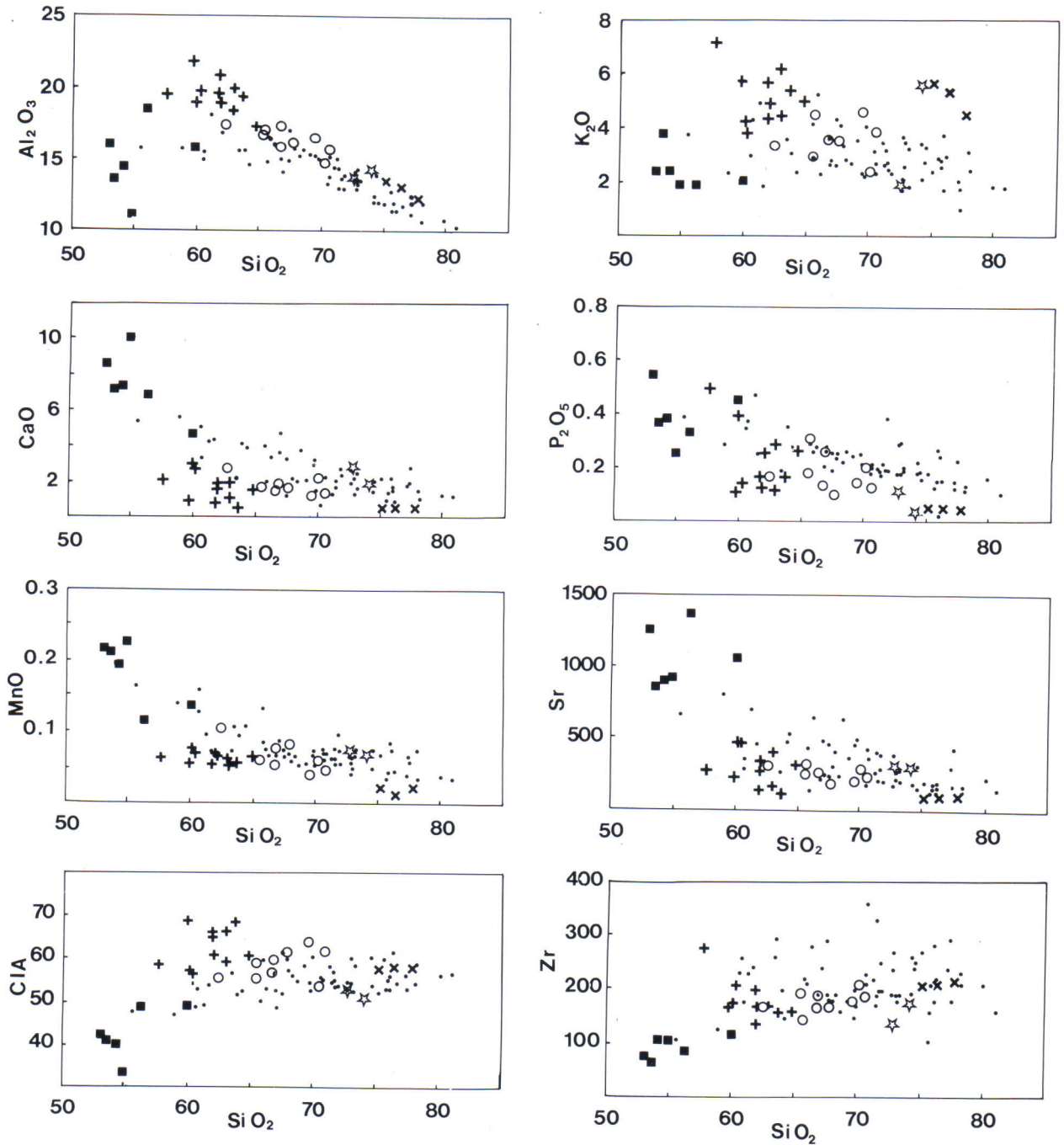


Fig. 2. Selected Harker diagrams of the TSB sedimentary rocks. Data from Table 2. Dots = graywackes and conglomerates in general, closed squares = Pulesjärvi graywackes, crosses = mudstones in general, open circles = silty mudstones and transitional or mixed mudstones - fine-grained graywackes, stars = felsic tuffaceous mudstones, inclined crosses = Mauri arkoses.

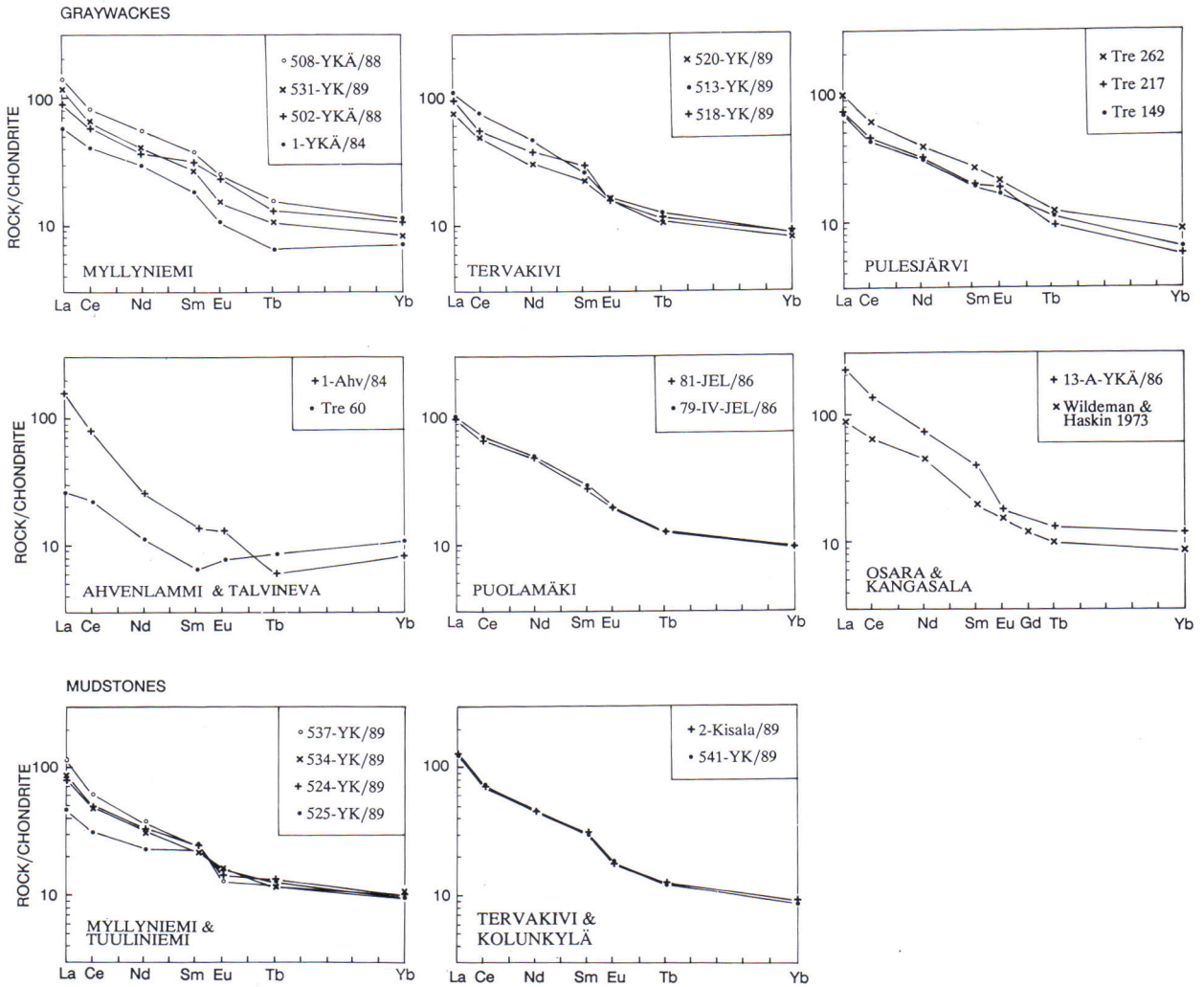


Fig. 3 Chondrite-normalized REE diagrams of the Tampere graywackes and mudstones. Chondrite values: Leedey-6 divided by factor 1.2 (Jahn et al. 1980, Tb from Koljonen & Rosenberg 1975). Sample 13a-YK-/86 is from the Osara Formation ca. 35 km NW from Tampere. The sample of Wildeman & Haskin (1973) is from the area of migmatites and veined gneisses south of the TSB.

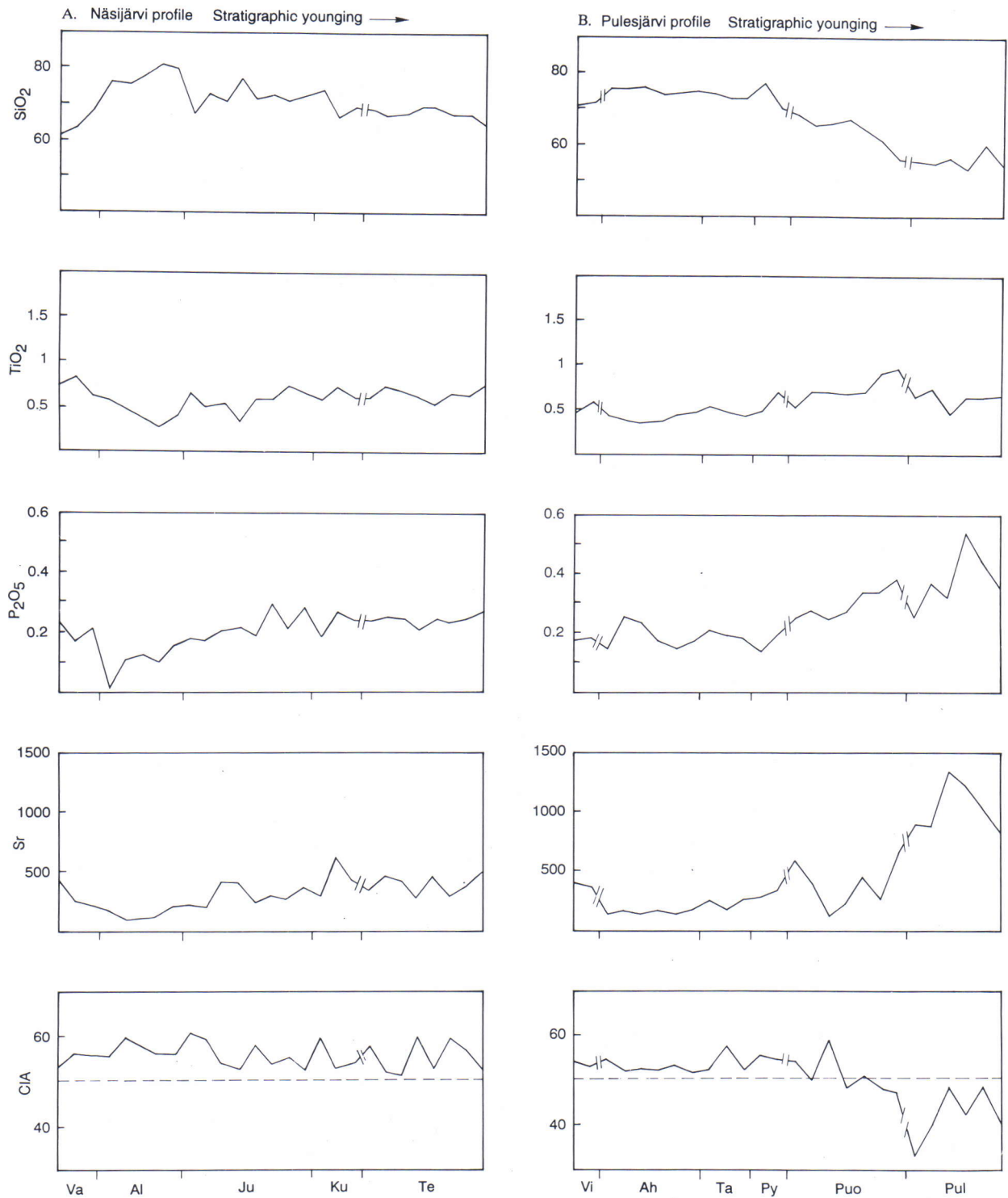


Fig. 4. Upward variation in the composition of the graywackes of the Näsijärvi and Pulesjärvi profiles. The distances between sample points not to true scale. Data from Table 2. Note that in the calculations for the CIA values, no corrections for carbonate and apatite were made. However, since the contents of P and C are low (Table 2) and since carbonate is generally absent or a minor component, the error is not severe. For the samples analyzed twice the diagrams show the analyses by Rautaruukki, and for sample 1-YKÄ/84 the second analysis is used. Oxides recalculated to 100%. Units and localities: Va = Vaarinniemi, Al = Alasenlahti, Ju = Jukonniemi, Ku = Kupinniemi, Te = Tervakivi, Vi = Viinaränninnotko, Ah = Ahvenlammi, Ta = Talvineva, Py = Pynnölänkangas, Puo = Puolamäki, Pul = Pulesjärvi.

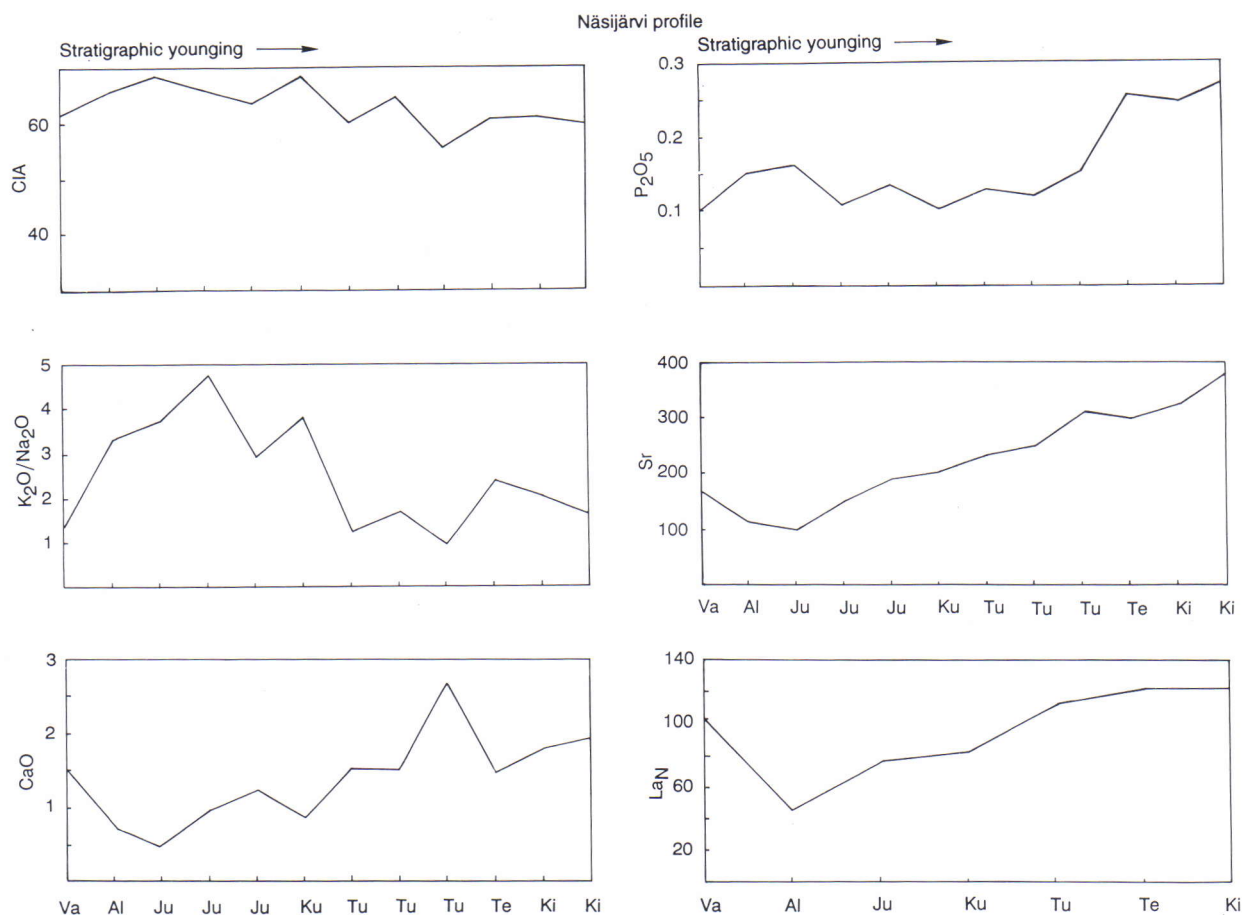


Fig. 5. Upward variation in the composition of mudstones of the Näsijärvi profile. The distances between the samples not to true scale. Oxides recalculated to 100%. Data from Tables 2 and 3. La_N is the chondrite-normalized value of La (Fig 3). Units and localities: Va, Al, Ju, Ku, Te as in Fig. 4. Tu = Tuuliniemi, Ki = Kisala from Kolunkylä.

VARIATION IN COMPOSITION WITH STRATIGRAPHIC POSITION

The chemical composition of the sedimentary rocks of the Näsijärvi and Pulesjärvi profiles varies according to stratigraphic position. In the graywackes, the contents of SiO₂, TiO₂, P₂O₅ and Sr show quite

systematic trends (Fig. 4). The CIA value also shows certain, although minor and fluctuating, variation. In addition, rather consistent variations are observed in the mudstones of the Näsijärvi profile.

Graywackes

In the Näsijärvi profile, the Vaarinniemi graywackes are lower in SiO₂ but higher in TiO₂, P₂O₅ and Sr than the overlying Alasenlahti graywackes (Fig. 4). Upward from Alasenlahti, the graywackes show a general decrease in SiO₂ and increases in TiO₂, P₂O₅ and Sr. The CIA trend fluctuates but, on the average, the Alasenlahti and the lowermost Jukonniemi graywackes have higher CIA values than the other graywackes. The LREE contents increase from the Alasenlahti member upward to the Kupinniemi member, but a similar trend is not observed in the Tervakivi formation.

The variation in the Pulesjärvi profile largely resembles that in the Näsijärvi profile. The Ahvenlammi conglomerates and graywackes are similar to the Alasenlahti graywackes in being relatively rich in SiO₂. The upward change towards less silicic compositions is accentuated in the Pulesjärvi graywackes.

The Ahvenlammi and Talvineva conglomerates and graywackes tend to have slightly lower CIA and SiO₂ than the Alasenlahti graywackes. Petrographically, the difference in CIA is attributed to the higher amount of sericite/muscovite, reflecting a

higher proportion of clayey matrix at Alasenlahti. In general terms, the divergences may be due to differences in distal vs. proximal turbidites (see Sawyer 1986). The detritus in distal turbidites has experienced more weathering than that in proximal ones but progressive weathering also increases the relative abundance of the weathering-resistant minerals, e.g. quartz. Another explanation may be that the Ahvenlammi and Alasenlahti members represent different fans. If they would belong to the same fan there should occur thickly bedded quartz-rich graywackes at Sorila, a village halfway between Ahvenlammi and Alasenlahti (Fig. 1). According to the observations by Y. Kähkönen, graywackes of this type are absent at Sorila.

The upward compositional variations are readily observed in petrography. The relatively high SiO_2 contents in the Alasenlahti and Ahvenlammi graywackes are indications of the abundance of quartz clasts. According to tentative observations by Y. Kähkönen, they also seem to be richer in granitoid clasts than the other graywackes studied. The upward decrease of the SiO_2 content within the Tervakivi and Puolamäki graywackes is related to the occurrence of hornblende in the uppermost graywackes (Appendix). Based on petrography only (Rautio 1987, unpub-

lished data of Y. Kähkönen), it is also clear that the graywackes at Kolunkylä are less silicic than the Myllyniemi graywackes and most of the Tervakivi graywackes.

The CIA values of the graywackes vary systematically according to the stratigraphic position but the trend in part fluctuates. The oscillations are partly due to analytical uncertainties since the samples analysed twice show differences of 0.5-3 CIA units (Table 2). There are also differences within beds. For instance, samples Tre 59-61 are from a single bed and show a range of 52-58 in CIA (Table 2). In addition to analytical uncertainties, these divergences may be due to sorting effects. The rather low CIA and high SiO_2 in sample 526a-YK-/89 is a result of washing; the rock is poor in intergranular mica which represents an original muddy matrix.

The composition of the TSB graywackes is partly controlled by sorting and grain size but other factors, such as differences in the provenance, must also be considered. For instance, the Alasenlahti and Jukonniemi graywackes are similar in grain size but the former are higher in SiO_2 than the latter. Also, the graywacke sample 1-Ahv/84 resembles the associated conglomerates in its SiO_2 content.

Mudstones

The data on the mudstones of the Näsijärvi profile are less abundant than the graywacke data but, in general, the Myllyniemi mudstones are lower in P_2O_5 , CaO, Sr and LREE contents but higher in CIA values and $\text{K}_2\text{O}/\text{Na}_2\text{O}$ ratios than those at Tervakivi and Kolunkylä (Fig. 5). The Tuuliniemi mudstones are intermediate between these types. The silty mudstone from Vaarinniemi has higher CaO and La contents, and lower CIA and $\text{K}_2\text{O}/\text{Na}_2\text{O}$ values than

the other Myllyniemi mudstones. Silt/clay grain-size effects explain a part of the oscillation of the variation trends in the Myllyniemi and Tuuliniemi mudstones (Table 2). The non-consistent upward variation in the mudstones of the Pulesjärvi profile (Table 2) is attributed to the problems of precise determination of the original grain size and character of the fairly recrystallized fine-grained schists.

GEOCHEMISTRY AND TECTONIC SETTING

Sedimentary basins may be classified according to their plate tectonic setting into some twenty types (Ingersoll 1988, Miall 1990) but in the classifications based on chemical composition of graywackes three to four plate tectonic settings are discerned (Bhatia 1983, Bhatia & Crook 1986, Roser & Korsch 1986). McLennan et al. (1990) distinguished six tectonic settings of depositional basins. These authors also emphasized that the plate tectonic setting of the provenance is more important than the tectonic

setting of deposition in controlling the composition of turbidites. While the basin and provenance generally have comparable tectonic settings, sediment may be transported into a tectonically distinctive basin and a basin may receive material from various source areas (see McLennan et al. 1990). This is one source of uncertainty when the discrimination diagrams (Figs. 6-9) are applied. A further problem in diagrams based on a $\text{K}_2\text{O}/\text{Na}_2\text{O}$ ratio is the eventual post-depositional mobility of alkali metals. Consid-

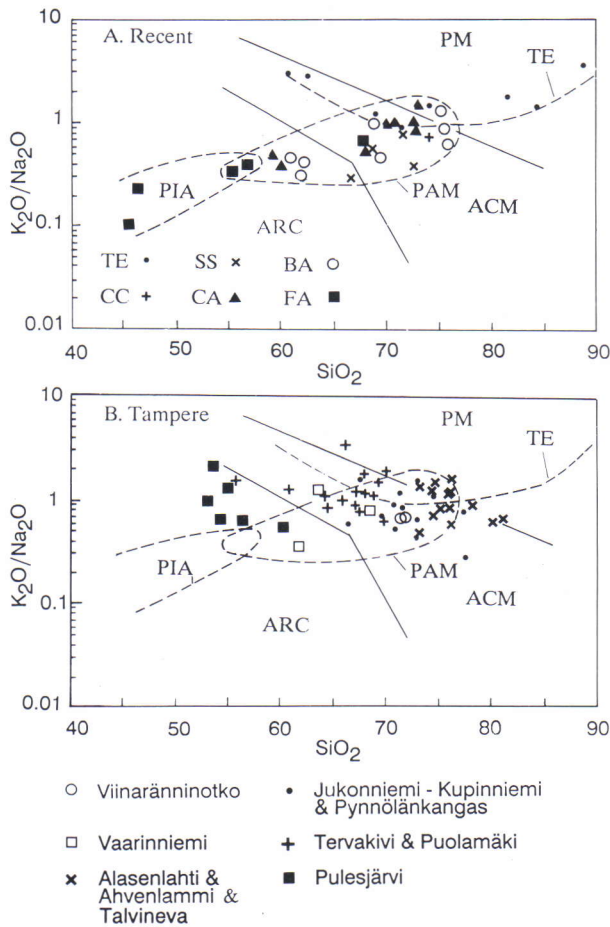


Fig. 6. K_2O/Na_2O vs. SiO_2 diagram of modern turbidite sands and Tampere graywackes. SiO_2 values recalculated to 100%.

A. Young sands and graywackes. Continuous lines indicate boundaries of the fields of graywackes derived from passive continental margins (PM), from active continental margins (ACM) and from oceanic island arcs (ARC), according to Roser & Korsch (1986). Symbols for modern sands: TE = trailing edge margins; CC = continental collision basins; SS = strike-slip margins; BA = back-arc basins; CA = continental arc basins; FA = forearc basins; data from McLennan et al. (1990), recalculated to 100%. Based on these symbols, we discriminate with dashed lines the fields of trailing edge (TE), primitive island arc (PIA) and pooled active margin (PAM) basins. The FA sample from Japan is excluded from the PIA field because its Nd isotopes show a significant component of old crust in the provenance and because northern Japan is not a primitive island arc. The sands from continental collisions are included in the PAM group (cf. Maynard et al. 1982), not in the TE group (cf. McLennan et al. 1990).

B. Tampere graywackes from the Näsijärvi and Pulesjärvi profiles. Data from Table 2. The TE, PAM, PIA, PM, ACM and ARC fields from Fig. 6A.

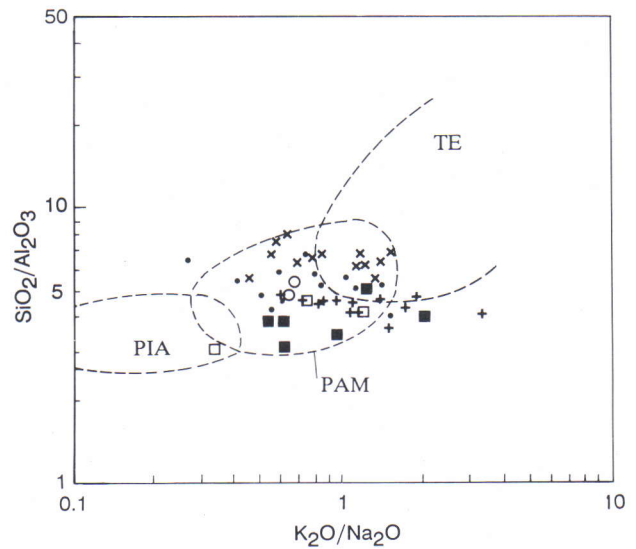


Fig. 7. SiO_2/Al_2O_3 vs. K_2O/Na_2O diagram of the Tampere graywackes from the Näsijärvi and Pulesjärvi profiles. Data and symbols as in Fig. 6B. The TE, PAM and PIA fields of recent sands were drawn according to Fig. 4 of McLennan et al. (1990) using criteria similar to those in Fig. 6A.

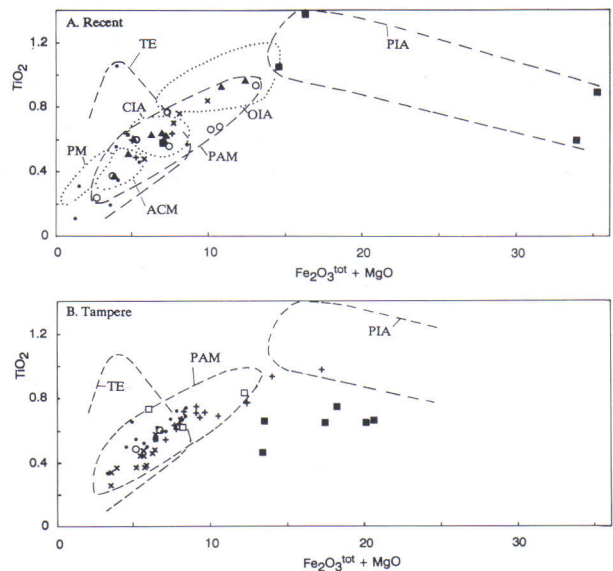


Fig. 8. TiO_2 vs. $Fe_2O_3^{tot} + MgO$ diagram of modern turbidite sands and Tampere graywackes. Data recalculated to 100% on a volatile-free basis. Total Fe as Fe_2O_3 . **A.** Modern sands, data from McLennan et al. (1990), symbols as in Fig. 6A. The TE, PAM and PIA fields (dashed lines) were drawn using criteria similar to those in Fig. 6A. Dotted lines give the major fields of sandstones from oceanic island arc (OA), continental island arc (CIA), active continental margin (ACM) and passive margin (PM) settings according to Bhatia (1983).

B. Tampere graywackes from the Näsijärvi and Pulesjärvi profiles. Data and symbols as in Fig. 6B. The TE, PAM and PIA fields from Fig. 8A.

ering the overlappings and uncertainties, a simple three-fold classification is used here: trailing edge settings (TE), settings close to primitive island arcs (PIA), and the pooled active margin (PAM) settings. It should be emphasized that the discrimination is tentative and future revisions will probably be necessary. We do not use mudstone data for tectonic setting discrimination (cf. Roser & Korsch 1986) since seawater salt may comprise a significant part of sodium in muds (McLennan et al. 1990).

In general, the graywackes of the Näsijärvi and Pulesjärvi profiles resemble PAM graywackes and sands (Figs. 6-9). The relatively silicic graywackes and conglomerates of Alasenlahti, Ahvenlammi and Talvineva fall closer to the TE field than the other TSB graywackes. Nevertheless, they may be classified as PAM sedimentary rocks. The TE imprint is slighter in the Tervakivi and Vaarinniemi graywackes

than in most of the Myllyniemi graywackes, and it is weakest in the Pulesjärvi graywackes.

The Pulesjärvi graywackes resemble PIA graywackes due to their low SiO_2 contents. However, features such as high ratios of $\text{K}_2\text{O}/\text{Na}_2\text{O}$, high La/Yb and high La/V distinguish them from the latter. They are evidently associated with a mature arc. The Vaarinniemi graywackes, the lowermost graywackes studied in the Näsijärvi profile, are also mainly derived from a mature arc, not from a primitive arc.

The TSB graywackes are more silicic than modern forearc sands of immature arcs. However, the forearc setting suggested by Ojakangas (1986) cannot be confirmed or refuted on this basis because some modern forearc basins, e.g. off northern Japan, contain fairly silicic sands which have a significant component of old continental crust in the provenance (Figs. 6, 8 and 9 in McLennan et al. 1990).

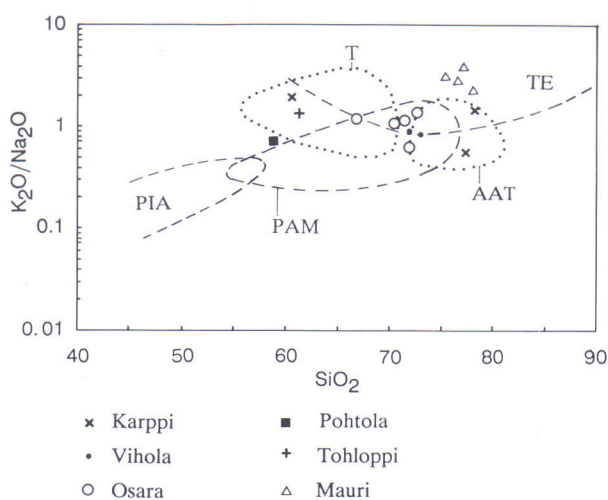
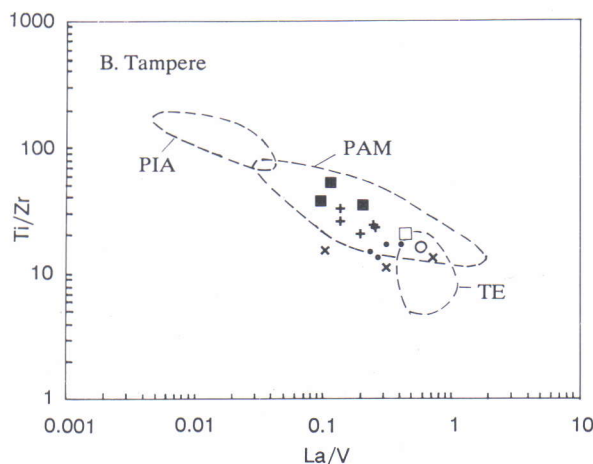
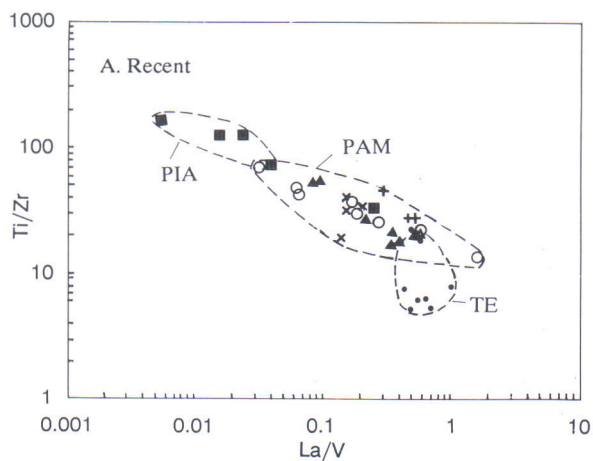


Fig. 10. $\text{K}_2\text{O}/\text{Na}_2\text{O}$ vs. SiO_2 diagram of the Tampere graywackes from dispersed localities, and of the Mauri arkoses. Data from Table 2. The PIA, PAM and TE fields from Fig. 6A. AAT gives the field of the Alasenlahti-Ahvenlammi-Talvineva graywackes, and T that of the graywackes of the Tervakivi formation.

Fig. 9. Ti/Zr vs. La/V diagram of modern turbidite sands and Tampere graywackes. A. Modern sands. Data, symbols and fields as in Fig. 6A. B. Tampere graywackes. Data from Tables 2 and 3. Symbols as in Fig. 6B, but the open circle indicates sample 13-A-YKÄ/86 from Osara. The TE, PAM and PIA fields from Fig. 9A.

COMPOSITION OF THE TSB SEDIMENTARY ROCKS OUTSIDE THE MAJOR PROFILES

The composition of the TSB sedimentary rocks outside the Näsijärvi and Pulesjärvi profiles emphasizes some of the features observed in the major profiles (Fig. 10). See Fig. 1 for the location of these samples.

The volcanic and sedimentary rocks at Tohloppi are considered lateral equivalents of the Kiviranta volcanic and sedimentary rocks but their stratigraphic position is problematic (Kähkönen, this volume). The Tohloppi graywacke is low in SiO_2 , high in alkalis and high in P_2O_5 . It resembles the Vaarinniemi graywackes more than the other Myllyniemi graywackes but it also has similarities with the Tervakivi graywackes. The Tohloppi mudstone differs from the typical Myllyniemi mudstones due to the high P_2O_5 and Sr contents and the low CIA value. In these respects, it is similar to the mudstones of Tervakivi and Kolunkylä, but has a higher $\text{K}_2\text{O}/\text{Na}_2\text{O}$ value.

According to the grade of recrystallization, the Vihola turbidites at Nokia are intermediate between the well-preserved TSB rocks and the migmatites to the south of the TSB. Their stratigraphic correlation is not definite since they lie south of the fault which separates the TSB from the migmatites. In general, the Vihola graywackes are like the Myllyniemi graywackes in chemical composition.

The graywackes of Karppi, in the southern limb of the major syncline at Orivesi, are lateral equivalents of the Myllyniemi formation. The two lower samples are rich in SiO_2 and thus similar to the graywackes at

Alasenlahti and Ahvenlammi. The third sample, ca. 100 m above the former in the succession, is low in silica.

The Osara graywackes (p. 119) are stratigraphically above the pillow-basalt bearing Haveri formation (Mäkelä 1980, Kähkönen & Nironen, this volume). They largely resemble the Myllyniemi graywackes, particularly those at Jukonniemi, in chemical composition. However, the Osara sample analyzed for REE deviates from most of the TSB sedimentary rocks due to its relatively high LREE and low Eu/Eu^* .

The sedimentary and volcanic rocks at Pohtola are stratigraphically above the Pulesjärvi sedimentary and volcanic rocks. The Pohtola graywacke is low in SiO_2 and resembles the Pulesjärvi graywackes. Since the Pohtola mudstones have high P_2O_5 and Sr contents, low $\text{K}_2\text{O}/\text{Na}_2\text{O}$ ratios and low CIA values, they differ from those of the Myllyniemi formation and are like the Tervakivi and Kolunkylä mudstones. The sedimentary rocks at Pohtola confirm the idea that the source areas of the uppermost TSB sedimentary rocks differ from those of the typical Myllyniemi turbidites.

As can be expected, the Mauri arkoses deviate from the TSB graywackes in many respects. They are fairly rich in SiO_2 and Ba, low in Sr and P_2O_5 , and the $\text{K}_2\text{O}/\text{Na}_2\text{O}$ ratios are high. The differences are attributed partly to the arkosic character and partly to different source areas since clasts of K-feldspar are common and clasts of mafic volcanics are absent in the Mauri arkoses (see also Matisto 1968).

DISCUSSION

Significance of the REE data

In general, three features are essential when discussing the chondrite-normalized REE patterns of siliciclastic sedimentary rocks (e.g. Taylor & McLennan 1985, McLennan & Taylor 1991). (1) Significant enrichment of LREE relative to HREE indicates evolved source areas while flat REE patterns are derived from geochemically primitive sources. (2) Steep REE patterns with HREE depletion are best explained by fractionation of garnet during the genesis of the igneous source rocks. Positively sloping HREE patterns may be due to the abundance of HREE-enriched clastic minerals such as zircon and garnet. (3) Significant Eu depletions in sedimentary rocks were formerly considered a post-Archean phe-

nomenon (Taylor & McLennan 1985). This concept was partly due to sampling bias; the Archean samples came mainly from greenstone belts which largely represent active settings while the post-Archean samples typically were from cratonic areas (e.g., Gibbs et al. 1986). Indeed, the turbidites from Archean greenstone belts tend to be less depleted in Eu than post-Archean turbidites. However, it is also clear that post-Archean siliciclastic sedimentary rocks without prominent Eu depletion are more common than was previously thought, and there are also Archean sedimentary rocks with significant Eu depletions (McLennan & Taylor 1991). As a conclusion, post-Archean turbidites which have both a significant

LREE enrichment and no or minute Eu depletion (Eu/Eu^* more than 0.85) have not been reported frequently. The basic reason of the significant Eu depletions is cratonization and associated intracrustal differentiation since this process includes formation of K-rich granitoids with plagioclase as a residual or fractionating phase.

The Nd isotopes and detrital zircon ages of the TSB turbidites indicate predominantly Paleoproterozoic provenances with minor input from Archean sources (Huhma 1987, Huhma et al. 1991). The considerable LREE enrichments in most of the TSB sedimentary rocks indicate that the bulk sources were fairly evolved. The LREE enrichments might be attributed to the mixing of material from primitive arc(s) with Archean crustal material. However, volcanics of immature arcs have La_N values lower than 50 and average Archean crust has La_N values lower than 80 (Taylor & McLennan 1985, McLennan & Taylor 1991). Although the Archean crust is partly high in LREE (e.g. Hyvärinen 1985, Wang et al. 1990) and although an Archean cobble from the Ahvenlammi member shows a pronounced LREE enrichment (La_N ca. 450, Kähkönen & Huhma 1993), the La_N values typically of ca. 80-120 in the TSB sedimentary rocks cannot be yielded by mixing average Archean crustal material with material from immature Proterozoic arc(s). Therefore, the LREE enrichments of the TSB sedimentary rocks imply fairly evolved Paleoproterozoic source rocks.

The REE patterns of the turbidites of the Alasenlahti, Ahvenlammi and Talvineva members tend to be slightly distinguishable from those of the other TSB sedimentary rocks. Excluding one sample, they have relatively low LREE contents (La_N 25-60). Thus their proportion of evolved material is lower than that which is typical for the TSB sedimentary rocks. Considering the differences in the LREE enrichments in the cobbles from the Ahvenlammi member (Kähkönen & Huhma 1993), the relatively high LREE in sample 1-Ahv/84 may result from heterogeneous sources but the possible role of LREE-rich accessory minerals, e.g. allanite, may also be considered. The three graywackes of the Alasenlahti, Ahvenlammi and Talvineva members are also distinguished in having positive HREE patterns. These slight HREE enrichments might be due to clastic zircon.

McLennan & Taylor (1991) defined Eu depletions

as significant when Eu/Eu^* is below 0.85. The Eu/Eu^* values in the TSB sedimentary rocks range from 0.65 to 1.23 but are mostly above or about 0.85 (Table 3). Based on the non-smooth Nd-Tb patterns in some samples, analytical uncertainties are possible. For instance, we infer that the actual $\text{Eu}:\text{Eu}^*$ value in sample 518-YK/89 is higher than the value given in Table 3. Considering the analytical problems, it is probable that significant Eu depletions are mostly absent in the TSB sedimentary rocks. Note also that the sample analyzed by Wildeman & Haskin (1973) has no Eu anomaly (Fig. 3). The data from the TSB sedimentary rocks indicate that the post-Archean siliciclastic sedimentary rocks, which are characterized both by no or minor Eu depletions and significant LREE enrichments, are more common than has been reported previously.

Because significant Eu depletions are rare in the TSB sedimentary rocks, the bulk of their provenance components were not cratonized, although the LREE enrichments indicate evolved sources. The obvious Eu depletions, particularly in the Osara graywacke (sample 13-A-YK-/86) which also has a strong LREE-enrichment, may be indications of a high proportion of intracrustally differentiated material. The data do not allow a conclusion as to whether the material was Archean or Paleoproterozoic. A certain, though not very wide, variation in the proportion of the Archean component is evident in the TSB sedimentary rocks (Huhma 1987, Welin 1987).

McLennan & Taylor (1991) consider the HREE depletions significant when Gd_N/Yb_N exceeds 2.0. The Gd_N/Yb_N value of 2.0 is equal to the Tb_N/Yb_N value of ca. 1.8. Thus the HREE depletions in the TSB sedimentary rocks are not significant in terms of McLennan & Taylor (1991). However, the Pulesjärvi graywackes have steeper HREE patterns ($\text{Tb}_N/\text{Yb}_N = 1.4-1.7$) than the other TSB sedimentary rocks ($\text{Tb}_N/\text{Yb}_N = 0.7-1.4$). Based on petrography, high alkali and phosphorus contents, and $\text{K}_2\text{O}/\text{Na}_2\text{O}$ ratios close to or above unity, the provenance of the Pulesjärvi graywackes was rich in potassic volcanic rocks or shoshonites. The relatively high Tb_N/Yb_N values agree with this interpretation since shoshonitic and potassic volcanic rocks tend to have higher Tb_N/Yb_N values than calc-alkaline volcanic rocks (Francalanci et al. 1989). Furthermore, a part of the volcanic rocks at Pulesjärvi have shoshonitic characteristics (unpublished data of the authors).

Reasons for the compositional differences between the units

The sedimentary rocks at Vaarinniemi, probably low in the succession, bear some compositional resemblances to the Tervakivi and Pulesjärvi sedimentary rocks, which are high in the succession. This might be interpreted to indicate repetition of strata by overthrusting or by early recumbent folding. However, rocks resembling those of the Alasenlahti, Ahvenlammi and Talvineva members were not observed in the other parts of the profiles studied. It is also difficult to find evidence for structural repetition of this scale in the field (Nironen 1989) or on airborne geophysical maps. Therefore, the Vaarinniemi member most probably belongs to low stratigraphic levels.

The pronounced variation in the composition of the sedimentary rocks in the study profiles indicates that the material was not homogenized due to repeated redeposition. Therefore, a very long bulk transportation on a wide shelf is not probable.

The upward compositional change near Lake Näsijärvi indicates variation in volcanic activity and in the character of the predominant provenance. The lowermost sedimentary rocks (at Vaarinniemi) are derived from a mature arc. Volcanic interbeds are not frequent in the Myllyniemi formation. The proportion of mafic and intermediate shoshonitic volcanic provenances is relatively low in the fairly silicic Alasenlahti, Ahvenlammi and Talvineva graywackes. The sedimentary rocks of these members are mostly lower in LREE, i.e. they are geochemically less evolved than the TSB sedimentary rocks typically. The mudstones have relatively high CIA values. The

Alasenlahti and Ahvenlammi graywackes seem to contain more granitoid clasts than the other Myllyniemi graywackes (p.130). Relatively advanced chemical weathering and deep erosion of provenances with a significant component of relatively primitive Paleoproterozoic material is probable. A marked contribution from Archean tonalite-trondhjemite-granodiorite-type sources is not evident since the HREE patterns are flat. Possibly a stage of relative quiescence in volcanic activity resulted in that relatively primitive sources characterize the composition of the Alasenlahti, Ahvenlammi and Talvineva sedimentary rocks.

From the Alasenlahti and Ahvenlammi members to the stratigraphically higher units, the graywackes change to more mafic. Coexistently, the CIA values decrease and the P_2O_5 , Sr and La contents increase in the mudstones. These features are attributed to the increase in volcanic activity in the source areas. This activity was first mainly intermediate in composition but the provenance of the units above the Tervakivi formation was rather mafic and also largely shoshonitic. Direct indications of the increase in volcanic activity are provided by the pyroclastic rocks of the Pirttiniemi formation and, particularly, the abundance of volcanic rocks at Pulesjärvi and Kolunkylä. The increased volcanic activity resulted in steeper relief, rapid volcanoclastic accumulations and limited chemical weathering, as indicated by the relatively low CIA values in the Tervakivi and Kolunkylä mudstones.

ACKNOWLEDGMENTS

This study is part of a project (No. 1011197), funded by the Academy of Finland, "Geology and Geochemistry of the Supracrustal Rocks of the Early Proterozoic Tampere Schist Belt", and it is a contribution to the IGCP project (No. 217) "Proterozoic Geochemistry". Financial support was also gratefully received from the Wilhelm Ramsay and Th. G. Sahama Memorial Foundation. We would like to thank Asko Kontinen and Richard W. Ojakangas for

the referee comments, as well as Jarmo Kohonen and Raimo Lahtinen for reviews. Sample 46-RWO/82 was provided by R.W. Ojakangas. We are grateful to Dr. Tim Brewer for the XRF analyses carried out at Nottingham University. The figures were drawn by Marja Tiuhonen, Riitta Virtanen and Riitta Fagerström, and the English language was revised by Anthony Meadows.

REFERENCES

- Ala-Vainio, I. 1986.** XRF routine analysis by the fundamental parameter method. Proceedings of the Thirty-ninth Chemist's Conference. Scarborough, June 17-19, 1986. Research and Development, British Steel Corporation, 51-54.
- Bhatia, M.K. 1983.** Plate tectonics and geochemical composition of sandstones. *J. Geol.* 91, 611-627.
- Bhatia, M.K. & Crook, K.A.W. 1986.** Trace element characteristics of graywackes and tectonic setting discrimination of sedimentary basins. *Contrib. Mineral. Petrol.* 92, 181-193.
- Dickinson, W.R. & Suzek, C.A. 1979.** Plate tectonics and sandstone compositions. *Ass. Am. Petrol. Geol., Bull.* 63, 2164-2182.
- Françalanci, L., Manetti, P. & Peccerillo, A. 1989.** Volcanological and magmatological evolution of Stromboli volcano (Aeolian Islands): the roles of fractional crystallization, magma mixing, crustal contamination and source heterogeneity. *Bull. Volcanol.* 51, 355-378.
- Huhma, H. 1987.** Provenance of early Proterozoic and Archean metasediments in Finland: a Sm-Nd isotopic study. *Precambrian Res.* 35, 127-143.
- Huhma, H., Claesson, S., Kinny, P.D. & Williams, I.S. 1991.** The growth of Early Proterozoic crust: new evidence from Svecofennian detrital zircons. *Terra Nova* 3, 175-179.
- Hyvärinen, T. 1985.** Kuhmon Kivivaaran-Kirkkokankaan alueen migmatiitit ja niihin liittyvät granitoidit. Arkeisten alueiden malmiprojekti. Raportti No 22. Univ. Oulu, 111 p. (in Finnish)
- Ingersoll, R.V. 1988.** Tectonics of sedimentary basins. *Geol. Soc. Am. Bull.* 100, 1704-1719.
- Jahn, B.M., Auvray, B., Blais, S., Capdevila, R., Cornichet, J., Vidal, P. & Hameurt, J. 1980.** Trace element geochemistry and petrogenesis of Finnish greenstone belts. *J. Petrol.* 21, 201-244.
- Kähkönen, Y. 1987.** Geochemistry and tectonomagmatic affinities of the metavolcanic rocks of the early Proterozoic Tampere Schist Belt, southern Finland. *Precambrian Res.* 35, 295-311.
- Kähkönen, Y. 1989.** Geochemistry and petrology of the metavolcanic rocks of the early Proterozoic Tampere Schist Belt, southern Finland. *Geol. Surv. Finland, Bull.* 345, 104 p.
- Kähkönen, Y. 1994.** Shoshonitic and high-K metavolcanic rocks in the southern parts of the Paleoproterozoic Tampere Schist Belt, southern Finland; evidence for an evolved arc-type setting. *Geol. Surv. Finland, Spec. Paper* 19, 101-115.
- Kähkönen, Y. & Huhma, H. 1993.** An Archaean cobble in a Svecofennian conglomerate near Tampere, southern Finland. *Geol. Surv. Finland, Spec. Paper* 18, 31-36.
- Kähkönen, Y., Huhma, H. & Aro, K. 1989.** U-Pb zircon ages and Rb-Sr whole-rock isotope studies of early Proterozoic volcanic and plutonic rocks near Tampere, southern Finland. *Precambrian Res.* 45, 27-43.
- Kähkönen, Y. & Nironen, M., 1994.** Structure and geochemistry of the supracrustal rocks around the extinct Paleoproterozoic Haveri Au-Cu mine, southern Finland; evidence for a change from an extensional setting to volcanic arc. *Geol. Surv. Finland, Spec. Paper* 19, 141-159.
- Koljonen, T. & Rosenberg, R. 1975.** Rare earth elements in Middle Precambrian volcanic rocks of Finland, with a discussion of the origin of the rocks. *Bull. Geol. Soc. Finland* 47, 127-138.
- Leveinen, J. 1990.** Tampereen liuskevyöhykkeen kerrostumat Pulesjärven profiilissa. M.Sc. thesis, Univ. Helsinki, 134 p. (unpublished, in Finnish)
- Matisto, A. 1968.** Die Meta-Arkose von Mauri bei Tampere. *Bull. Comm. géol. Finlande* 235, 21 p.
- McLennan, S.M., Taylor, S.R., McCulloch, M.T. & Maynard, J.B. 1990.** Geochemical and Nd-Sr isotopic composition of deep-sea turbidites: Crustal evolution and plate tectonic associations. *Geochim. Cosmochim. Acta* 54, 2015-2050.
- McLennan, S.M. & Taylor, S.R. 1991.** Sedimentary rocks and crustal evolution: Tectonic setting and secular trends. *J. Geol.* 99, 1-21.
- Miall, A.D. 1990.** Principles of Sedimentary Basin Analysis. 2nd ed. New York: Springer-Verlag, 668 p.
- Nesbitt, H.W. & Young, G.M. 1982.** Early Proterozoic climates and plate motions inferred from major element chemistry of lutites. *Nature* 299, 715-717.
- Nironen, M. 1989.** The Tampere Schist Belt: structural style within an early Proterozoic volcanic arc system in southern Finland. *Precambrian Res.* 43, 23-40.
- Ojakangas, R.W. 1968.** Cretaceous sedimentation, Sacramento Valley, California. *Geol. Soc. Am. Bull.* 79, 973-1008.
- Ojakangas, R.W. 1986.** An early Proterozoic metagraywacke-slate turbidite sequence: The Tampere schist belt, southwestern Finland. *Bull. Geol. Soc. Finland* 58, 241-261.
- Rautio, T. 1987.** Tampereen liuskejackson litostratigrafia ja paleosedimentologia Kolunkylän ja Veittijärven alueilla. M.Sc. thesis, Univ. Oulu, 108 p. (unpublished, in Finnish)
- Rosenberg, R. J., Kaistila, M. & Zilliagus, R. 1982.** Instrumental neutron activation analysis of solid geochemical samples. *J. Radioanal. Chem.* 71, 419 - 428.
- Roser, B.P. & Korsch, R.J. 1986.** Determination of tectonic setting of sandstone-mudstone suites using SiO₂ content and K₂O/Na₂O ratio. *J. Geol.* 94, 635-650.
- Roser, B.P. & Korsch, R.J. 1988.** Provenance signatures of sandstone-mudstone suites determined using discriminant function analysis of major-element data. *Chem. Geol.* 67, 119-139.
- Sawyer, E.W. 1986.** The influence of source rock type, chemical weathering and sorting on the geochemistry of clastic sediments from the Quetico Metasedimentary Belt, Superior Province, Canada. *Chem. Geol.* 55, 77-95.
- Simonen, A. 1953.** Stratigraphy and sedimentation of the Svecofennian early Archean supracrustal rocks in southwestern Finland. *Bull. Comm. géol. Finlande* 160, 64 p.
- Simonen, A. & Kouvo, O. 1951.** Archean varved schists north of Tampere in Finland. *Bull. Comm. géol. Finlande* 154, 93-114.
- Taylor, S.R. & McLennan, S.M. 1985.** The Continental Crust: Its Composition and Evolution. Oxford: Blackwell, 312 p.
- Valloni, R. & Maynard, J.B. 1981.** Detrital modes of recent deep-sea sands and their relation to tectonic setting: a first approximation. *Sedimentology* 28, 75-83.
- van de Kamp, P.C. & Leake, B.E. 1985.** Petrography and geochemistry of feldspathic and mafic sediments of the northeastern Pacific margin. *Trans. R. Soc. Edinburgh: Earth Sci.* 76, 411-449.
- Wang, K., Windley, B., Sills, J. & Yan, Y. 1990.** The Archaean gneiss complex in E. Hebei Province, North China: geochemistry and evolution. *Precambrian Res.* 48, 245-265.
- Welin, E. 1987.** The depositional evolution of the Svecofennian supracrustal sequence in Finland and Sweden. *Precambrian Res.* 35, 95-113.
- Wildeman, T.R. & Haskin, L.A. 1973.** Rare earths in Precambrian sediments. *Geochim. Cosmochim. Acta* 37, 419-438.

APPENDIX. Sample description. xx cm indicates thickness of the bed. ϕ gives the maximum diameters of the clasts in sections approximately perpendicular to elongation. Am = amphibole. Cpx-clasts are now composed of amphibole. x and y give grid coordinates.

NÄSIJÄRVI PROFILE

MYLLYNIEMI FORMATION

Vaarinniemi member

- 1-B-YK/91. Graywacke. 11 cm, graded. ϕ to 1x2.2 mm. x 6825.82, y 2490.44.
- 1-Bm-YK/91. Silty mudstone. 5 cm, immediately above 1-B-YK/91.
- 4-YK/91. Graywacke. 40 cm, massive. ϕ to 1x1 mm. x 6825.86, y 2490.45.
- 46-RWO/82. Graywacke. 12 cm, graded. ϕ to 1.2x2 mm. x 6825.89, y 2490.42.

Alasenlahti member

- 10-YK/91. Graywacke. 30 cm, graded. ϕ to 1x1.5 mm. x 6825.95, y 2490.27.
- 11-YK/91. Graywacke. 20 cm, graded. ϕ to 0.8x0.9 mm. x 6825.97, y 2490.30.
- 1-YKÄ/84. Graywacke. 1.2 m, graded. ϕ to 0.9x1.6 mm. x 6826.20, y 2490.26.
- 525-YK/89. Clayey mudstone. Laminated. About 1.5 m above 1-YKÄ/84.
- 2-YKÄ/84. Graywacke. 1 m, graded. ϕ to 1.2x1.3 mm. Ca. 7 m above 1-YKÄ/84. x 6826.21, y 2490.27.
- 501-YKÄ/88. Graywacke. 30 cm Bouma A. ϕ to 0.8x1.2 mm. x 6826.55, y 2489.78.

Jukonniemi member

- 502-YKÄ/88. Graywacke. 70 cm Bouma A. ϕ to 1.5x2.1 mm. x 6826.65, y 2489.65.
- 503-YKÄ/88. Graywacke. 35 cm Bouma A. ϕ to 1x1.4 mm. Ca. 4 m above 502-YKÄ/88.
- 504-YKÄ/88. Graywacke. 2 m, massive. ϕ to 1x1.6 mm. Ca. 6 m above 503-YKÄ/88. x 6826.66, y 2489.66.
- 526-a-YK/89. Fine-grained conglomerate. 15 cm thick lense. Matrix-poor. ϕ to 3x8 mm. x 6826.64, y 2489.72.
- 524-YK/89. Clayey mudstone. 0.5 m, laminated. x 6826.79, y 2489.63.
- 531-YK/89. Graywacke. > 70 cm. ϕ to 1.5x1.5 mm. x 6826.89, y 2489.56.
- 527-YK/89. Clayey mudstone. Thinly laminated. x 6826.93, y 2489.62.
- 528-YK/89. Siltstone/fine-grained graywacke. 15 cm. ϕ to 0.25x0.32 mm. 40 cm above 527-YK/89.
- 505-YKÄ/88. Graywacke. 14 cm Bouma A. ϕ to 0.8x0.8 mm. x 6827.02, y 2489.71.
- 506-YKÄ/88. Graywacke. 35 cm, massive. ϕ to 0.7x1.6 mm. x 6827.08, y 2489.79.
- 533-YK/89. Fine-grained graywacke. Tuffaceous. ϕ mostly to 0.3x0.4 mm, rare clasts to 0.8x1.2 mm. x 6827.21, y 2490.03.
- 532-YK/89. Felsic tuffaceous mudstone. 10 cm. ϕ mostly to 0.1x0.15 mm; scarce oversized Pl-clasts to 1x1 mm, possible shards to 0.2x0.8 mm. x 6827.22, y 2490.04.

Kupinniemi member

- 507-YKÄ/88. Graywacke. 40 cm, massive. ϕ to 0.5x0.6 mm. x 6827.56, y 2489.82.
- 508-YKÄ/88. Graywacke. 20 cm. ϕ to 1x1.1 mm. Mud chips, 2-3%, ϕ to 0.6x 5 mm. 2 m above 507-YKÄ/88. x 6827.56, 2489.83.
- 509-YKÄ/88. Graywacke. 20 cm Bouma AB. ϕ to 0.8x1.5 mm. 5 m above 508-YKÄ/88. x 6827.57, y 2489.85.
- 534-YK/89. Clayey mudstone. Laminated. 1 m above 509-YKÄ/88. x 6827.57, y 2489.84.

TUULINIEMI FORMATION

- 535-YK/89. Silty mudstone. 70 cm, massive. ϕ to 0.2x0.2 mm. x 6829.41, y 2489.49.
- 537-YK/89. Clayey mudstone. Thinly laminated. x 6829.46, y 2489.47.
- 540-YK/89. Silty mudstone. Massive, rich in biotite. ϕ to 0.1x0.15 mm. x 6829. x 6829.51, y 2489.49.

TERVAKIVI FORMATION

- 541-YK/89. Mudstone. Laminated. x 6830.58, y 2489.77.
- 511-YK/89. Graywacke. 14 cm, graded. ϕ to 0.7x1.8 mm. 4 m above 541-YK/89. x 6830.59, y 2489.77.
- 513-YK/89. Graywacke. 1.4 m, massive. ϕ to 0.8x1.3 mm. 7.3 m above 511-YK/89. x 6830.60, y 2489.77.
- 514-YK/89. Graywacke. 60 cm, massive. ϕ to 0.5x1.6 mm. 4.5 m above 513-YK/89.
- 515-YK/89. Graywacke. 13 cm Bouma A. ϕ to 0.5x3 mm. x 6830.64, y 2489.81.
- 517-YK/89. Graywacke. 11 cm Bouma A. ϕ to 0.6x0.7 mm. 10.7 m above 515-YK/89. x 6830.65, y 2489.81.
- 518-YK/89. Graywacke. 35 cm, massive. ϕ to 0.6x1 mm. 4.1 m above 517-YK/89. x 6830.65, y 2489.82.
- 519-YK/89. Graywacke. 50 cm, massive. ϕ to 0.7x1.3 mm. 6.3 m above 518-YK/89. x 6830.66, y 2489.82.
- 520-YK/89. Graywacke. 80 cm Bouma AB. ϕ to 0.8x1.5 mm. Am-bearing. x 6830.70, y 2490.00.

KOLUNKYLÄ

- 2-Kisala/89. Mudstone. Laminated. 6831.54, y 2491.05.
- 1-Kisala/89. Mudstone. About 6 m above 2-Kisala/89.

PULESJÄRVI PROFILE

VIINARÄNNINNOTKO

Two samples from interbeds in a minor conglomerate:

14-Ahv/85. Graywacke. 20 cm. ϕ to 0.5x2 mm. x 6831.49, y 2502.97.

16-Ahv/85. Graywacke. ϕ to 0.8x1.1 mm. x 6831.48, y 2502.95.

MYLLYNIEMI FORMATION

Ahvenlammi member

1-Ahv/84. Graywacke. 5 cm, graded. ϕ to 0.9x5.5 mm. x 6831.56, y 2502.80.

Four samples from a 2 m thick graded conglomerate-graywacke; x 6831.58, y 2502.76:

21-Ahv/85. Conglomerate. 0.1 m above the base. ϕ to 7x17 mm.

22-Ahv/85. Conglomerate/coarse-grained graywacke. 0.55 m above the base. ϕ to 3x3.5 mm.

23-Ahv/85. Coarse-grained graywacke. 1 m above the base. ϕ to 1.5x3.7 mm.

24-Ahv/85. Graywacke. 1.5 m above the base. ϕ to 1.2x3 mm.

Tre 53. Graywacke. > 2 m. Massive. ϕ to 0.5 mm. x 6832.09, y 2503.31.

Talvineva member

Four samples from a 3 m thick Bouma AB unit; x 6832.36, y 503.26:

Tre 59. Coarse-grained graywacke. ϕ to 4 mm.

Tre 60. Graywacke. 0.4 m above the former. ϕ to 0.9x1.8 mm.

Tre 61. Graywacke. 2.2 m above the former. ϕ to 0.7x1.3 mm.

Tre 62. Silty mudstone.

Pynnölänkangas member

Four samples from a single outcrop; x 6832.04, y 2503.06:

Tre 77H. Graywacke. 2.5 cm, graded.

Tre 77S. Mudstone + fine-grained graywacke.

Tre 76H (stratified graywacke, ϕ to 1x1.2 mm) and Tre 76S (graded mudstone) from a 3 cm thick graded unit ca. 10 cm above Tre 77S.

MULTIVUORI

Tre 82. Fine-grained graywacke + mudstone. Laminated. 1 mm wide quartz-vein. x 6833.22, y 2502.61.

51-JEL/86. Silty mudstone/fine-grained graywacke. Massive. x 6833.25, y 2502.65.

Tre 85. Felsic tuffaceous mudstone. x 6833.33, y 2502.53.

TERVAKIVI FORMATION at Puolamäki

Tre 103. Graywacke. 5 cm, Bouma A. ϕ to 0.4x0.5 mm. x 6833.73, y 2502.12.

79-IV-JEL/86. Graywacke. 30 cm, graded. ϕ to 0.7x0.9 mm. x 6834.05, y 2502.16.

80-III A-JEL/86. Graywacke. 10 cm, graded. ϕ to 0.6x1.2 mm. x 6834.08, y 2502.16.

80-III B-JEL/86. Graywacke. > 1 m. ϕ to 0.9x1.8 mm. x 6834.08, y 2502.16.

80-V-JEL/86. Graywacke. > 25 cm, massive. ϕ to 0.6x1.4 mm. x 6834.08, y 2502.16.

81-JEL/86. Graywacke. Am-bearing. ϕ to 0.8x1.4 mm. x 6834.09, y 2502.11.

Tre-112. Graywacke. 26 cm. Am-bearing, few Cpx-clasts. ϕ to 0.7x2.0 mm. x 6833.74, y 2502.15.

PULESJÄRVI GRAYWACKES

Tre 149. Graywacke. Tuffaceous, stratified, rich in Cpx-clasts. ϕ to 2x2 mm. x 6834.23, y 2501.31.

Tre 149B. Graywacke. Tuffaceous, stratified, rich in Cpx-clasts. x 6834.23, y 2501.31.

Tre 192. Coarse-grained graywacke. Tuffaceous, stratified, rich in Cpx-clasts. ϕ to 2x3.5 mm. x 6834.80, y 2501.47.

Tre 217. Coarse-grained graywacke. Tuffaceous, stratified, rich in Cpx-clasts. ϕ to 2x3.5 mm. x 6835.37, y 2501.33.

Tre 262. Coarse-grained graywacke. Tuffaceous, stratified. Am-bearing. x 6835.69, y 2501.37.

Tre 266. Coarse-grained graywacke. Tuffaceous, stratified, rich in Cpx-clasts. x 6835.82, y 2501.30.

SAMPLES OUTSIDE THE STUDY PROFILES

Pohtola

Tre 350. Graywacke. 6 cm, graded. Am-bearing. x 6838.54, y 2499.85.
Tre 351. Mudstone. x 6838.44, y 2499.83.
Tre 352. Silty mudstone. Pronounced deformation. x 6837.52, y 2499.59.

Vihola, Nokia.

61-A-RWO/82. Graywacke. 1 m, graded. ϕ to 1.6x2.3 mm. x 6817.9, y 2474.5.
2-Vihola/84. Graywacke. 5x20 cm coarse-grained lense below a graded graywacke. ϕ to 2.5x4 mm. x and y as in the former.

Karppi

Two samples from a stratum > 1 m thick; x 6836.55, y 2516.94:
1-Karp/84. Coarse-grained graywacke. ϕ to 1.2x5.3 mm.
2-Karp/84. Coarse-grained graywacke. ϕ to 2x4.5 mm.
4-YKÄ/86. Graywacke. Tuffaceous. 25 cm, graded. ϕ to 1.3x2 mm. x 6836.61, y 2517.27.

Osara formation

11-YKÄ/86. Graywacke. From the upper part of a 2-3 m thick stratum. ϕ to 0.7x1.2 mm. One 1x5 mm clast rich in apatite. x 6844.00, y 2458.14.
12-B-YKÄ/86. Graywacke. Graded. ϕ to 0.9x1.1 mm. x 6844.40, y 2457.86.
13-A-YKÄ/86. Graywacke. 40 cm, graded. ϕ to 2.1x3 mm. x 6844.74, y 2456.78.
13-B-YKÄ/86. Graywacke. 20 cm above 13-A-YKÄ/86, same stratum. ϕ to 0.5x1 mm.
13-C-YKÄ/86. Graywacke. 50 cm bed below the two former. ϕ to 1x1.5 mm.

Tohloppi

18-YKÄ/83. Graywacke. 5 cm, graded. ϕ to 1x2 mm. Pl-clasts and fine-grained rock fragments dominate, one Qtz-clast. Underlies the Tohloppi conglomerates. x 6821.90, y 2481.40.
5-3-YKÄ/83. Mudstone. Faintly stratified. Overlies the lower Tohloppi conglomerate but underlies the Tohloppi Pl+Ur-phyric lava. x 6822.20, y 2479.88.

Mauri arkose. x 6818.7, y 2461.0.

10-A-YKÄ/86. Cross-bedded pebbly sandstone. 20 cm.
10-B-YKÄ/86. Sandstone from the same stratum as the former.
10-C-YKÄ/86. Pebble-bearing sandstone. 0.5 m below 10-B-YKÄ/86.

SUPRACRUSTAL ROCKS AROUND THE PALEOPROTEROZOIC HAVERI AU-CU DEPOSIT, SOUTHERN FINLAND: EVOLUTION FROM A SPREADING CENTER TO A VOLCANIC ARC ENVIRONMENT

by
Yrjö Kähkönen and Mikko Nironen

Kähkönen, Yrjö & Nironen, Mikko 1994. Supracrustal rocks around the Paleoproterozoic Haveri Au-Cu deposit, southern Finland: evolution from a spreading center to a volcanic arc environment. *Geological Survey of Finland, Special Paper 19*, 141–159, 15 figures, one table and two appendices.

The volcanic and sedimentary rocks around the former Haveri Au-Cu mine belong to the well-preserved Tampere Schist Belt. The volcanic rocks are mainly mafic lavas, metamorphosed at amphibolite facies. In addition to massive lithologies, metalavas with pillow and breccia structures are present, as are intercalations of mafic to intermediate metatuffs and metatuffites, limestone and chert. The Au-Cu deposit is hosted by lava breccia. The metatuffs and metatuffites grade into sulfide-bearing metasedimentary rocks. Together these rocks constitute the Haveri Formation which is overlain by metaturbidites (the Osara Formation) and metavolcanic rocks of predominantly intermediate composition (the Harhala Formation). Felsic and intermediate subvolcanic and dyke rocks as well as granitoids intrude the supracrustal rocks.

Depositional younging determinations, combined with observations of primary layering and S_1 foliation, subparallel to the layering, suggest that the study area is on the northern limb of a major F_1 syncline. In the eastern part of the study area, porphyroblasts grew in the metasedimentary rocks before the end of D_1 deformation, and migmatization in the western part probably also occurred during D_1 but certainly before D_2 . D_3 deformation, associated with retrograde metamorphism, is expressed as minor synforms and antiforms. Two faults cross the study area. The earlier fault is associated with an early shear zone with mainly horizontal movement. The later, vertical fault caused the slight difference in metamorphic grade between the eastern and western parts of the study area.

The Haveri metalavas are mostly low-K/medium-K tholeiitic basalts. Tectonomagmatic affinities suggest that they are not arc-type rocks, but instead are more reminiscent of marginal basin basalts. The attendant chemical variation trends may be explained by low-pressure fractional crystallization but there are also indications of combined assimilation. The metavolcanic rocks of the Harhala Formation, the subvolcanic and dyke rocks, and the granitoids are medium-K calc-alkaline rocks having rather evolved arc-type affinities. The difference between the rocks of the Haveri Formation and adjacent rocks records the change from a restricted, shallow extensional basin to a larger arc-related basin environment.

Key words (GeoRef Thesaurus, AGI): metavolcanic rocks, basalts, pillow lava, gold ores, geochemistry, structural geology, marginal basins, island arcs, Proterozoic, Paleoproterozoic, Haveri, Viljakkala, Finland

Yrjö Kähkönen, Department of Geology, P.O. Box 11 (Snellmaninkatu 3), FIN-00014 University of Helsinki, Finland

Mikko Nironen, Geological Survey of Finland, FIN-02150 Espoo, Finland

INTRODUCTION

The Paleoproterozoic Svecofennian Domain of Finland (Fig. 1) was formed ca. 1.9 Ga ago, from predominantly mantle-derived material (e.g. Patchett & Kouvo 1986, Huhma 1986). The Domain has been variously interpreted as the result of amalgamation and accretion of one or several terranes to the Archean craton (e.g. Hietanen 1975, Gaál & Gorbatshev 1987, Park 1991). Studies of paleoenvironments within the Svecofennian have been carried out within several well-preserved schist belts, separated from each other by migmatitic gneiss belts. Correlation between the schist belts is still premature and perhaps impossible without precise U-Pb zircon ages, which is one of the main reasons for the diverging opinions about the extent and number of terranes. Detailed studies of stratigraphic successions within individual belts nevertheless provide clues to the nature of the terranes (island arcs, continental arcs or collided microplates), and also assist in assessing the number of terranes that were juxtaposed against the Archean craton.

The Paleoproterozoic supracrustal rocks around the Haveri Au-Cu deposit, at Viljakkala, are part of the 200 km long Tampere Schist Belt (TSB) which extends along the southern boundary of the Central Finland Granitoid Complex (Fig. 1). In the central part of the TSB, east of Viljakkala, the epiclastic rocks consist mainly of turbiditic graywackes,

mudstones and conglomerates, metamorphosed under greenschist facies - amphibolite facies transition conditions (e.g. Sederholm 1897, Simonen & Neuvonen 1947, Ojakangas 1986). The metavolcanic rocks were mafic to felsic pyroclastics and minor lavas. Intermediate rocks with calc-alkaline affinities are the most common metavolcanics in the TSB (Kähkönen 1987).

The Haveri Au-Cu mine, which was mined from 1942 to 1960, is located within breccia-type mafic metalavas (Stigzelius 1944, Mäkelä 1980). According to Mäkelä (1980), the deposit is volcanic-exhalative in origin, and the ore and host rocks have Cyprus-type characteristics. The rocks were metamorphosed at amphibolite facies.

In this study, an analysis of the structures in the supracrustal rocks surrounding the Haveri mine is presented. The supracrustal sequence is divided into three Formations: the Haveri Formation (see also Mäkelä 1980), the Osara Formation, and the Harhala Formation (Fig.1). The geochemical studies of Mäkelä (1980) are supplemented, and inferences concerning paleoenvironment are discussed. Emphasis is placed whether or not the mafic metavolcanic rocks are closely related or exotic with respect to the rest of the TSB. Y. Kähkönen is responsible for the geochemical-petrological and M. Nironen for the structural interpretation.

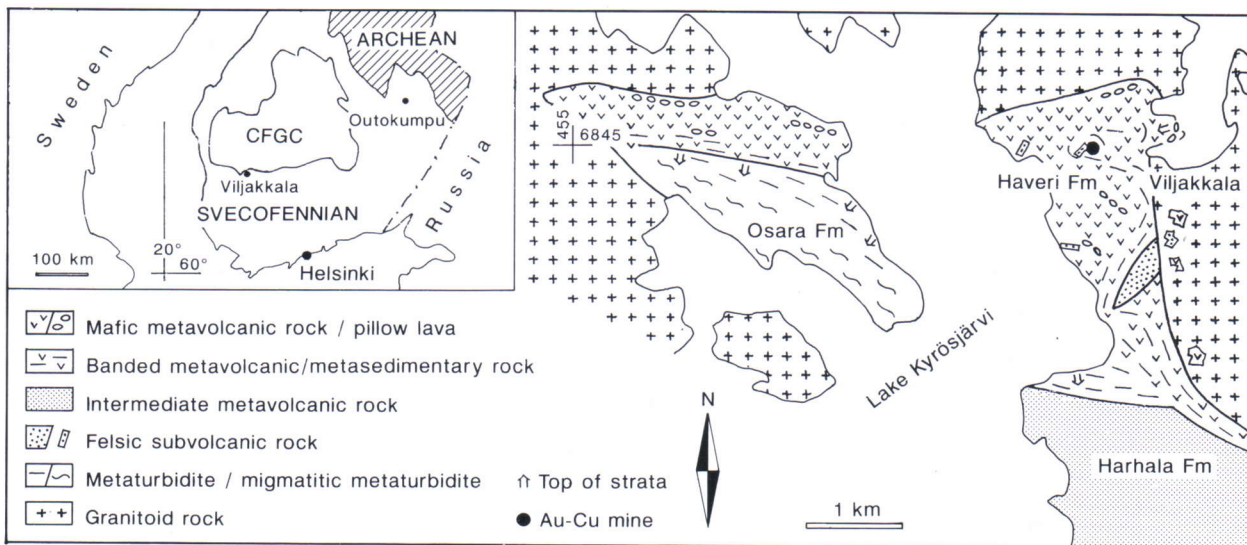


Fig. 1. Geological map of the Viljakkala area. The location of the study area in the Svecofennian Domain is shown in the inset. CFGC = Central Finland Granitoid Complex.

ROCK TYPES

The predominant volcanic rocks of the Haveri Formation are mafic metalavas. These rocks are usually rather massive, but pillow structures, flow breccias, and hyaloclastic breccias have been identified (Figs. 2a and 2b). In places the pillows contain amygdules near their margins. Uralite and plagioclase phenocrysts are present in the metalavas, but distinctly porphyritic rocks are rare. Skarn and limestone interlayers, 10-30 cm in width, as well as cherty bands occur in the metalavas (Mäkelä 1980).

Mafic metatuffs and intermediate metatuffites are associated with the metalavas, e.g. at the Au-Cu deposit. These streaky or banded rocks are usually sulfide-bearing to various degrees; the weathering surface of the rocks is brownish due to the sulfide content. White mica is an abundant mineral in the sulfide-rich lithologies. Fine-grained, graphite-rich black schists are also present. These rocks grade into rocks containing garnet, cordierite and staurolite porphyroblasts. Hence, there seems to be a continuous gradation from volcanoclastic rocks to epiclastic ones. The epiclastic rocks (metagraywackes) in the southern part of the map area (Fig. 1) also contain sulfides.

To the south and southwest of the Haveri Formation, metaturbidites occur that differ markedly from the banded rocks described above. These rocks, designated in this study as the Osara Formation, are grayish, and the content of opaque minerals is low. They are well-preserved on the eastern shore of Lake Kyrösjärvi, consisting mostly of sand-dominated turbidites (bed thickness up to 2 m), with the silty/muddy upper portions being only several cm thick. The muddy units contain slightly elongate gray spots 1-4 cm in diameter that have a core of fine-grained white mica, biotite and opaque minerals, and a rim of larger muscovite laths (Fig. 2c). In places the spots consist solely of muscovite laths. The mineral composition and elongate form suggest that the spots are pseudomorphs of andalusite or staurolite.

Outcrop evidence and drilling on the western shore of Lake Kyrösjärvi through the contact between the Haveri and Osara Formations show that the sulfide-bearing banded rocks of the Haveri Formation grade

into the metaturbidites of the Osara Formation, i.e. the contact west of Lake Kyrösjärvi is not a fault. The metamorphic grade is slightly higher in the mica schists west of Lake Kyrösjärvi than on the eastern shore. Moreover, the mica schists grade into migmatitic mica gneisses towards the SW.

To the south of the Osara Formation, various metavolcanic rocks occur (streaky/banded tuffs and tuffites, tuff breccias and lapilli tuffs). The rocks are mostly of intermediate composition, but felsic varieties also exist. These rocks form part of a poorly exposed unit, termed here as the Harhala Formation.

The plutonic rocks intruding the Haveri Formation are intermediate to felsic in composition. West of Lake Kyrösjärvi, the igneous rocks are medium-grained tonalites and granodiorites containing xenoliths of supracrustal rocks. East of the Haveri Formation, there is a roundish pluton of granodioritic composition which contains dioritic/gabbroic portions. The western contact of this granodiorite brecciates the supracrustal and subvolcanic rocks.

The granodioritic rock to the north of the mine is porphyritic, with a fine-grained groundmass. The porphyritic texture with distinctly zoned plagioclase phenocrysts gives the rock a subvolcanic appearance. In addition, sulfide-bearing felsic rocks containing quartz aggregates in a fine-grained matrix occur as enclaves within the granodiorite.

Felsic and intermediate dyke rocks cut the rocks of the Haveri Formation around the Au-Cu deposit. A rather extensive felsic rock (labelled as felsic subvolcanic rock in Fig. 1) cuts the supracrustal rocks south of the mine. The fine-grained rock contains abundant quartz aggregates (recrystallized phenocrysts?) and anhedral feldspar phenocrysts 1-3 mm in diameter. The rock is granodioritic/rhyodacitic in composition, and presumably subvolcanic in origin. Felsic dyke rocks of similar mineralogy are also present elsewhere within the mafic metalavas. A dyke rock of intermediate (dacitic) composition occurs at the western border of the open pit. It is porphyritic, with small (1-2.5 mm) plagioclase and quartz phenocrysts.

STRUCTURES

Pillow-structures in metalavas, banding in metatuffs, limestone interlayers, and bedding in sedimentary rocks were used to identify primary layering. Primary younging indicators were found both in the metavolcanic and metasedimentary rocks.

To the east of the Haveri deposit, near the contact with the intrusive rocks, the mafic metalava has a

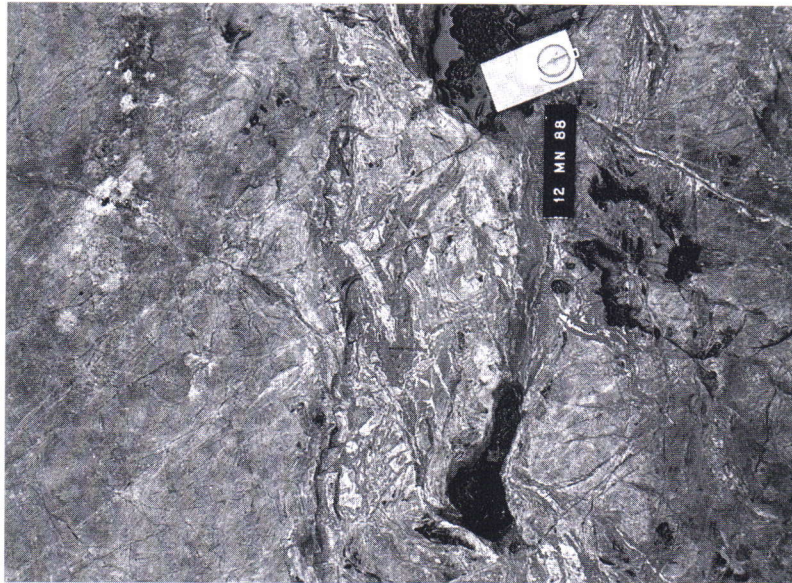
well-preserved pillow structure. The "tails" of the pillows and the preferential occurrence of amygdules at the margins of the pillows opposite to the "tails" indicate that the top is to the SW (Fig. 2a). A banded, sulfide-bearing tuffite overlies the mafic metalava.

Mäkelä (1980) identified only one younging

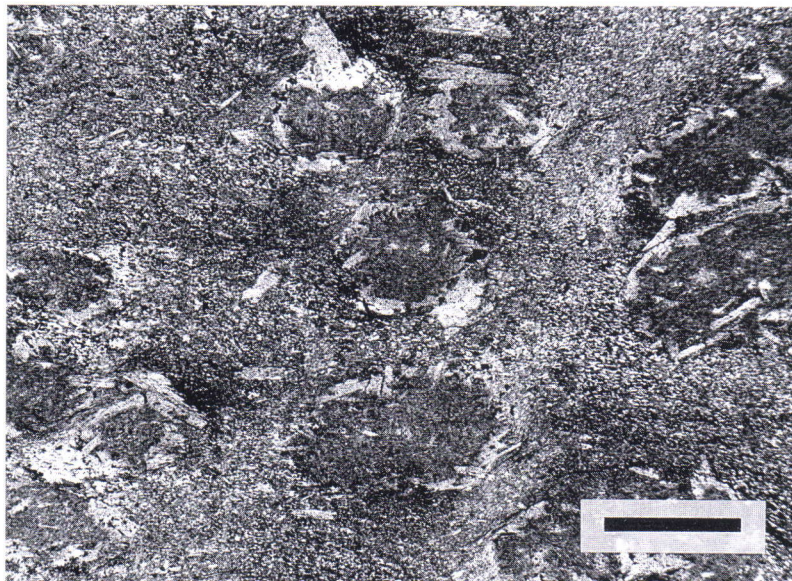
2a)



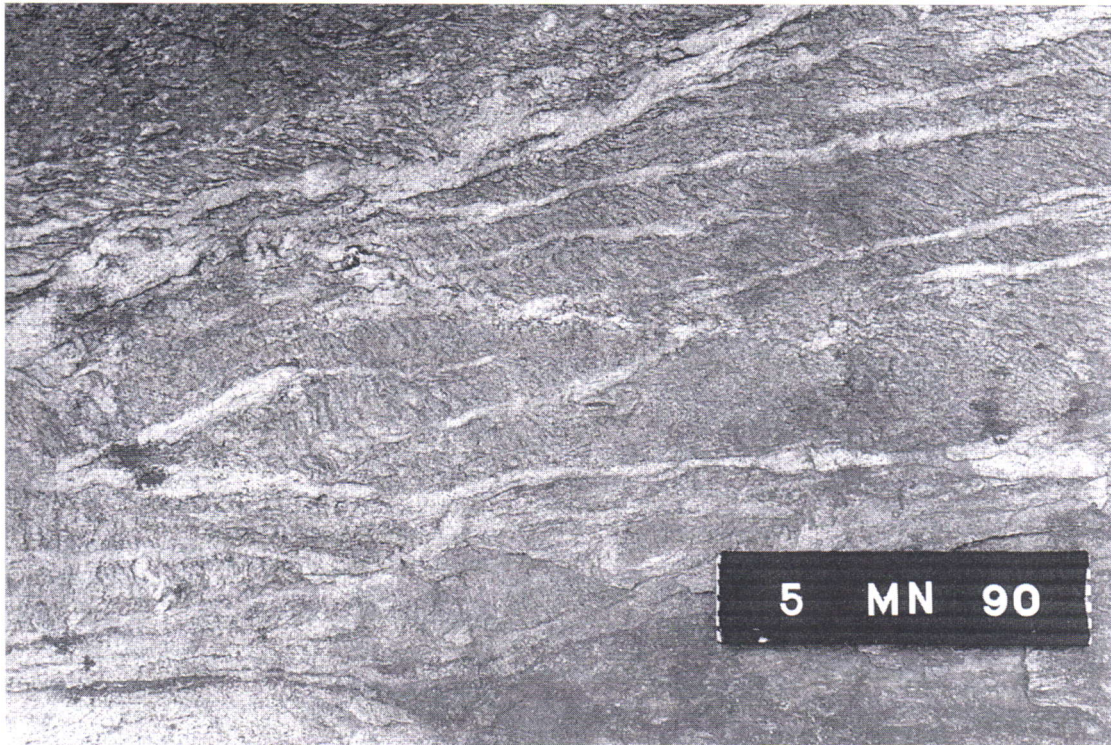
2b)



2c)



2d)



2e)

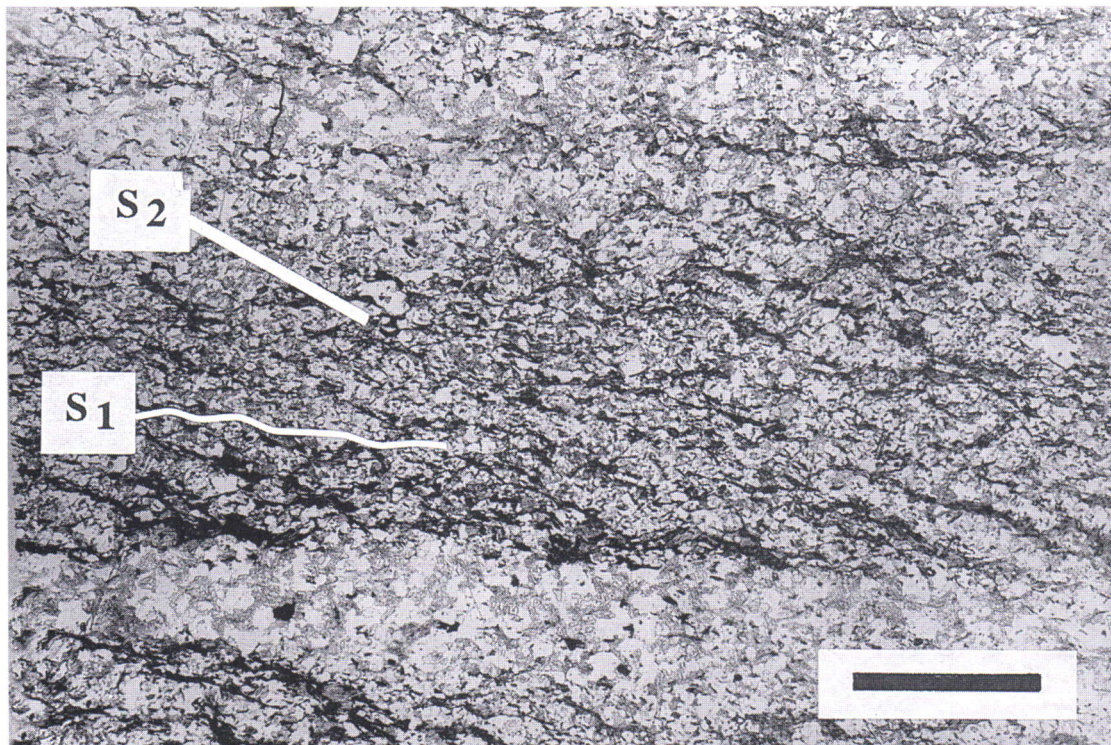


Fig. 2. **a)** Pillow lava. Note the amygdules in the margin of the pillow. Peltosaari, 1 km east of the Haveri mine. Length of pen is 13 cm. **b)** Hyaloclastic breccia between massive lava (left) and pillow lava (right). Ansomäki, 1 km south of the Haveri mine. Length of code bar is 16 cm. **c)** Photomicrograph of S_1 schistosity wrapping around pseudomorphosed porphyroblasts in muddy part of metaturbidite. The pseudomorphs consist mainly of fine-grained muscovite. The randomly oriented larger muscovite laths have overgrown S_1 . Eastern shore of Lake Kyrösjärvi. Scale bar 2 mm. **d)** Leucosome veins, subparallel with weakly developed S_1 schistosity, crenulated by S_2 . Western shore of Lake Kyrösjärvi. Length of code bar is 16 cm. **e)** Photomicrograph of S_1 schistosity, subparallel leucosome veins, and S_2 crenulation cleavage. Same site as in Fig. 2d. Scale bar 5 mm.

indicator in the Osara area, and inferred from this that the metaturbidites overlie or are the lateral extensions of the Haveri Formation. During this study, several other younging directions were measured in the metasediments near the contact with the metavolcanic rocks, and all of them imply younging to the S-SW. Moreover, the stratigraphic top is also to the SW at the contact between the sulfide-bearing schists and the metaturbidites. This confirms that the metaturbidites do in fact overlie the Haveri Formation rather than represent lateral facies variations. The position of the Harhala Formation to the south of the Osara Formation also suggests that the former overlies the latter.

The layered volcanic and sedimentary rocks contain a penetrative schistosity parallel or subparallel to the primary layering (Fig. 3). This was named S_1 , by analogy with the structures in the central TSB (Nironen 1989). In the metalavas, pillows and breccia fragments are elongate parallel to S_1 . In the metatuffs, S_1 is expressed as a weak preferred orientation of hornblende, while in the metatuffites and muddy units of the metaturbidites S_1 is defined by the alignment of micas. S_1 is rather weakly developed in the sandy units of the metaturbidites.

In the metatuffites, S_1 wraps around garnet porphyroblasts, indicating that garnet grew before the termination of D_1 . In the muddy parts of the metaturbidites, S_1 wraps around the muscovite-rich andalusite/staurolite pseudomorphs (Fig. 2c). The muscovite laths overgrow S_1 , implying that pseudomorphism was a post- D_1 event. In the areas where F_2 folding is evident, S_1 is crenulated in the mica-rich streaky/banded rocks. Chlorite flakes par-

allel to S_2 overgrow biotite, indicating that D_2 deformation was associated with retrograde metamorphism. The relationship between D_2 and pseudomorphism in the well-preserved metaturbidites is unclear, because no signs of D_2 deformation are visible in these rocks.

West of Lake Kyrösjärvi, the leucosomes in the migmatitic metaturbidites are parallel to the weakly developed S_1 (Figs. 2d and 2e). Because S_2 crenulates S_1 , migmatization occurred before D_2 deformation, probably during D_1 . The L_2 mineral lineation is intensely developed in the migmatites.

Airborne and ground geophysical measurements indicate a fairly continuous magnetic and electromagnetic anomaly within the Haveri Formation, caused by the sulfide- and graphite-bearing banded rocks, which curves around the Haveri mine (Fig. 4). The same horizon can be traced as an anomaly west of Lake Kyrösjärvi. The geophysical anomalies and the curvature of banding suggest a large fold at the site of the open pit. F_2 folding with a subvertical axial plane and moderately SW plunging fold axes can be seen around the open pit.

In the Haveri Formation, F_3 is manifested as open, fairly symmetric folding in the streaky rocks. At the microscale, retrograde chlorite flakes are strained at microfold hinges, indicating limited recovery/re-crystallization of chlorite during D_3 . D_3 fractures also occur in the intrusive felsic rock south of the mine and in the roundish body of granodiorite in the east. F_3 folding can be seen in several outcrops of migmatites W of Lake Kyrösjärvi. The F_3 fold axis is subparallel with L_2 , although no mineral orientation

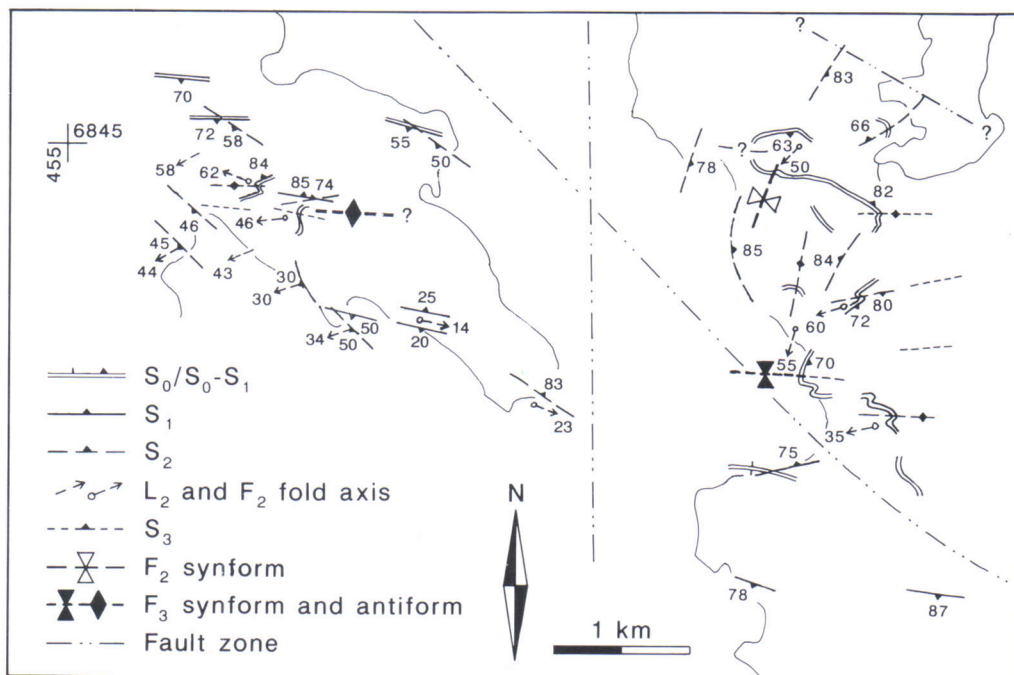


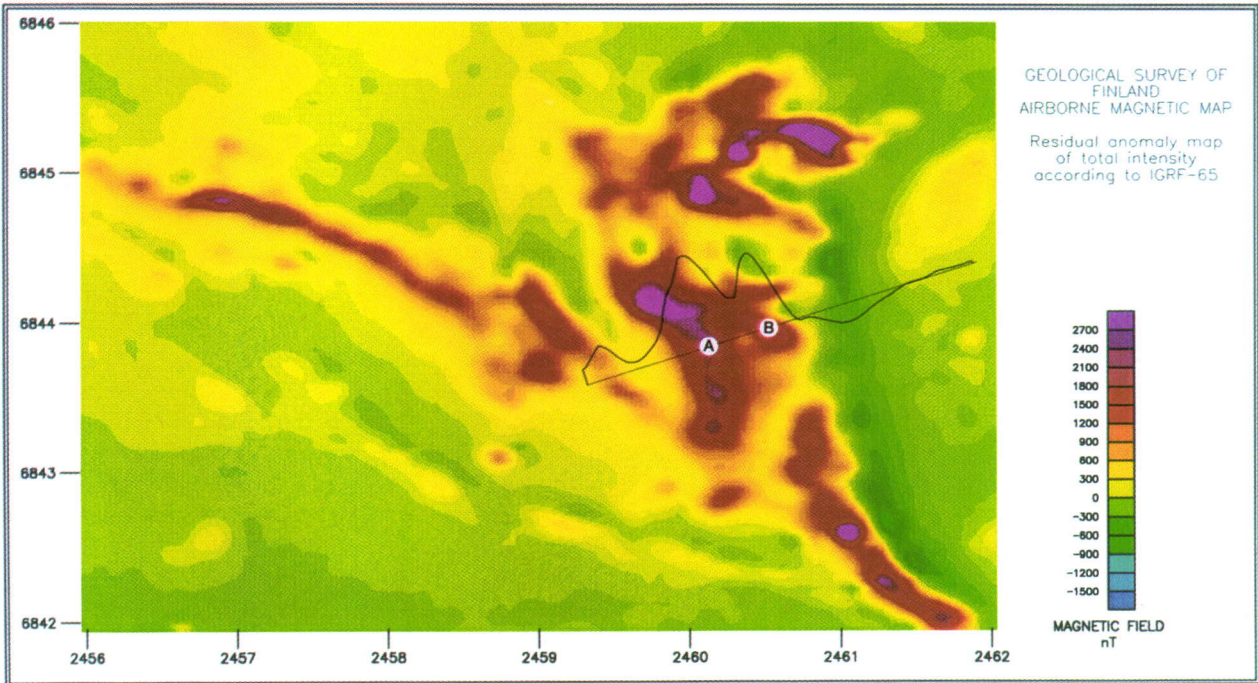
Fig. 3. Structural map of the Viljakkala area.

is mesoscopically evident in the axial plane.

Regional airborne magnetic measurements reveal the presence of two major faults crossing the study area. The older, NW-SE trending fault was delineated by the deflections in the magnetic anomalies (Fig. 4a) and it probably had a mainly horizontal sense of movement. This fault marks the contact E of Lake Kyrösjärvi

between the banded sulfide-bearing rocks of the Haveri Formation and the metaturbidites of the Osara Formation. The younger, N-S trending fault explains the slightly higher metamorphic grade in the mica schists W of Lake Kyrösjärvi. Offset along the fault is presumably vertical (west side up), because there is no major lateral deflection in the geophysical anomalies.

4a)



4b)

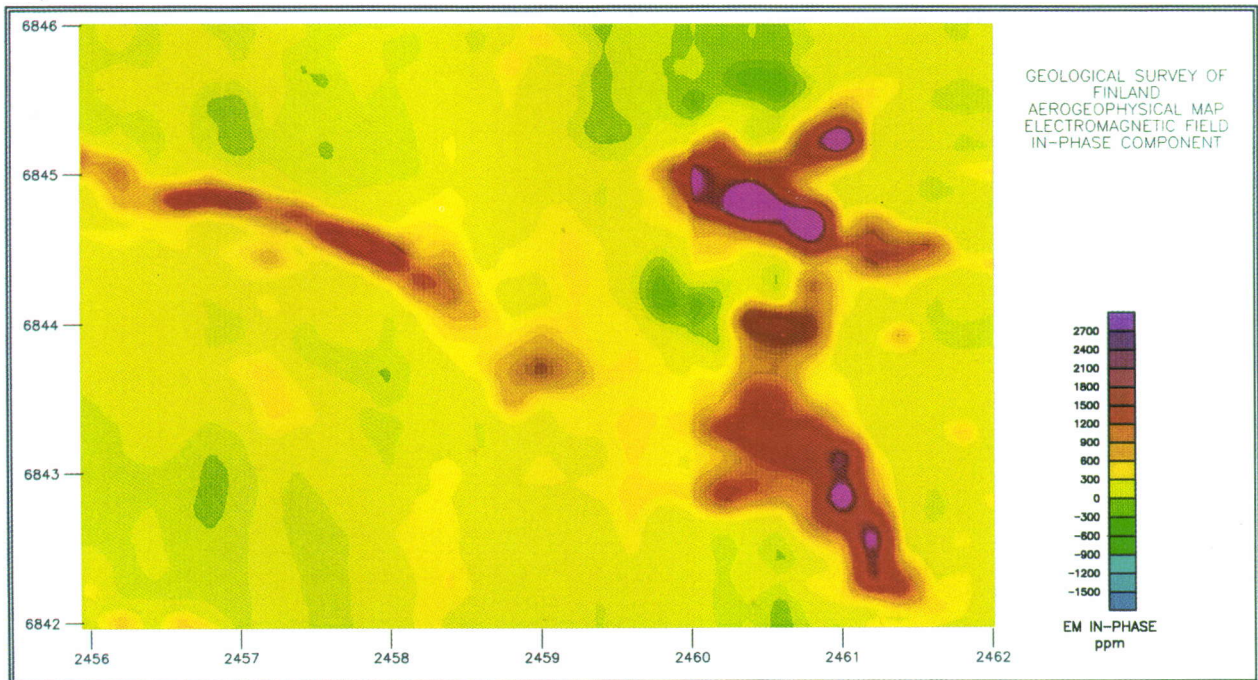


Fig. 4. Low altitude airborne geophysical maps of the area around the Haveri mine (Geological Survey of Finland, Geophysical Department). **a)** Magnetic map. Two positive anomalies (A and B) are marked along the cross-section. See text for explanation. **b)** Electromagnetic map (inphase component).

STRUCTURAL ANALYSIS

An unequivocal analysis could not be made of the structures in the study area. This is largely due to the fact that large areas of bedrock are covered by water or overburden. A structural analysis of the central part of the TSB, near Tampere (Fig. 1), has been carried out by Nironen (1989). In the central TSB, the structure is rather simple, with a major upright F_1 syncline trending E-W. Considering the observed younging to the SW at Viljakkala, the supracrustal rocks as a whole probably represent the northern limb of a major F_1 syncline.

The scarcity of younging observations makes it difficult to outline a stratigraphic sequence within the Haveri Formation. Based on the lithology W of Lake Kyrösjärvi, a pillow-structured metalava unit is at the base of the stratigraphic sequence. Pillow lavas probably exist at several stratigraphic levels between the massive and breccia-type metalavas. Moreover, the S_1 - S_2 relationship is not clear in the hinge zone of the large fold in the area around the Au-Cu mine. In the western part, the scarcity of outcrops makes a detailed analysis impossible. Although all the younging directions are to the south, the S_1 - S_2 relationship and the distinct L_2 in the Osara Formation implies F_2 folding, in places overprinted by almost

coaxial F_3 folding.

The zonal magnetic anomaly in the center of the Haveri Formation (Fig. 4a, anomaly A) and the negative anomaly at the same site in the electromagnetic map (Fig. 4b) were studied in detail. A best-fit polygon model across a WNW trending section suggests a magnetic layer at a depth of 60-100 m at anomaly A, whereas anomaly B extends up to ground level (compatible with the observed sulfide-bearing layers at site B). Such a deep-seated magnetic/conductive layer would explain the lack of an electromagnetic anomaly at site A.

Two models are presented for the structural evolution (Fig. 5). The first model is partly based on the above geophysical modelling. In this model, progressive sinistral shear and contemporaneous pluton emplacement during D_2 caused clockwise rotation and folding of strata in a contractional imbricate fan-type setting (cf. Woodcock and Fischer 1986). In the second model, the large fold is an F_1 fold, and the structure around the Au-Cu deposit is an F_1 - F_2 interference pattern. In both models subsequent N-S compression during D_3 caused folding with E-W axial trend and dextral faulting.

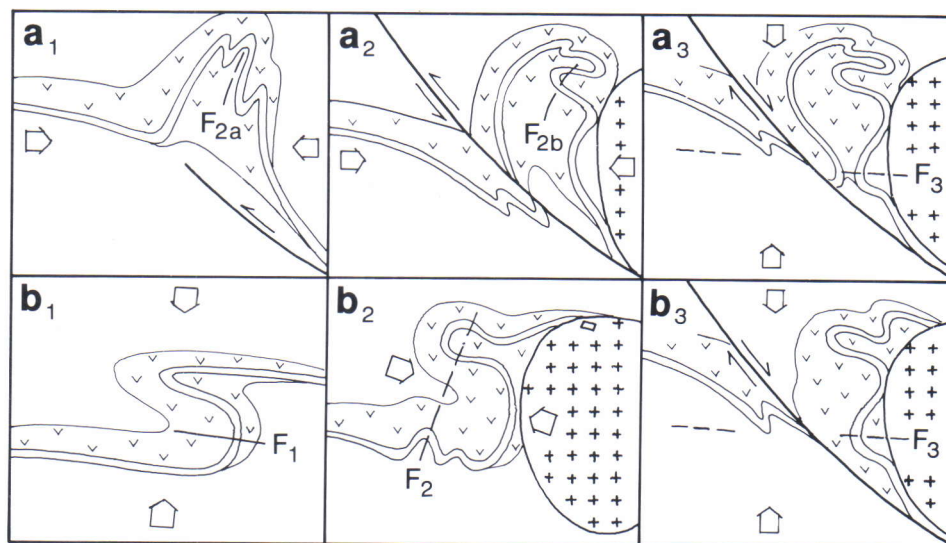


Fig. 5. Two models for the structural evolution of the supracrustal rocks around the Haveri mine. Only the rocks of the Haveri Formation are shown. Symbols as in Fig. 1 (sulfide-bearing rocks indicated by two parallel lines). Also the greatest principal stress (arrows) and the fold axial trends are shown. In the first model (a_1 - a_3), folds are formed in a contractional imbricate fan-type setting at the termination of a propagating sinistral fault (a_1). During progressive sinistral shear the strata are rotated clockwise, and the earlier foliation is overprinted by a later one. The granodiorite pluton is emplaced contemporaneously (a_2). N-S compression causes dextral shear along the fault together with folding (a_3). In the second model (b_1 - b_3), an early fold (b_1) is refolded, and the pluton is emplaced contemporaneously (b_2). N-S compression causes folding and dextral faulting (b_3).

GEOCHEMISTRY

Sampling sites and short descriptions of the analyzed samples are given in Appendix 1. Most of the analyses were made from pressed rock powder briquettes with a Philips 1480 XRF instrument at the Geological Survey of Finland (Table 1). The samples lacking Y determination were analyzed with a

Philips PW 1400/AHP XRF instrument at the Laboratory of Rautaruukki Oy (Ala-Vainio 1986). The rare earth elements, Ta, Hf, Th, Sc and Rb were determined by instrumental neutron activation analysis at the Technical Research Centre of Finland (Rosenberg et al. 1982).

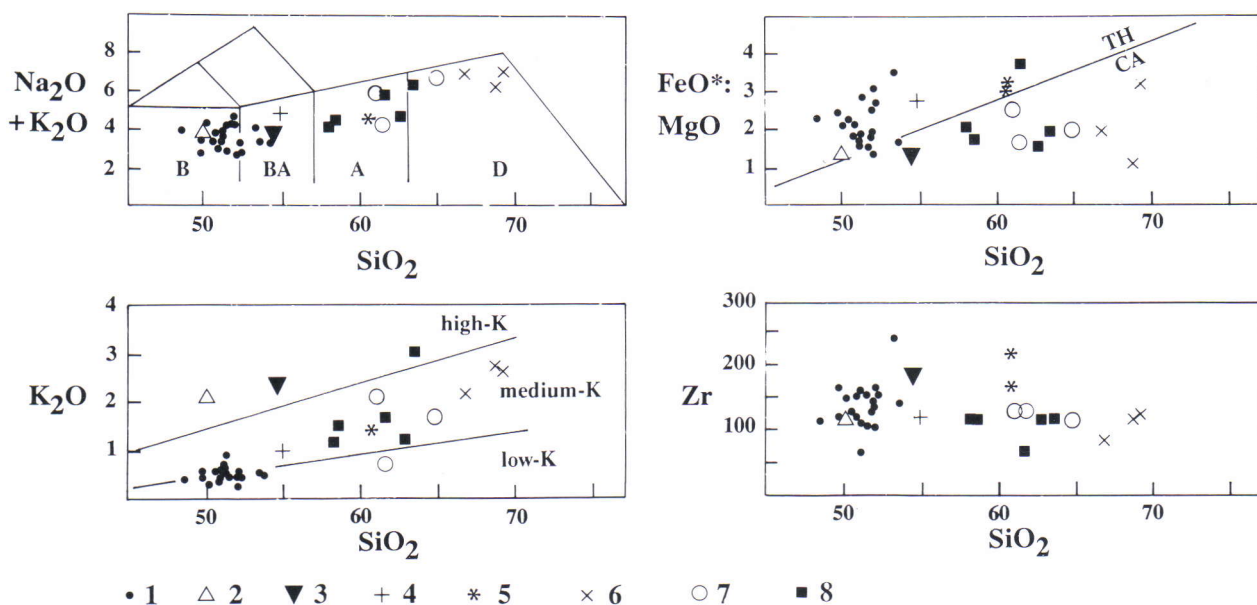


Fig. 6. SiO_2 variation diagrams of the rocks around the Haveri mine. Data from Table 1. a) Total alkali vs. SiO_2 (TAS) diagram. Fields from Le Maitre (1989, Fig. B13). B = basalt, BA = basaltic andesite, A = andesite, D = dacite. b) K_2O vs. SiO_2 diagram. Low-K, medium-K, and high-K fields from Le Maitre (1989, Fig. B15). c) FeO^*/MgO vs. SiO_2 diagram. Tholeiitic (TH) and calc-alkaline (CA) fields from Miyashiro (1974). d) Zr vs. SiO_2 diagram. 1 = Haveri metalavas, 2 = breccia lava (12-br-MN/88), 3 = Haveri metatuffite (18-MN/88), 4 = mafic dyke (12-dyke-MN/88), 5 = intermediate dykes (4-Hav/87, 5-Hav/87), 6 = felsic subvolcanic rocks (6-MN/88) and dykes (28-fels-MN/88, 29-S-fels-MN/88), 7 = granitoids (11-MN/89, 20-MN/89, Gr-Os/89), 8 = Harhala metavolcanic rocks.

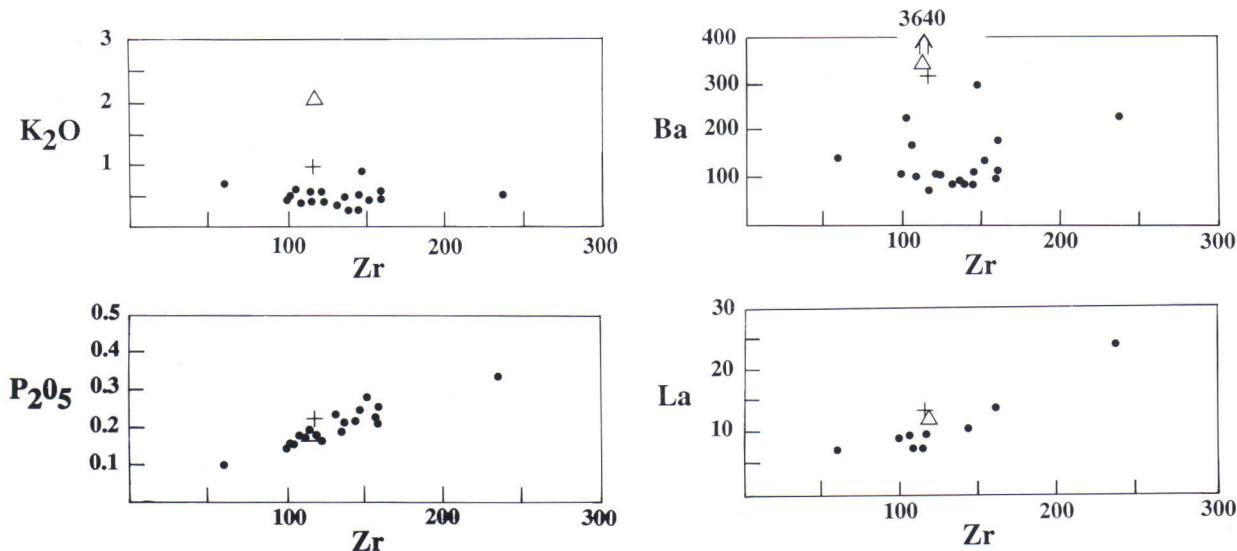


Fig. 7. Zr variation diagrams for the Haveri metalavas and the mafic dyke (12-dyke-MN/88). Data from Table 1, symbols as in Fig. 6.

Table 1. Major and trace element data for the rocks around the Haveri Au-Cu deposit. Oxides in weight%, trace elements in ppm. Total Fe as FeO. Most analyses by XRF at the Geological Survey of Finland and Rautaruukki (Ala-Vainio 1986). REE, Ta, Hf, Th, Sc and Rb by INAA (Rosenberg et al. 1982).

sample	METALAVAS EAST OF LAKE KYRÖSJÄRVI									META-TUFFITE					METALAVAS WEST OF LAKE KYRÖSJÄRVI				
	South of the mine									North and east of the mine									
	12-ty	12-ev	12-br	29-aft-	29-ur-	28-maf	29-S-ev	3-	17-	21-1	21-N	4-	6-B-	6-C-	18-	1-B-	101-	109-	102-
	MN/88	MN/88	MN/88	MN/88	MN/88	MN/88	MN/88	Hav/87	MN/88	MN/88	MN/88	MN/89	MN/89	MN/89	MN/88	MN/89	YK/89	YK/89	YK/89
SiO ₂	49.83	49.83	47.55	49.27	51.75	52.20	48.97	49.40	47.74	49.16	50.15	47.89	48.87	49.85	51.20	48.95	47.56	45.64	48.79
TiO ₂	1.24	1.31	1.46	1.69	1.58	2.32	1.91	1.50	1.86	1.77	1.71	1.51	1.50	1.49	0.39	0.81	1.67	1.76	1.81
Al ₂ O ₃	14.53	14.12	15.81	13.32	12.65	12.91	12.91	13.40	13.59	13.88	13.53	12.76	13.61	13.69	14.20	14.07	13.33	13.03	11.90
FeO	9.28	8.15	7.24	12.35	10.25	14.04	10.68	12.87	12.58	12.39	10.48	12.59	11.00	9.93	8.87	11.03	14.19	15.13	14.72
MnO	0.15	0.21	0.27	0.15	0.19	0.20	0.19	0.26	0.21	0.11	0.11	0.17	0.15	0.15	0.19	0.19	0.23	0.26	0.24
MgO	6.60	6.41	5.68	6.03	6.38	4.20	7.13	5.28	5.47	6.23	5.63	5.90	6.33	5.84	6.45	6.84	6.13	6.96	5.47
CaO	11.20	12.11	13.77	10.61	10.60	8.11	11.02	10.00	11.98	10.51	10.65	11.11	11.48	11.37	9.18	10.71	9.39	7.91	9.57
Na ₂ O	3.46	3.43	1.67	3.01	2.64	3.28	2.59	2.10	2.22	3.90	4.10	2.47	3.14	3.50	1.20	2.67	2.70	3.22	1.81
K ₂ O	0.35	0.43	1.95	0.47	0.41	0.46	0.46	0.27	0.38	0.21	0.20	0.49	0.31	0.37	2.24	0.64	0.47	0.32	0.77
P ₂ O ₅	0.13	0.14	0.16	0.20	0.18	0.32	0.21	0.22	0.20	0.21	0.20	0.16	0.17	0.15	0.14	0.09	0.16	0.16	0.23
sum	96.77	96.14	95.56	97.10	96.63	98.04	96.07	95.30	96.23	98.37	96.76	95.05	96.56	96.34	94.05	96.00	95.83	94.39	95.31
S	0.03	0.04	0.13	0.05	0.09	0.18	0.03		0.01	0.00	0.40	0.00	0.03	0.00	0.92	0.00	0.04	0.09	0.24
Cl	638	510	237	525	420	425	479		457	473	500	1795	1023	937		269	114	202	193
Zr	98	100	115	144	135	235	157	130	158	143	137	119	115	122	190	58	113	107	146
Cr	286	286	323	72	81	39	183	80	46	82	82	87	150	154	90	317	101	135	150
Ni	105	89	79	66	77	42	97	50	72	75	67	41	91	71	250	74	76	99	89
Sr	224	207	259	213	215	239	181	110	188	208	197	184	240	224	180	203	227	139	177
Ba	101	218	3621	104	86	222	92	80	104	79	81	100	66	99	620	140	123	94	291
V	342	350	369	381	356	515	409	370	448	445	416	395	412	401	830	261	413	437	468
Zn	76	95	124	75	81	97	87	90	128	63	54	86	75	76	140	99	132	125	131
Cu	21	154	107	130	231	130	28	150	13	9	582	0	19	0	300	0	143	52	256
Nb	7	5	8	13	10	16	12		8	7	6	6	7	3		6	7	5	13
Ta	0.367		0.426			0.926			0.474	0.497			0.451					0.381	0.345
Hf	2.38		2.43			5.66			3.72	3.39			3.03			1.21	2.91	2.6	
Th	0.635		0.669			2.76			0.586	0.81			0.595			0.387	0.439		
Sc	46.2		52.1			41.7			53.6	51			50			45.7	45.7	49.4	
Rb			49.8															12.8	
La	8.5		11.9			23.9			12.6	10.2			9.22			6.47	6.67	6.87	
Ce	17.5		20.7			42.6			23.9	21.2			17.9			12.6	14.9	15	
Nd	12		11.7			24.9			15.2	15.3			13.4			8.18	10.8	10.6	
Sm	3.25		3.68			6.84			4.92	4.66			3.81			2.11	3.91	4.08	
Eu	1.21		1.55			2.16			1.84	1.73			1.51			0.811	1.52	1.57	
Tb	0.652		0.703			1.09			0.886	0.896			0.807			0.511	0.795	0.839	
Yb	1.94		2.15			3.62			2.62	2.79			2.52			1.61	2.31	2.46	
Y	22	20	24	23	23	39	31		36	28	31	27	31	28		19	29	28	34
La _N :Yb _N	2.89		3.65			4.35			3.17	2.41			2.41			2.65	1.90	1.84	

Table 1. (cont.)

sample	METALAVAS WEST OF LAKE KYRÖSJÄRVI				MAFIC DYKE	SUBVOLCANIC ANDESITES		FELSIC DYKES AND PORPHYRIES			HARHALA VOLCANICS					GRANITOIDS		
	103-1 YK/89	104-4 YK/89	106-6 YK/89	7- Hav/87	12-dyke MN/88	4- Hav/87	5- Hav/87	28-fels MN/88	29-S-fels MN/88	6- MN/88	1- Korpela	112-a YK/89	113- YK/89	114- YK/89	16- MN/89	Gr- Os/89	11- MN/89	20- MN/89
SiO ₂	50.24	49.17	48.84	50.90	53.22	59.70	59.80	67.80	67.40	65.20	60.80	61.50	55.20	54.60	61.10	60.50	64.20	60.40
TiO ₂	1.97	1.31	1.51	1.60	1.06	0.79	0.76	0.24	0.24	0.24	0.64	0.48	0.71	0.67	0.70	0.68	0.34	0.76
Al ₂ O ₃	12.48	13.98	12.77	13.60	15.85	17.80	17.70	15.80	16.20	16.60	18.50	15.00	15.80	14.90	15.80	15.80	16.40	16.90
FeO	14.42	11.03	12.70	13.51	10.43	7.25	7.21	2.93	2.28	2.90	5.97	5.89	7.43	7.09	5.28	6.53	3.99	6.31
MnO	0.21	0.19	0.26	0.24	0.17	0.12	0.15	0.04	0.06	0.10	0.12	0.13	0.13	0.14	0.12	0.13	0.10	0.14
MgO	4.86	6.17	6.36	5.26	3.88	2.42	2.26	0.93	2.14	1.49	1.64	3.18	3.75	4.42	3.40	4.09	2.02	2.50
CaO	9.27	10.79	10.84	9.81	7.67	5.98	6.04	3.34	3.66	4.38	5.09	4.54	8.04	7.33	6.44	6.57	5.39	5.90
Na ₂ O	2.43	3.00	2.40	2.18	3.68	3.02	3.18	4.28	3.45	4.64	4.13	3.18	2.85	2.82	3.38	3.50	4.91	3.71
K ₂ O	0.50	0.54	0.37	0.37	0.91	1.35	1.33	2.49	2.60	2.02	1.57	2.85	1.03	1.30	1.11	0.65	1.62	2.06
P ₂ O ₅	0.24	0.14	0.17	0.27	0.21	0.25	0.26	0.12	0.13	0.13	0.46	0.28	0.21	0.20	0.21	0.18	0.22	0.36
sum	96.62	96.32	96.22	97.74	97.08	98.68	98.69	97.98	98.16	97.70	98.92	97.04	95.15	93.48	97.54	98.62	99.18	99.04
S	0.03	0.01	0.01	0.32				0.28	0.17	0.17	0.15	0.09	0.01	0.01	0.01	0.02	0.14	0.04
Cl	71	181	267		294													
Zr	158	104	114	150	115	160	160	120	110	80	60	110	110	110	110	120	110	120
Cr	141	288	153	40	36	50	80				100	110	140	80	130			
Ni	74	100	75	50	10	20	10	10	20	10	10	30	30	20	20	50	20	10
Sr	216	204	209	140	381	340	360	490	240	720	1470	640	500	370	620	350	860	590
Ba	173	164	125	130	318	510	500	1010	1520	790	1010	780	470	670	880	380	920	750
V	486	353	408	390	309	140	120	50	60	80	150	140	190	190	190	160	90	140
Zn	138	111	140	130	118	100	100	30	40	70	110	90	70	80	80	90	60	90
Cu	90	61	14	90	74	160	80	170	100	20	50	90	70	20	50	10	10	20
Nb	10	6	5		8													
Ta	0.714	0.383			0.36	0.522		0.965						0.639			0.623	
Hf	3.9	2.7			2.66	3.26		4.21						3.28			3.12	
Th	0.867	0.636			1.73	2.59		4.26						2.65			4.44	
Sc	50.7	47.4			37.5	24.1		5.74						34.2			13.4	
Rb					43.7	36.4		57.1						28.6			22.9	
La	13.1	8.81			13.1	22.9		20.5						16.3			24.8	
Ce	25.6	17.5			27.9	38.7		35.2						27.7			40.4	
Nd	18.9	12.2			18.6	23.8		16.5						12.8			18.6	
Sm	5.73	3.35			4.04	4.07		2.67						3.04			3.03	
Eu	1.83	1.3			1.31	1.27		0.918						1.09			1.14	
Tb	0.948	0.69			0.639	0.641		0.375						0.514			0.399	
Yb	3.19	2.01			1.93	2.16		1.14						1.66			1.41	
Y	37	25	27		24													
La _N :Yb _N	2.71	2.89			4.47	6.98		11.85						6.47			11.59	

Haveri Formation

The Haveri metalavas are low-K/medium-K basalts with tholeiitic affinities (Fig. 6; see also Mäkelä 1980). The tholeiitic trend is corroborated by the increase in V and Ti contents with increasing Zr (Figs. 7 and 10). The REE patterns are largely parallel (Fig. 8) and display slight enrichment in LREE ($La_N:Yb_N = c. 3-7$; see also Kähkönen et al. 1981). Eu anomalies are lacking.

The hyaloclastic breccia (sample 12-br-MN/88)

differs from the other metalavas in having relatively high K, Rb, Al, Ca and high Ba contents, and a low Na content (Table 1). The breccia also displays a slight positive Eu anomaly. These features are probably due to primary alteration. Based on Fig. 9, the Haveri metatuffite does not correspond to any primary igneous composition.

As the metalavas fall mostly within the igneous spectrum, severe alteration is not evident in these

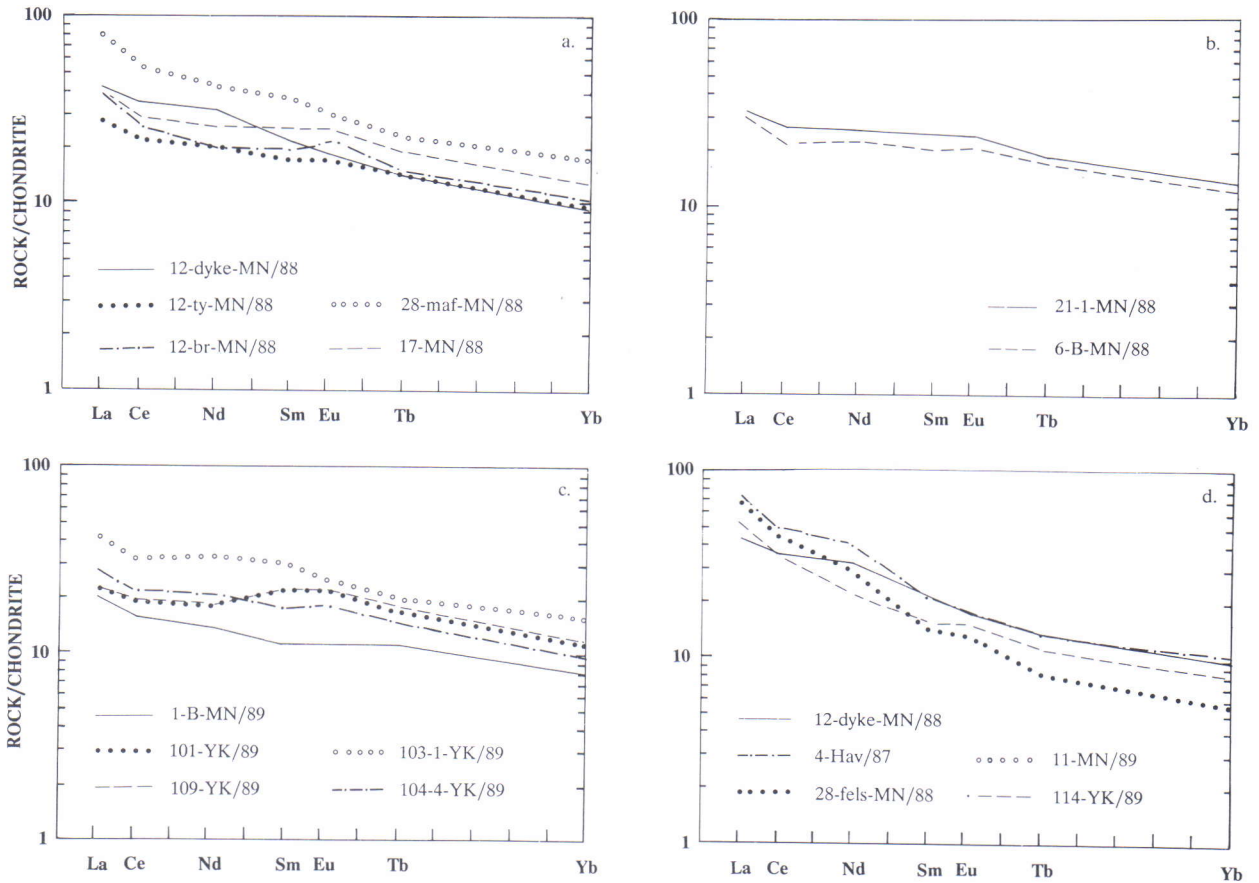


Fig. 8. Chondrite-normalized REE patterns of the rocks around the Haveri mine. Data from Table 1. Chondrite values: Leedeey-6 divided by factor 1.2 (Jahn et al. 1980, Tb from Koljonen & Rosenberg 1975).

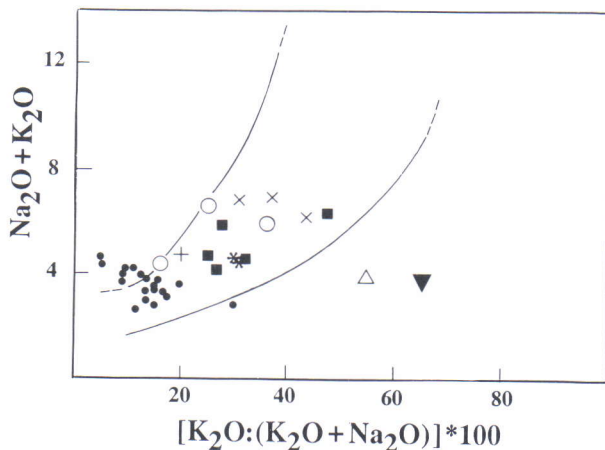


Fig. 9. Rocks around the Haveri mine plotted on the igneous spectrum of Hughes (1973). The lines delineate the field of relatively unaltered volcanic rocks. Data from Table 1, symbols as in Fig. 6.

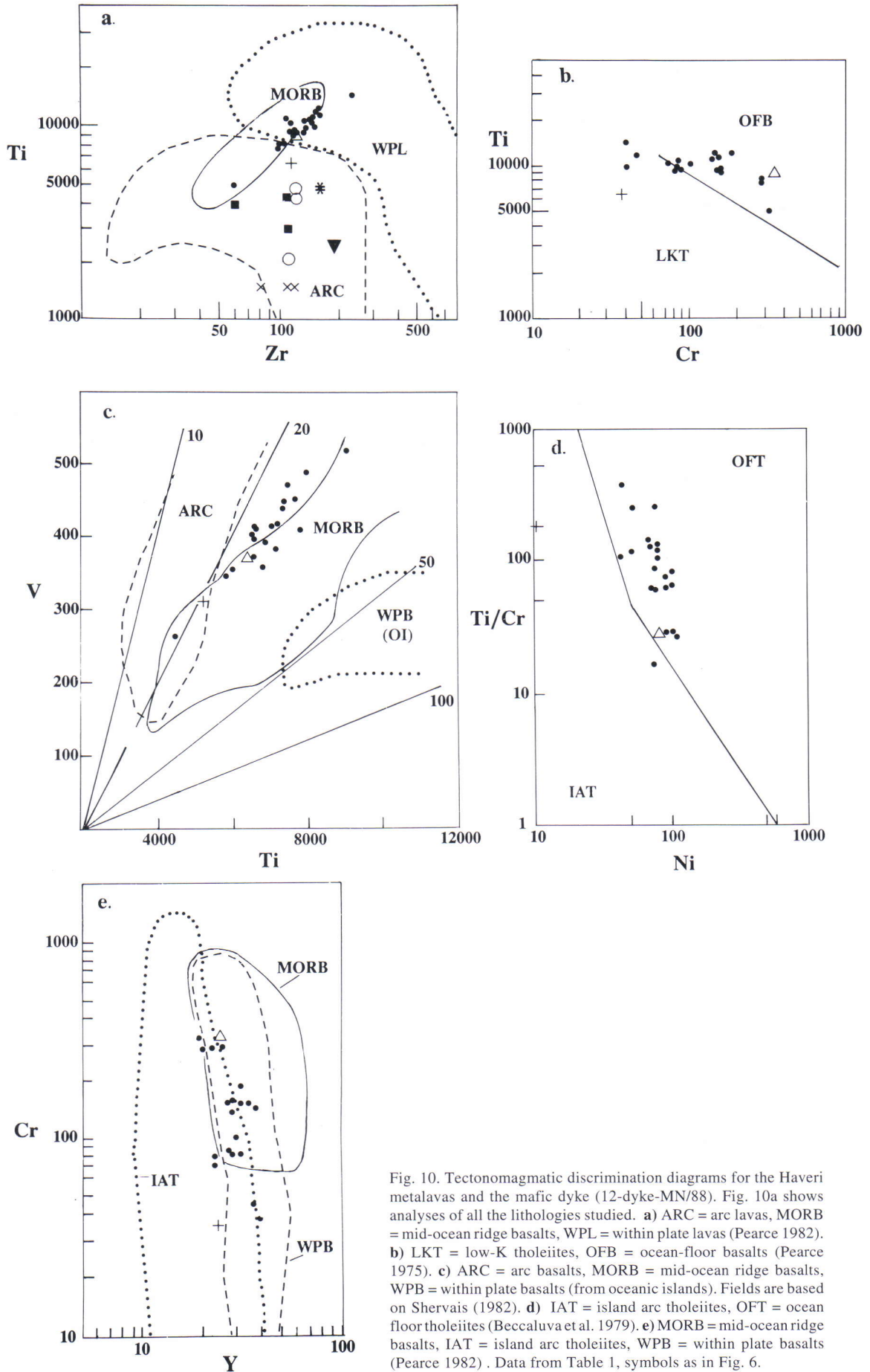


Fig. 10. Tectonomagmatic discrimination diagrams for the Haveri metalavas and the mafic dyke (12-dyke-MN/88). Fig. 10a shows analyses of all the lithologies studied. **a)** ARC = arc lavas, MORB = mid-ocean ridge basalts, WPL = within plate lavas (Pearce 1982). **b)** LKT = low-K tholeiites, OFB = ocean-floor basalts (Pearce 1975). **c)** ARC = arc basalts, MORB = mid-ocean ridge basalts, WPB = within plate basalts (from oceanic islands). Fields are based on Shervais (1982). **d)** IAT = island arc tholeiites, OFT = ocean floor tholeiites (Beccaluva et al. 1979). **e)** MORB = mid-ocean ridge basalts, IAT = island arc tholeiites, WPB = within plate basalts (Pearce 1982). Data from Table 1, symbols as in Fig. 6.

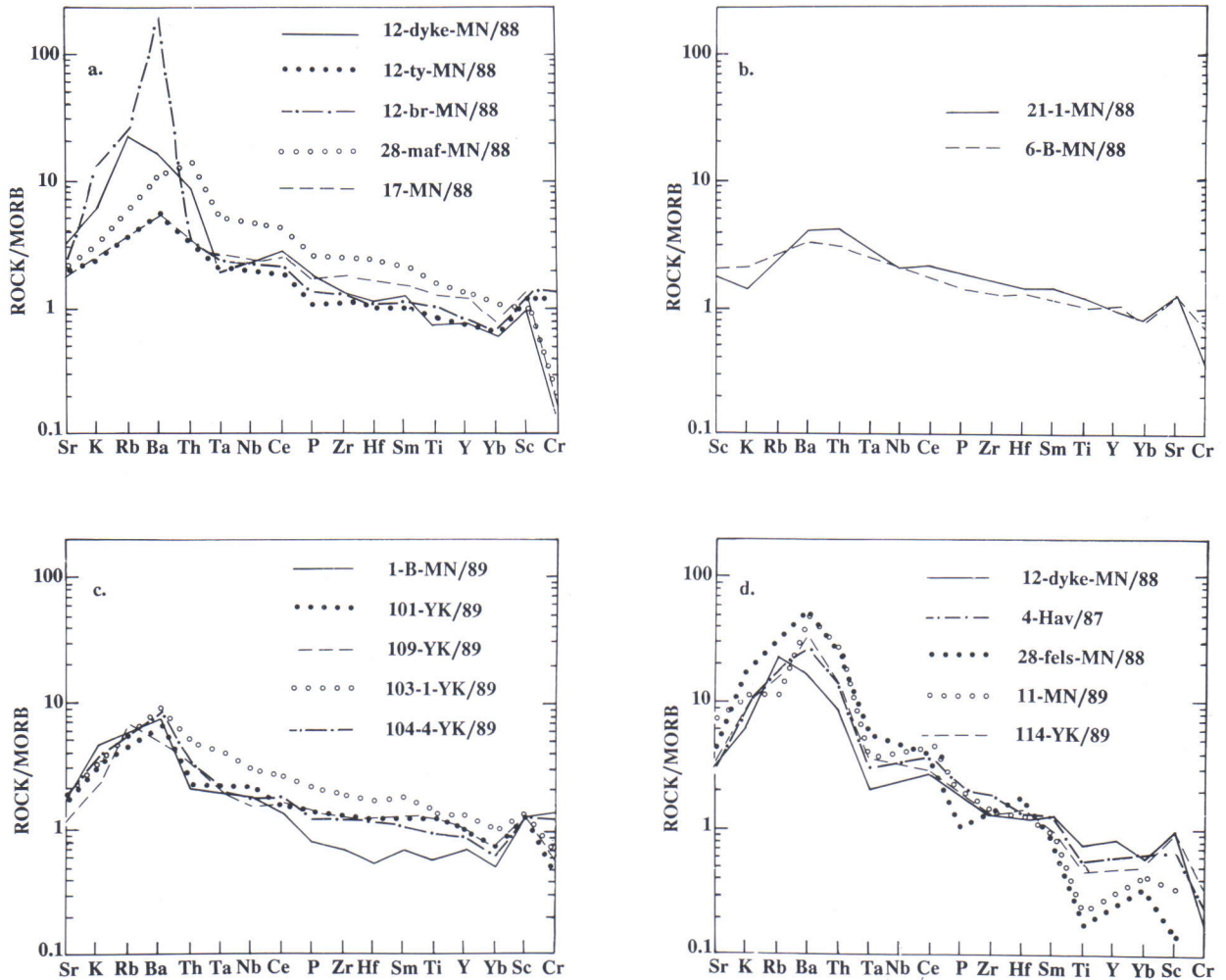


Fig. 11. Normal mid-ocean ridge basalt (N-MORB) normalized trace element patterns of the rocks around the Haveri mine. MORB values from Pearce (1982). Data from Table 1.

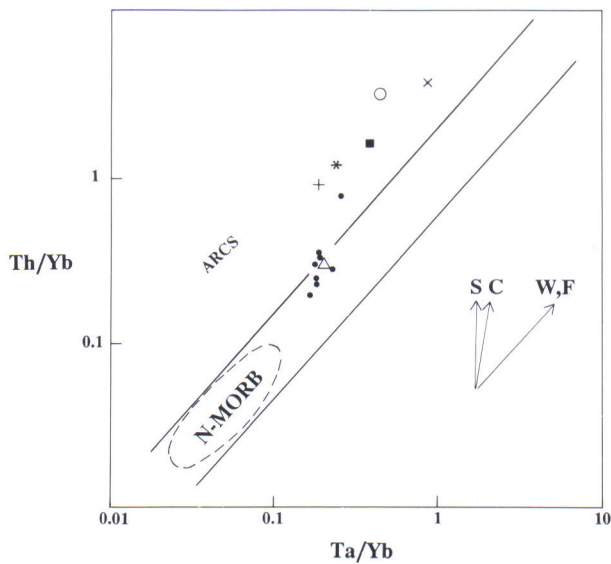


Fig. 12. Th/Yb vs. Ta/Yb diagram of the rocks around the Haveri mine. Data from Table 1, symbols as in Fig. 6. The parallel lines limit the field of mid-ocean ridge basalts and within plate basalts. Arc basalts (ARC'S) are above this array. Vectors: S = subduction zone enrichment, C = crustal contamination, W = within plate enrichment, F = fractional crystallization (Pearce 1983).

rocks. However, K and Ba do not show consistent variations with increasing Zr, unlike other incompatible elements such as P, Th, Ta and Nb (Nb not shown) (Fig. 7; see also Fig. 14). It is thus evident that alteration affected the distribution of K and Ba. The slight Ce minima in the REE patterns (Fig. 8) may be explained by circulation of seawater in the system, because seawater is depleted in Ce relative to other rare earth elements (Fleet 1984).

The Cl contents in the Haveri metalavas west of Lake Kyrösjärvi are lower (70-270 ppm; Table 1) than in those east of the lake (400-1800 ppm, with the exception of the breccia, 240 ppm). This difference is probably attributable to the higher metamorphic grade in the west, the content of Cl in the system having decreased due to volatile loss in the higher grade rocks.

Based on the contents and ratios of Ti, Zr, Cr, V, Ni and Y, the Haveri metalavas (including the breccia) resemble mid-ocean ridge basalts (MORB) or within plate basalts (WPB) rather than arc basalts (Fig. 10). In the MORB-normalized spidergrams, the metalava patterns from Th to Yb are mostly gently sloping and lacking prominent Ta and Nb depletions, confirming that the metalavas are not of arc type (Fig. 11; cf. Pearce 1982). In the Th/Yb vs. Ta/Yb diagram, the metalavas mostly lie within the MORB & WPB array (Fig. 12). Because of their relatively high LREE, P

and Zr contents, the Haveri metalavas can be distinguished from N-type MORB and they bear some resemblance to T-type (transitional between N-type and P-type) MORB and tholeiitic WPB (Wilson 1989, p. 138-142). They are also reminiscent of certain marginal basin basalts since these latter have tectonomagmatic affinities intermediate between arc basalts, various MORB and WPB.

Considering the position of the study area within the TSB, an extensional setting in a marginal basin (*sensu lato*; see Carey & Sigurdsson 1984) for the metalavas of the Haveri Formation is preferred over an oceanic divergent plate margin or oceanic within plate setting. However, it is not clear which type of marginal basin they represent, i.e., whether the basin was associated with subduction, transtension or spreading/rifting independent of subduction. The absence of pronounced Ta and Nb depletions in most of the Haveri metalavas distinguishes them from typical back-arc basalts, which tend to be depleted in these elements. However, back-arc basin basalts formed during the earliest stages of development of a subduction system lack this feature (Saunders & Tarney 1984). The arc affinity of the Haveri metalava in the Ti vs. Zr diagram (Fig. 10a) may be explained by mixing of heterogeneous material during redeposition.

Metavolcanic rocks of the Harhala Formation, subvolcanic and dyke rocks, and granitoids

The metavolcanic rocks of the Harhala Formation are andesitic in composition, and the felsic subvolcanic and dyke rocks as well as the granitoids are mostly dacitic (Fig. 6). Unlike the Haveri metalavas, however, the rocks have calc-alkaline affinities. They plot in the igneous spectrum and hence do not show signs of strong alteration (Fig. 9).

Sample 12-dyke-MN/88 is from a mafic dyke which crosscuts the Haveri metalavas. The sample is richer in SiO₂, K, Ba, Sr, Th and LREE than the metalavas. These characteristics might be explained by a simple differentiation process, but the relatively low Zr content of the dyke rock precludes the dyke

and the metalavas from being consanguineous.

The granitoids, dykes and subvolcanic rocks as well as the Harhala metavolcanics show arc affinities on the Ti vs. Zr and Th/Yb vs. Ta/Yb diagrams (Figs. 10 and 12). The LIL element (including LREE) enrichment and especially the deep slopes from Th to Ta and Nb in the MORB-normalized spidergrams are also typical of arc magmas (Pearce 1982). In this respect, the Harhala metavolcanics resemble the mafic dyke crosscutting the Haveri metalavas, corroborating the interpretation that the Harhala metavolcanics are younger than the Haveri Formation.

Petrogenesis of the Haveri metalavas

The steep Cr vs. Y trend (Fig. 10e) is explained by fractional crystallization rather than partial melting of mantle (Pearce 1982). The positive Ti vs. Zr trend (Fig. 10a) may be caused by fractional crystallization

of an assemblage without magnetite. However, the steep Th/Yb vs. Ta/Yb trend (Fig. 12) cannot be due to fractional crystallization alone and instead indicates either crustal contamination (assimilation) or

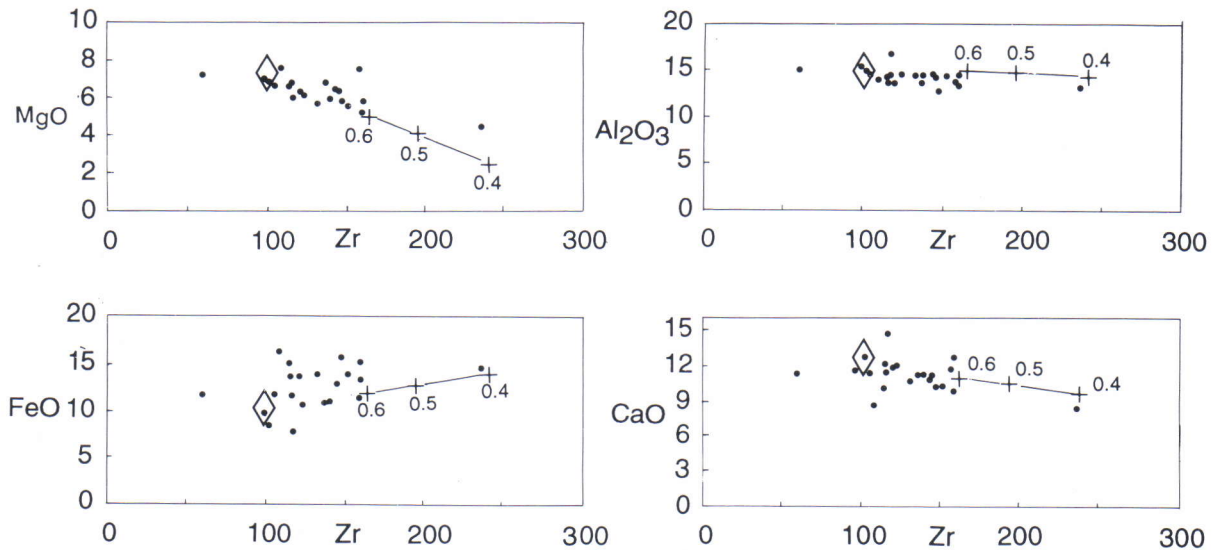


Fig. 13. Major element vs. Zr variation diagrams for the Haveri metalavas (dots) and of model compositions produced by closed-system fractional crystallization of the assemblage $OL_{0.1}CPX_{0.4}PLG_{0.5}$ (crosses). Major elements were calculated using mass-balance equations (e.g. Hanson 1980) with mineral compositions given in Appendix 2. Zr values were calculated as explained in Fig. 14. The assumed initial composition (open diamond; 15% Al_2O_3 , 10% FeO, 7% MgO, 12% CaO, 100 ppm Zr) was approximated from the composition of the Haveri metalavas with about 100 ppm Zr. Numbers 0.6, 0.5, 0.4 denote fractions of residual liquid.

the influence of a subduction zone component.

The analyzed material was modelled assuming a combination of fractional crystallization and assimilation, i.e. the AFC process (Figs. 13 and 14). Based on major elements (Mg, Fe, Ti, Ca, P) and most trace elements, the variation may be due to fractional crystallization of an assemblage $OL_{0.05-0.1}CPX_{0.4}$

$PL_{0.5}$ (Figs. 13 and 14; see also Appendix 2). In Fig. 14, the Th content in particular of the most evolved sample deviates from the closed system fractional crystallization trend and implies the assimilation of average fractional continental crust by a ratio of $r = 0.1$ (DePaolo 1981).

DISCUSSION

Mäkelä (1980, p. 73) inferred that the paleo-environment of the Haveri Formation was a low-energy one, in contrast to the high-energy environment indicated by the metaturbidites of the Osara Formation. The existence of amygdules, with diameters up to 10 mm, in the pillow lavas (Mäkelä 1980) indicates a shallow-water environment (approximately 100-1000 m; Jones 1969, Fischer 1984). The metatuffites and the sulfide-bearing epiclastic rocks in the southern part of the Haveri Formation are interpreted as mixtures of chemical sediments and weathering products of predominantly volcanic rocks. The gradation from volcanoclastic through sulfide-bearing epiclastic to purely epiclastic rocks of the Osara Formation records the change from a shallow basin with local sources to one with a more regional provenance.

The metavolcanics of the Harhala Formation are probably lateral equivalents of the 1904-1898 Ma old andesite- and dacite-rich units in the northern limb of

the major syncline (see Kähkönen et al. 1989). Based on their andesitic composition and the La/Yb and Th/Yb ratios, they resemble volcanics of fairly evolved arcs rather than primitive arcs (cf. Leeman 1983). The lack of primitive arc rocks is attributed to evolution near a slightly older magmatic arc.

Petrogenetic modelling suggests an AFC process for the evolution of the Haveri metalavas. The assimilated material may have been either sialic crust or crustally-derived sediments. The Haveri Formation was formed in an extensional setting, probably in a marginal basin. Oceanic marginal basins are floored by a sheeted dike complex and ultramafic to mafic plutonic units beneath the lava sequence, and together these units comprise ophiolites. Since there are relatively few outcrops of the Haveri Formation, the existence of a dyke complex or ultramafic units cannot be proved, or disproved. It is possible that the Haveri Formation represents an ensialic, relatively small extensional basin floored by attenuated

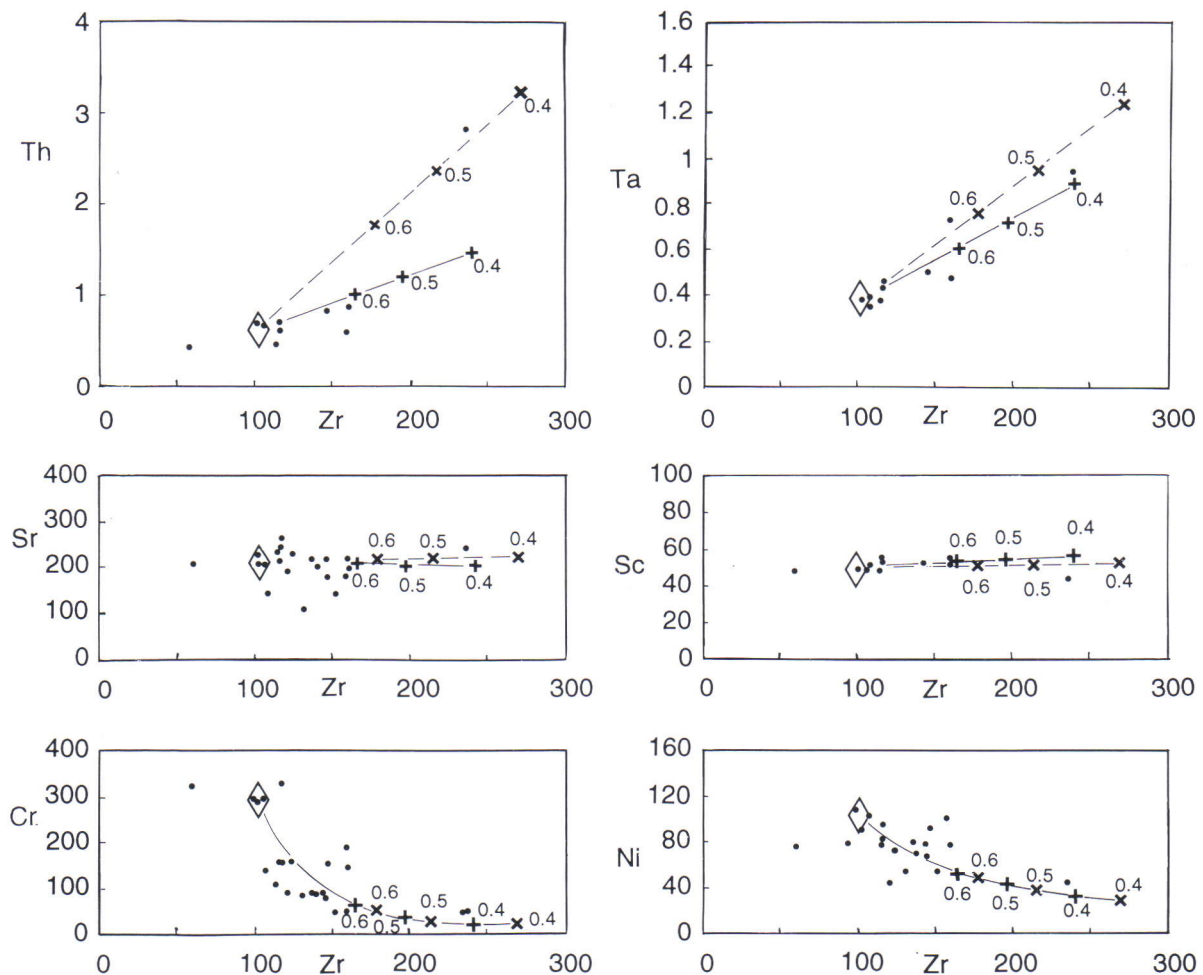


Fig. 14. Trace element vs. Zr variation diagrams for the Haveri metalavas (dots) and modelled liquids (crosses and inclined crosses). The model calculations were made using the MODULUS-program of Knoper (1990). Initial composition for the model calculations (open diamond; 100 ppm Zr, 0.6 ppm Th, 0.37 ppm Ta, 210 ppm Sr, 48 ppm Sc, 290 ppm Cr, 100 ppm Ni) is based on the composition of the Haveri metalavas with about 100 ppm Zr. Crosses and continuous lines denote closed-system fractional crystallization (FC, Rayleigh equation) of the assemblage $OL_{0.1}CPX_{0.4}PLG_{0.5}$. Inclined crosses and broken lines denote combined assimilation-fractional crystallization (AFC-process, DePaolo 1981) of the above assemblage with r (ratio of mass assimilation rate to fractional crystallization rate) of 0.1 using the average upper continental crust composition of Taylor and McLennan (1985) for the assimilant. Numbers 0.6, 0.5, 0.4 give fractions of residual liquid.

Distribution coefficients from Knoper (1990) and for Cr and Ni from Cox et al. (1979):

	OL	CPX	PLG
Zr	0.02	0.1	0.01
Th	0.02	0.02	0.05
Ta	0.03	0.06	0.04
Sr	0.015	0.1	2
Sc	0.3	2	0.04
Cr	1	10	0.004
Ni	15	2	0.004

(Paleoproterozoic) continental crust. A model for basin evolution, based on the one presented by Carey and Sigurdsson (1984), is given in Fig. 15. In their model, a magmatic arc is split to form a backarc between an active part of the arc and an inactive remnant arc. The active magmatic arc is the source of volcanoclastics, the backarc spreading center produces hyaloclastites and hydrothermally derived sediments, and the remnant arc is the source of gravity-flow deposits.

The Pb composition of the sulfides and the metalavas surrounding the Haveri Au-Cu mine differ from typical Svecofennian Pb compositions in being of mantle-type (Vaasjoki & Huhma 1987). Because Pb isotopes are sensitive to crustal contamination, extrusion of the Haveri metalavas through a thick sialic crust is improbable. The metalavas assimilated either primitive crust such as in an island arc, or crustally-derived sediments. The least radiogenic Pb in the sulfides of the Haveri deposit has

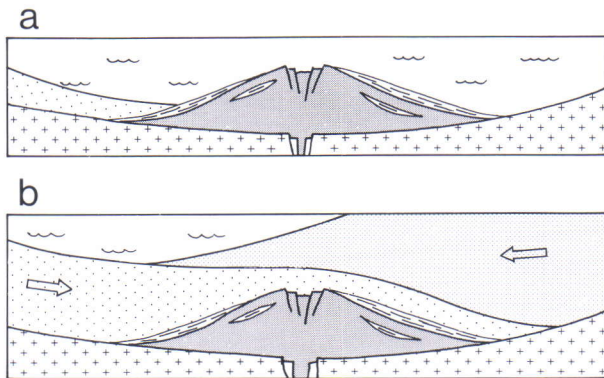


Fig. 15. A model for the evolution of the rocks around the Haveri Au-Cu deposit (modified from Carey & Sigurdsson 1984). Note the exaggerated vertical section. **a**) The mafic volcanic rocks (Haveri Formation; dark shaded area) extruded through a slightly older magmatic arc or thin continental crust (crosses) into a shallow, spreading subaqueous basin. Hydrothermal, sulfide-bearing sediments, mixed with redeposited, largely volcanic material, were deposited at the flanks of the spreading center. **b**) Voluminous turbidites (Osara Formation) covered the mafic volcanic rocks. These, in turn, were overlain by intermediate volcanic rocks (Harhala Formation; light-shaded area). The arrows show the interpreted transport directions.

the same isotopic composition as the galenas at the Outokumpu mine (Fig. 1; M. Vaasjoki 1992, personal communication).

The Pb isotopes, made of whole rock samples from Haveri, yielded an age of 1990 ± 25 Ma (Vaasjoki & Huhma 1987). The U-Pb zircon age of a gabbro body within the Outokumpu ophiolitic association is 1972 ± 18 Ma (Koistinen 1981). On the basis of this data, an episode of ocean spreading, lasting for some 70 Ma, might be envisaged. This scenario would mean that the Haveri Formation is an exotic remnant of an older ocean basin within an arc complex. However, the structures in the rocks hosting the deposit do not indicate a protracted evolutionary history, e.g. older folding episodes, for the Haveri Formation with respect to the overlying sequence. Rather, the geological and geochemical evidence suggest that tholeiitic mafic volcanism in an extensional setting was followed, possibly continuously, by arc-type magmatism.

ACKNOWLEDGMENTS

This study is part of the project 1011197, funded by the Academy of Finland, "Geology and geochemistry of the supracrustal rocks of the early Proterozoic Tampere Schist Belt", and is a contribution to the IGCP project 217 "Proterozoic Geochemistry". Financial support was also gratefully received from the Wilhelm Ramsay and Th. G.

Sahama Memorial Foundation. Maija Kurimo and Tarmo Jokinen provided the geophysical maps and geophysical modelling, respectively. The figures were drawn by Mikko Nironen and Riitta Fagerström, and the English language was revised by Peter Sorjonen-Ward.

REFERENCES

- Ala-Vainio, I. 1986.** XRF routine analysis by the fundamental parameter method. Proceedings of the Thirty-ninth Chemist's Conference. Scarborough, June 17-19, 1986. Research and Development, British Steel Corporation, 51-54.
- Basaltic Volcanism Study Project 1981.** Basaltic Volcanism on the Terrestrial Planets. New York: Pergamon Press, 1286 p.
- Beccaluva, L., Ohnenstetter, D. & Ohnenstetter, M. 1979.** Geochemical discrimination between ocean-floor and island-arc tholeiites - application to some ophiolites. *Can. J. Earth Sci.* 16, 1874-1882.
- Carey, S. & Sigurdsson, H. 1984.** A model of volcanogenic sedimentation in marginal basins. In: Kokelaar, B.P. & Howells, M.F. (eds.) *Marginal Basin Geology*. Oxford: Blackwell, 37-58.
- Cox, K.G., Bell, J.D. & Pankhurst, R.J. 1979.** *The Interpretation of Igneous Rocks*. London: Allen & Unwin, 450 p.
- DePaolo, D.J. 1981.** Trace element and isotopic effects of combined wallrock assimilation and fractional crystallization. *Earth Planet. Sci. Lett.* 53, 189-202.
- Fischer, R.V. 1984.** Submarine volcanoclastic rocks. In: Kokelaar, B.P. & Howells, M.F. (eds.) *Marginal Basin Geology*. Oxford: Blackwell, 5-27.
- Fleet, A.J. 1984.** Aqueous and sedimentary geochemistry of the rare earth elements. In: Henderson, P. (ed.) *Rare Earth Element Geochemistry*. Amsterdam: Elsevier, 343-373.
- Gaal, G. & Gorbatshev, R. 1987.** An outline of the Precambrian evolution of the Baltic Shield. *Precambrian Res.* 35, 15-52.
- Hanson, G.N. 1980.** Rare earth elements in petrogenetic studies of igneous systems. *Ann. Rev. Earth Planet. Sci.* 8, 371-406.
- Hietanen, A. 1975.** Generation of potassium-poor magmas in the northern Sierra Nevada and the Svecofennian of Finland. *J. Res. U.S. Geol. Surv.* 3, 631-645.
- Hughes, C.J. 1973.** Spilites, keratophyres, and the igneous spectrum. *Geol. Mag.* 109, 513-527.
- Huhma, H. 1986.** Sm-Nd, U-Pb and Pb-Pb isotopic evidence for the origin of the Early Proterozoic Svecokarelian crust in Finland. *Geol. Surv. Finland, Bull.* 337, 48 p.
- Isokangas, P. 1978.** Finland. In: Bowie, S.H.U., Kvalheim, A. & Haslam, H.W. (eds.) *Mineral Deposits of Europe, Vol. 1: Northwest Europe*. Inst. Min. Metall. Miner. Soc., Dorking, 39-92.
- Jahn, B.M., Auvray, B., Blais, S., Capdevila, R., Cornichet, J., Vidal, P. & Hameurt, J. 1980.** Trace element geochemistry

- and petrogenesis of Finnish greenstone belts. *J. Petrol.* 21, 201-244.
- Jones, J.G. 1969.** Pillow lavas as depth indicators. *Am. J. Sci.* 267, 181-195.
- Kähkönen, Y. 1987.** Geochemistry and tectonomagmatic affinities of the metavolcanic rocks of the early Proterozoic Tampere Schist Belt, southern Finland. *Precambrian Res.* 35, 295-311.
- Kähkönen, Y., Huhma, H. & Aro, K. 1989.** U-Pb zircon ages and Rb-Sr whole-rock isotope studies of early Proterozoic volcanic and plutonic rocks near Tampere, southern Finland. *Precambrian Res.* 45, 27-43.
- Kähkönen, Y., Mäkelä, K. & Rosenberg, R.J. 1981.** Rare earth elements in Proterozoic metabasalts and associated volcanogenic sulphide ore from Haveri, southwestern Finland. *Bull. Geol. Soc. Finland* 53, 11-16.
- Koistinen, T.J. 1981.** Structural evolution of an early Proterozoic strata-bound Cu-Co-Zn deposit, Outokumpu, Finland. *Trans. R. Soc. Edinburgh, Earth Sci.* 72, 115-158.
- Koljonen, T. & Rosenberg, R. 1975.** Rare earth elements in Middle Precambrian volcanic rocks of Finland, with a discussion of the origin of the rocks. *Bull. Geol. Soc. Finland* 47, 127-138.
- Knoper, M.W. 1990.** Geochemistry of Early Proterozoic supracrustal rocks, West-Central Colorado: evidence for their petrogenesis and tectonic setting. PhD dissert., New Mexico Institute of Mining and Technology, Socorro, N.M.
- Leeman, W.P. 1983.** The influence of crustal structure on compositions of subduction-related magmatism. *J. Volcanol. Geotherm. Res.* 18, 561-588.
- LeMaitre, R.W. (ed.) 1989.** A Classification of Igneous Rocks and Glossary of Terms. Oxford: Blackwell, 193 p.
- Mäkelä, K. 1980.** Geochemistry and origin of Haveri and Kiiyu, Proterozoic strata-bound volcanogenic gold-copper and zinc mineralizations from southwestern Finland. *Geol. Surv. Finland, Bull.* 310, 79 p.
- Miyashiro, A. 1974.** Volcanic rock series in island arcs and active continental margins. *Am. J. Sci.* 274, 321-355.
- Morris, P.A. 1984.** MAGFRAC: a basic program for least-squares approximation of fractional crystallization. *Computers & Geosciences* 10, 437-444.
- Nironen, M. 1989.** The Tampere Schist Belt: structural style within an early Proterozoic volcanic arc system in southern Finland. *Precambrian Res.* 43, 23-40.
- Ojakangas, R.W. 1986.** An early Proterozoic metagraywacke-slate turbidite sequence: The Tampere schist belt, southwestern Finland. *Bull. Geol. Soc. Finland* 58, 241-261.
- Park, A.F. 1991.** Continental growth by accretion: A tectonostratigraphic terrane analysis of the evolution of the western and central Baltic Shield, 2.50 to 1.75 Ga. *Geol. Soc. Am. Bull.* 103, 522-537.
- Patchett, P.J. & Kouvo, O. 1986.** Origin of continental crust of 1.9-1.7 age: Nd isotopes and U-Pb zircon ages in the Svecokarelian terrain of South Finland. *Contrib. Mineral. Petrol.* 92, 1-12.
- Pearce, J.A. 1975.** Basalt geochemistry as used to investigate past tectonic environments on Cyprus. *Tectonophysics* 25, 279-297.
- Pearce, J.A. 1982.** Trace element characteristics of lavas from destructive plate boundaries. In: Thorpe, R.S. (ed.) *Andesites. Orogenic Andesites and Related Rocks*. Chichester: Wiley and Sons, 525-548.
- Pearce, J.A. 1983.** Role of the subcontinental lithosphere in magma genesis at active continental margins. In: Hawkesworth, C.J. & Norry, M.J. (eds.) *Continental Basalts and Mantle Xenoliths*. Cheshire: Shiva, 230-249.
- Rosenberg, R. J., Kaistila, M., & Zilliacus, R. 1982.** Instrumental epithermal neutron activation analysis of solid geochemical samples. *J. Radioanal. Chem.* 71, 419-428.
- Saunders, A.D. & Tarney, J. 1984.** Geochemical characteristics of basaltic volcanism within back-arc basins. In: Kokelaar, B.P. & Howells, M.F. (eds.) *Marginal Basin Geology*. Oxford: Blackwell, 59-76.
- Sederholm, J.J. 1897.** Über eine archaische Sedimentformation im Südwestlichen Finnland und ihre Bedeutung für die Erklärung der Entstehungsweise des Grundgebirges. *Bull. Comm. géol. Finlande* 6, 254 p.
- Shervais, J.W. 1982.** Ti-V plots and the petrogenesis of modern and ophiolitic lavas. *Earth Planet. Sci. Lett.* 59, 101-118.
- Simonen, A. & Neuvonen, K. 1947.** On the metamorphism of the schists in the Ylöjärvi area. *Bull. Comm. géol. Finlande* 140, 247-260.
- Stigzelius, H. 1944.** Über die Erzgeologie des Viljakkalagebietes im südwestlichen Finnland. *Bull. Comm. géol. Finlande* 134, 91 p.
- Taylor, S.R. & McLennan, S.M. 1985.** *The Continental Crust: its Composition and Evolution*. Oxford: Blackwell, 312 p.
- Vaasjoki, M. & Huhma, H. 1987.** Lead isotopic results from metabasalts of the Haveri Formation, southern Finland: an indication of early Proterozoic mantle derivation. *Terra Cognita* 7, 159.
- Wilson, M. 1989.** *Igneous Petrogenesis*. London: Unwin Hyman, 466 p.
- Woodcock, N. H. & Fischer, M. 1986.** Strike-slip duplexes. *J. Struct. Geol.* 8, 725-735.

Appendix 1. Sample sites and sample description. The pillow lava samples are from pillow interiors. Pl (plagioclase), Hbl (hornblende), Act (actinolite), Cpx (clinopyroxene, mostly diopside), Ep (epidote), Bt (biotite), Op (opaques), Chl (chlorite), Sph (sphene) indicate major minerals.

12-ty-MN/88. Pillow lava. Pl, Hbl, Cpx. x = 6843.97, y = 2460.25.
 12-ev-MN/88. Lava with large pillows. Pl, Hbl, Ep. x = 6843.97, y = 2460.25.
 12-br-MN/88. Hyaloclastic breccia. Hbl, Pl, Cpx, Ep. x = 6843.97, y = 2460.25.
 29-aft-MN/88. Pillow lava. Hbl, Pl. x = 6844.06, y = 2459.90.
 29-ur-MN/88. Ur-phyric lava. Pl, Hbl, Ep. x = 6844.06, y = 2459.90.
 28-maf-MN/88. Massive lava. Pl, Hbl, Op, Bt. x = 6843.90, y = 2460.00.
 29-S-ev-MN/88. Massive lava. Hbl, Pl, Ep. x = 6843.99, y = 2459.92.
 3-Hav/87. Massive lava. Hbl, Pl. x = 6843.95, y = 2460.46.
 17-MN/88. Pillow lava. Hbl, Pl. x = 6844.47, y = 2460.50.
 21-1-MN/88. Pillow lava. Hbl, Pl, Sph, Op. x = 6845.53, y = 2460.64.
 21-N-MN/88. Pillow lava. Hbl, Pl, Cpx. x = 6845.63, y = 2460.59.
 4-MN/89. Massive lava. Hbl, Pl. x = 6845.22, y = 2461.01.
 6-B-MN/89. Pillow lava. Hbl, Pl, Cpx, Ep. x = 6845.16, y = 2461.21.
 6-C-MN/89. Pillow lava. Hbl, Pl. x = 6845.16, y = 2461.21.
 18-MN/88. Stratified tuffite. Act, Cpx. x = 6844.51, y = 2460.90.
 1-B-MN/89. Pillow lava. Hbl, Pl. x = 6845.08, y = 2457.52.
 101-YK/89. Massive lava. Hbl, Pl. x = 6845.14, y = 2457.58.
 109-YK/89. Massive lava. Hbl, Pl. x = 6845.53, y = 2456.88.
 102-YK/89. Massive lava. Hbl, Pl. x = 6845.16, y = 2456.21.
 103-1-YK/89. Massive lava. Hbl, Pl. x = 6845.14, y = 2456.25.
 104-4-YK/89. Pillow lava. Hbl, Pl. x = 6845.09, y = 2456.32.
 106-6-YK/89. Pillow lava. Hbl, Pl. x = 6845.04, y = 2456.33.
 7-Hav/87. Massive lava. Hbl, Pl, Op. x = 6845.02, y = 2456.79.
 12-dyke-MN/88. 15 cm wide dyke. Hbl, Pl, Bt, Qtz, Op. x = 6843.97, y = 2460.25.
 4-Hav/87. 50-80 cm wide deformed dyke. Pl, Hbl, Bt, Qtz. x = 6844.55, y = 2460.86.
 5-Hav/87. Dyke with indefinable boundaries. Pl, Qtz, Hbl, Bt. x = 6844.55, y = 2460.86.
 6-MN/88. Felsic porphyry. Pl, Kfs, Qtz, Bt, Chl. x = 6843.78, y = 2460.93.
 28-fels-MN/88. Porphyritic felsic dyke. Pl, Qtz, Kfs, Bt. x = 6843.90, y = 2460.00.
 29-S-fels-MN/88. Porphyritic felsic dyke. Pl, Qtz, Kfs. x = 6843.99, y = 2459.92.
 6-Korpela. Lithics- and crystals-bearing tuff. Pl, Qtz, Bt, Chl. x = 6840.06, y = 2464.06.
 112-a-YK/89. Lithics- and crystals-bearing tuff. Pl, Qtz, Hbl, Bt. x = 6841.50, y = 2460.11.
 113-YK/89. Pl-phyric massive rock from an area dominated by tuff breccias. Pl, Hbl, Qtz. x = 6839.98, y = 2461.32.
 114-YK/89. Pl-phyric rock from the matrix of tuff breccias. Pl, Hbl, Qtz, Chl. x = 6840.04, y = 2461.24.
 16-MN/89. Porphyritic lapilli tuff. Pl, Hbl, Qtz, Bt. x = 6840.63, y = 2463.56.
 Gr-Os/89. Porphyritic granitoid with pronounced orientation. Pl, Qtz, Hbl. x = 6845.15, y = 2456.49.
 11-MN/89. Porphyritic granitoid (subvolcanic?). Pl, Qtz, Hbl, Kfs, Bt. x = 6846.17, y = 2461.26.
 20-MN/89. Even-grained granitoid. Pl, Qtz, Hbl, Bt. x = 6845.47, y = 2460.00.

Appendix 2. Least-squares major element modelling of the Haveri metalavas using the approximation program MAGFRAC (Morris 1984).

The initial assumed composition is an approximation based on the Haveri samples with about 100 ppm Zr and the evolved assumed composition is based on sample 28-maf-MN/88. The mineral compositions are based on means in MORB (Basaltic Volcanism Study Project 1981, Tables 1.3.2.2, 1.3.2.3a, 1.3.2.4a).

	Model liquid compositions			Mineral compositions		
	Initial assumed	Initial calculated	Evolved assumed	Ol	Cpx	Pl
SiO ₂	50.00	50.32	52.00	38.00	50.00	53.00
TiO ₂	1.30	1.11	2.30	0.00	0.90	0.00
Al ₂ O ₃	15.00	14.71	13.00	0.00	3.00	29.00
FeO	10.00	9.51	14.00	22.00	12.00	0.70
MnO	0.20	0.17	0.20	0.40	0.30	0.00
MgO	7.00	6.97	4.00	40.00	15.00	0.10
CaO	12.00	11.52	8.00	0.40	18.00	13.00
Na ₂ O	3.00	2.44	3.00	0.00	0.20	4.00
K ₂ O	0.40	0.22	0.50	0.00	0.00	0.10
P ₂ O ₅	0.13	0.12	0.32	0.00	0.00	0.00

Fractionating assemblage: 7% olivine, 41% clinopyroxene, 52% plagioclase
 F (fraction of residual liquid) = 0.39.
 Sum of squared residuals = 1.04

POST-DEPOSITIONAL K-FELDSPAR BREAKDOWN AND ITS IMPLICATIONS FOR METAGRAYWACKE PROVENANCE STUDIES - AN EXAMPLE FROM NORTH KARELIA, EASTERN FINLAND

by
Jarmo Kohonen

Kohonen, Jarmo 1994. Post-depositional K-feldspar breakdown and its implications for metagraywacke provenance studies - an example from north Karelia, eastern Finland. *Geological Survey of Finland, Special Paper 19*, 161–171, 10 figures.

The low- to medium-grade metamorphic Kaleva graywackes and pelites of north Karelia are typically free of K-feldspar (Kfs). However, in places granitoid-quartzite pebble conglomerates and associated coarse-grained psammites do contain abundant Kfs.

The 125 m Hovinvaara section in the Höytiäinen area was studied in detail. The sequence consists of psammite-dominated (sand-shale ratio 5) ABE turbidites. The coarsest grained units have a distinctly blastoclastic, nearly arenitic texture with feldspar (both Kfs and plagioclase) and quartz grains generally equal in size. As the modal grain size decreases the proportion of mica (interpreted mainly as primary clay matrix) increases, Kfs disappears and the texture becomes clearly bimodal, with large clasts of quartz 'floating' in a biotite-sericite-plagioclase-quartz groundmass.

The common absence of Kfs in metagraywackes is considered to be due to its breakdown in diagenetic processes and metamorphic reactions producing biotite. The local preservation of detrital Kfs is attributed to its relative stability in matrix-poor and coarse-grained sediments which contained very little or no primary chlorite. Consequently, variations in Kfs content of Höytiäinen metagraywackes do not necessarily reflect changes in provenance.

Major component analyses (25 samples) of psammites from the Höytiäinen area show a clear correlation between grain size and SiO₂ content. The samples containing Kfs are rich in SiO₂, but do not differ remarkably in K₂O/Na₂O ratios when compared with the Kfs-free samples from Hovinvaara and other localities. The whole data set shows intermediate to high values for K₂O/Na₂O and SiO₂ excluding an immature volcanic arc as the main source.

Key words (GeoRef Thesaurus, AGI): metagraywacke, K-feldspar, grain size, provenance, Proterozoic, Kalevian, Hovinvaara, Kontiolahti, Finland

Jarmo Kohonen, Geological Survey of Finland, FIN-02150, Espoo, Finland

INTRODUCTION

Metagraywackes and associated fine-grained sediments form the major part of the early Proterozoic Kaleva association in eastern Finland. In North Karelia these low- to medium-grade metamorphic graywackes have been reported to be totally free of K-feldspar (Kfs) over large areas (e.g. Pelkonen 1966, Nykänen 1968, Nykänen 1971, Huhma 1975). However, in the Höytiäinen Province (Fig. 1) coarse psammites, and associated granitoid and quartzite pebble conglomerates, locally contain abundant detrital Kfs. These lithologies occur among Kfs-free graywackes without a clear boundary.

The sporadic distribution of Kfs might be attribut-

ed either to changing source areas or to selective preservation of Kfs in post-depositional processes (diagenesis and metamorphism). The question is of primary interest from the viewpoint of provenance studies and basin models of the Kaleva association.

The section studied in detail, Hovinvaara, includes both Kfs-bearing and Kfs-free metapsammites, and in the present paper the preliminary petrographic observations are discussed. In addition, major element chemical analyses from Hovinvaara are compared with data from Kfs-free metagraywackes of the northern Höytiäinen Province.

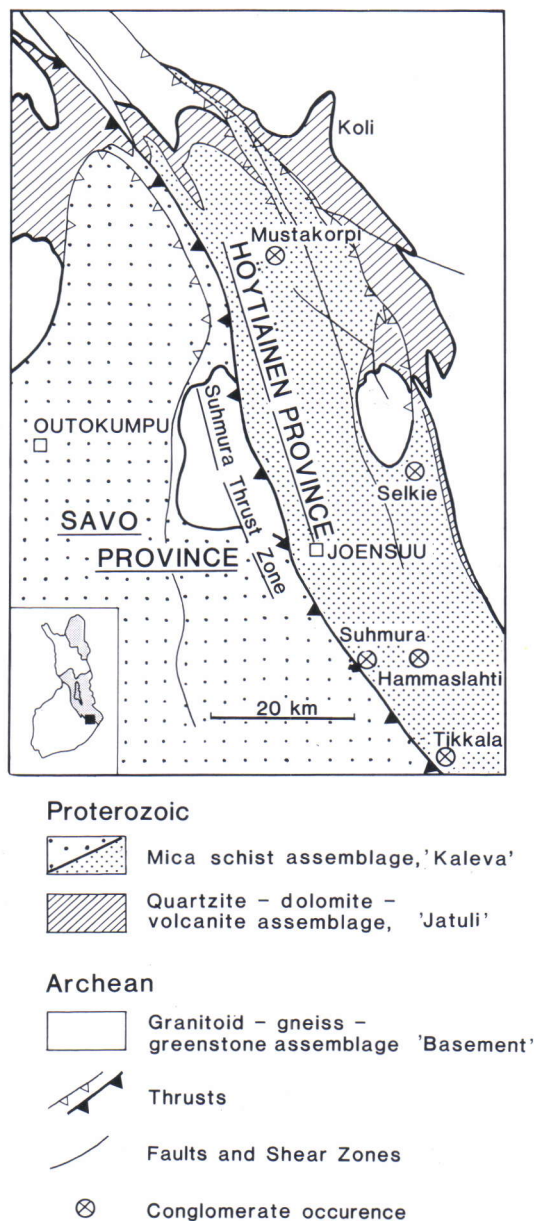


Fig. 1. Location of reported granitoid-quartzite pebble conglomerates and associated coarse psammites within the Höytiäinen Province. Map showing the geological main units of the North Karelia Schist Belt is modified after Koistinen (1987) and Ward (1987). Inset shows the location of the study area (black square) at the boundary of Archean basement (shaded) and Proterozoic rocks.

HOVINVAARA SECTION

The studied section is located east of Lake Höytiäinen near the Romppala village (map sheet 4313 07). The Mustakorpi (Romppala) conglomerate, which contains pebbles of felsic plutonics, quartzites, carbonate rocks and graphitic schists, is situated about 3 km along strike (NNW) from Hovinvaara (Fig. 2). The conglomerate, associated with coarse- to very-coarse grained psammites, was interpreted as part of the same lithological unit as the Hovinvaara sequence (Kohonen 1991). The area east of the studied section is characterized by phyllitic mica schists whereas the area in the west consists mainly of monotonous metapsammites.

The 125 m long, in detail mapped profile at Hovinvaara is a psammite-dominated section showing top of strata mainly to the east (Fig. 2). The most striking feature of the section is the frequent grain size variation, but also massive psammitic units several meters in thickness are present (A-A-sequences in Fig. 3). Although grading is not well-developed, the major part of the sequence gives the appearance of an ABE turbidite (i.e., showing A, B and E Bouma sections). The psammitic units com-

monly contain fragments (intraclasts) of dark graphitic schist but true conglomerates are lacking. The primary grain size of the coarsest units corresponds to that of very coarse sand. Load casts, flame structures and erosional features were locally observed at the base of the psammitic beds.

The rocks show pronounced deformation, although mesoscopic folds are rare. The whole system is dipping steeply to the west and has a slightly overturned position. Foliation is subparallel to bedding and prominent in all lithologies. It is defined by flattening of the framework grains and by a preferred orientation of the micas. Quartz has largely recrystallized to a smaller grain size.

The westernmost part of the section was sampled in detail and the coarse units were observed to contain abundant K-feldspar whereas the adjacent, more fine-grained psammites lack Kfs. This seems to be the case also with the units interpreted as parts of a single Bouma sequence (Figs. 3 and 4). The Kfs-bearing samples show a distinct blastoclastic texture with quartz, plagioclase and Kfs equal in size (Figs. 5a and 6a). In these samples the amount of matrix is typical-

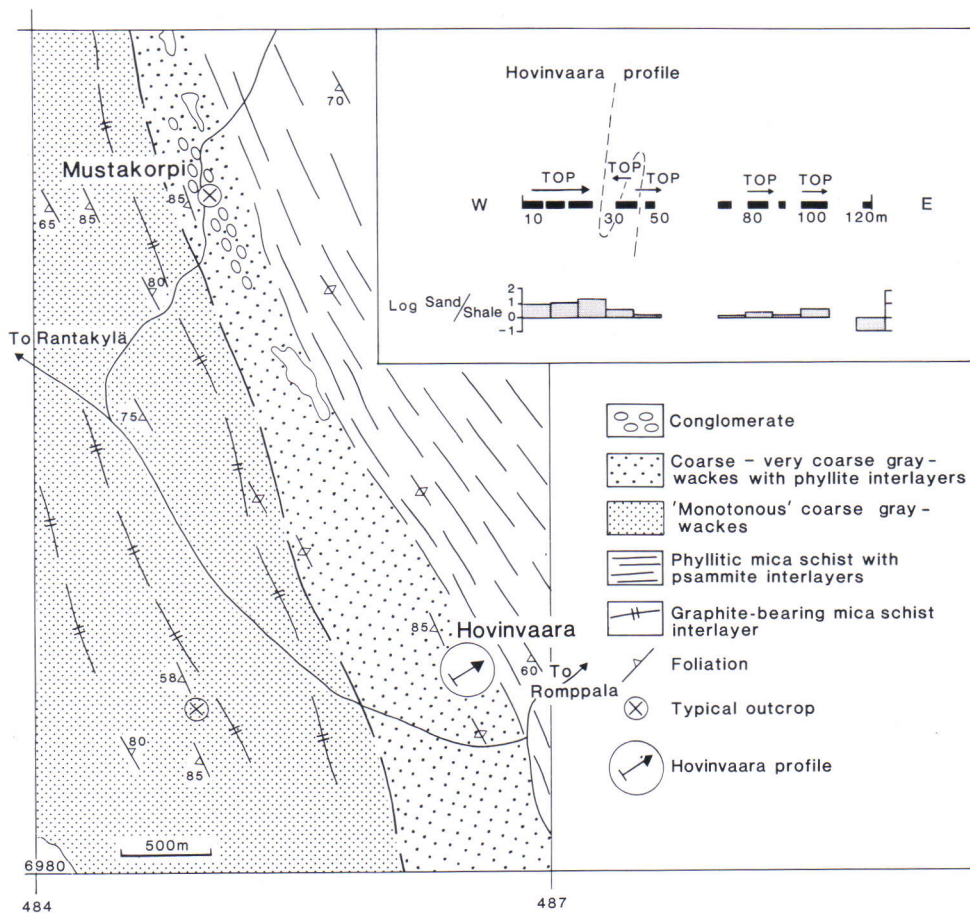


Fig. 2. Geological map of the Hovinvaara-Mustakorpi area with exposure and sand-shale ratio diagram of the Hovinvaara Profile. For location see 'Mustakorpi' in Fig. 1.

ly low and the rocks are almost arenitic in character. Some detrital K-feldspar grains are mantled by biotite and indicate partial destruction.

In contrast, the Kfs-free samples show quartz grains, clearly clastic in origin, 'floating' in a more fine-grained groundmass consisting of quartz, biotite, sericite and plagioclase (Figs. 5b and 6b; see also Figs. 22, 32 and 33 by Pelkonen 1966). Because quartz and feldspars are nearly equal in density, detrital grains about equivalent in size are normally expected in depositional settling processes. Hence,

an authigenic origin for most of the fine-grained, albitic plagioclase forming the groundmass is suggested.

It is hard to imagine conditions where the sediment source was changing between adjacent beds within a single depositional system or where K-feldspar was originally present only in coarse grain size fractions. If this reasoning is correct, one has to assume a process or processes decomposing potassium feldspar selectively, in this case, in the sediments representing a smaller modal grain size.

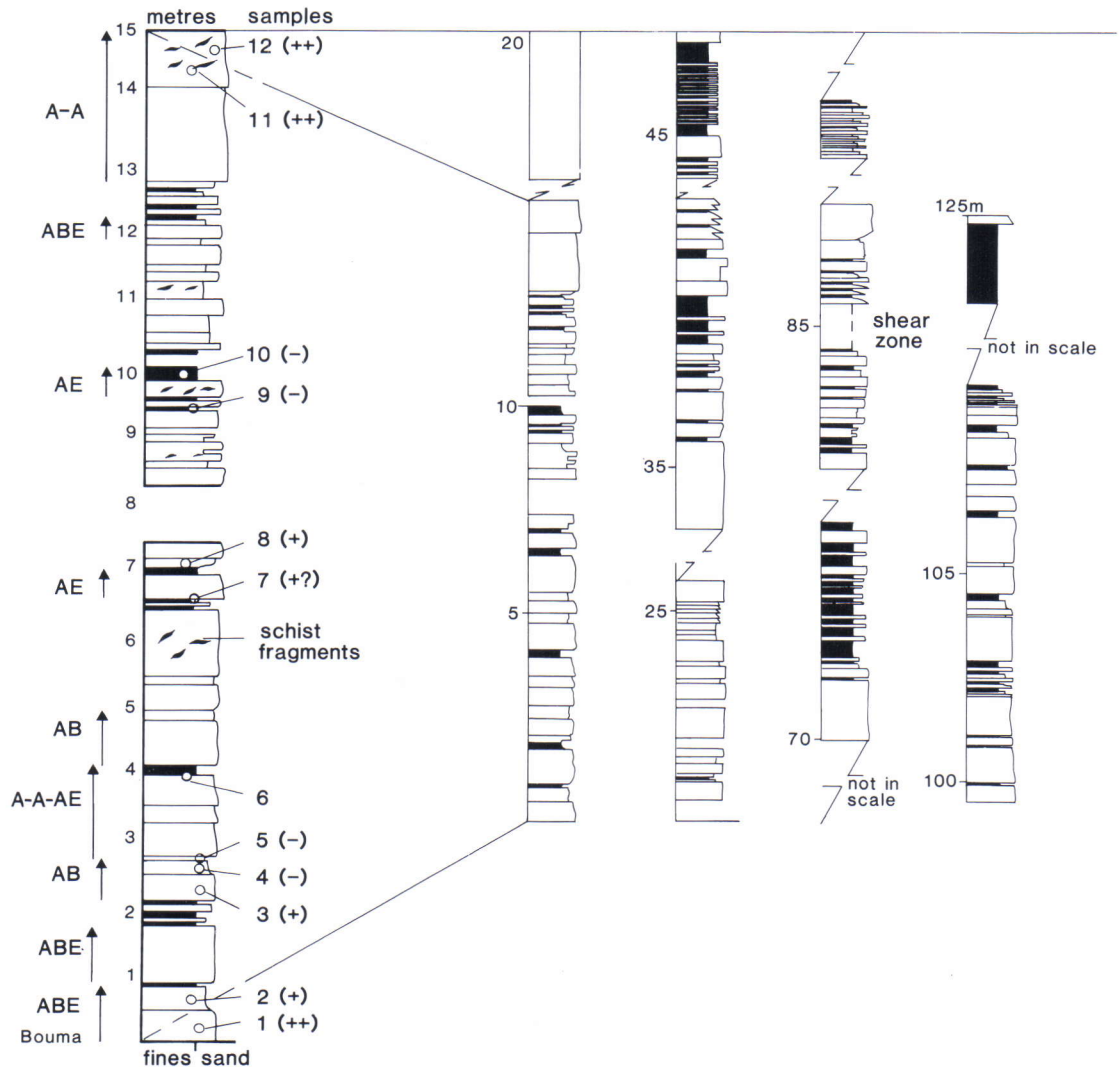


Fig. 3. Schematic vertical section indicating grain size variation within the Hovinvaara profile. Also examples of Bouma sequences, sampling sites (numbers refer to the last number of the code in Figs. 4 - 6) and appearance of K-feldspar are shown (++ = abundant Kfs, + = Kfs present, - = no Kfs).

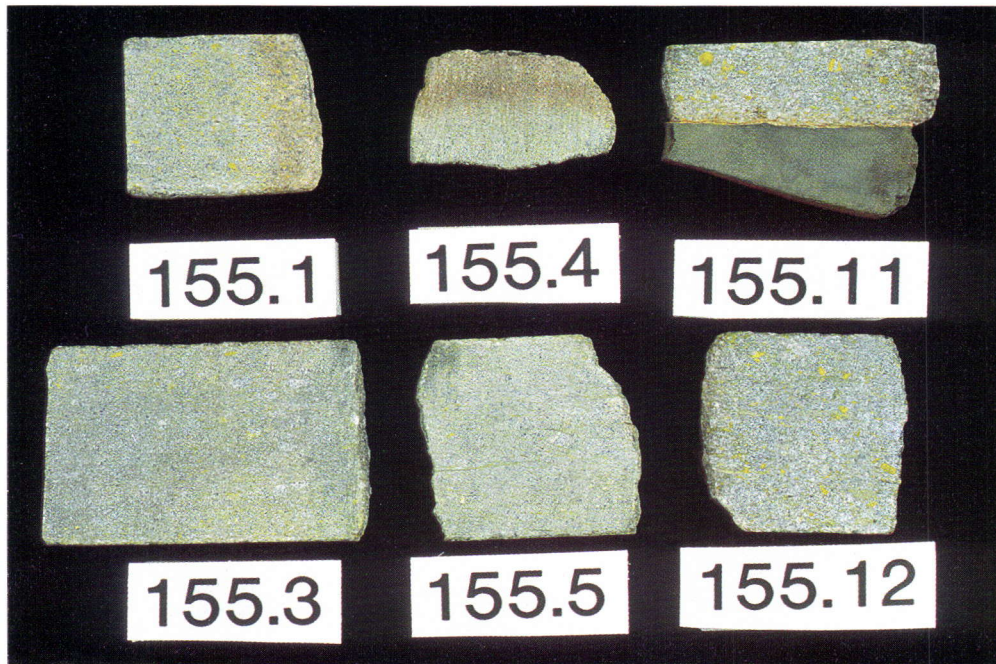


Fig. 4. Hovinvaara samples etched by sodium-cobalt-nitrite showing various amounts of K-feldspar (bright yellow). Height of numbers is 6 mm. Photo: J. Väättäinen.

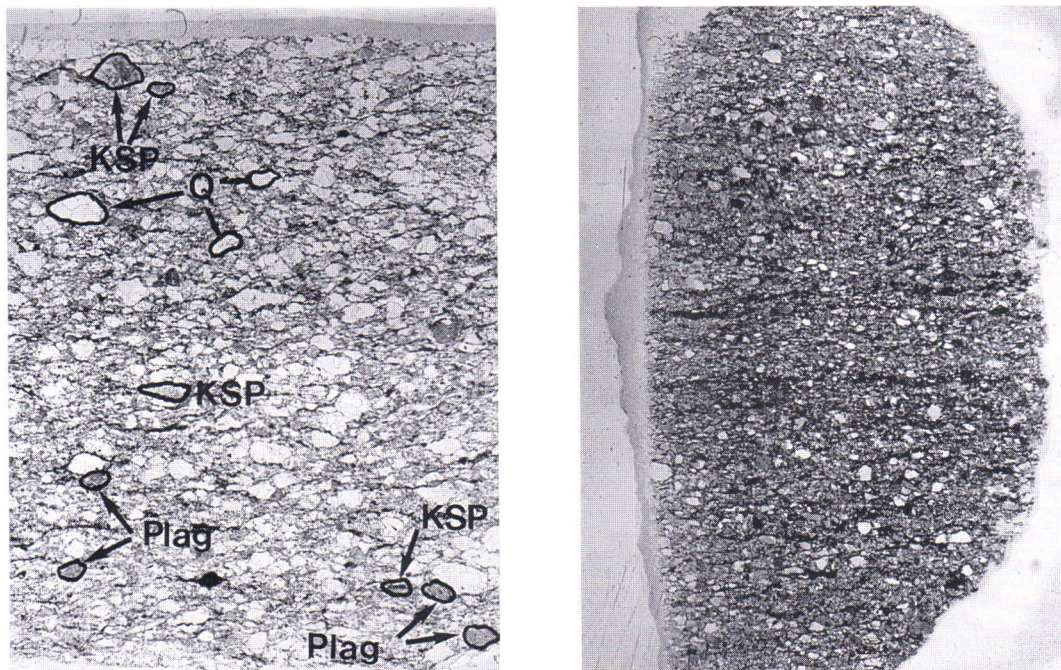
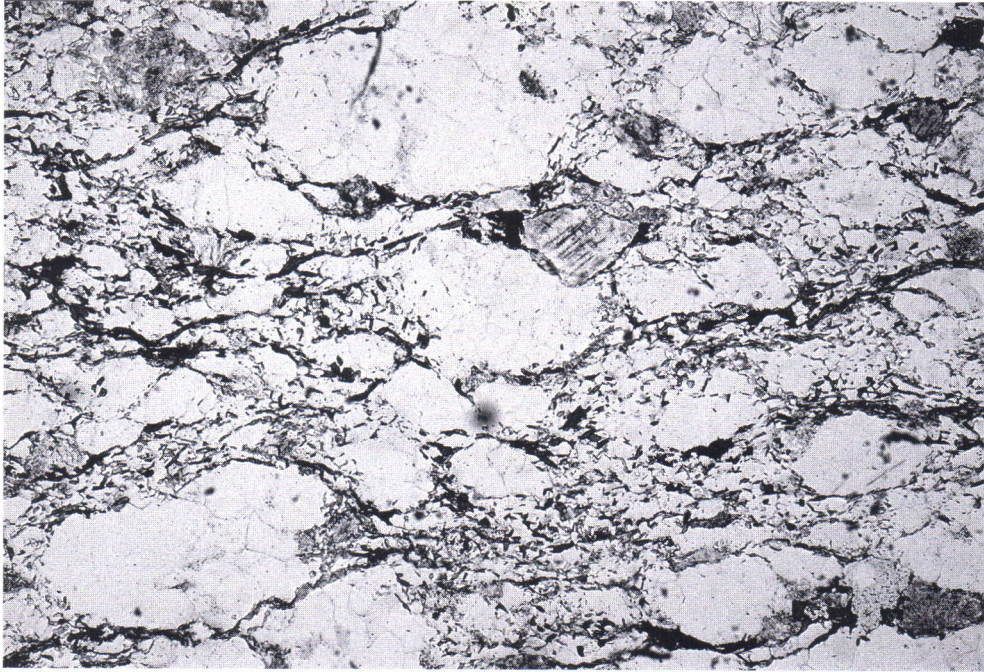


Fig. 5. a) Sample 155.1 showing clast-supported framework. Note also the equal size of quartz and feldspar clasts. KSP = K-feldspar, Plag = plagioclase. b) Sample 155.4 with clastic quartz in a more fine-grained groundmass. Height of the picture is 2 cm, nicols parallel. Photos: J. Väättäinen.

6a)



6b)

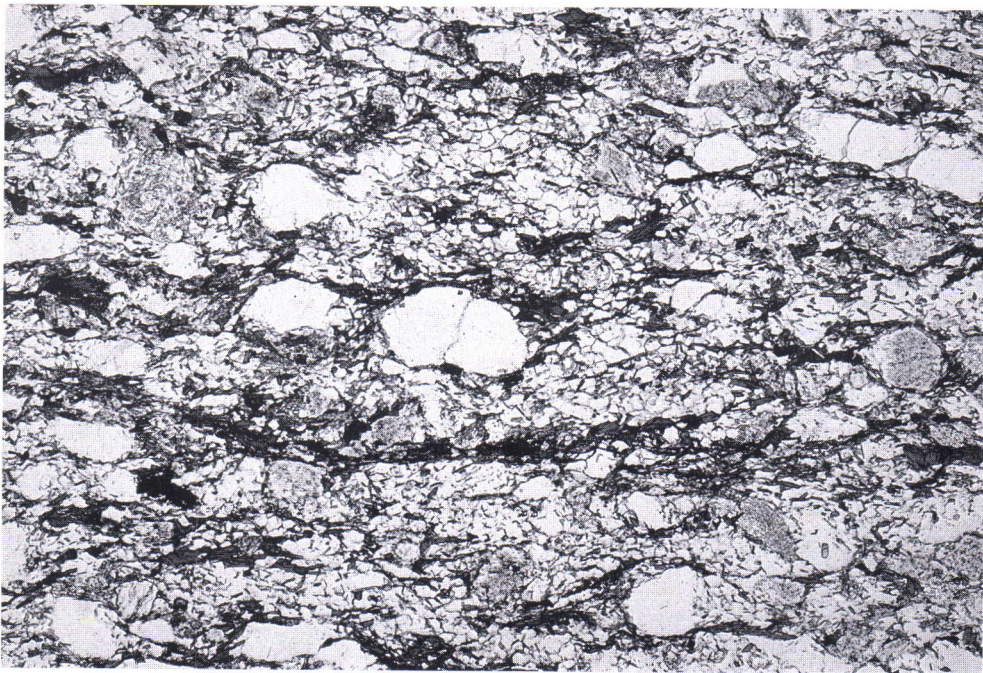


Fig. 6. **a)** Blastoclastic texture of sample 155.1. **b)** Bimodal grain size distribution in sample 155.4. Width of the pictures is 3.7 mm.

CHEMICAL CHARACTERISTICS

As work concerning the geochemistry of the whole Kaleva association is currently in progress, the geochemical part of the present study is to be taken as a preliminary one. The aim is to connect the

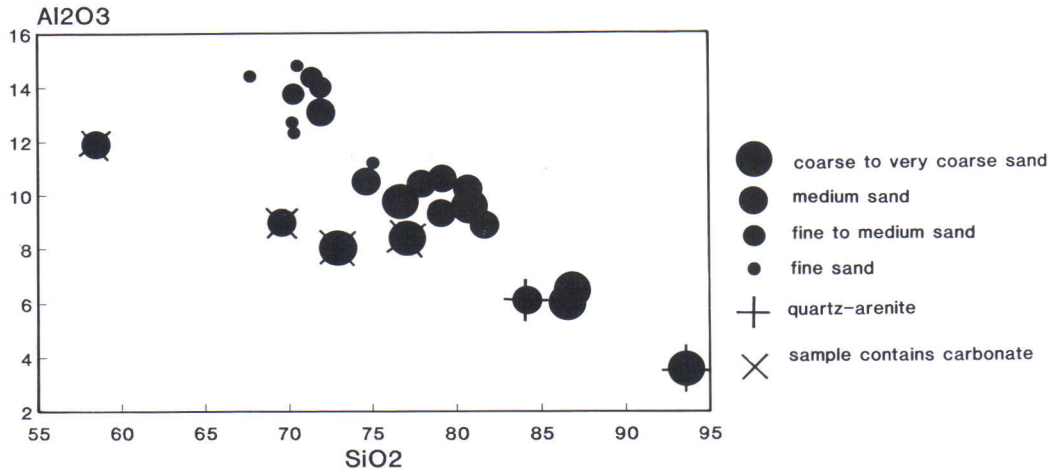


Fig. 7. Al_2O_3 - SiO_2 - grain size relations in metapsammites of the Höytiäinen area (grain size estimated by hand lens from samples). Analyses (Figs. 7 - 10) by Rautaruukki and Geological Survey of Finland; unpublished data by the author.

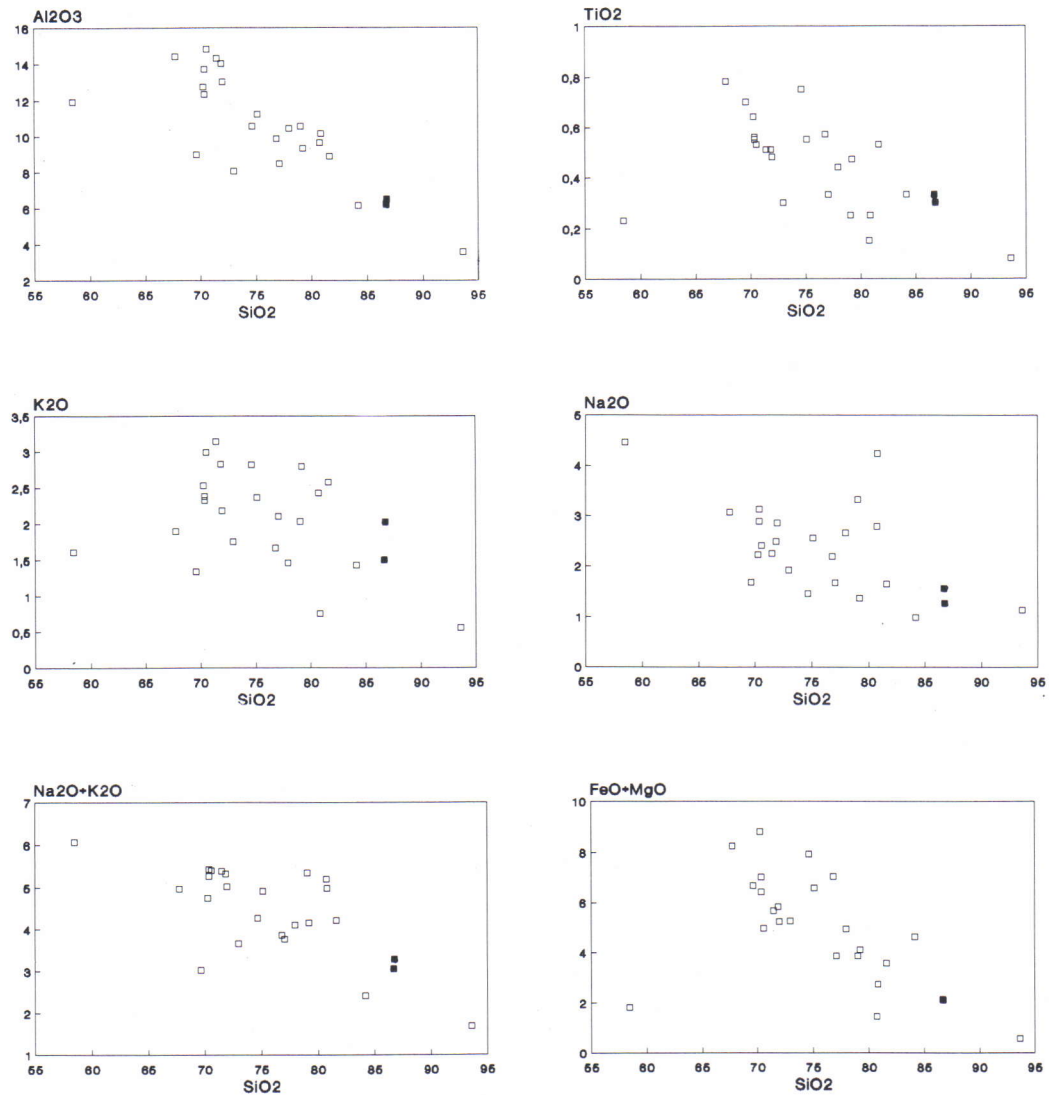


Fig. 8. Plots of selected major elements vs. SiO_2 in the samples of the Höytiäinen area. The samples containing abundant K-feldspar are shown as filled boxes.

Hovinvaara samples to a more broad context and discuss, along with inferences from petrographical data, the most apparent major element characteristics of the Höytiäinen area metagraywackes. The analytical data will be published as part of more detailed analysis of the geochemistry in the Höytiäinen area.

The most striking feature in the geochemical data for the psammites from the northern part of the Höytiäinen Province is the dependence between grain size and SiO₂ content (Fig. 7). Most major elements correlate positively with Al₂O₃ and, conversely, show negative correlation against SiO₂. K₂O and Na₂O show large variation which, however, decreases remarkably when the alkalis are summed as Na₂O+K₂O.

The poor correlation between Na₂O and K₂O

against SiO₂ could indicate variable detritus compositions. If this was true, similar features should be noticeable also in other major component plots. Alternatively, post-depositional mobility of these elements, together with albitization of feldspars and uptake of potassium by clay minerals forming micas, for example, might explain the sample scale variability observed.

The Hovinvaara samples containing K-feldspar show the highest SiO₂ contents in the whole population if a quartz arenitic sample is ignored (Fig. 8). In turn, their K₂O/Na₂O ratios do not drastically differ from those of the Kfs-free psammites (see Fig. 10). Interestingly, the two samples from Hovinvaara not containing Kfs show rather high K₂O/Na₂O values.

DISCUSSION

Decomposition of K-feldspar has been reported (e.g. Dickinson et al. 1969, Middleton 1972, Aagaard et al. 1990) and experimentally proven (e.g. Chermak & Rimstidt 1990) to occur in diagenetic conditions. Diagenetic destruction of feldspars occurs both through replacement and dissolution (McBride 1985, Milliken et al. 1989). These reactions are mainly functions of temperature, depth and time. Substantial loss of detrital feldspars is proposed to occur at temperatures greater than 100°C (e.g. Land & Milliken 1981, Boles 1982), and decreasing amount of Kfs with increasing sample depth has been reported from many oilfields (e.g. Milliken 1988, Saigal et al. 1988).

Minerals such as chlorite, montmorillonite, smectite and kaolinite seem to play an important role as a 'potassium sink' during diagenetic decomposition of Kfs through albitization (Aagaard et al. 1990). Without co-existing clay minerals, capable of removing the released K⁺ ions by illitization, the reaction $\text{Na}^+ + \text{KAlSi}_3\text{O}_8 \rightarrow \text{NaAlSi}_3\text{O}_8 + \text{K}^+$ would rapidly set in equilibrium and terminate.

Although K-feldspar may have largely disappeared from the Kaleva graywackes during diagenesis, metamorphic modification of the original framework minerals is possible as well. Metamorphic biotite is one of the main minerals in the Kaleva metasediments, and following low-grade (greenschist facies) reactions involving K-feldspar and producing biotite have been presented (Thompson & Norton 1968, Mather 1970):

(1) {dolomite + Kfs + H₂O} = {biotite + calcite + CO₂}

(2) {chlorite + Kfs} = {biotite + muscovite + quartz + H₂O}

(3) {phengite + chlorite + Kfs} = {biotite + quartz + Mg,Fe-poor phengite}.

Metapsammites of arkosic composition may well retain clastic Kfs up to medium-grade metamorphism (above staurolite isograd of pelites; e.g. Allen & Ragland 1972), but in graywackes of suitable bulk composition, e.g. low Al₂O₃/(FeO+MgO) ratio, the breakdown reaction (3) occurs even below the biotite isograd of pelites (Mather 1970).

The samples containing Kfs are exceptionally coarse-grained within the graywackes of the Höytiäinen region and their texture is nearly arenitic. In other words, the primary proportion of matrix and, consequently, the amount of minerals such as chlorite, montmorillonite, smectite and kaolinite was low. The amount of clay minerals has a major impact on the whole rock compositions, and above the biotite isograd of pelites (at the biotite-phengite stage) the amount of chlorite is critical for preservation of Kfs (Fig. 9). It seems that in the metagraywackes originally poor in chlorite the (Mg+Fe)/K ratio was not high enough for the disappearance of Kfs.

In summary, the preservation potential of detrital K-feldspar, in both diagenetic and metamorphic processes, seems to be enhanced by the scarcity of primary clay and unstable (mafic) lithic fragments. The selective metamorphic breakdown of Kfs in reactions producing biotite explains quite well the observed distribution of Kfs within the Höytiäinen Province. The coarse grain size itself is undoubtedly an additional factor contributing to the preservation of primary minerals, because the relative reactive surface is smaller than in finer-grained rocks.

The chemical composition of graywackes reflects,

at least generally speaking, their source and tectonic setting during deposition (e.g. Crook 1974, Bhatia 1983, Roser & Korsch 1986). A wide variety of parameters may be used, but K_2O/Na_2O vs. SiO_2 is a simple and significant plot indicating the 'maturity' of the depositional system (Fig. 10). However, the

effect of various grain sizes on the SiO_2 content (see Fig. 7) and the possible mobility of sodium and potassium, must be borne in mind. It is pointed out that this kind of plots are to be taken only as an approximate, especially in the case of small samples. In any case, the values of K_2O/Na_2O in Fig. 10 do not

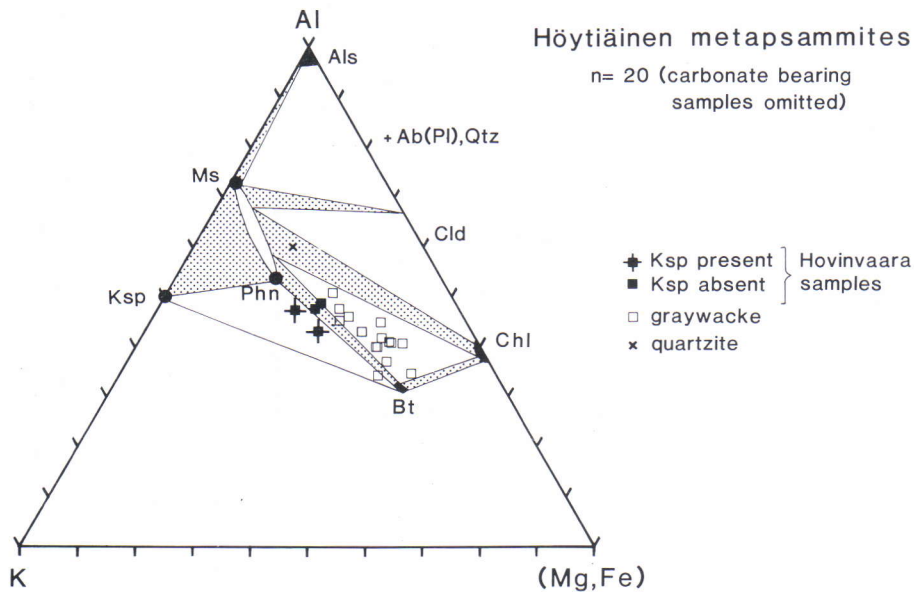


Fig. 9. Höytiäinen area metapsammities analyses plotted on the Al-K-(Mg,Fe) diagram (Al: $Al_{tot} - [(Al \equiv Na) + (2Al \equiv Ca)]$, at.% ; K: K_{tot} , at.% ; (Mg,Fe): Mg+Fe, at.% ; cf. Korikovsky 1973). Ms = muscovite, Ksp = K-feldspar, Phn = Prehnite, Bt = biotite, Chl = chlorite, Cld = chloritoid, Als = Al-silicate. The samples containing K-feldspar plot on left side of the Bt-Phn connod. Filled boxes = Hovinvaara samples, filled boxes with crosses = samples containing abundant Kfs, open boxes = Kfs-free samples of the Höytiäinen area.

METAPSAMMITES Höytiäinen area

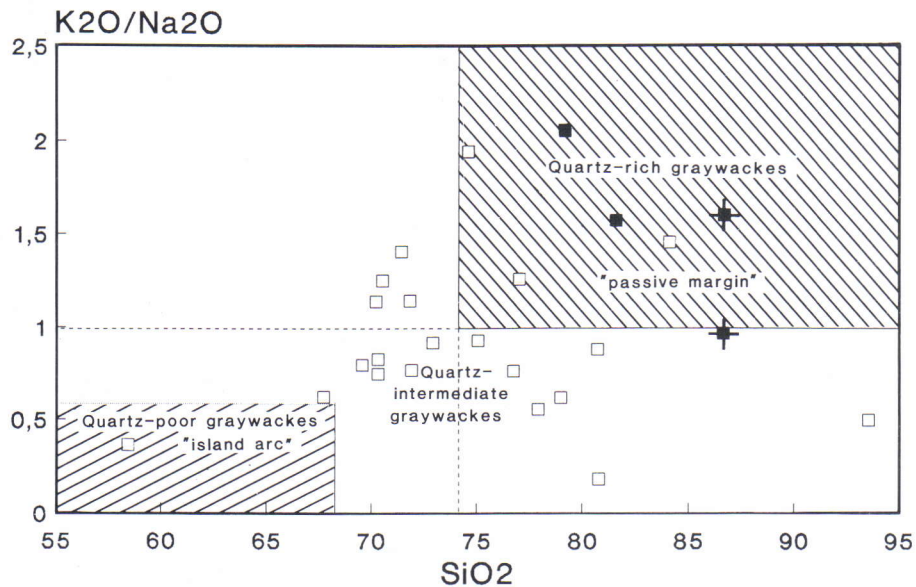


Fig. 10. Tectonic setting discrimination (cf. Crook 1974) of the Höytiäinen area metapsammities by the K_2O/Na_2O vs. SiO_2 plot. Symbols as in Fig. 9.

indicate a provenance low in potassium. Consequently, at least an immature arc can be ruled out as a major source. This may, perhaps, indirectly support the possibility that K-feldspar once was an essential component in the detritus, but largely disappeared during burial and metamorphism.

Finally, in light of this study, and taking into account the granitoid-quartzite pebble conglomer-

ates and the Sm-Nd isotope results with model ages of around 2.2 - 2.4 Ga (Huhma 1987), the intracratonic basin model for the Höytiäinen Province (Ward 1987) is supported. The most plausible source area for the 'east Kaleva' graywackes might be simply the adjacent Archean craton partly covered by Paleoproterozoic sedimentary and volcanic rocks.

CONCLUSIONS

1. A major part of the clastic K-feldspar in the Kaleva graywackes of the Höytiäinen Province may have been destroyed during diagenesis and metamorphism. Provenance estimations derived from the mineral composition of metagraywackes, even in the presence of blastoclastic features, may be of limited value.

2. The local preservation of K-feldspar is en-

hanced by the scarcity of matrix (arenitic nature of the rock), coarse grain size and, in consequence of the former, high SiO₂ content.

3. The psammites of the northern Höytiäinen Province resemble 'quartz-intermediate to quartz-rich graywackes' in major element geochemistry and a depositional setting intimately related to an immature volcanic arc is hardly probable.

ACKNOWLEDGEMENTS

This study was partly supported by the Academy of Finland. I thank many colleagues at GSF for fruitful discussions. S.P. Korikovsky, Y. Kähkönen

and K. Laajoki made many helpful suggestions and criticisms. The English language was revised by Christopher Cunliffe.

REFERENCES

- Aagaard, P., Egeberg, P.K., Saigal, G.C., Morad, S. & Bjorlykke, K. 1990. Diagenetic albitization of detrital K-feldspars in Jurassic, Lower Cretaceous and Tertiary clastic reservoir rocks from offshore Norway, II. Formation water chemistry and kinetic considerations. *J. Sed. Petrol.* 60, 575-581.
- Allen, G.C. & Ragland, P.C. 1972. Chemical and mineralogical variations during prograde metamorphism, Great Smoky Mountains, North Carolina and Tennessee. *Geol. Soc. Am. Bull.* 83, 1285-1298.
- Bhatia, M.R. 1983. Plate tectonics and geochemical composition of sandstones. *J. Geol.* 91, 611-627.
- Boles, J.R. 1982. Active albitization of plagioclase, Gulf Coast Tertiary. *Am. J. Sci.* 282, 165-180.
- Chermak, J.A. & Rimstidt, J.D. 1990. The hydrothermal transformation rate of kaolinite to muscovite/illite. *Geochim. Cosmochim. Acta* 54, 2979-2990.
- Crook, K.A.W. 1974. Lithogenesis and geotectonics: the significance of compositional variation in flysch arenites (graywackes). In: Dott, R.H. & Shaver, R.H. (eds.) *Modern and Ancient Geosynclinal Sedimentation*. SEPM Spec. Publ. 19, 304-310.
- Dickinson, W.R., Ojakangas, R.W. & Stewart, R.J. 1969. Burial metamorphism of the late Mesozoic Great Valley sequence, Cache Creek, California. *Geol. Soc. Am. Bull.* 80, 519-526.
- Huhma, A. 1975. Outokummun, Polvijärven ja Sivakkavaaran kartta-alueiden kallioperä. Summary: Precambrian rocks of the Outokumpu, Polvijärvi and Sivakkavaara map-sheet areas. Explanation to the maps of Pre-Quaternary rocks, sheets 4222, 4224 and 4311. Geological map of Finland 1 : 100 000. 151 p.
- Huhma, H. 1987. Provenance of early Proterozoic and Archaean metasediments in Finland: a Sm-Nd isotopic study. *Precambrian Res.* 35, 127-143.
- Kohonen, J. 1991. Nunnanlahden - Kolin - Kontiolahden alueen stratigrafia ja rakenne. In: Piirainen, T. & Vuollo, J. (eds.) *Arkeinen ja proterotsooinen geologinen evoluutio ja malminmuodostus: Pohjois-Karjalan malmiprojektin loppuraportti, Pohjois-Karjalan malmiprojekti. Raportti n:o 31*. Univ. Oulu, 70-99. (in Finnish)
- Koistinen, T. 1987. Review of the geology of North Karelia. In: Häkli, T.A. (ed.) *Otto Trüstedt symposium in Finland on June 3-5, 1985*, *Geol. Surv. Finland. Spec. Pap.* 1, 35-40.
- Korikovsky, S.P. 1973. The biotite isograd and mineral associations of the biotite zone of metamorphism in CaO-poor rocks. *Int. Geol. Rev.* 15, 936-946.
- Land, L.S. & Milliken, K.L. 1981. Feldspar diagenesis in the

- Frio Formation, Brazoria County, Texas Gulf Coast. *Geol.* 9, 314-318.
- Mather, J.D. 1970.** The biotite isograd and the lower greenschist facies in the Dalradian rocks of Scotland. *J. Petrol.* 11, 253-275.
- McBride, E.F. 1985.** Diagenetic processes that affect provenance determinations in sandstone. In: Zuffa, G.G. (ed.) *Provenance of Arenites*. Boston: Riedel, 95-113.
- Middleton, G.V. 1972.** Albite of secondary origin in Charny Sandstones, Quebec. *J. Sed. Petrol.* 42, 341-349.
- Milliken, K.L. 1988.** Loss of provenance information through subsurface diagenesis in Plio-Pleistocene sandstones, Northern Gulf of Mexico. *J. Sed. Petrol.* 58, 992-1002.
- Milliken, K.L., McBride, E.F. & Land, L.S. 1989.** Numerical assesment of dissolution versus replacement in the subsurface destruction of detrital feldspars, Oligocene Frio Formation, South Texas. *J. Sed. Petrol.* 59, 740-757.
- Nykänen, O. 1968.** Kallioperäkartan selitys, Tohmajärvi. Summary: Explanation to the map of rocks, sheet 4232-4234. Geological map of Finland 1 : 100 000, 66 p.
- Nykänen, O. 1971.** Kallioperäkartan selitys, Kiihtelysvaara. Summary: Explanation to the map of rocks, sheet 4241. Geological map of Finland 1 : 100 000, 68 p.
- Pelkonen, K. 1966.** Piirteitä Pohjois-Karjalan liuskealueen geologiasta Kontiolahden ja Polvijärven pitäjissä. M.Sc. Thesis, Univ. Helsinki. (unpublished, in Finnish)
- Roser, B.P. & Korsch, R.J. 1986.** Determination of tectonic setting of sandstone-mudstone suites using SiO₂ content and K₂O/Na₂O ratio. *J. Geol.* 94, 635-650.
- Saigal, G.C., Morad, S., Bjorlykke, K., Egeberg, P.K. & Aagaard, P. 1988.** Diagenetic albitization of detrital K-feldspar in Jurassic, Lower Cretaceous, and Tertiary clastic reservoir rocks from offshore Norway, I. Textures and origin. *J. Sed. Petrol.* 58, 1003-1013.
- Thompson, J.B. & Norton, S.A. 1968.** Paleozoic regional metamorphism in New England and adjacent areas. In: E-An Zen et al. (eds.) *Studies of Appalachian Geology, Northern and Maritime*. New York: John Wiley & Sons, 319-327.
- Ward, P.G. 1987.** Early Proterozoic deposition and deformation at the Karelian craton margin in southeastern Finland. *Precambrian Res.* 35, 71-93.

EMPLACEMENT, DEFORMATION AND GEOCHEMISTRY OF BIMODAL VOLCANICS IN VESTLAX, SW FINLAND

by

Alf Lindroos and Carl Ehlers

Lindroos, Alf & Ehlers, Carl 1994. Emplacement, deformation and geochemistry of bimodal volcanics in Vestlax, SW Finland. *Geological Survey of Finland, Special Paper 19*, 173–184, 9 figures and one table.

Bimodal volcanics in SW Finland formed a primitive Svecofennian crust some 1.89 Ga ago. In Vestlax, on the Kemiö island some of these volcanics are well-preserved. Primary volcanic structures, like pillowed lavas and pyroclastic and rheomorphic flow structures were mapped and one of the felsic units was identified as a metaignimbrite. A stratigraphic sequence was constructed from the pile of metavolcaniclastic rocks. The geochemistry of the pillowed metalavas is tholeiitic, with element patterns resembling those of recent mid-ocean ridge basalts (MORB). Early deformation folded the volcanoclastics recumbently and thrust them westwards, preferably along limestone horizons. The overturned volcanic sequence was subsequently refolded and a mushroom-shaped fold interference pattern developed. The axial plane of the second fold phase is steep east-westerly, which is the general strike of the Svecofennides in southern Finland.

Key words (GeoRef Thesaurus, AGI): metavolcanic rocks, volcanoclastics, pillow lava, ignimbrite, structural geology, deformation, geochemistry, Proterozoic, Paleoproterozoic, Vestlax, Kemiö, Finland

Alf Lindroos and Carl Ehlers, Department of Geology, Åbo Akademi University, FIN-20500 Åbo 50, Finland

INTRODUCTION

The Vestlax area on the Kemiö island is situated within a zone of intensely deformed Svecofennian gneisses in southern Finland (Fig. 1). This zone has been called the “Zone of Late Svecofennian granites” by Gaál (1990) and the “Late Svecofennian granite-migmatite or LSGM zone” by Ehlers et al. (1993). It transects southern Finland in a WSW-ENE direction as a 100 km wide and 500 km long belt. Characteristic features are thrust and sheared subaqueous metasediments and younger anatectic, sheet-like,

late orogenic granite bodies and migmatites.

The regional geological mapping of the Vestlax area and its surroundings was carried out by Seitsaari (1955). Lithologically the Vestlax area belongs to the “leptite zone” or the “Orijärvi leptite zone” (Eskola 1963), an eastward continuation of the Bergslagen ore province in south-central Sweden. This zone, and especially the Orijärvi part, about 50 km to the east of Vestlax, is well known from Eskola's (1914, 1915, 1920) now classical papers on metamorphic facies.

The structural geology of the Vestlax area and other parts of the Kemiö island has lately been described by several authors. Verhoef & Dietvorst (1980) presented a local geological map from an adjacent area and described two regional and two local fold phases. Dietvorst (1982) and Van Staal & Williams (1983) recognized metamorphic jumps and explained them by thrusting along marble horizons during the second fold phase as important factors in the structural development of the area. They also emphasized that the structural and metamorphic history of the area is similar to that of Phanerozoic orogenic belts. Westra (1988) gave a resume on the structural geology of the Vestlax area, based on publications mentioned in this chapter and several unpublished reports from the Free University of Amsterdam. He also gave a "tentative evolution model" for the Svecofennides of southern Finland. Another regional interpretation of the volcano-tectonic setting of the Kemiö-Orijärvi belt was presented by Colley & Westra (1987). They compared the belt to the present day back-arc setting in New Zealand.

Geological mapping of the area by the authors and by the students of the Åbo Akademi University has enabled us to compile a detailed geological map in which the fold interference pattern of an extensive but rather thin pillowed metalava marker horizon is utilized in interpreting the structural development of the area. A local stratigraphy is presented and stratigraphical sequence is used in connecting displaced or discontinuous parts of the marker-horizon. The structural interference pattern is then discussed in a regional context as a part of the "LSGM zone". Whole rock major and trace element analyses from the Vestlax metavolcanics are also presented and used for a discussion of petrogenesis and tectonic setting.

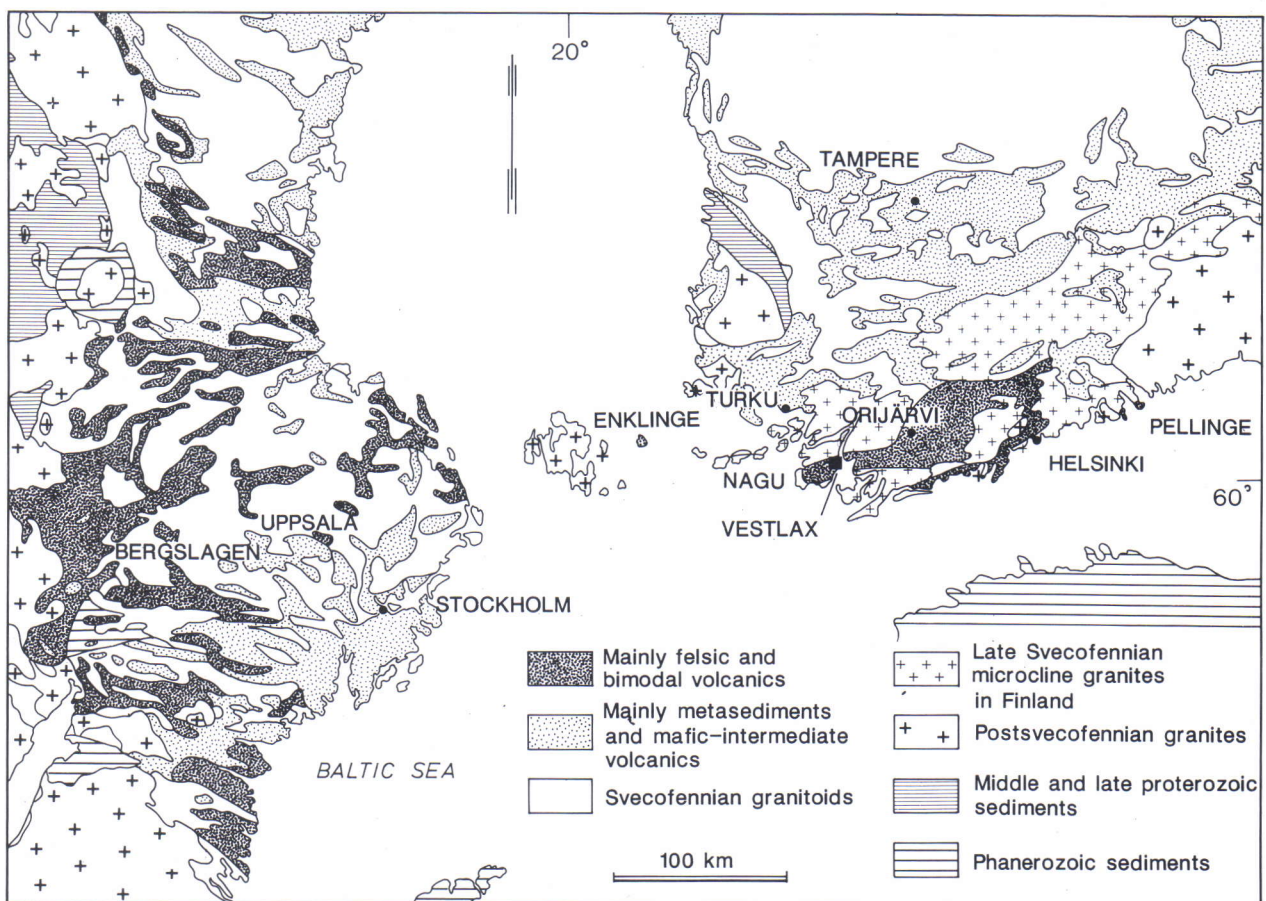


Fig. 1. Geological map of the southern Svecofennides. Modified from Boyd et al. (1985).

GEOLOGICAL SETTING

The Svecofennian Domain of Finland formed about 1.9 Ga ago during a major crust-forming event (Huhma 1986, Patchett & Kouvo 1986). The age of the oldest Svecofennian schists is poorly known, but a few U-Pb zircon datings on volcanogenic rocks (Patchett & Kouvo 1986, Kähkönen et al. 1989) place them around 1.90-1.89 Ga. Synorogenic calc-alkaline plutonism was most extensive somewhat later, around 1.89 Ga (Huhma 1986, Nurmi & Haapala 1986, Patchett & Kouvo 1986, Front & Nurmi 1987). In Pellinge, about 170 km to the east of Vestlax, metadacites, highest up in the local stratigraphy (Laitala 1984), are 1887 ± 14 Ma old (Patchett & Kouvo 1986). In Enklinge 120 km to the west, tonalitic veins, with local dacitic breccia pipes are dated at 1885 ± 15 Ma (Suominen 1987). Both these dacites are, however, more evolved than the felsic volcanics in the bimodal Vestlax and Orijärvi areas. They also occur stratigraphically above more primitive felsic volcanics, similar to those in Vestlax (Ehlers & Lindroos 1990a, Lindroos 1990)

In Sweden numerous datings on the early felsic volcanics (leptites) have been made. In the Uppsala and Bergslagen areas, 300-400 km to the west of Vestlax, rhyolitic and unspecified leptitic metavolcanics have ages around 1880-1900 Ma (Åberg et al. 1983, Åberg & Strömberg 1984, Welin 1987). The felsic metavolcanics of Vestlax and Orijärvi are in many ways similar to the early felsic metavolcanics of the Uppsala and Bergslagen areas. They have similar lithologies, geochemistry and mineralisations and we therefore consider them synchronous. The dated dacites in Pellinge and Enklinge are slightly younger and contemporaneous with the main Svecofennian plutonic phase.

Tectono-magmatically the Svecofennides have been regarded as a former convergent plate margin (Hietanen 1975, Mäkelä 1980, Gaál & Gorbatshev 1987, Kähkönen et al. 1989). The metavolcanic rocks in Vestlax and Orijärvi (Fig. 1) belong to a bimodal calc-alkaline suite, which may have erupted in a back-arc environment (Colley & Westra 1987). Our chemical analyses of the Vestlax pillowed metalavas show an even more primitive tholeiitic geochemistry, which has also been encountered in Orijärvi (Mäkelä 1989). It is probable that some of the pillowed metalavas in Vestlax and Orijärvi can be correlated.

Pillowed metalavas west of the Kemiö island are different. In Nagu and Iniö, about 50 km to the west, they show a HFS (High Field Strength) element enriched tholeiitic geochemistry (Ehlers et al. 1986,

Lindroos et al. 1990). According to Ehlers et al. (1986), the tholeiitic pillowed metalavas of Nagu represent early continental rift volcanism followed by transgression and precipitation of limestone and sulfides.

The earliest Svecofennian fold phases predate the major plutonic activity (Ehlers & Lindroos 1990a, b) or they are coeval with it (Colley & Westra 1987). Within a 100 km wide belt along the south coast of Finland, running across the Kemiö island, stacking of offshore sediments and volcanics took place during the early Svecofennian. Piles of volcanoclastics, turbidites and chemical sediments were thrust on top of each other (e.g. Väisänen 1988) and occasionally they were overturned. Typically the thrusting took place along limestone horizons (Van Staal & Williams 1983, Ehlers & Lindroos 1990b). The direction of the early thrusts has not been determined yet but most of the sequences we have observed in southwestern Finland are overturned towards the north and the west. Ploegsma & Westra (1990) on the other hand suggest an early fold phase with recumbent folds verging towards ESE-SSE in Orijärvi.

About 40 Ma after the major granitoid emplacement stage, the area was sheared by dextral movements along steep E-W trending planes (Ehlers & Lindroos 1990b) and microcline granites were emplaced along synchronous subhorizontal shear zones (Ehlers et al. 1993). The Hanko granite, southeast of Vestlax, has been dated at 1.83 Ga (Huhma 1986) and the Perniö granite on the northern side at 1.84 Ga (Suominen 1991). According to Ehlers et al. (1993), portions of the upper crust moved westwards relative to deeper parts of the crust as a result of the shearing, and the microcline granites were mainly emplaced along these flat-lying planes. Final stages of the deformation folded the microcline granites into upright folds.

The Vestlax area is situated within a block bordered to the north and to the south by steeply dipping marble horizons along which E-W strike slips have taken place. Within the block the Svecofennian schists are well-preserved and characterized by a muscovite + quartz assemblage while high-grade cordierite + K-feldspar rocks occur on both sides of the block (Dietvorst 1982). According to Van Staal & Williams (1983), the block movements and metamorphic jumps are more easily explained by northward thrusting than by normal faulting. If that is the case, then the steep strike slips bordering the Vestlax block are the flanks of curved thrust planes along marble horizons.

ROCK SEQUENCE

Within the Vestlax block there is a conspicuous closed interference pattern consisting of pillowed metalavas and mafic metavolcaniclastics interlayered between felsic metavolcaniclastics (Fig. 2). A section from the inside of the figure to the outside gives

the following sequence of rocks, which we consider a stratigraphic sequence: (1) an inner felsic unit, (2) a mafic horizon, (3) a volcanoclastic and partly tectonic breccia, and (4) an outer felsic unit.

Inner felsic unit

Felsic metavolcaniclastics occur inside the interference structure. Primary structures, such as fiamme-

like fragments, xenolithic fragments (mostly gabbroic) and rheomorphic flow structures (Fig. 3)

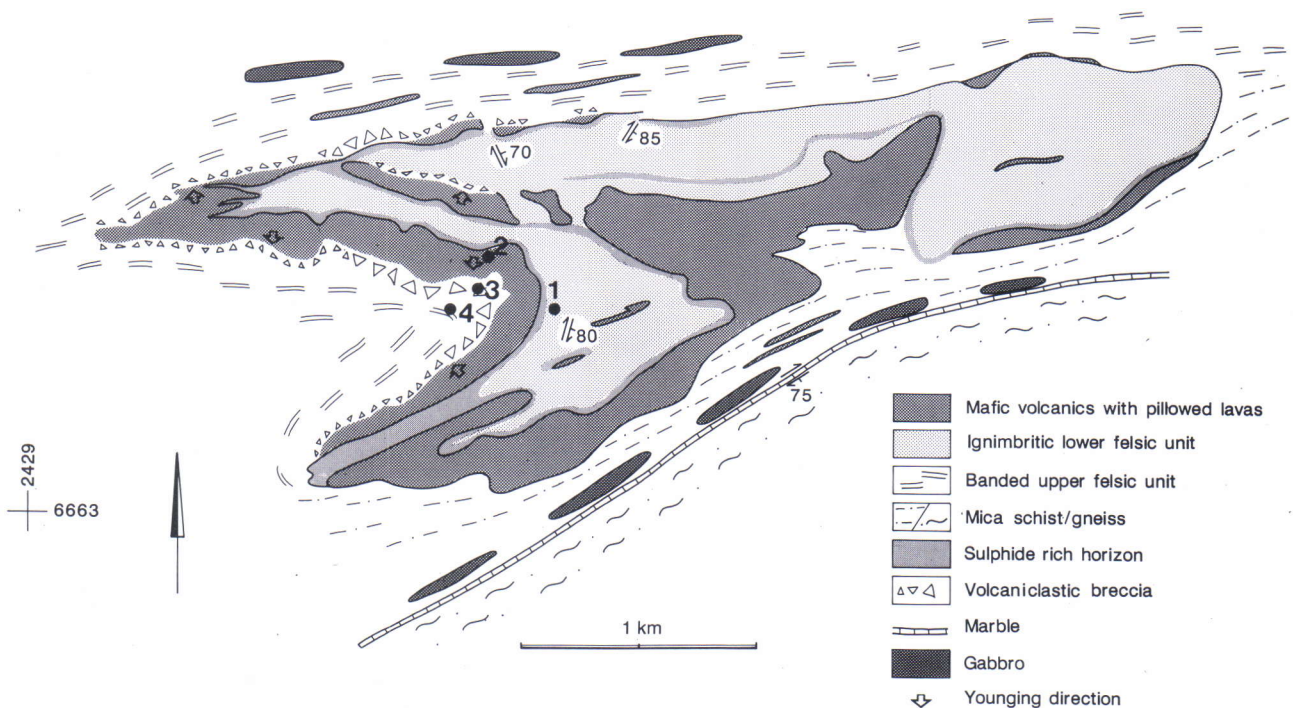


Fig. 2. Geological form surface map of the Vestlax area. Numbers 1-4 refer to the rock sequence in the text.

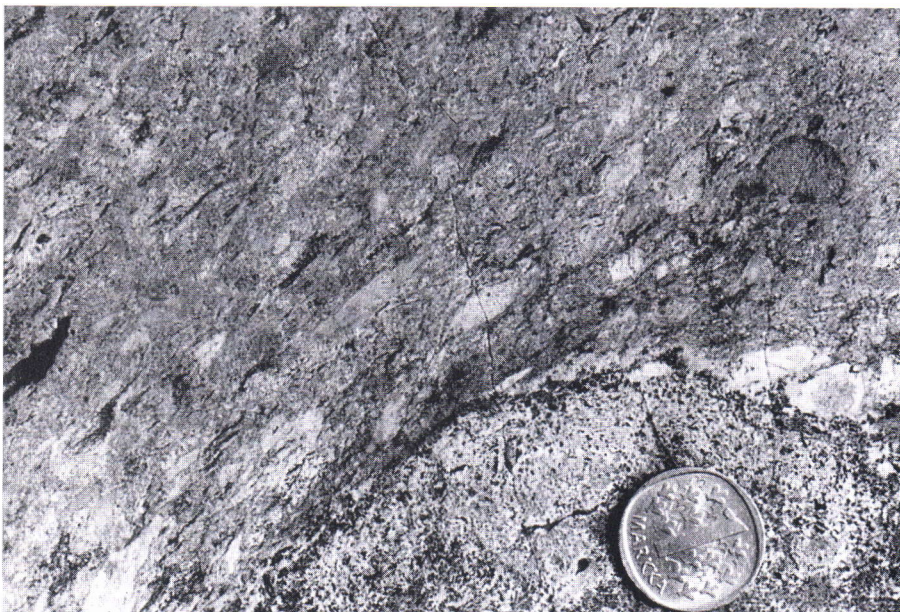


Fig. 3. The ignimbritic lower felsic unit. Welded felsic fragments, and a xenolithic gabbro fragment. Diameter of the coin is 24 mm.

suggest that this felsic horizon is a metaignimbrite.

The rock is composed of quartz with minor plagioclase and biotite, and frequent centimeter scale hollow or calcite filled voids. It is very fine but uneven in grain size. Grain boundaries and void contours are stained by opaques and sericite. Small clusters of larger quartz grains occur frequently. No orientation of individual quartz grains can be seen, but the clusters are elongated and have a preferred

orientation parallel with the fiammes. Greenish brown mica occurs together with the quartz clusters and as smaller grains together with the opaques. Mica is also concentrated along the margins of the fiammes. Retrograde chlorite overprints a few mica grains and defines a preferred orientation. The margin (stratigraphically the upper part) of the felsic unit is sericitized and mineralized with pyrrhotite and pyrite.

Mafic unit

Mafic pillowed metalavas cover the mineralized horizon. The pillows are in places well preserved, so that top of strata can be determined. The interpillow matrix is cherty. The metalavas occur together with massive lenticular bodies of uralite porphyries of unknown origin. The latter were probably mafic pyroclastics which might have been enriched in crystals during subaqueous transport and deposition.

The mineral composition of the metalavas is dominated by a dense network of very fine-grained, dirty green hornblende; only a few plagioclase, sphene, biotite and quartz grains occur together with a fine-grained opaque impregnation. Hornblende is clearly metamorphic; the grains are arranged as a mosaic, which reveals a more coarse-grained primary flow structure.

Breccia unit

The mafic metavolcanic pile in many places terminates with a layered, clast-supported volcanic metabreccia consisting of mafic lava fragments and hyaloclastic rubble in a biotitic matrix. Polymictic varieties also occur where fragments from the underlying ignimbritic and sulfide-rich horizons occur together with and, in places, outnumber the mafic fragments. The strata may be normally or inversely graded or ungraded, which suggests that they were redeposited after sliding down subaqueous slopes.

On the western and northern flank of the interference structure there is a thin (<3 m) but extensive (several km long) polymictic clast-supported meta-

breccia between the mafic formation and the surrounding felsic horizon. The clasts consist of fragments of mafic volcanics chaotically mixed with fragments from the underlying felsic formation, coarse plagioclase and quartz grain clusters, cherty fragments and quartz vein fragments in a biotitic matrix. The clasts are in general deformed, attenuated vertically and flattened horizontally. In our opinion, this is a tectonic breccia formed by shearing along the contact between the mafic and felsic units. The tectonic breccia partly overprints the volcanic breccia described above.

Outer felsic unit

Structurally outside the interference figure and the polymictic metabreccia follows a felsic, fine-grained and banded volcanoclastic metasediment. The lowermost bands are locally rich in fragmental plagioclase crystals. The bulk of the unit consists of fine-grained quartz-feldspar-biotite rocks with only accessory opaques. A fine-grained matrix of quartz and sericitized plagioclase encloses slightly larger quartz and occasional K-feldspar grains. The unit is thickest on the northern and western side of the interference figure. Along the southern margin it is thin, sheared and mica-rich. The outer felsic unit is interpreted as a distal subaqueous volcanoclastic

metasediment probably of ash-cloud origin. It was possibly transported subaqueously and locally mixed with epiclastic material.

Further outwards from the structure the metasediments are pelitic and generally they are strongly sheared and sericitic. Sill-like gabbroic bodies are common in the sheared metapelites. Strongly sheared marble horizons border the Vestlax block on the northern and southern sides. In general the marbles occur concordantly within the metapelites, but they are always sheared and in places they are mobilized along shear zones and occur discordantly in respect to the pelitic layers and their axial plane schistosity.

The marble layer in Fig. 2 is the locus of a metamorphic jump which requires a vertical displacement of several kilometers (Dietvorst 1982).

On the southern side of the marble, gabbros and sillimanite-bearing mica gneisses, with amphibolitic metadykes, are encountered. Further south the entire sequence reappears, which suggests that the inner and outer felsic units are stratigraphically separate units with a regional distribution and not a proximal ignimbritic facies folded over its distal facies.

GEOCHEMISTRY

Metavolcanic rocks from the southern parts of the Kemiö island were analysed for the major elements and some trace elements, including REE. Major elements and Ti, P, Sr, Zr, Cr and Ni were determined using XRF in the Research Laboratory of Rautaruukki Oy (for details see Ala-Vainio 1986). Ba, Rb, Cs, U, Th, Sc, Ta and the REE were analysed using INA techniques in the Technical Research Centre of Finland (Rosenberg 1977). Ba values under 80 ppm, as well as Ta values under 0.5 ppm and Cs values under 0.6 ppm are near the detection limit of the INA method and therefore imprecise. Rb in samples 3B and 4B was under the detection limit for the INA method. It was therefore determined together with Y and Ga by external millibeam PIXE multipoint analysis directly on polished samples at the Accelerator Laboratory of Åbo Akademi University (Lill et al. 1993). Table 1 presents some of the analyses from the Vestlax area.

The mafic metavolcanics plot in two distinct groups in Figs. 4 and 5: one basaltic and one andesitic, along a subalkaline and tholeiitic trend. They are rich in Al, Fe, Ti, P, Sc, heavy alkalis and actinides,

We consider the section from the inside of the interference figure to the outside a true stratigraphic sequence. A transgressive evolution from silicic ignimbritic volcanism to basaltic volcanism with pillow lavas and finally to coverage by distal volcanics can be deduced from the stratigraphy. However, major displacements along the marbles and more local displacements, due to folding, along the upper and lower contacts of the mafic metavolcanics have affected the sequence.

but low in Mg, Ni, Cr, Sr and Ga. Their chondrite-normalized REE patterns (Fig. 7) are flat and nearly parallel with a slight LREE fractionation and a negative Eu anomaly. The MORB-normalized minor and trace element patterns (Fig. 6) of the Vestlax pillowed metalavas show a rather primitive geochemistry similar to MORB or back-arc basin basalt.

Some elements are, however, enriched compared with MORB. K, Rb, Th (Fig. 6) and U (Table 1) are up to seven times enriched, while Cs (Table 1) is about two orders of magnitude enriched compared with the Cs concentrations for MORB given, e.g. by Wilson (1989). Note also that the Cs concentrations are higher in the metabasalts than in the metaandesites, which cannot be a primary feature. Heavy alkali and actinide element mobilization during the deformational phases described below, is suggested as the cause of the anomalous concentrations. Similar, but even more extreme enrichment of alkalis and actinides have been encountered in several pillowed metalavas with secondary micas from southern Finland (our unpublished analyses).

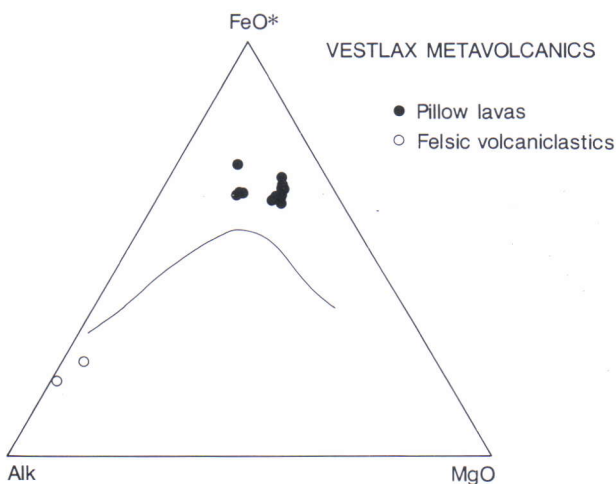


Fig. 4. AFM diagram (Irvine & Baragar 1971) of the metavolcanics from the Vestlax area. Data from Table 1.

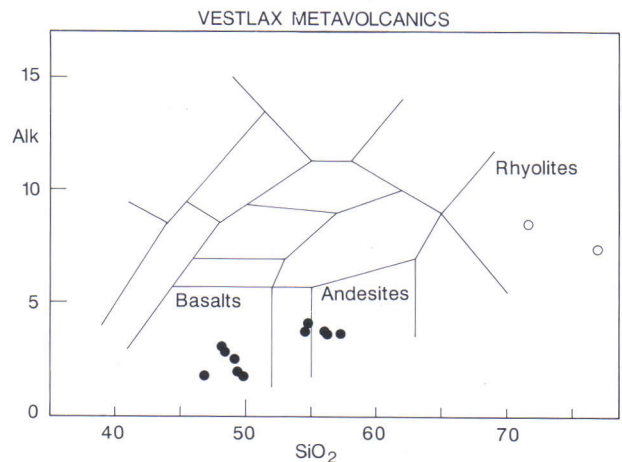


Fig. 5. Total alkali ($\text{Na}_2\text{O} + \text{K}_2\text{O}$) vs. silica diagram for classification of volcanic rocks (Cox et al. 1979). Symbols as in Fig. 4.

Table 1. Chemical analyses of the Vestlax mafic and felsic units. The analytical methods are described in the text.

	1A	1B	1C	2A	2B	2C	3A	3B	3C	4A	4B	4C	5	6	7	8
SiO ₂	56.73	54.09	57.27	57.61	57.01	55.02	49.60	49.10	49.20	46.70	48.30	48.00	48.30	52.50	76.80	71.40
TiO ₂	2.38	2.56	2.39	2.46	2.33	2.36	1.51	1.45	1.44	1.29	1.42	1.46	2.22	0.84	0.16	0.41
Al ₂ O ₃	12.70	13.23	12.81	13.21	12.58	12.68	15.20	17.80	16.80	22.60	16.50	16.60	14.10	16.50	13.00	14.40
FeO*	12.58	13.34	11.91	13.18	12.25	12.55	14.00	12.60	13.20	11.90	13.90	14.10	18.50	8.85	1.80	2.80
MnO	0.20	0.21	0.18	0.22	0.20	0.21	0.19	0.21	0.20	0.18	0.20	0.20	0.27	0.16	0.01	0.04
MgO	2.92	3.37	2.82	3.37	3.15	3.09	4.70	5.18	4.86	4.29	5.15	5.17	3.92	6.58	0.11	0.54
CaO	6.93	7.00	8.15	7.70	7.45	7.59	11.40	10.10	11.10	10.00	10.50	10.00	8.84	9.93	0.30	1.20
Na ₂ O	3.20	3.20	3.19	3.32	3.12	3.13	1.60	2.23	1.77	1.54	2.55	2.77	1.57	3.46	2.13	3.17
K ₂ O	0.66	0.89	0.48	0.38	0.55	0.61	0.26	0.23	0.23	0.32	0.24	0.35	0.43	0.32	5.28	5.40
P ₂ O ₅	0.24	0.28	0.23	0.23	0.24	0.22	0.25	0.25	0.24	0.22	0.23	0.23	0.45	0.09	0.01	0.17
Sum	98.54	98.17	99.43	101.68	98.88	97.46	98.71	98.35	99.04	99.04	98.99	98.88	98.60	99.23	99.60	99.53
Rb	11	24.2	11	-	-	-	-	13.1	-	-	15.2	-	15.4	-	114	113
Cs	0.88	2.3	0.73	-	-	-	1.6	0.93	1.1	4.1	0.4	1.4	1.8	1.1	1.6	4.3
Sr	120	100	129	128	120	117	110	110	110	100	130	130	130	140	20	90
Ba	175	245	50	-	-	-	20	50	40	40	40	80	50	110	816	670
Th	5.23	5.51	5.02	-	-	-	1.29	1.42	1.31	1.19	1.07	1.07	1.85	2.83	19.9	22.8
U	1.85	1.92	1.94	-	-	-	0.53	0.44	0.52	0.44	0.39	0.41	1.07	0.97	5.53	3.49
Ta	0.7	0.7	0.8	-	-	-	0.2	0.2	0.2	0.2	0.2	0.2	0.4	0.5	1.2	0.9
Zr	156	162	118	163	164	153	100	100	100	80	90	90	220	70	250	340
Y	48	49	47	48	47	47	-	35.6	-	-	35.6	-	-	-	-	-
Sc	41	47	47	-	-	-	64	63	61	56	62	66	66	52	4	7
Cr	40	40	40	-	-	-	174	155	150	148	110	144	30	224	20	20
Ni	30	30	30	-	-	-	40	20	30	30	20	20	30	20	10	20
Ga	-	-	-	-	-	-	-	17.4	-	-	18.8	-	-	-	-	-
La	14.5	17.1	17.1	-	-	-	6.9	6.67	6.4	6.5	7.4	5.7	8.3	8.6	17.1	55.3
Ce	-	33.5	-	-	-	-	-	12.9	-	-	-	-	-	-	37.7	107
Nd	-	18.9	-	-	-	-	-	8.78	-	-	-	-	-	-	20.8	48.6
Sm	5.92	6.37	6.40	-	-	-	3.59	3.30	3.30	3.06	3.11	3.20	5.81	3.18	5.02	7.63
Eu	-	1.54	-	-	-	-	-	1.02	-	-	-	-	-	-	0.67	0.92
Tb	-	1.10	-	-	-	-	-	0.78	-	-	-	-	-	-	1.13	0.99
Yb	-	4.09	-	-	-	-	-	3.10	-	-	-	-	-	-	9.49	2.81
Lu	-	0.60	-	-	-	-	-	0.49	-	-	-	-	-	-	1.27	0.33

Numbers 1-4 refer to lava pillows. (Coordinates: 1 and 2, X=660.150, Y=420.800; 3 and 4, X=664.150, Y=430.800). 5 massive mafic lava, (X=664.360, Y=431.660). 6 gabbro, (X=662.550, Y=430.570). 7 the lower felsic unit, (X=664.000, Y=431.250). 8 the upper felsic unit, (X=663.950, Y=430.650).

Because of the alkali and actinide element behavior discussed above and since the Ta analyses are imprecise and Nb is not analyzed, we do not consider it possible to speculate about whether there is a subduction zone component present in the metavolcanics. Anyway they represent a rather primitive crust.

The positive Sc anomalies in Fig. 6 might be a primary feature, typical for Fe-, Ti- and P- rich Svecofennian metabasalts. The anomaly arises from the well-established Sc-Fe (III) diadochy. The small Y anomaly could have a similar origin, but Y is more like the HREE and the anomaly is therefore smaller.

The genetic relationship between the andesite and the basalt can be modelled in several ways. The REE patterns in Fig. 7 can be interpreted so that they represent partial melts of similar source rocks. The higher REE values of sample 1B (andesite) represent a smaller fraction of melt than those of sample 3B (basalt). Residual plagioclase would cause the nega-

tive Eu anomaly and residual clinopyroxene the slight LREE fractionation from the HREE.

The andesite and basalt could also be produced by fractional crystallization of a parent magma with a composition similar (but slightly more basic) to that of the gabbro in Table 1. The low Mg, Ni, Cr and Sr contents and the Ti and Fe enrichment trend suggest that their parent magma fractionated Mg-Cr spinel, olivine and plagioclase, but not ilmenite nor clinopyroxene. The andesite did probably not evolve from the basalt directly by fractional crystallization, since phryic plagioclase is absent in the basalt, but they more likely developed along separate paths with separate parent magmas in small magma chambers. The negative Eu anomaly was probably present already in the parent magmas. Their upper mantle source rocks were most likely similar, since the Vestlax area is geographically restricted.

A third model for their genetic relation is to consider them as increments of melt from the same source rock. In this case the andesite represents an earlier batch of melt and the basalt a later batch of melt from the same source. We consider the first two processes more important, while the third one is more theoretical. (For modelling trace element behaviour during melting and fractional crystallization see, e.g. Haskin 1984).

Our limited material does not allow us to model the melting process in detail since we do not know the composition of the source rock. Some constraints on the composition of the source can, however, be deduced from the REE patterns if the simple melting models are basically correct. Firstly, our melting models require that the REE composition of the source rock does not differ very much from a low

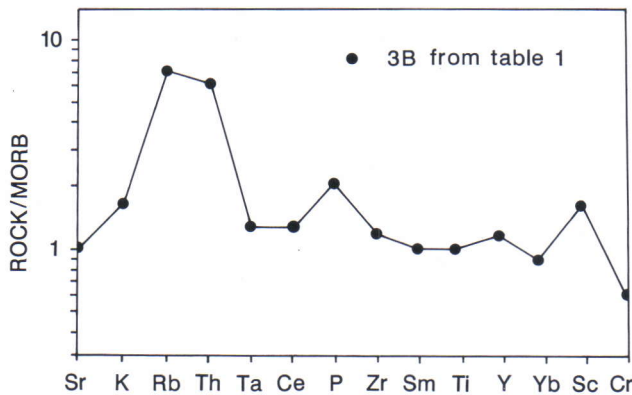


Fig. 6. MORB-normalized (values from Pearce 1982) trace element variation diagram for a basaltic pillow lava from the Vestlax area. Sample 3B, Table 1.

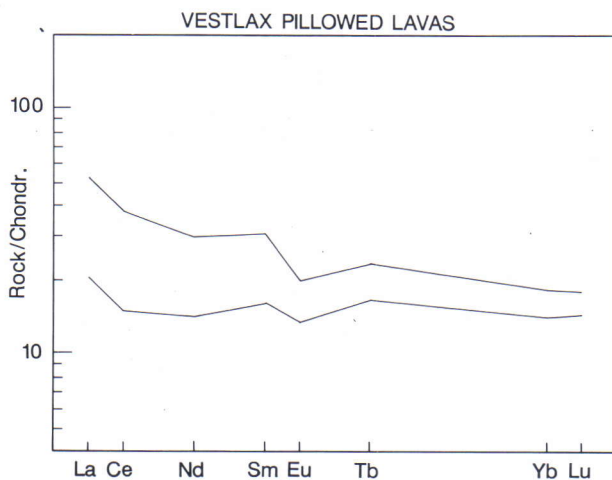


Fig. 7. Chondrite-normalized (Nakamura 1974) REE patterns of the mafic rocks from the Vestlax area. The lower graph represents the samples which plot in the field of basalts in Fig. 5; the upper graph represents the andesitic samples. Samples 1B and 3B, Table 1.

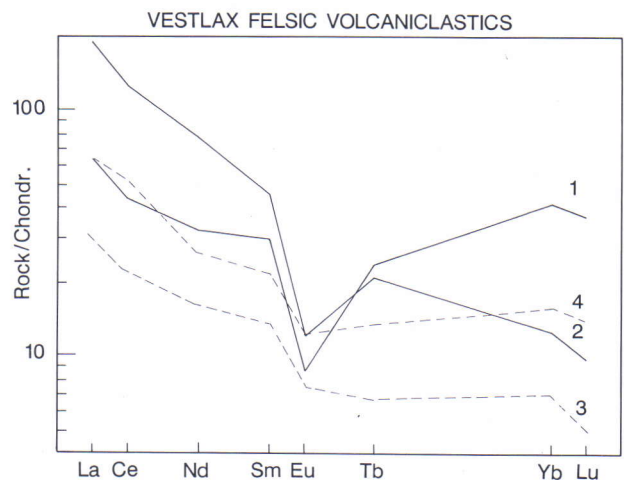


Fig. 8. Chondrite-normalized (Nakamura 1974) REE patterns for the inner (1) and outer felsic units (2) in Vestlax (samples 7 and 8, Table 1) compared with two felsic metavolcanics from Orijärvi (Mäkelä 1989); 3 = "quartz-eyed acid meta-agglomerate"; 4 = "equigranular metatuff".

multiple of chondritic REE concentrations. Secondly, the small negative Eu anomaly, which is somewhat deeper in the andesites, requires the presence of plagioclase in solid residue (or as a fractionating mineral in parent magmas). Thirdly, the fractionation of the LREE relative to the HREE, is explained with clinopyroxene being present.

It is suggested that the Vestlax basalts and andesites formed by partial melting of the upper mantle leaving clinopyroxene and plagioclase in the residue. The melts ascended and were collected into small, shallow magma chambers where Mg-Cr spinel, plagioclase and olivine crystallized leaving an Fe- and Ti -rich liquid which eventually erupted. The gabbro in Table 1 could represent a small magma chamber with a less fractionated magma, where olivine was the most important fractionating mineral

as seen from the low Ni but moderate Mg, Cr and Sr content.

The felsic units were not sampled in any detail because pyroclastic silicic rocks do not generally represent their parent magma. However, in Table 1 the two last samples represent the felsic units. Fig. 8 shows REE patterns for the inner and the outer felsic units together with REE patterns for silicic metavolcanic rocks from the Orijärvi area (Mäkelä 1989). The patterns are not related to each other nor to those of the mafic metavolcanics by simple melting/crystal fractionation processes. A comparison with the felsic metavolcanics from Orijärvi shows no similarity either. The strong negative Eu anomalies indicate that plagioclase played an important role in the formation of both felsic units either as a solid residue during partial melting or as a fractionating mineral.

STRUCTURAL ANALYSIS

The pillow lava marker horizon in Vestlax defines a closed fold interference structure (Fig 2). Stratigraphic order determined from top of strata observations in well-preserved parts of the pillowed metalava indicates that it is an anticlinal structure,

overturned towards the west, later folded into a synform with a steep E-W striking axial surface. We therefore identify two major deformation phases D_1 and D_2 , which interfere and produce the structure in Fig. 2.

D_1 phase

In this study D_1 comprises structures which are transposed and overprinted by the more easily discerned and regionally consistent D_2 structures. The definition is principally the same as that used by Verhoef & Dietvorst (1980) and Westra (1988).

A few mesoscopic F_1 folds have been observed in mafic interlayers in the inner felsic lithologies. They are isoclinal and had originally subhorizontal fold axes later steepened by D_2 . The westwards pointing southern and northern horns in Fig. 9 as well as the

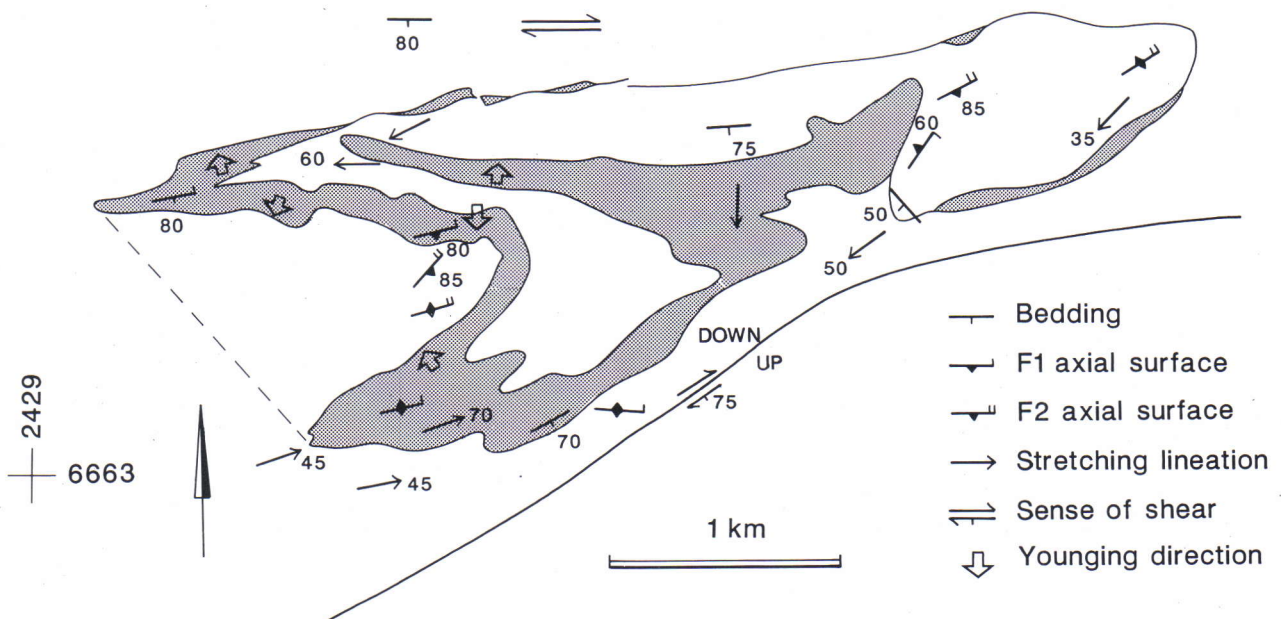


Fig. 9. Structural interpretation of the Vestlax area, simplified from surface map.

southwestwards pointing bend in the eastern part are macroscopic isoclinal F_1 folds. A line connecting the southern horn with the northern horn (the dashed line in Fig. 9) gives the approximate original strike of the F_1 axis. We do not, however, know whether the F_1 fold was cylindrical or non-cylindrical (sheath or tubular fold), but early folds from other areas in southwestern Finland are usually non-cylindrical.

S_1 axial plane schistosity consists of a preferred orientation of micas and hornblende and is occasionally formed by flattening of the clasts in the volcanoclastic breccias. It is concordant with the volcanoclastic layering S_0 around the interference figure, except for the southern and northern horns, which are F_1 fold apices (Fig. 9). An early generation of quartz veins developed concordantly with S_1 or possibly already with S_0 .

Early linear structures consist of a preferred orientation of hornblende and elongated pillows and volcanoclastic fragments; south from the interference

figure an orientation of sillimanite is formed. The linear elements have a rather uniform moderate plunge towards the east in the southern parts of the area (Fig. 9) and gentle to moderate westerly plunges in the eastern and northern parts, while steep southerly plunges prevail in the central parts.

Some of the linear elements could be D_1 transport lineations, or they could have formed along intersections between F_1 and F_2 axial surfaces. The observations of Verhoef and Dietvorst (1980) that hornblende and sillimanite crystallized after the culmination of D_1 and before and during D_2 , support the latter interpretation, but do not exclude the former. The generally steep to moderate plunge of the lineations on the other hand cannot have formed from intersection between a subhorizontal axial surface of a recumbent D_1 fold and a steep F_2 axial surface. This problem will be discussed further in the structural interpretation.

D_2 phase

D_2 in the Kemiö area is seen as tight to isoclinal folds with E-W striking steep axial surfaces. It is generally defined as a N-S oriented compressive phase (Verhoef & Dietvorst 1980, Van Staal & Williams 1983, Westra 1988). In Vestlax a macroscopic F_2 synform dominates the interference figure. Together with the two isoclinal F_1 folds it forms two successive inclined fold interference mushroom figures with eastward pointing apices. The western mushroom is well-developed, while the northern half

of the eastern mushroom was difficult to map because the mafic horizon is thin or discontinuous in the northeastern parts of the area.

The E-W axial surface is upright or tilted slightly towards the north. A well-developed S_2 axial surface schistosity diverges from S_1+S_0 in the apices of the mushroom figures. Stereographically constructed F_2 fold axis and measured D_2 stretching lineations plunge moderately to steeply towards the west or the southwest.

Structural interpretation

The Vestlax structure is formed by interference of two fold phases. The D_1 phase is represented by two successive isoclinal anticlines overturned towards the west. The D_2 phase folds the subhorizontal axial surfaces of the D_1 phase into an east-westerly synform with a steep axial surface and a westwards plunging axis.

The pillowed metalavas were folded recumbently and overturned together with the felsic units during D_1 . The tectonic component of the breccia on the west side of the interference figure may have formed during a westward thrust of the recumbent fold. During folding the contact between the ignimbritic and the mafic unit was sheared and the sulfides from the upper part of the ignimbritic unit were locally mobilized into the F_1 hinges.

The well-developed southern parts of the two

successive mushroom figures have lineations in opposite directions (Fig. 9). In the western figure the plunges are towards east and in the eastern figure they are towards the west. In a fold interference mushroom model this would mean that erosion has revealed the lower limb of the western recumbent fold but only scraped off parts of the upper limb of the eastern one. The observed outward dip of the lithologic layering in the eastern F_1 fold is also consistent with this interpretation.

The different trend of plunges of early lineations in the northern and southern horns of the larger western mushroom can be explained in several ways. We believe that most of the measured lineations are F_1 transport lineations and the angle between the F_1 axis and the D_2 axial surfaces is oblique. If the F_2 axial plane is taken as east-westerly then the F_1 fold

axis must have had a flat NW-SE trend. This is consistent with the simple geometrical fact that the northern leg of the well-developed westerly F_2 fold is longer than the southern leg. A model where the lineations are parallel with F_1 axis is unlikely because in that case a longer southern and a shorter northern leg would have developed.

A third possibility is that the compressive D_2 phase had a dextral strike slip component, that was not completely taken up by the limestones, but also transposed the lineations. Field evidence, however, indicate that dextral shearing was concentrated in the marble horizons and the micaceous schists south of the interference figure.

DISCUSSION

The early Svecofennian volcanism of southern Finland is poorly known. Stratigraphic successions generally commence with metagraywackes covered by or interspersed with tholeiitic pillowed metalavas and banded gabbros. In places these thin primitive metabasalts are overlain by thicker piles of bimodal metavolcanics. The bimodal metavolcanics of Vestlax are together with their counterparts in Orijärvi the most primitive tholeiitic volcanics in southern Finland.

The depositional environment for the metavolcanics was a young ensialic crust. This has been verified by zircon analyses of stratigraphically low-lying metagraywackes from different parts of the Svecofennian Domain (Huhma et al. 1991). Zircons with U-Pb ages between 1.9 and 2.0 Ga are abundant, which indicates that a Proterozoic crust with felsic igneous rocks developed already before 1.9 Ga ago.

The age of the first Svecofennian fold phase is synchronous with, or older than the major Svecofennian granitoid plutonism about 1.88 Ga ago, because these granitoids were emplaced along F_1 axial surfaces (Ehlers et al. 1993). The direction of

the D_1 stress field was E-W to NE-SW. A direction perpendicular to a NW-SE directed subduction zone along the margin of the Archean craton about 500 km to the northeast is plausible and was suggested by e.g. Nironen (1989). Westward and northwestward vergences of folds synchronous with the main Svecofennian plutonic phase are also common in the Stockholm area in Sweden as pointed out by Stålhös (1969, 1972, 1991). We have also observed similar vergences in the northern parts of the archipelago near Turku (Fig. 1). Clockwise rotation of originally southwesterly vergences may have occurred during a long period of dextral shearing after the recumbent folding (Ehlers et al. 1993).

The second phase of deformation predates, or is approximately synchronous with the emplacement of microcline granites and migmatites. Ehlers et al. (1993) describe it as a combination of WSW-ENE directed dextral strike-slip with a NW-SE directed compression. D_2 structural elements in Vestlax have the same orientation as the general trend of D_2 elements described by Ehlers et al. (1993), and we therefore correlate them.


REFERENCES

- Åberg, G., Levi, B. & Fredrikson, G. 1983. Zircon ages of metavolcanic and synorogenic rocks from the Svärdsjö and Yxsjöberg areas, south central Sweden. *Geol. Fören. Stockholm Förh.* 105, 199-204.
- Ala-Vainio, I. 1986. XRF routine analysis by the fundamental parameter method. Proceedings of the Thirty-ninth Chemists' Conference. Scarborough, June 17-19, 1986. Research and Development, British Steel Corporation, 51-54.
- Åberg, G. & Strömberg, A. 1984. Radiometric dating of Svecokarelian metarhyolites and prekinematic granitoids from Bergslagen south central Sweden. *Geol. Fören. Stockholm Förh.* 106, 209-213.
- Boyd, R., Nilsson, G., Papunen, H., Vormaa, A., Zagorodny, V. & Robonen, W. 1985. General geological map of the Baltic shield 1:2 500 000. In: Papunen, H. & Gorbunov, G.I. (eds) Nickel-copper Deposits of the Baltic Shield and Scandinavian Caledonides. *Geol. Surv. Finland, Bull.* 333.
- Colley, H. & Westra, L. 1987. The volcano-tectonic setting and mineralisation of the early Proterozoic Kemiö-Orijärvi-Lohja belt, SW Finland. In: Pharaoh, T.C., Beckinsale, R.D. & Rickard, D. (eds) *Geochemistry and Mineralisations of Proterozoic Volcanic Suites*. Oxford: Blackwell. *Geol. Soc. Spec. Publ.* 33, 95-107.
- Cox, K.G., Bell, J.D. & Pankhurst, R.J. 1979. *The Interpretation of Igneous Rocks*. London: Allen & Unwin, 450 p.
- Dietvorst, E.J.L. 1982. Prograde metamorphic zoning in amphibolite facies pelitic gneisses from Kemiö, southwest Finland. *Geol. Rundschau* 71, 245-262.
- Ehlers, C., Lindroos, A. & Jaanus-Järkkälä, M. 1986. Stratigraphy and geochemistry in the Proterozoic mafic volcanic rocks of the Nagu-Korpo area, SW Finland. *Precambrian Res.* 32, 297-315.
- Ehlers, C. & Lindroos, A. 1990a. Early Proterozoic Svecofennian volcanism and associated plutonism in Enklinge, SW Finland. *Precambrian Res.* 47, 307-318.
- Ehlers, C. & Lindroos, A. 1990b. Low angle ductile shears in


- the Early Proterozoic rocks of SW Finland. *Geol. Fören. Stockholm Förh.* 112, 177-178.
- Ehlers, C., Lindroos, A. & Selonen, O. 1993.** The late Svecofennian granite-migmatite zone of SW Finland - a belt of transpressive deformation and granite emplacement. *Precambrian Res.* 64, 295-309.
- Eskola, P. 1914.** On the petrology of the Orijärvi region in southwestern Finland. *Bull. Comm. géol. Finlande* 40, 277 p.
- Eskola, P. 1915.** Om sambandet mellan kemisk och mineralogisk sammansättning hos Orijärvitraktens metamorfa bergarter. *Bull. Comm. géol. Finlande* 44, 145 p.
- Eskola, P. 1920.** Om metasomatiska omvandlingar i silikatbergarter. *Norsk geol. Tidsskr.* 6, 89-107.
- Eskola, P. 1963.** The Precambrian of Finland. In Rankama, K. (ed.) *The Precambrian*, vol. 1. New York: John Wiley, 145-263.
- Front, K. & Nurmi, P. 1987.** Characteristics and geological setting of synkinematic Svecofennian granitoids in southern Finland. *Precambrian Res.* 35, 207-224.
- Gaál, G. 1990.** Tectonic styles of early Proterozoic ore deposition in the Fennoscandian Shield. *Precambrian Res.* 46, 83-114.
- Gaál, G. & Gorbatshev, R. 1987.** An outline of the Precambrian evolution of the Baltic Shield. *Precambrian Res.* 35, 15-52.
- Haskin, L.A. 1984.** Petrogenetic modelling - use of rare earth elements. In: Henderson, P. (ed.) *Rare Earth Element Geochemistry*. Amsterdam: Elsevier, 115-152.
- Hietanen, A. 1975.** Generation of potassium-poor magmas in the northern Sierra Nevada and the Svecofennian of Finland. *U.S. Geol. Surv. J. Res.* 3, 631-645.
- Huhma, H. 1986.** Sm-Nd, U-Pb and Pb-Pb isotopic evidence for the origin of the Early Proterozoic Svecofennian crust in Finland. *Geol. Surv. Finland, Bull.* 337, 48 p.
- Huhma, H., Claesson, S., Kinny, P.D. & Williams, I.S. 1991.** The growth of early Proterozoic crust: new evidence from Svecofennian detrital zircons. *Terra Nova* 3, 175-179.
- Irvine, T.N. & Baragar, W.R.A. 1971.** A guide to the classification of the common volcanic rocks. *Can. J. Earth Sci.* 8, 523-548.
- Kähkönen, Y., Huhma, H. & Aro, K. 1989.** U-Pb zircon ages and Rb-Sr whole rock isotope studies of early Proterozoic volcanic and plutonic rocks near Tampere, southern Finland. *Precambrian Res.* 45, 27-42.
- Laitala, M. 1984.** Pellingin ja Porvoon kartta-alueiden kallioperä. Summary: Pre-Quaternary rocks of the Pellinki and Porvoo map-sheet areas, sheets 3012 and 3021. Geological map of Finland. 1 : 100 000. 53 p.
- Latvalahti, U. 1979.** Cu-Zn-Pb ores in the Aijala-Orijärvi area, Southwest Finland. *Econ. Geol.* 74, 1035-1059.
- Lill, J.-O., Saarela, K.-E., Hernberg, F.J., Heselius, S.-J. & Harju, L. 1993.** A novel method for charge integration in external beam TPIXE-application to analyses of biological materials. *Nuclear Instruments and methods in physics research.* B83, 387-393.
- Lindroos, A. 1990.** Early Proterozoic volcanic rocks in SW Finland, their stratigraphy and geochemistry. In: Kähkönen, Y. (ed.) *Symposium Proterozoic Geochemistry, Helsinki '90* December 13-14, 1990, Abstracts, 35-38.
- Lindroos, A., Ehlers, C. & Åberg, G. 1990.** A Rb-Sr isochron of 1.5 Ga in early Proterozoic pillow lavas in SW Finland. *Geol. Fören. Stockholm Förh.* 112, 51-58.
- Mäkelä, K. 1980.** Geochemistry and origin of Haveri and Kiipu, Proterozoic strata-bound volcanogenic gold-copper and zinc mineralisations from southwestern Finland. *Geol. Surv. Finland, Bull.* 310, 79 p.
- Mäkelä, U. 1989.** Geological and geochemical environments of Precambrian sulphide deposits in southwestern Finland. *Ann. Acad. Sci. Fennicae. Ser. A, III Geol.-Geogr.* 151, 102 p.
- Nakamura, N. 1974.** Determination of REE, Ba, Fe, Mg, Na and K in carbonaceous and ordinary chondrites. *Geochim. Cosmochim. Acta* 38, 757-775.
- Nironen, M. 1989.** Emplacement and structural setting of granitoids in the Early Proterozoic Tampere and Savo Schist Belts, Finland - implications for contrasting crustal evolution. *Geol. Surv. Finland, Bull.* 346, 83 p.
- Nurmi, P. & Haapala, I. 1986.** The Proterozoic granitoids of Finland; Granite types, metallogeny and related crustal evolution. *Bull. Geol. Soc. Finland* 58, 241-261.
- Patchett, P.J. & Kouvo, O. 1986.** Origin of continental crust of 1.9-1.7 Ga age: Nd isotopes and U-Pb zircon ages in the Svecofennian terrain of South Finland. *Contrib. Mineral. Petrol.* 92, 279-297.
- Pearce, J.A. 1982.** Trace element characteristics of lavas from destructive plate boundaries. In: Thorpe, R.S. (ed.) *Andesites*. New York: Wiley and Sons, 724 p.
- Ploegsma, M. & Westra, L. 1990.** The early Proterozoic Orijärvi triangle (southwest Finland): a key area on the tectonic evolution of the Svecofennides. *Precambrian Res.* 47, 51-69.
- Rosenberg, R.J. 1977.** Instrumental neutron activation analysis as a routine method for rock analysis. Technical Research Centre of Finland, Electric and Nuclear Technology Publ. 19.
- Seitsaari, J. 1955.** Pre-Quaternary rocks, sheet 2012 Perniö. Geological map of Finland 1 : 100 000.
- Stålhös, G. 1969.** Description to the geological map of the Stockholm area, nr 24, ser. Ba, 133-145. (in Swedish with English summary)
- Stålhös, G. 1972.** Description to the geological map of Sweden; solid rocks of the Uppsala region, map sheets Uppsala SW and SE. Series Af Nr 105-106, 111-117. (in Swedish with English summary)
- Stålhös, G. 1991.** Description to the geological map of Sweden. Sheets Östhammar NW, NO, SW, SE. Series Af 161, 166, 169, 172, 136-157. (in Swedish)
- Suominen, V. 1987.** Mafic dyke rocks in southwestern Finland. *Geol. Surv. Finland, Rep. Invest.* 76, 151-172.
- Suominen, V. 1991.** The chronostratigraphy of southwestern Finland with special reference to Postjotnian and Subjotnian diabases. *Geol. Surv. Finland, Bull.* 356, 100 p.
- Väisänen, M. 1988.** Geology of the Aijala-Orijärvi area. In: Gaál, G. & Gorbatshev, R. (eds) *Tectonic setting of Proterozoic volcanism and associated ore deposits. Field guide for IGCP 217 and 247 excursion.* *Geol. Surv. Finland, Guide* 22, 81-86.
- Van Staal, C.R. & Williams, P.F. 1983.** Evolution of a Svecofennian mantled gneiss dome in SW Finland, with evidence for thrusting. *Precambrian Res.* 21, 101-128.
- Verhoef, P.N.W. & Dietvorst, E.J.L. 1980.** Structural analysis of differentiated schists and gneisses in the Taalintehdas area, Kemiö island, southwest Finland. *Bull. Geol. Soc. Finland* 52, 147-164.
- Welin, E. 1987.** The depositional evolution of the Svecofennian supracrustal sequence in Finland and Sweden. *Precambrian Res.* 35, 95-113.
- Westra, L. 1988.** Thermotectonic setting of an early Proterozoic volcanic belt in SW Finland. In: Gaál, G. & Gorbatshev, R. (eds.) *Tectonic setting of Proterozoic volcanism and associated ore deposits. Field guide for IGCP 217 and 247 excursion.* *Geol. Surv. Finland, Guide* 22, 69-80, 94-98.
- Wilson, M. 1989.** *Igneous Petrogenesis. A Global Tectonic Approach.* London: Harper Collins Academic, 466 p.

Tätä julkaisua myy


GEOLOGIAN
TUTKIMUSKESKUS (GTK)
Julkaisumyynti
02150 Espoo

 (90) 46 931
Teleksi: 123185 geolo sf
Telekopio: (90) 462 205

GTK, Väli-Suomen
aluetoimisto
Kirjasto
PL 1237
70211 Kuopio


 (971) 205 111
Telekopio: (971) 205 215

GTK, Pohjois-Suomen
aluetoimisto
Kirjasto
PL 77
96101 Rovaniemi


 (960) 3297 111
Teleksi: 37295 geolo sf
Telekopio: (960) 3297 289

Denna publikation säljes av

GEOLOGISKA
FORSKNINGSCENTRALEN (GFC)
Publikationsförsäljning
02150 Esbo

 (90) 46 931
Telex: 123185 geolo sf
Telefax: (90) 462 205

GFC, Distriktsbyrån för
Mellersta Finland
Biblioteket
PB 1237
70211 Kuopio

 (971) 205 111
Telefax: (971) 205 215

GFC, Distriktsbyrån för
Norra Finland
Biblioteket
PB 77
96101 Rovaniemi


 (960) 3297 111
Telex: 37295 geolo sf
Telefax: (960) 3297 289

This publication can be obtained
from


GEOLOGICAL SURVEY
OF FINLAND (GSF)
Publication sales
FIN-02150 Espoo, Finland

 +358 0 46 931
Telex: 123185 geolo sf
Telefax: +358 0 462 205

GSF, Regional office of
Mid-Finland
Library
P.O. Box 1237
FIN-70211 Kuopio, Finland

 +358 71 205 111
Telefax: +358 71 205 215

GSF, Regional office of
Northern Finland
Library
P.O. Box 77
FIN-96101 Rovaniemi

 +358 60 3297 111
Telex: 37295 geolo sf
Telefax: +358 60 3297 289